VAPOR-LIQUID EQUILIBRIUM MEASUREMENTS FOR SELECTED ETHANE AND CARBON DIOXIDE MIXTURES AND MODIFICATION OF THE SPHCT EQUATION OF STATE

By

RONALD D. SHAVER

Bachelor of Science
Oklahoma State University
Stillwater, Oklahoma
1988

Master of Science
Oklahoma State University
Stillwater, Oklahoma
1990

Submitted to the Faculty of the
Graduate College of the
Oklahoma State University
in partial fulfillment of
the requirements for
the Degree of
DOCTOR OF PHILOSOPHY
July, 1993

VAPOR-LIQUID EQUILIBRIUM MEASUREMENTS FOR SELECTED ETHANE AND CARBON DIOXIDE MIXTURES AND MODIFICATION OF THE SPHCT EQUATION OF STATE

Thesis Approved:

K. A. M. Gasem
Thesis Adviser

Robert L. Robinson Jr.

Arland H. Johannes

James R. Wiese

Lionel M. Raff

Thomas C. Collins
Dean of the Graduate College

PREFACE

A recently automated experimental apparatus has been used to measure the vapor-liquid equilibrium phase behavior for three selected binary mixtures (CO_2 + n-decane, CO_2 + *trans*-decalin, and ethane + 1-methylnaphthalene) at 160 °F at pressures up to the mixture critical points. Properties measured include vapor and liquid phase compositions, phase densities, and interfacial tensions. The data for CO_2 + n-decane agree well with existing literature data and confirm the proper operation of new computer automation systems. The data for the ethane + 1-methylnaphthalene system represent an addition to the literature of previously unavailable data.

Modifications have been proposed for the simplified-perturbed-hard-chain theory (SPHCT) equation of state that results in significantly improved pure fluid vapor pressure and phase density predictions. The modified equation is comparable to the original SPHCT equation in its ability to represent ethane + n-paraffin mixtures. However, worsened predictions are observed for prediction of CO2 + n-paraffin mixtures. This is attributed to deficiencies in the partition function of the original framework and the resulting uncertainties in the mixing rules used. Simple correlations have been developed to represent the critical point constraints without the need for numerically solving the critical point constraint equations.

I would like to express my sincere appreciation to my advisor, Dr. K. A. M. Gasem, for his continued assistance during the course of this work. His enthusiasm and dedication to his work helped maintain a high level of motivation throughout this work.

I would also like to thank the members of my graduate committee, Dr. R. L. Robinson, Jr., Dr. A. H. Johannes, Dr. J. Wagner, and Dr. L. M. Raff, for their time and valuable suggestions about this work.

Finally, I would like to thank my friends and family whose unconditional support over the last three years has allowed me to pursue my goals. To them I humbly dedicate this work, especially to my father who was unable to see its completion.

TABLE OF CONTENTS

LIST OF TABLES

Table Page

LIST OF FIGURES

Figure Page

SECTION 1

Figure Page

Figure Page

SECTION 2

NOMENCLATURE

a	Cubic equation of state parameter
A	Coefficient for density meter period, coefficient for scaling laws, Helmoltz energy, cubic equation of state parameter
AAD	Average absolute deviation
%AAD	Percent average absolute deviation
AAPD	Average absolute percent deviation
AR	Area ratio
b	Cubic equation of state parameter
B	Coefficient for density meter period, coefficient for scaling laws, cubic equation of state parameter
c	Degrees of freedom parameter
c_1, c_2	Volume translation parameters
C	Coefficient for density meter period, binary interaction parameter
d	Distance parameter
D	Coefficient for density meter period, binary interaction parameter
E	Energy, binary interaction parameter
F1	Equation of state solution function
F2	Equation of state solution function
F_t	SPHCT modifying function
F_g	SPHCT modifying function
g	Radial distribution function
G	Coefficient for interfacial tension scaling law, radial distribution function integral
h	Planck's constant
k	Boltzmann's constant
m	Molecular mass
M	Number of terms in extended power law equations

MW	Molecular weight
n	Number of injections
N	Number of moles, number of terms, number of particular species
N_c	Coordination number
N_a	Avogodro's number
P	Pressure
q	Single component partition function, external molecular surface area
Q	Canonical partition function
r	Distance from center of molecular segment
$\tilde{r}$	Reduced distance (r/σ)
R	Gas constant, interaction distance
RF	Response factor
RMSE	Root mean square error
RMSPE	Root mean square percentage error
s	Number of segments
S	Volume translation function
SS	Objective function
T	Temperature
$\tilde{T}$	Reduced temperature (T/T^*)
U	Internal energy
v	Specific volume
$\tilde{v}$	Partial molar volume
V	Volume
w	Volume translation parameter
x	Liquid mole fraction
X	Saturation property
y	Vapor mole fraction
Y	Physical property, SPHCT function
z	Compressibility factor

Z_M Maximum coordination number

Greek Symbols

α Scaling law exponent, cubic equation of state function

β Scaling law exponent

γ Interfacial tension

δ Volume translation parameter

Δ Wegner correction term, difference of phase values

ε Uncertainty

η Volume translation parameter, reduced density ($v^*\tau/v$)

Λ de Broglie wavelength

ν Scaling law exponent

ρ Density

$\tilde{\rho}$ Reduced density (v^*/v)

σ Weighting factor, hard-core diameter

τ Density meter period, geometrical constant (0.74048)

ϕ Order parameter, intermolecular potential energy, fugacity coefficient

Ψ Ratio of radial distribution function integrals

ω Acentric factor

Subscripts

a Air

att Attractive

c Critical state

calc Calculated

exp Experimental

ext External

EOS Equation of state

f Free

int	Internal
i,j	Component identification numbers
m	Mixture
min	Minimum
rep	Repulsive
r,v	Rotational and vibrational modes
t	Translational modes
w	Water
1,2	Solute and solvent, respectively
+,-	Ordered phases

Superscripts

c	Classical
CONF	Configurational
EOS	Equation of state
L	Liquid phase
nc	Non-classical
r	Residual
V	Vapor phase
*	Scaled property, characteristic parameter
',''	Phase designations

Additional Symbols

< >	Mixture property

SECTION 1 - EXPERIMENTAL WORK

CHAPTER I

INTRODUCTION

Accurate prediction of thermodynamic properties plays a vital role in nearly every area of chemical engineering as well as in our fundamental understanding of fluid phase behavior of pure fluids and mixtures. The most convenient form for representation of equilibrium phase behavior for process design and optimization calculations has long been recognized as that of analytic equations of state (1-3). The ability to evaluate the phase behavior predictive capabilities of existing equations of state and to develop new equations requires accurate experimental data on mixtures of selected compounds.

The present work represents an effort to expand the necessary database for such evaluations and to explore modifications to a recent theoretically based equation of state. Section 1 of this work is devoted to the experimental work while Section 2 documents the equation of state evaluation and development for the simplified-perturbed-hard-chain theory (SPHCT) equation of state. Each section includes its own list of references and appendixes for ease of use.

The primary experimental objectives of the present work were to collect phase equilibrium data to be used in equation of state model development and evaluation. Specifically, phase equilibrium data encompassing vapor and liquid phase compositions, phase densities and

interfacial tensions were measured for three systems: CO_2 + n-decane at 160 °F, ethane + 1-methylnaphthalene at 160 °F and CO_2 + *trans*-decahydronaphthalene (*trans*-decalin) at 160 °F. Data for all three systems were collected at pressures up to the mixture critical point. The first system (CO_2 + n-decane) was studied as a test system to demonstrate the capabilities of a recently automated experimental facility (4), while the second and third systems were studied to complement similar data obtained at Oklahoma State University.

Chapter II of the present section includes a brief review of the experimental apparatus used and previous experimental data reported in the literature which pertain to this study. Chapter III provides more detailed descriptions of the experimental apparatus and procedures. Chapter IV presents the results and discussions pertaining to each of the systems studied.

CHAPTER II

LITERATURE REVIEW

This chapter provides a brief review of experimental work directly related to the present experimental efforts. Two topics are reviewed: the experimental facility used to measure the equilibrium phase behavior data and previous experimental data collected on the systems studied in this work.

Experimental Apparatus

The experimental apparatus used to obtain the data reported here has been described in detail by other workers (4,5). The apparatus was originally constructed to measure vapor-liquid equilibrium phase behavior data (phase densities and compositions) and interfacial tensions for systems consisting of hydrocarbon solvents and light solute gases at reservoir conditions (up to 300 °F and 3000 psia) for a consortium of oil companies (4-17). The equipment has undergone many modifications with the most recent improvements described by Roush (4) aimed at automating the data acquisition and control.

The apparatus consists of a high pressure equilibrium cell, two density meters for measurement of vapor and liquid phase densities, an interfacial tension cell, a gas chromatograph sampling system for composition analysis, and a magnetic circulation pump all housed in a temperature controlled oven. Also present are the necessary equipment

for injection of liquid solvents and gas solutes. Detailed descriptions of each piece of equipment and the calibration and operating procedures used appear in the next chapter.

Previous Experimental Data

Prior to the collection of experimental data, a thorough search of the literature was done to identify previous experimental data on the mixtures of interest at or near the temperature studied (160 °F). The first system studied (CO_2 + n-decane) was chosen as a test system for the new automation equipment because this system has been well studied by several investigators (7,19-20,30-31). Nagarajan and Robinson (7) report phase densities, phase compositions and interfacial tensions from 926 psia to the mixture critical point. Reamer and Sage (19) report phase densities and compositions from 200 psia to the critical point. Seagraves (30) presents solubilities of CO_2 in n-decane at pressures from 653 to 1477 psia, Bufkin (31) presents CO_2 solubilities from 182.7 to 1252.4 psia, and Chou, et al. (20) presents vapor and liquid phase compositions from 590 psia to 1730 psia.

Mixtures of CO_2 and *trans*-decalin have been studied by several investigators (11,21-22). Gasem and Robinson (11) report phase compositions, phase densities and interfacial tensions at 160 °F from 750 psia to the mixture critical point. Tiffin and coworkers (21) present liquid phase compositions and specific volumes at 75 °C (167 °F) from 147 psia to 1029 psia. Anderson and coworkers (22) report liquid phase compositions at 75 °C (167 °F) from 370 psia to 1348 psia. This mixture was studied for two reasons. First, the original data of Gasem and Robinson (11) remains questionable due to experimental difficulties

encountered during its collection. The vapor and liquid phase data were collected on separate experimental runs because of equipment problems and the vapor phase compositions were suspected of being too lean in solute mole fraction (32). Second, the composition data of Tiffin (21) and Anderson (22) are in disagreement and new measurements are required to alleviate this discrepancy.

No experimental data for mixtures of ethane and 1-methylnaphthalene at or near the temperature studied (160 °F) was located in the literature. Therefore, the data collected here represents an addition to the literature of previously unavailable information.

CHAPTER III

EXPERIMENTAL APPARATUS AND PROCEDURES

The experimental apparatus used to obtain the data reported here has been described in detail by other workers (4-9). The apparatus is used to measure vapor-liquid equilibrium phase behavior data (phase densities and compositions) and interfacial tensions. The apparatus is currently limited to a temperature of 300 °F and a pressure of 3000 psia. Figures 1 and 2 show schematic diagrams of the apparatus in vapor and liquid circulation flow patterns, respectively. Following is a brief description of each of the main components of the system.

Constant Temperature Oven

The experimental apparatus is housed in a Hotpack oven (model 212052-29). Vigorous air circulation within the oven is achieved by operating the two internal oven blowers at their highest rate with additional circulation provided by a ten inch aluminum fan run by an electric motor located outside of the oven doors. The externally driven fan was added during this work to reduce temperature profiles within the oven and has greatly improved the stability of temperature control. Temperatures are monitored by five thermocouples and five resistance temperature detectors (RTD's) linked to a Northgate 386 personal computer through an Acro Systems computer interface module. All temperature probes are calibrated against a Minco platinum resistance

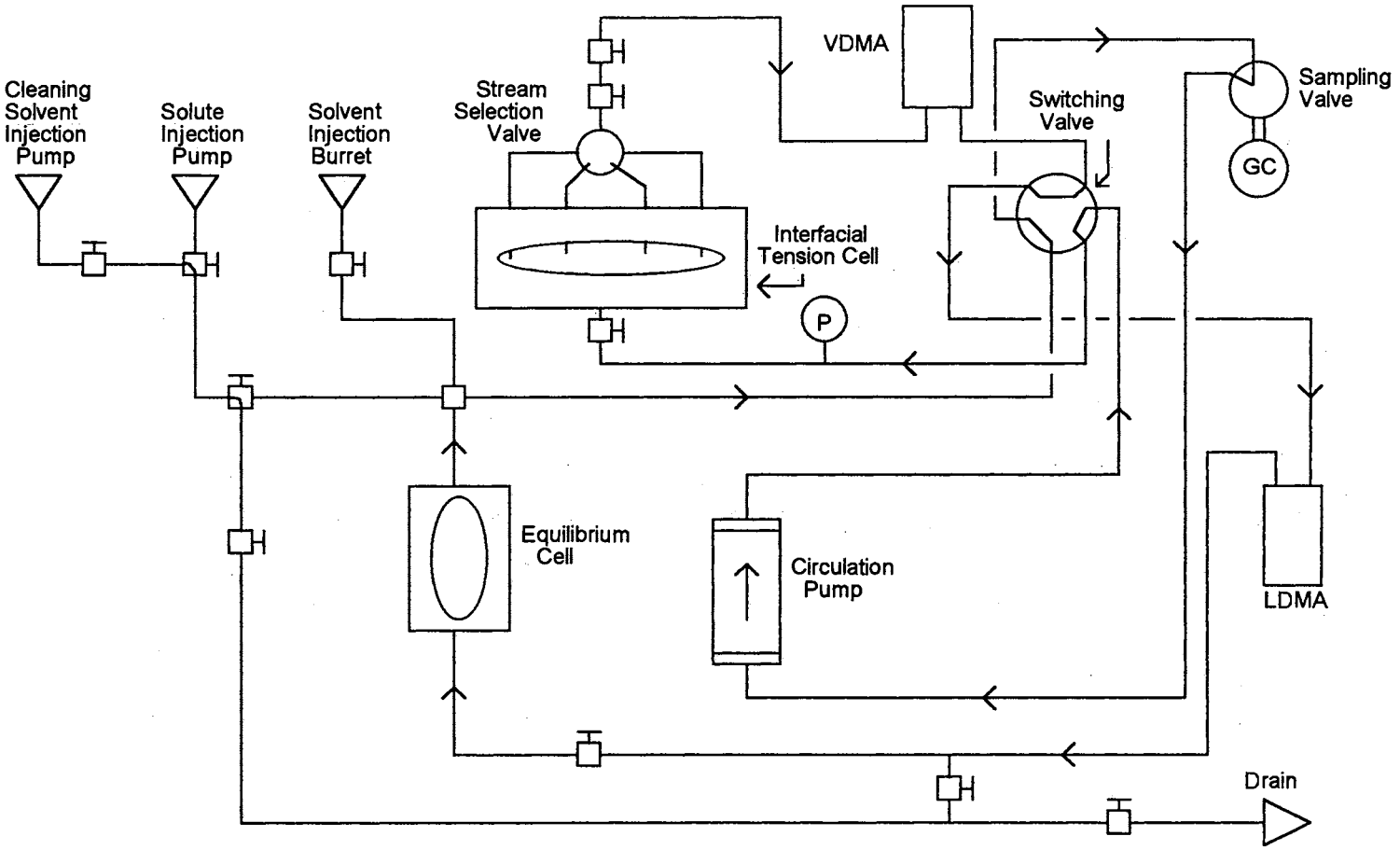

Figure 1. Experimental Apparatus Showing the Vapor Circulation Path

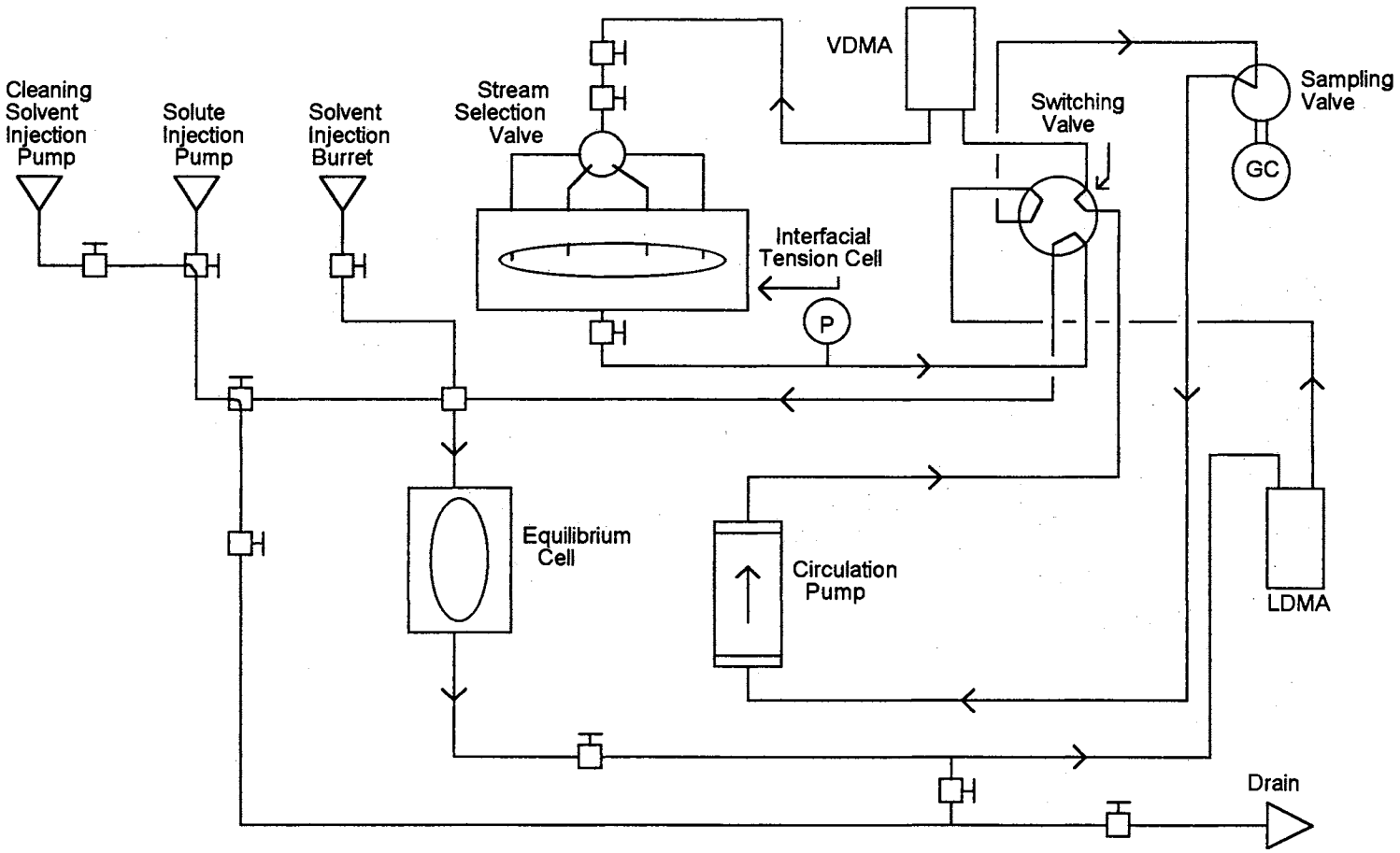

Figure 2. Experimental Apparatus Showing the Liquid Circulation Path

thermometer. Equipment temperatures in the oven are controlled to within ±0.1 °F by five small heaters controlled through the computer software described in a later section.

Interfacial Tension Cell

The interfacial tension cell (IFT cell) used in this work is the prototype first installed by Roush (4) for the measurement of IFT's using the pendant drop technique. The cell consists of a modified high pressure flow meter positioned horizontally with four 5/8 inch holes bored into the top and one into the bottom to be used as an outlet port. A simplified schematic diagram of the cell is shown in Figure 3. Each of the four inlet holes is used to hold a 2 inch-long needle (Unimetrics) which is held in place by a teflon plug. Needle diameters are chosen so that a wide range of interfacial tensions can be measured without maintenance of the cell. For very low interfacial tensions, a small wire is installed inside one of the needles with about 1/8 inch of wire extending below the end of the needle. Pendant drops are then suspended on the tip of the wire.

The original cell contained oval gaskets for sealing between the windows and the cell body. The gaskets were not capable of sealing high pressure gases. Therefore, the cell was modified further by having an oval groove machined into each side of the central cell section. A standard 4 inch diameter composite O-ring (Viton encapsulated by Teflon) was then seated into the groove and compressed against the windows by the sealing nuts. The cell has been successfully tested at pressures ranging from vacuum to 2000 psia. However, above 2000 psia the O-rings failed several times and further modification of the cell will be

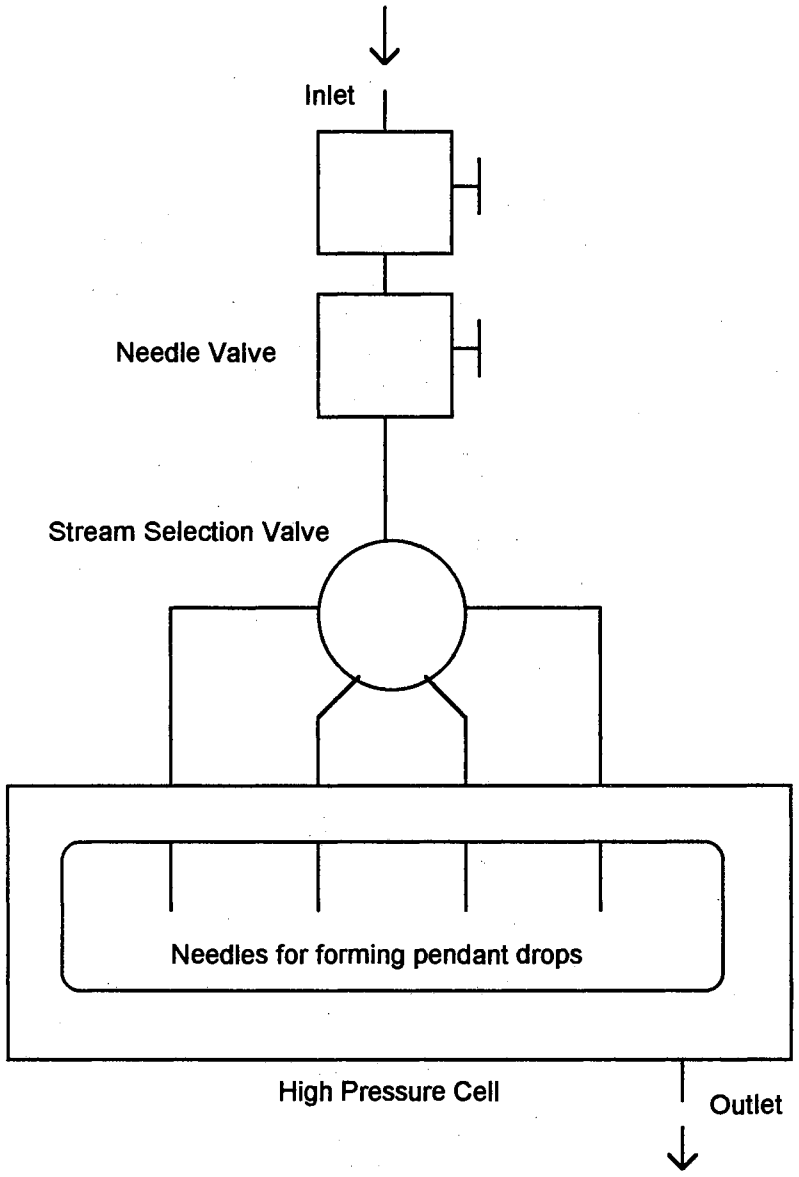

Figure 3. Simplified Diagram of Interfacial Tension Cell

required to achieve operation at high pressures. The new cell contains no moving parts and eliminates plugging of the system tubing due to deterioration of the O-rings and seals (32). The new composite O-rings are inert to the chemicals studied and eliminate problems of swelling of the O-rings.

The entire interfacial tension cell is mounted on a steel platform which extends through the oven wall and is attached to a vibration free table. Illumination of the pendant drops is provided by a Volpi fiberoptic light source with the fiberoptic tip attached to a track behind the IFT cell. The track allows the light source to be moved horizontally to provide illumination behind any of the four needles. Descriptions of the equipment and procedures for analysis of pendant drops is included in a later section.

The original IFT cell contained a cluster of four Autoclave high pressure valves to control the flow of liquid through the IFT needles (4). These valves were replaced with a single 6-position Valco stream selection valve as shown in Figure 3 to allow selection of the desired needle. The new configuration reduces the potential for leaks and provides for simpler operation of the IFT cell.

Gas Chromatograph

The gas chromatograph (GC) used for composition analysis in this work was a Varian 3700 with a Varian CDS-111 integrator, a Varian 9176 chart recorder, a Varian external events module and a Varian digital valve sequence programmer. A thermal conductivity detector was used for all of the systems studied. Table I lists specific information on the GC configuration for each system studied.

TABLE I

GAS CHROMATOGRAPH CONFIGURATION AND OPERATING CONDITIONS FOR EACH SYSTEM STUDIED

	System		
	CO_2 + n-Decane	Ethane + 1-Methylnaphthalene	CO_2 + *trans*-Decalin
Column	24' OV-101	24' OV-101 + 10' 3% OV-17	24' OV-101
Carrier gas	He	He	He
Carrier gas inlet pressure	54 psig	54 psig	40 psig
Injector Temperature	220 °C	220 °C	270 °C
Column Temperature	220 °C	200 °C	200 °C
Detector Temperature	240 °C	240 °C	270 °C
Filament Temperature	270 °C	270 °C	300 °C

The GC sampling system is a pneumatically controlled pair of valves actuated by the digital valve sequence programmer. The sampling valve is a 1-μL Valco high pressure sampling valve. The valve sequence positions are shown in Figure 4. During the course of this work, the GC sampling valve was inverted with the inlet and outlet ports facing down and was relocated near the top of the apparatus to improve vapor sampling. The new configuration provides more reliable vapor composition measurements at higher pressures. However, measurement of vapor phase compositions for low density vapors remains troublesome. This is due in part to the presence of liquid droplets in the GC sampling valve. Vapor circulation at low pressures does not sweep liquid from the sampling valve as efficiently as at higher pressures. Consequently, vapor composition analysis at pressures below 1000 psia is difficult to obtain. A possible remedy may be to install two separate sampling valves: one located at the bottom of the equilibrium cell for sampling of the liquid phase and one near the top of the cell for sampling the vapor phase. The system lines should be configured so that only vapor phase is circulated through the vapor sampling valve to prevent contamination of samples with liquid droplets.

Density Meters

The density meters are Mettler/Paar type 512 vibrating U-tube density meters. The liquid density meter is located on the floor of the oven with both the inlet and outlet ports pointing upward to aid in removal of any vapor bubbles which may become trapped in the instrument. Likewise, the vapor density meter is placed near the top of the

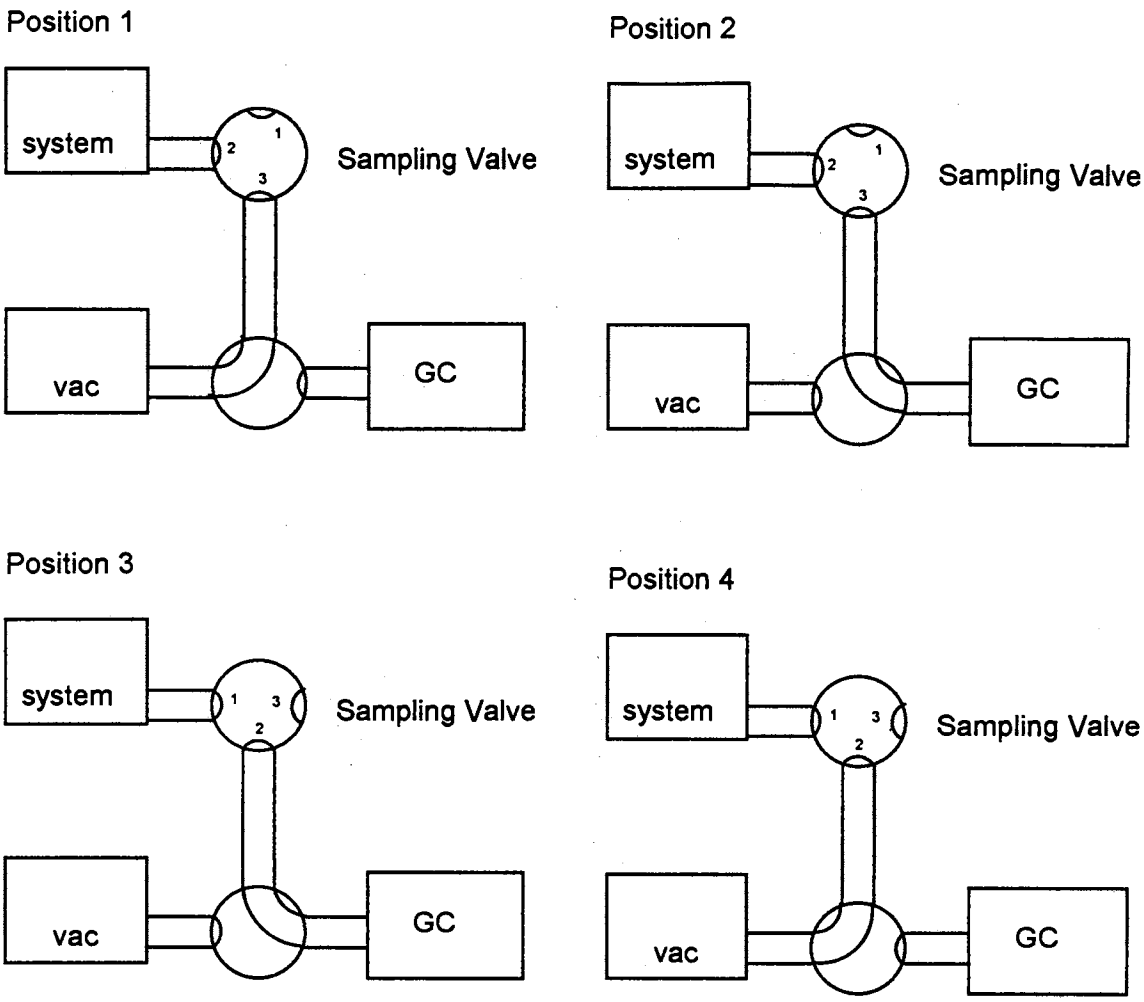

Figure 4. Gas Chromatograph Sampling Valve Sequence

apparatus and is inverted to aid in draining any liquid present in the instrument.

Video System and Drop Analysis

Interfacial tension measurements are made from drops pendant on the needles of the IFT cell described earlier. Digital images of the pendant drops are obtained with a Javelin CCTV B/W camera (model JE2362A) connected to a Wild microscope system. A PC Vision plus Frame Grabber card installed in a Dell 286 personal computer is used to freeze digital images of the drops. Jandel Scientific's JAVA software is then used to manipulate the digitized images to produce the data necessary for calculation of interfacial tension. The JAVA software has the capability to trace the drop profile and store the pixel values of the profile in a data file. A Fortran program originally written by Roush (4) (included in Appendix A) is then used to convert the drop profile data so that the apex of the drop is at the origin of a Cartesian coordinate system. The program also adjusts for the video system aspect ratio and rescales the pixel values to units of centimeters. A final Fortran program written by Pallas (18) (adopted for PC use) is then used to calculate the interfacial tension from the converted drop profile data. The program uses a rotational discrimination technique to solve the Young-Laplace equations describing the drop profile and is described in detail elsewhere (4,18,23). An example of the digitized drop profile data is presented in Figure 5. The left and right halves of the drop are shown superimposed to illustrate the symmetry of the drop about the drop centerline. Figure 6 shows the residuals of the fit obtained from the Pallas program for a typical drop. The figure again indicates that

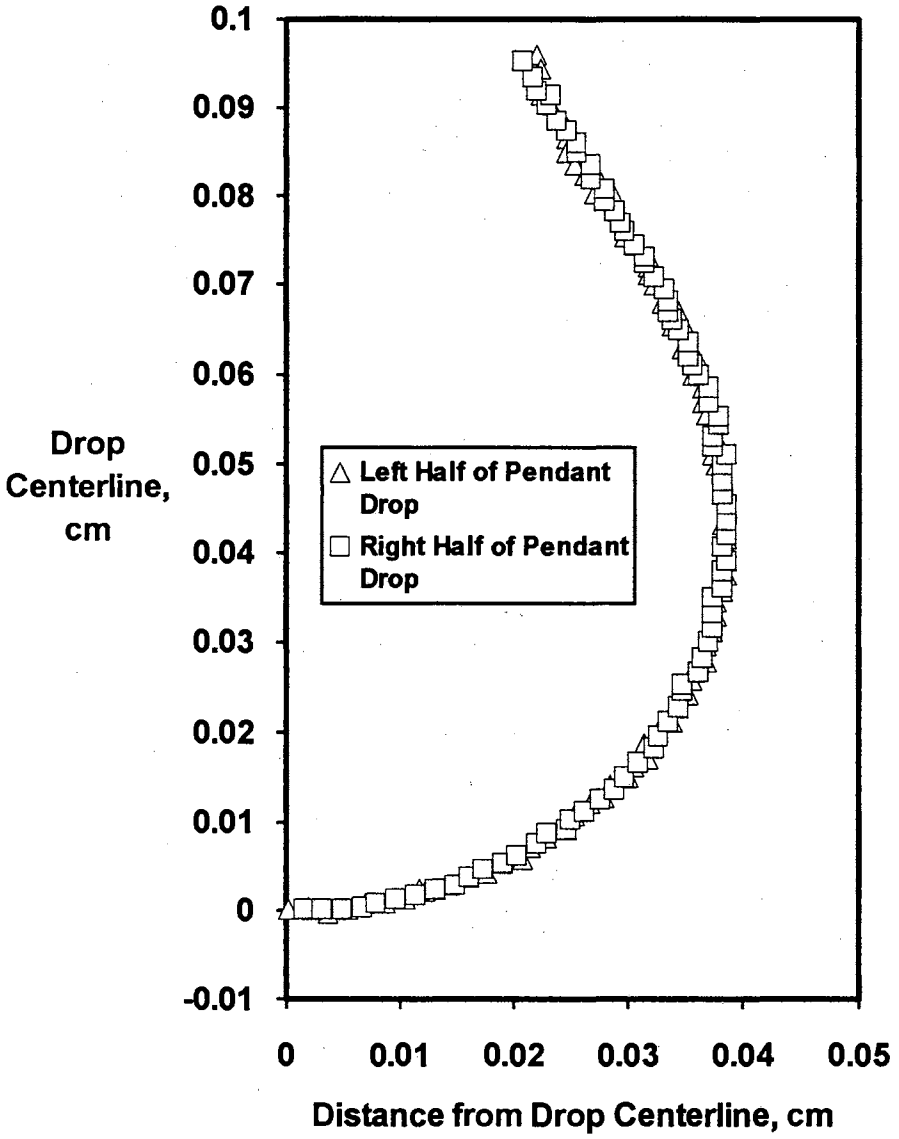

Figure 5. Example of Digitized Pendant Drop Profile Data

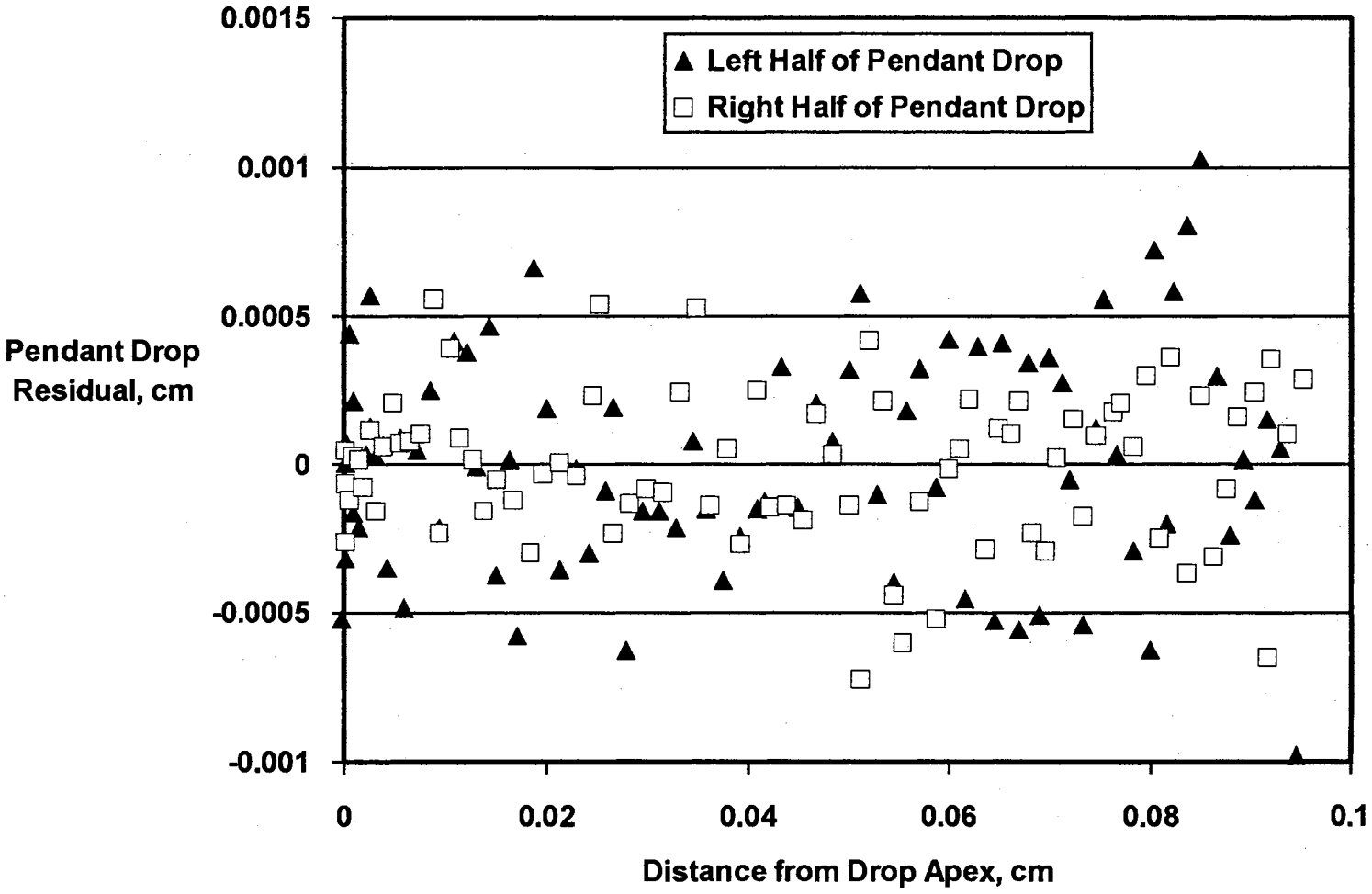

Figure 6. Residuals of Calculated Pendant Drop

the drop is symmetrical about the centerline and is quite close to the shape of a true pendant drop.

Computer System

Data acquisition and control is maintained through a computer system installed by Roush (4). All equipment except for the gas chromatograph is interfaced to a Northgate 386 personal computer through an ACRO 900 interface unit and monitored through Labtech Control software. Temperatures within the oven are controlled to within ±0.1 °F by five separate heaters located strategically in the oven to compensate for heat losses. Each heater is controlled through a customized circuit board which proportions a 0-10 volt signal from the ACRO interface to 0-120 volt heater input utilizing a proportional-integral (PI) control strategy.

Calibrations and Integrity Checks

During the course of experimental data acquisition, several calibrations and integrity tests are performed to verify proper operation of all equipment. Before the start of each experimental run, the temperature sensors, the pressure gage, the two density meters and the gas chromatograph response factor are all calibrated. The thermocouples and RTD's are calibrated against a Minco platinum resistance thermometer at the temperature of interest. The pressure transducer (a Sensotec TJE/743-03 3000 psig transducer) is calibrated using helium as the working fluid against a Ruska deadweight tester with a calibration traceable to NBS.

The density meters are calibrated with air and water as reference fluids. The period of oscillation of the vibrating density meter U-tube is fitted to an equation of the following form for each reference fluid for each density meter:

$$\tau = A + BP + CP^2 + DP^3 \qquad (1)$$

where

τ = period of oscillation of the density meter U-tube

P = pressure

A,B,C,D = fitted constants

Sample densities are then found by interpolation between the reference fluid values using:

$$\rho = K\left(\tau^2 - \tau_w^2\right) + \rho_w \qquad (2)$$

where

$$K = \frac{\left(\rho_a - \rho_w\right)}{\left(\tau_a^2 - \tau_w^2\right)} \qquad (3)$$

τ_a, τ_w = density meter period of oscillation for air and water

ρ, ρ_a, ρ_w = sample, air and water densities, respectively

The gas chromatograph is calibrated by preparing mixtures of known composition within the apparatus and determining a response factor for the GC system. The procedure for determining the response factor was similar to procedures described elsewhere (5,11,12). The response factor is determined from the relation:

$$RF = (AR)N_2/N_1 \tag{4}$$

where

AR = ratio of GC integrated areas of solute to solvent

N_1 = number of moles of solute in calibration mixture

N_2 = number of moles of solvent in calibration mixture

An estimate of the uncertainty in the response factor due to uncertainties in the area ratio and in N_1 and N_2 is given by standard error propagation methods as:

$$\left(\frac{\varepsilon_{RF}}{RF}\right)^2 = \left(\frac{\varepsilon_{AR}}{AR}\right)^2 + \left(\frac{\varepsilon_{N_1}}{N_1}\right)^2 + \left(\frac{\varepsilon_{N_2}}{N_2}\right)^2 \tag{5}$$

where

ε_{RF} = uncertainty in response factor

ε_{AR} = uncertainty in measured area ratio

$\varepsilon_{N_1}, \varepsilon_{N_2}$ = uncertainty in N_1 and N_2, respectively

Two different methods were used to determine the response factor since each method provides favorable error analysis in different ranges of composition and the use of two separate methods provides a convenient check on the experimental procedures. The difference in the two methods is in the technique used to determine the amount of solute in the calibration mixture. The first method (referred to as the material balance method) uses a material balance to calculate the composition of the calibration mixture where:

$$N_1 = \sum_{i=1}^{n_1}\left(\frac{\rho_1 V_1}{MW_1}\right)_i \tag{6}$$

and

$$N_2 = \sum_{i=1}^{n_2} \left(\frac{\rho_2 V_2}{MW_2} \right)_i \tag{7}$$

where

n_1, n_2 = number of solute and solvent injections

ρ_1, ρ_2 = solute and solvent density

V_1, V_2 = volume of injected solute and solvent (for injection "i")

MW_1, MW_2 = solute and solvent molecular weights

By applying error propagation to Equations (6) and (7), the following uncertainties in N_1 and N_2 can be obtained:

$$\left(\frac{\varepsilon_{N_1}}{N_1} \right)^2 = \sum_{i=1}^{n_1} \left[\left(\frac{\varepsilon_{V_1}}{V_1} \right)_i^2 + \left(\frac{\varepsilon_{\rho_1}}{\rho_1} \right)_i^2 \right] \tag{8}$$

and

$$\left(\frac{\varepsilon_{N_2}}{N_2} \right)^2 = \sum_{i=1}^{n_2} \left[\left(\frac{\varepsilon_{V_2}}{V_2} \right)_i^2 + \left(\frac{\varepsilon_{\rho_2}}{\rho_2} \right)_i^2 \right] \tag{9}$$

where

$\varepsilon_{V_1}, \varepsilon_{V_2}$ = uncertainty in solute and solvent volumes injected

$\varepsilon_{\rho_1}, \varepsilon_{\rho_2}$ = uncertainty in solute and solvent injection density

For the second method (referred to as the density method), the amount of solute injected is calculated from the measured density (ρ_M) of the calibration mixture as follows:

$$N_1 = \frac{1}{MW_1}\left[\rho_M V - \sum_{i=1}^{n_2}(\rho_2 V_2)_i\right] \tag{10}$$

Thus, the uncertainty in N_1 is:

$$\left(\frac{\varepsilon_{N_1}}{N_1}\right)^2 = \left(\frac{1}{N_1 MW_1}\right)^2\left\{\left(\varepsilon_{\rho_M} V\right)^2 + \left(\varepsilon_V \rho_M\right)^2 + \sum_{i=1}^{n_2}\left[\left(\varepsilon_{\rho_2} V_2\right)_i + \left(\varepsilon_{V_2}\rho_2\right)_i\right]\right\} \tag{11}$$

where

ε_{ρ_M} = uncertainty in measured system density

ε_V = uncertainty in measured system volume

ρ_M = measured system density

V = measured system volume

Figures 7-9 show the results of the response factor determinations for several mixtures using the above two approaches for each of the systems studied in this work. Error bars are also included based on the following uncertainties in the input variables in the above equations:

$\varepsilon_{V_1} = 0.05\ cm^3$

$\varepsilon_{V_2} = 0.10\ cm^3$

$\varepsilon_{\rho_1} = \varepsilon_{\rho_2} = \varepsilon_{\rho_M} = 0.003\ g/cm^3$

$\varepsilon_V = 1.0\ cm^3$

and where ε_{AR} is estimated from the standard error of a series of repeated GC samples. As shown in Figures 7-9, the response factor is dependent upon composition. Therefore, a weighted-least-squares regression was performed on the response factor as a function of the solute compositions (x_{solute}) obtained from the material balance method and the density method. The weighting factors for the data points were

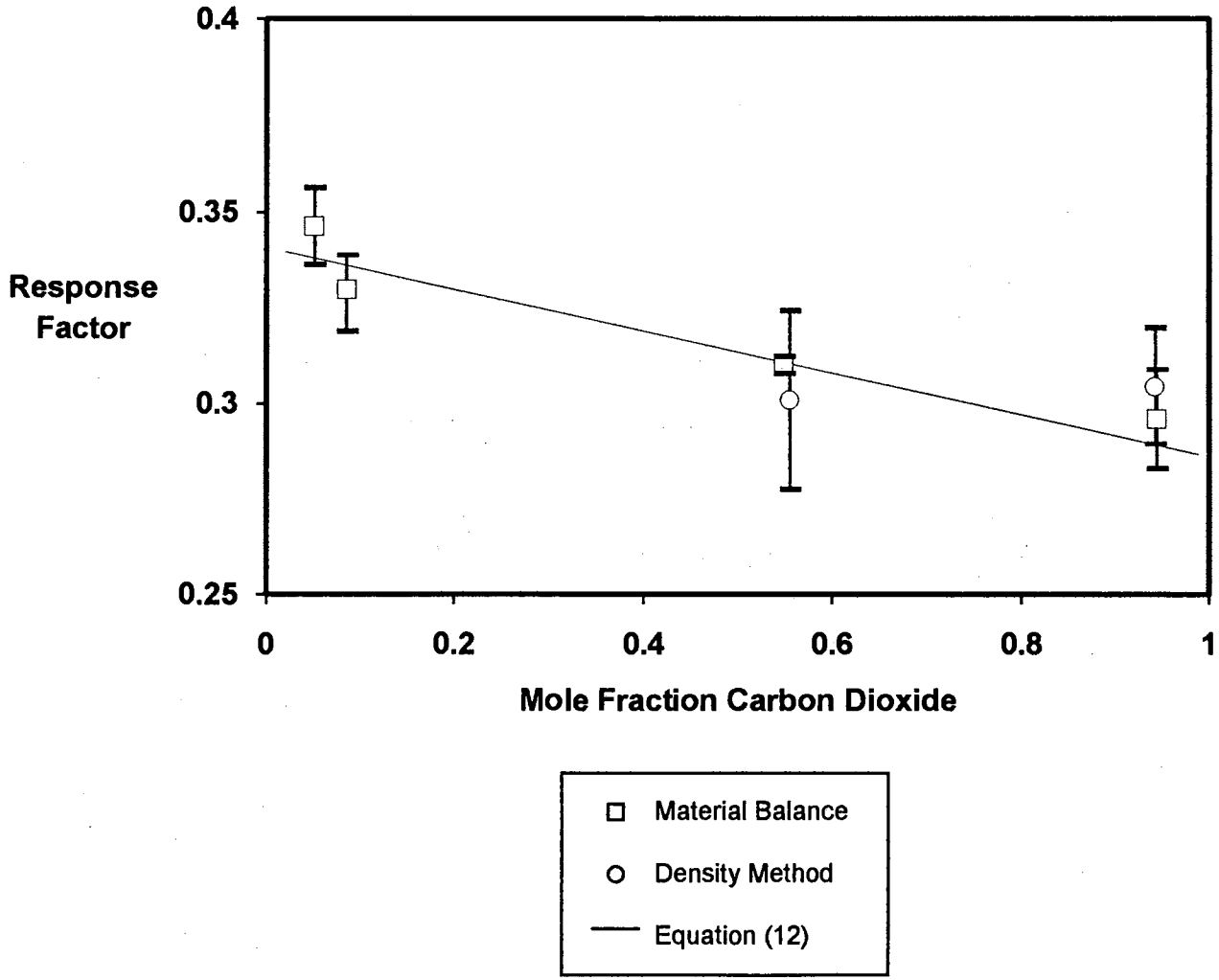

Figure 7. Response Factor Composition Dependence for the CO_2 + n-Decane System at 344.3 K (160 °F)

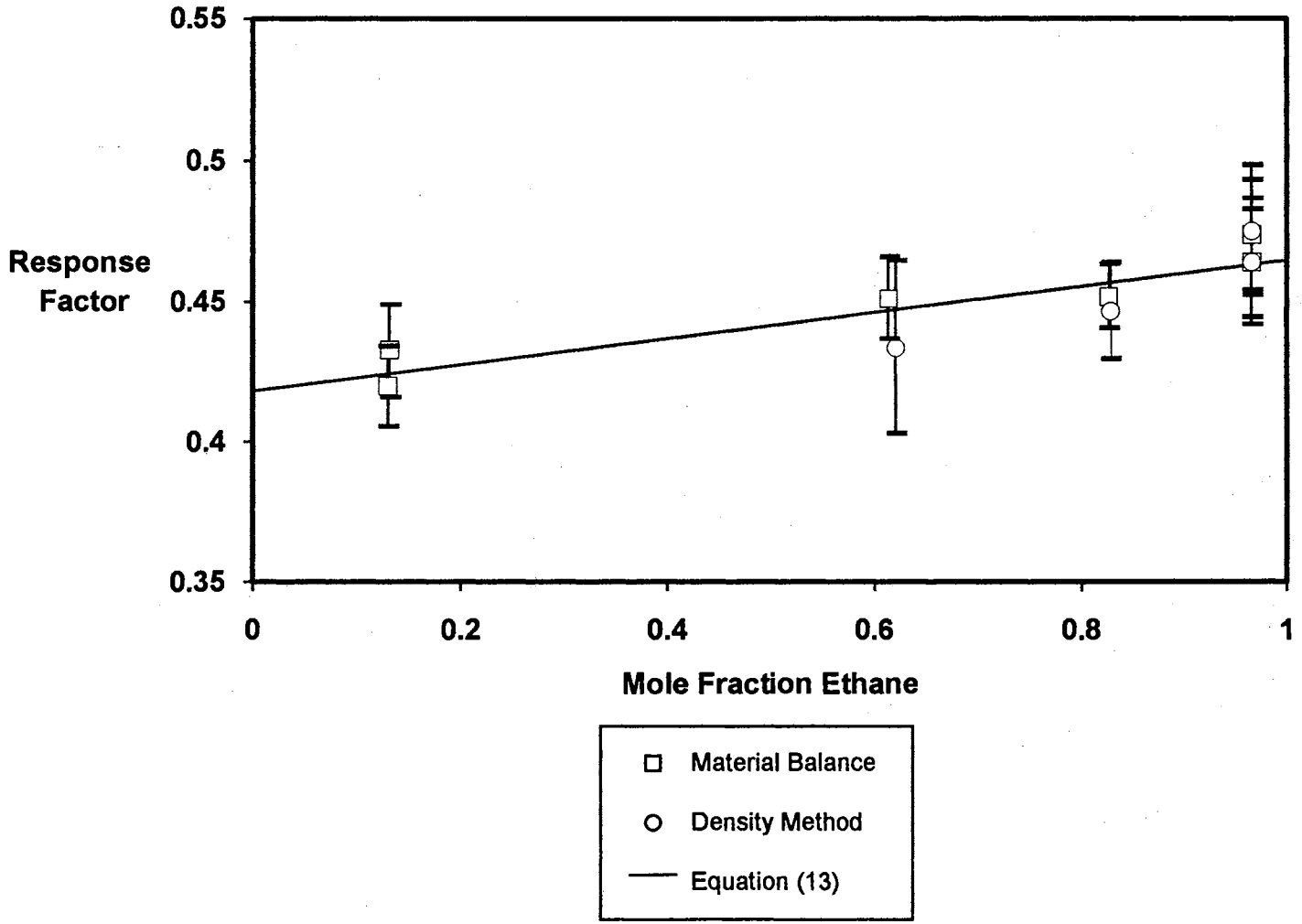

Figure 8. Response Factor Composition Dependence for the Ethane + 1-Methylnaphthalene System at 344.3 K (160 °F)

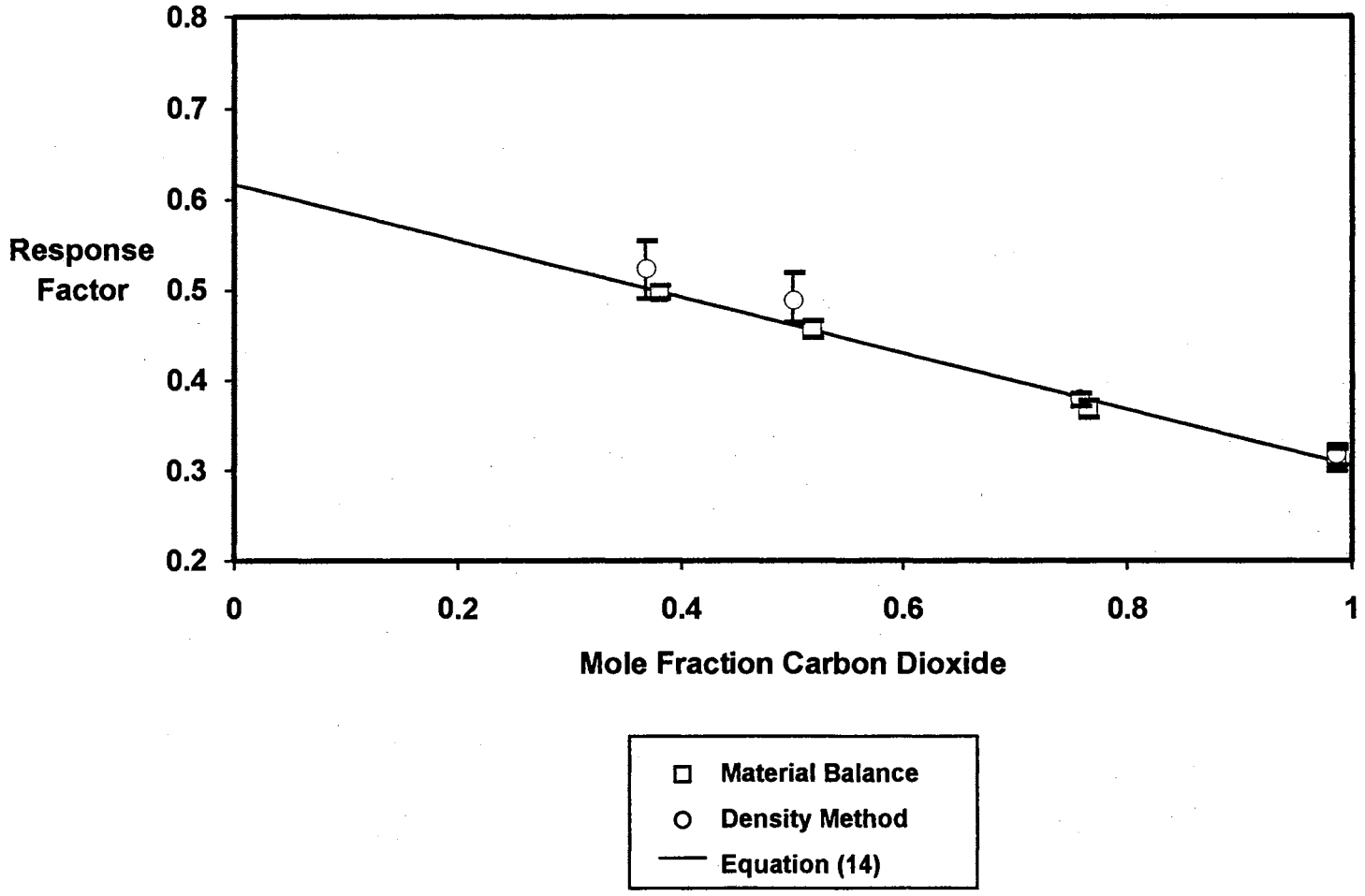

Figure 9. Response Factor Composition Dependence for the CO_2 + *trans*-Decalin System at 344.3 K (160 °F)

given by the uncertainties calculated from the above equations. The resulting equations for response factor composition dependence are as follows.

For CO_2 + n-decane at 344.3 K (160 °F):

$$RF = 0.3410 - 0.05488x_{CO_2} \quad (12)$$

For ethane + 1-methylnaphthalene at 344.3 K (160 °F):

$$RF = 0.4182 + 0.04663x_{ethane} \quad (13)$$

For CO_2 + *trans*-decalin at 344.3 K (160 °F):

$$RF = 0.6173 - 0.3123x_{CO_2} \quad (14)$$

The compositional dependence of the response factors is believed to be due to adsorption effects in the sample transfer line and to non-linear response of the TCD detector to the solvent. The compositional dependence of response factor for the CO_2 + *trans*-decalin system is quite strong as indicated in Equation (14). However, as shown in Figure 9 this dependence is accounted for through the calibration.

Experimental Procedures

After each piece of equipment has been calibrated and the system has been tested for leaks, the system is cleaned using n-pentane and CO_2. The system is then drained and placed under vacuum. When the system is thoroughly evacuated (as indicated by a VacTorr thermocouple vacuum gauge) the system is isolated from the vacuum pump and hydrocarbon is injected. Usually 40 to 50 cm^3 of hydrocarbon is injected through the burret shown in Figures 1 and 2. Solute gas is then injected from a Ruska hand pump (the solute injection pump) until

the system pressure reaches the first desired pressure. The system is placed in the vapor circulation pattern and the circulation pump is operated until equilibrium is established. The state of equilibrium is determined as the point at which both the pressure gauge and density meter readings become stable (usually within two hours of solute injection).

Once equilibrium is established, vapor samples are analyzed with the GC until a series of four or five consistent chromatograms are obtained. The average of the GC area ratios is then recorded in the summary data file by running the data acquisition program included in Appendix A. Next, the circulation pump is stopped and vapor phase density is recorded. The circulation pump is then turned on, the system is placed in the liquid circulation pattern and liquid phase samples are analyzed by the GC. Again, after a series of four or five consistent chromatograms are obtained, the average liquid phase area ratio is recorded by the data acquisition program. The circulation pump is then stopped and liquid phase density is recorded as above.

The final step in the data acquisition at each pressure is photographing pendant drops for IFT determination. The appropriate needle of the IFT cell is selected by the manipulation of the stream selection valve located upstream of the IFT cell (shown in Figures 1-3). The circulation pump is started with the system in the liquid flow pattern until liquid is seen flowing from the needle of interest. The circulation pump is stopped and the top valve of the IFT valve cluster is closed. By slowly turning the needle valve located just upstream of the IFT cell, liquid drops can be squeezed out of the selected needle. Images of pendant drops are then digitized using the Frame Grabber board

and Jandel Scientific software and stored on floppy disk for later analysis as described earlier.

After all required data have been collected at a given pressure, additional solute is injected until the next desired pressure is reached and the entire procedure for data collection is repeated. The procedure is repeated up to the critical pressure of the mixture being studied. As the critical point is approached, a visual observation of the critical point is made for comparison with that obtained from the extended scaling law analysis of the final data (discussed in detail in Chapter IV). The critical point is characterized by a distinct change of color (usually orange or red) of the contents of the equilibrium cell. The level of liquid in the equilibrium cell is observed to determine if the mixture is approaching a bubble point, a dew point or the critical point. If the mixture is approaching the bubble point, a small amount of liquid is drained from the system and more solute is injected to enrich the mixture and another attempt is made to pass through the critical point. If the mixture is approaching the dew point, this observation is recorded and the experimental run is concluded since the current system configuration does not allow for hydrocarbon injections at positive gage pressure.

Materials

The n-decane used in this work was supplied by Johnson Matthey Electronics (Alfa Products) with a reported purity of 99%. The 1-methylnapthalene was supplied by Aldrich Chemical Company with a reported purity of 99%. The *trans*-decalin was obtained from Aldrich Chemical Company with a reported purity of 99%. The CO_2 used was

supplied by Linde Specialty Gases with a reported purity of 99.99%. The ethane was supplied by Matheson Gas Products with a reported purity of 99.99%. No further purification of any of the chemicals was attempted.

CHAPTER IV

EXPERIMENTAL RESULTS AND DISCUSSION

Experimental data on equilibrium phase densities (ρ^L, ρ^V), phase compositions (x, y) and interfacial tensions (γ) have been measured for the following systems: CO_2 + n-decane at 160 °F, ethane + 1-methylnaphthalene at 160 °F and CO_2 + *trans*-decalin at 160 °F. The measurements cover the pressure range from the lowest pressure at which data could be collected to the critical pressure of each mixture studied (P_c = 1844 psia for the CO_2 + n-decane system, P_c = 2295 for the ethane + 1-methylnaphthalene system and P_c = 2280 for the CO_2 + *trans*-decalin system). Presentation of the experimental data and discussion of each system follows.

Carbon Dioxide + n-Decane at 160 °F

Experimental Data

The raw data for this system appears in Tables II through IV. Table II includes all of the phase density data and Table III contains all of the phase composition data. In Table IV, values of $\gamma/\Delta\rho$ are given rather than values for the interfacial tension, γ, since $\gamma/\Delta\rho$ is the quantity obtained from the analysis of the pendant drops. The accuracy of the experimental data has been estimated in previous work (5,6,24) as:

TABLE II

COMPARISON OF EXPERIMENTAL AND CALCULATED PHASE DENSITIES
FOR CO_2 + N-DECANE AT 344.3 K (160 °F)

PRESSURE psia	PHASE DENSITIES (g/cm^3) Exp.	Calc.	ERROR IN CALCULATED DENSITY g/cm^3	% Dev.	Wt. Dev.	WEIGHTING FACTOR g/cm^3
----------LIQUID PHASE----------						
1839.6	0.628066	0.631929	0.003863	0.615031	1.155553	0.003343
1838.6	0.638044	0.635026	-0.003018	-0.473083	-1.039272	0.002904
1833.5	0.645732	0.646485	0.000753	0.116668	0.412582	0.001826
1823.0	0.660478	0.660815	0.000337	0.051004	0.304334	0.001107
1809.2	0.673308	0.672647	-0.000661	-0.098198	-0.869015	0.000761
1783.6	0.685979	0.686328	0.000349	0.050901	0.684507	0.000510
1737.4	0.699982	0.699934	-0.000048	-0.006920	-0.132472	0.000366
1712.4	0.704605	0.704413	-0.000192	-0.027271	-0.570664	0.000337
1647.3	0.711221	0.711360	0.000139	0.019512	0.450043	0.000308
1616.5	0.713178	0.713201	0.000023	0.003252	0.076280	0.000304
1515.0	0.715836	0.715928	0.000092	0.012796	0.305139	0.000300
1399.3	0.716061	0.715981	-0.000080	-0.011195	-0.267135	0.000300
1312.8	0.715241	0.715128	-0.000113	-0.015866	-0.377951	0.000300
1206.7	0.713651	0.713594	-0.000057	-0.008044	-0.191072	0.000300
1124.2	0.712180	0.712176	-0.000004	-0.000525	-0.012442	0.000301
1014.5	0.709951	0.710073	0.000122	0.017221	0.406614	0.000301
921.3	0.708008	0.708129	0.000121	0.017108	0.402714	0.000301
815.3	0.705712	0.705790	0.000078	0.011072	0.259713	0.000301
717.4	0.703645	0.703567	-0.000078	-0.011052	-0.258468	0.000301
615.2	0.701373	0.701254	-0.000119	-0.016921	-0.394495	0.000301
503.7	0.698939	0.698814	-0.000125	-0.017909	-0.416183	0.000301
409.0	0.696839	0.696830	-0.000009	-0.001256	-0.029099	0.000301
316.0	0.694815	0.694914	0.000099	0.014293	0.330235	0.000301
222.6	0.692700	0.692880	0.000180	0.026051	0.599718	0.000301
128.8	0.690587	0.690452	-0.000135	-0.019548	-0.447835	0.000301

TABLE II (Continued)

PRESSURE psia	PHASE DENSITIES (g/cm^3) Exp.	Calc.	ERROR IN CALCULATED DENSITY g/cm^3	% Dev.	Wt. Dev.	WEIGHTING FACTOR g/cm^3
			VAPOR PHASE			
1842.2	0.547684	0.552457	0.004773	0.871536	0.671716	0.007106
1838.3	0.532183	0.533544	0.001361	0.255674	0.371551	0.003662
1833.3	0.520215	0.518401	-0.001814	-0.348754	-0.697024	0.002603
1822.7	0.498685	0.495910	-0.002775	-0.556503	-1.521566	0.001824
1808.6	0.474275	0.473835	-0.000440	-0.092811	-0.310460	0.001418
1785.9	0.444532	0.446337	0.001805	0.405995	1.616822	0.001116
1782.5	0.442464	0.442735	0.000271	0.061191	0.249232	0.001086
1767.9	0.428393	0.428331	-0.000062	-0.014394	-0.062819	0.000982
1755.3	0.415787	0.417029	0.001242	0.298667	1.360465	0.000913
1737.5	0.402814	0.402432	-0.000382	-0.094798	-0.456177	0.000837
1714.3	0.384806	0.385277	0.000471	0.122367	0.617458	0.000763
1711.0	0.383726	0.382979	-0.000747	-0.194554	-0.990640	0.000754
1648.4	0.345260	0.344444	-0.000816	-0.236312	-1.298387	0.000628
1617.4	0.327688	0.328096	0.000408	0.124520	0.695498	0.000587
1612.5	0.326355	0.325642	-0.000713	-0.218418	-1.227115	0.000581
1515.4	0.282883	0.282747	-0.000136	-0.048177	-0.274979	0.000496
1514.0	0.281956	0.282195	0.000239	0.084841	0.483560	0.000495
1408.8	0.244433	0.244790	0.000357	0.146133	0.810797	0.000441
1398.5	0.241289	0.241496	0.000207	0.085734	0.473904	0.000437
1394.2	0.239531	0.240137	0.000606	0.253094	1.394026	0.000435
1312.7	0.216631	0.216055	-0.000576	-0.266071	-1.409704	0.000409
1213.2	0.190566	0.190191	-0.000375	-0.196848	-0.970471	0.000387
1211.4	0.189569	0.189753	0.000184	0.096855	0.475414	0.000386
1124.2	0.170029	0.169575	-0.000454	-0.266785	-1.218446	0.000372
1044.0	0.152075	0.152596	0.000521	0.342300	1.435910	0.000363
1014.7	0.146688	0.146713	0.000025	0.016831	0.068674	0.000359
921.6	0.129018	0.129003	-0.000015	-0.011684	-0.042908	0.000351
815.8	0.110485	0.110454	-0.000031	-0.028291	-0.090877	0.000344
717.2	0.094411	0.094458	0.000047	0.050110	0.139823	0.000338
615.5	0.079606	0.079100	-0.000506	-0.635440	-1.516555	0.000334
503.7	0.062893	0.063375	0.000482	0.766909	1.464585	0.000329
409.4	0.050720	0.050881	0.000161	0.318007	0.493617	0.000327
316.7	0.038971	0.039066	0.000095	0.243055	0.291115	0.000325
222.5	0.027820	0.027215	-0.000605	2.175026	-1.858576	0.000326
128.4	0.014776	0.015066	0.000290	1.962190	0.883605	0.000328
*1768.1	0.689887					
*508.4	0.062249					

* These data points were not included in the final regressions because they contained weighted deviations of greater than 2.5.

TABLE III

COMPARISON OF EXPERIMENTAL AND CALCULATED PHASE COMPOSITIONS FOR CO_2 + N-DECANE AT 344.3 K (160 °F)

PRESSURE psia	MOLE FRACTION CO_2 Exp.	Calc.	ERROR IN CALCULATED MOLE FRACTION Mol. Frac.	% Dev.	Wt.Dev.	WEIGHTING FACTOR Mol. Frac.
			----------LIQUID PHASE----------			
1837.5	0.9067	0.9063	-0.000392	-0.043189	-0.226615	0.001728
1833.4	0.8986	0.9003	0.001748	0.194504	1.252633	0.001395
1822.4	0.8897	0.8882	-0.001476	-0.165903	-1.354251	0.001090
1809.3	0.8767	0.8766	-0.000068	-0.007805	-0.071231	0.000961
1783.1	0.8568	0.8571	0.000299	0.034866	0.350898	0.000851
1768.1	0.8461	0.8471	0.001002	0.118402	1.226266	0.000817
1737.4	0.8297	0.8282	-0.001444	-0.174057	-1.874292	0.000771
1712.0	0.8129	0.8138	0.000920	0.113130	1.234608	0.000745
1649.0	0.7811	0.7809	-0.000175	-0.022400	-0.248063	0.000705
1616.3	0.7652	0.7650	-0.000229	-0.029954	-0.330974	0.000693
1514.9	0.7185	0.7183	-0.000188	-0.026153	-0.280496	0.000670
1399.2	0.6673	0.6677	0.000408	0.061090	0.617086	0.000661
1312.7	0.6300	0.6305	0.000493	0.078304	0.748422	0.000659
1206.7	0.5856	0.5849	-0.000711	-0.121374	-1.076085	0.000661
1124.2	0.5490	0.5491	0.000140	0.025573	0.211789	0.000663
1014.6	0.5016	0.5011	-0.000502	-0.100071	-0.752405	0.000667
921.3	0.4593	0.4596	0.000294	0.063942	0.437382	0.000671
815.3	0.4115	0.4116	0.000144	0.034895	0.212028	0.000677
717.2	0.3657	0.3664	0.000689	0.188473	1.008332	0.000684
615.2	0.3188	0.3183	-0.000515	-0.161646	-0.745408	0.000691
503.7	0.2648	0.2643	-0.000537	-0.202832	-0.765735	0.000701
409.0	0.2168	0.2170	0.000232	0.106872	0.325785	0.000711
316.0	0.1690	0.1693	0.000323	0.191362	0.448169	0.000722
222.5	0.1201	0.1200	-0.000116	-0.096203	-0.157783	0.000732
129.1	0.0694	0.0694	-0.000029	-0.042416	-0.039663	0.000742

TABLE III (Continued)

PRESSURE psia	MOLE FRACTION CO_2 Exp.	Calc.	ERROR IN CALCULATED MOLE FRACTION Mol. Frac.	% Dev.	Wt.Dev.	WEIGHTING FACTOR Mol. Frac.
			-----VAPOR PHASE-----			
1841.7	0.9524	0.9528	0.000364	0.038264	0.157550	0.002313
1839.8	0.9572	0.9561	-0.001084	-0.113257	-0.722352	0.001501
1832.4	0.9628	0.9628	0.000033	0.003385	0.040529	0.000804
1823.1	0.9672	0.9674	0.000189	0.019507	0.297054	0.000635
1808.3	0.9722	0.9720	-0.000200	-0.020596	-0.357277	0.000560
1795.7	0.9745	0.9748	0.000301	0.030919	0.560888	0.000537
1709.4	0.9851	0.9848	-0.000302	-0.030690	-0.598891	0.000505
1607.5	0.9894	0.9895	0.000082	0.008284	0.163642	0.000501
1500.4	0.9915	0.9917	0.000216	0.021814	0.432385	0.000500
1313.6	0.9938	0.9937	-0.000130	-0.013111	-0.260567	0.000500
1211.6	0.9946	0.9944	-0.000157	-0.015767	-0.313610	0.000500
1043.9	0.9948	0.9954	0.000635	0.063832	1.269944	0.000500
1041.8	0.9959	0.9954	-0.000456	-0.045756	-0.911336	0.000500
667.8	0.9952	0.9951	-0.000055	-0.005526	-0.109988	0.000500
508.5	0.9941	0.9941	0.000021	0.002088	0.041511	0.000500
*1824.7	0.9636					

* This data point was not included in the final regressions because it contained a weighted deviation of greater than 2.5.

TABLE IV

COMPARISON OF EXPERIMENTAL AND CALCULATED IFT/DENSITY DIFFERENCE RATIOS FOR CO_2 + N-DECANE AT 344.3 K (160 °F)

PRESSURE psia	$\gamma/\Delta\rho$ (mN/m)/(g/cm^3) Exp.	Calc.	ERROR IN CALCULATED $\gamma/\Delta\rho$ (mN/m)/(g/cm^3)	% Dev.	Wt.Dev.	WEIGHTING FACTOR (mN/m)/(g/cm^3)
129.5	26.418	26.712	0.293583	1.111286	0.572776	0.512561
222.7	25.323	25.336	0.013268	0.052394	0.027003	0.491355
316.2	23.984	23.960	-0.024312	-0.101367	-0.051739	0.469892
409.1	22.353	22.592	0.239164	1.069926	0.533444	0.448339
503.8	21.375	21.198	-0.177204	-0.829015	-0.415887	0.426086
615.5	19.487	19.549	0.062270	0.319545	0.155909	0.399396
717.5	18.452	18.037	-0.414976	-2.248950	-1.108019	0.374521
815.6	16.517	16.574	0.056928	0.344667	0.162626	0.350053
921.5	15.402	14.980	-0.421268	-2.735189	-1.304544	0.322924
1014.7	13.624	13.564	-0.060433	-0.443565	-0.202578	0.298318
1124.2	11.800	11.878	0.077964	0.660726	0.290522	0.268358
1206.6	10.639	10.590	-0.049206	-0.462491	-0.200908	0.244919
1312.9	8.697	8.901	0.204332	2.349455	0.957939	0.213304
1398.5	7.421	7.515	0.093871	1.264916	0.503398	0.186474
1514.8	5.446	5.588	0.142762	2.621657	0.967737	0.147522
1617.3	3.780	3.845	0.065444	1.731331	0.594753	0.110036
1649.0	3.296	3.298	0.002518	0.076418	0.025786	0.097669
1712.7	2.235	2.189	-0.045833	-2.050897	-0.641770	0.071417
1737.4	1.718	1.757	0.038992	2.269348	0.642839	0.060656
1768.0	1.284	1.224	-0.060583	-4.716811	-1.293833	0.046824
1783.6	1.015	0.9541	-0.060359	-5.949648	-1.525347	0.039571
1810.4	0.4884	0.5000	0.011623	2.379784	0.431243	0.026952
1822.0	0.3034	0.3109	0.007545	2.486712	0.349521	0.021586
1820.4	0.3330	0.3366	0.003571	1.072409	0.160027	0.022316
1824.6	0.2598	0.2697	0.009904	3.812040	0.485279	0.020408
*1831.4	0.1230					
*1835.3	0.04234					

* These data points were not included in the final regressions because they contained weighted deviations of greater than 2.5.

Compositions (x, y), mole fraction:	±0.003
Densities (ρ^L, ρ^V), g/cm^3:	±0.001
Interfacial Tensions (γ), mN/m:	$\pm 0.04\gamma^{0.8}$
Pressure (P), psi:	±2.0
Temperature (T), °F:	±0.1

The experimental phase densities, phase compositions, and $\gamma/\Delta\rho$ values are shown in Figures 10-12, respectively. The $\gamma/\Delta\rho$ values are plotted as a function of "scaled" pressure, $P^*=(P_c-P)/P_c$, since (a) this expands the near-critical low interfacial tension region and (b) "scaling laws" require this relationship to be linear as the critical point is approached with a universal value for the slope of $2\upsilon-\beta=0.935$ (25). The two data sets in Figure 12 are plotted using the optimum critical point pressure for each data set separately (1844 psia for the current work and 1848 psia for that of Nagarajan (7)). The following relationship for $\gamma/\Delta\rho$ as a function of pressure has been used for the near-critical region:

$$\frac{\gamma}{\Delta\rho} = A(P^*)^{2\nu-\beta} \qquad (15)$$

where A is a constant for the specific system of interest and υ and β are system-independent universal scaling exponents. The commonly accepted values for υ and β are $\upsilon=0.63$ and $\beta=0.325$ (26).

Functions for Smoothing Experimental Phase Behavior Data

For convenience of operation, each experimental measurement (x, y, ρ^L, ρ^V, $\gamma/\Delta\rho$) is obtained at a slightly different pressure. This procedure eliminates the need for adjustments of pressure between each

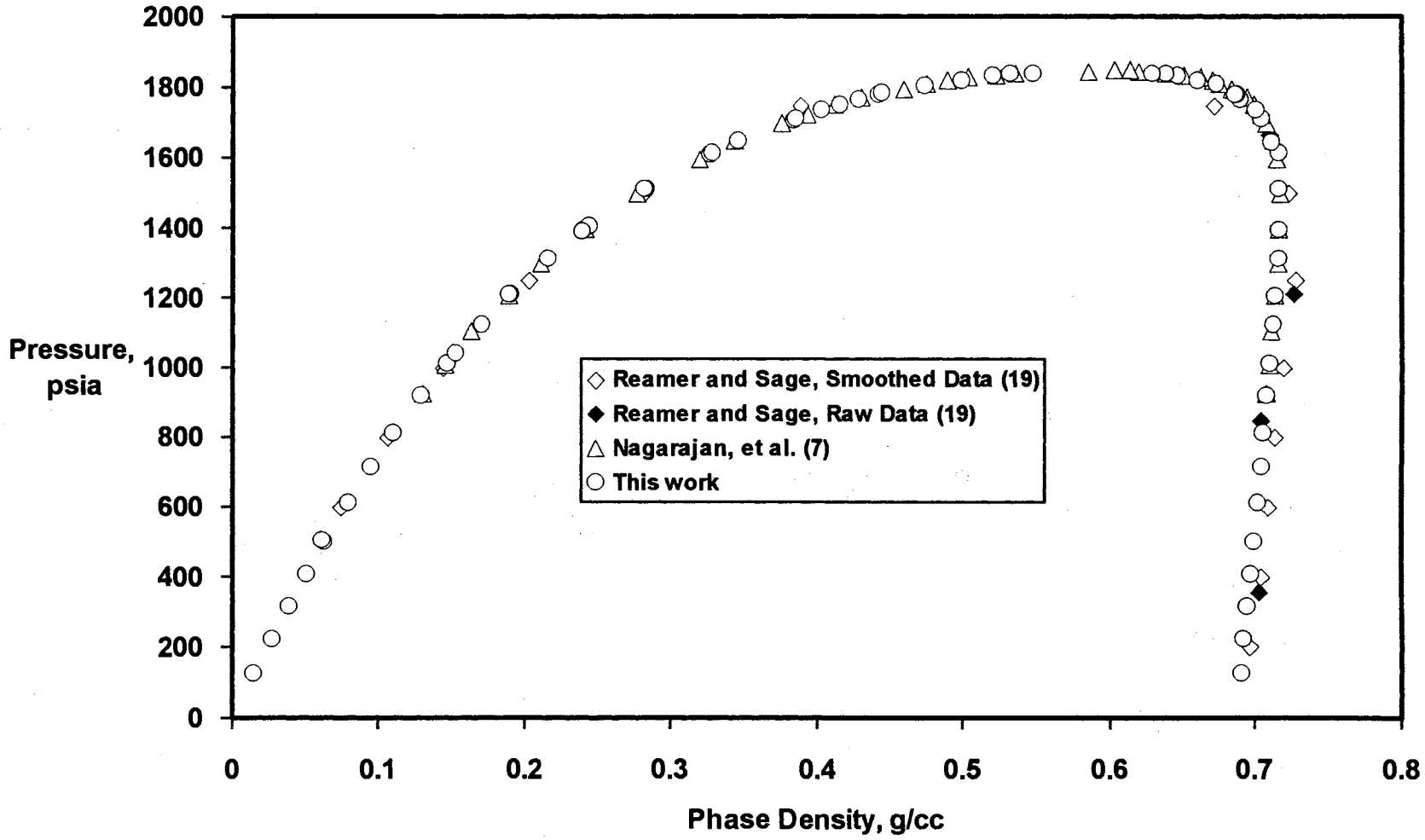

Figure 10. Phase Density Data for CO_2 + n-Decane at 344.3 K (160 °F)

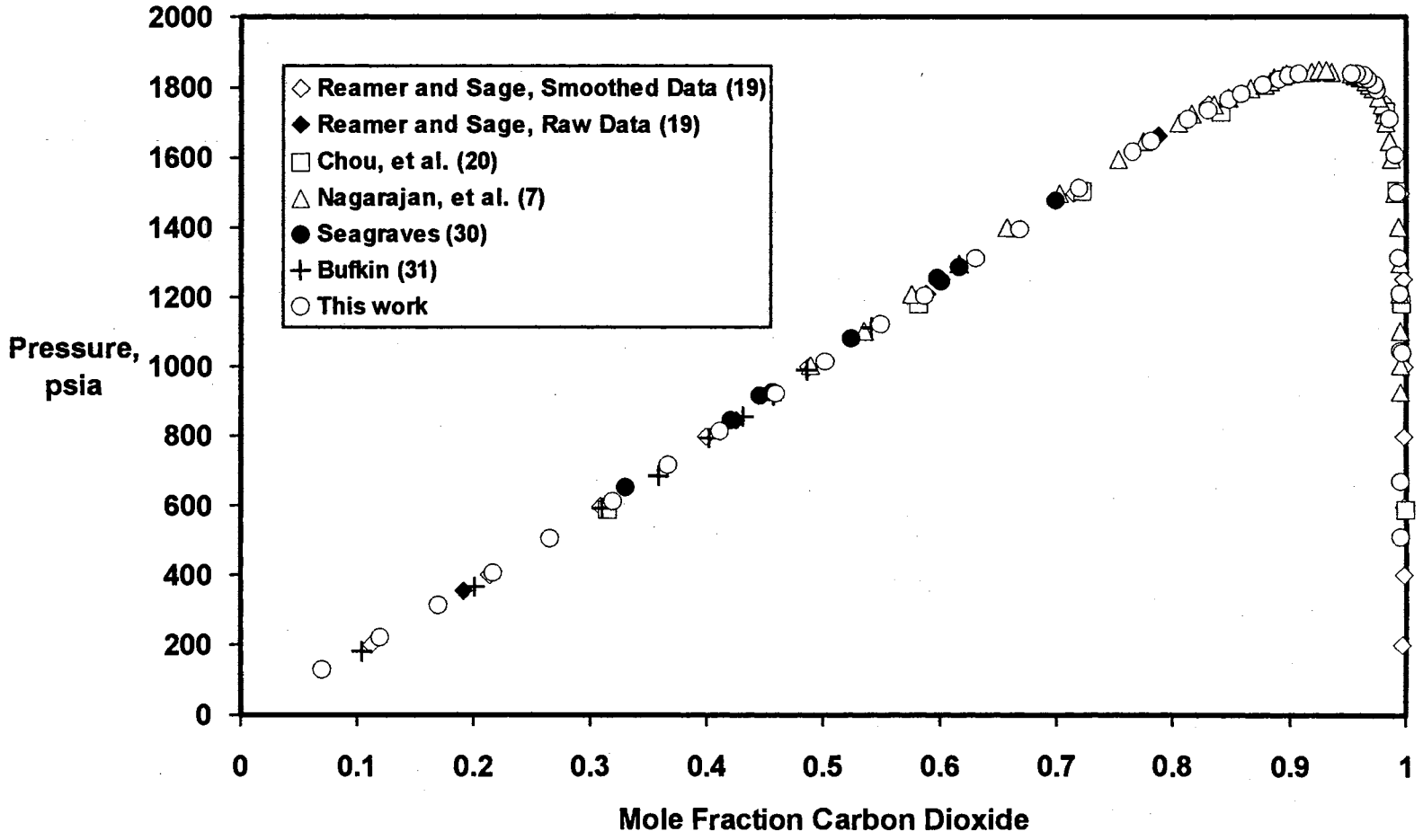

Figure 11. Phase Composition Data for CO_2 + n-Decane at 344.3 K (160 °F)

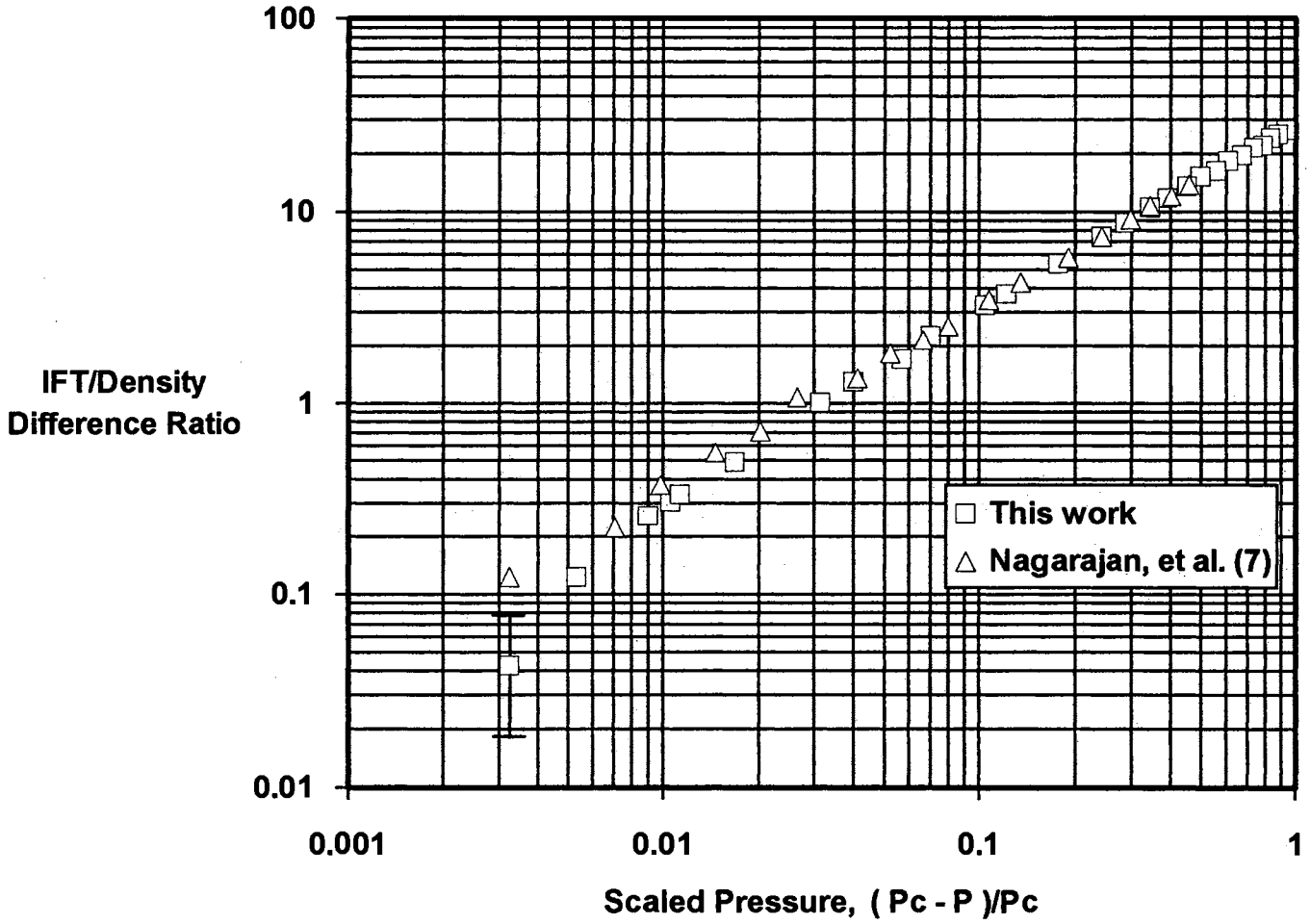

Figure 12. Pendant Drop IFT Data for CO_2 + n-Decane at 344.3 K (160 °F)

measurement. However, the resultant data are not in an optimum form for the final users of the data. Therefore, smoothing functions have been used for the interpolation and extrapolation of the experimental results. To be useful, these functions should (a) represent the experimental data within the expected uncertainties and (b) obey known scaling law behavior in the near-critical region. The following procedures have been described previously and have been used several times (5,8,11).

Wichterle, et al. (27) and Charoensombut-amon (28) used functions of the type shown below to represent the difference in values of an "order parameter, ϕ," in two equilibrium phases (denoted by "+" and "-"):

$$\phi_+ - \phi_- = \sum_{i=0}^{N} B_i (P^*)^{\beta+i\Delta} \tag{16}$$

where the leading term (i=0) is the limiting "scaling (or power) law" exponent of the order parameter, ϕ, and the subsequent terms in the summation are the Wegner (29) corrections to scaling behavior.

When the above relation is combined with the "rectilinear diameter" equation of the form

$$\frac{(\phi_+ - \phi_-)}{2} = \phi_c + A_0 (P^*)^{1-\alpha} + \sum_{j=1}^{M} A_j (P^*)^j \tag{17}$$

then the following expressions can be obtained for ϕ_+ and ϕ_-

$$\phi_\pm = \phi_c + A_0 (P^*)^{1-\alpha} + \sum_{j=1}^{M} A_j (P^*)^j \pm \frac{1}{2} \sum_{i=0}^{N} B_i (P^*)^{\beta+i\Delta} \tag{18}$$

where ϕ_+ and ϕ_- represent properties of vapor and liquid phases. One of the advantages of the above equation is that the exponents α, β and Δ are universal constants, independent of the fluid of interest.

Charoensombut-amon used Equation (18) to fit isothermal P-x,y data for CO_2 + n-hexadecane using $\alpha=1/8$, $\beta=1/3$, and $\Delta=1/2$ for the scaling exponents with M=3 and N=6 for a total of 12 constants (including z_c). Following the work of Gasem, et al. (8) and Dulcamara (5), Equation (18) has been used to represent the P vs ρ^L,ρ^V and P vs x,y behavior with

$$\text{for } P\text{-}\rho^L,\rho^V \; : \; \phi_c = \rho_c,\ \phi_+ = \rho^L,\ \phi_- = \rho^V,\ M=6,\ N=6$$

$$\text{for } P\text{-}x,y \; : \; \phi_c = z_c,\ \phi_+ = y,\ \phi_- = x,\ M=6,\ N=6$$

The values of $\gamma/\Delta\rho$ (which are the quantities determined from the measurements of the pendant drop digitized images) are expressed as:

$$\frac{\gamma}{\Delta\rho} = \sum_{k=0}^{L} G_i (P^*)^{2\nu-\beta+k\Delta} \tag{19}$$

with L=2 (only two correction terms).

Smoothed Experimental Data

Tables II, III, and IV document the ability of Equations (18) and (19) to fit the experimental data. The parameters obtained from the data regressions are shown in Table V. The results are based on weighted regressions of the data in which the sum of squares of weighted residuals was minimized:

$$SS = \sum_{i=1}^{K} \left[\frac{\left(Y_{calc} - Y_{exp}\right)}{\sigma_Y} \right]_i^2 = \sum_{i=1}^{K} \left(\frac{\Delta Y}{\sigma_Y} \right)_i^2 \tag{20}$$

TABLE V

PARAMETERS USED TO GENERATE SMOOTHED PROPERTIES FOR CARBON DIOXIDE + N-DECANE AT 344.3 K (160 °F)

PHASE DENSITIES
Units: $(kg/m^3)x10^{-3}$ or g/cm^3

P_c	1844.000
ρ_c	0.5874844
AR_0	-0.3709024
AR_1	-0.1358517
AR_2	0.6708606
AR_3	-0.5529693
AR_4	-0.2357940
AR_5	0.7372108
AR_6	-0.3588569
BR_0	0.6623708
BR_1	0.8146192
BR_2	-1.685781
BR_3	0.07663496
BR_4	3.102426
BR_5	-3.543098
BR_6	1.261702

PHASE COMPOSITIONS
Units: Mole Fraction CO_2

P_c	1844.000
z_c	0.9348942
AZ_0	-0.2214591
AZ_1	-0.2115755
AZ_2	0.3659545
AZ_3	-1.103288
AZ_4	1.619049
AZ_5	-1.378501
AZ_6	0.4996235
BZ_0	0.3643833
BZ_1	-0.6525278
BZ_2	6.626090
BZ_3	-20.33164
BZ_4	33.16005
BZ_5	-26.52762
BZ_6	8.375429

IFT/DENSITY DIFFERENCE RATIO
Units: $[(mN/m)/(kg/m^3)]x10^{-3}$ or $[(mN/m)/(g/cm^3)]$

P_c	1844.000
G_0	150.7520
G_1	-145.4775
G_2	23.35589

where K is the number of experimental observations and

$$\sigma_Y^2 = \varepsilon_Y^2 + \left(\frac{\partial Y}{\partial P}\right)^2 \varepsilon_P^2 \qquad (21)$$

Y represents the compositions (x,y), densities (ρ^L,ρ^V) or IFT/density difference ratio ($\gamma/\Delta\rho$). The experimental uncertainties, ε, were taken to be the following in the regressions:

$$\varepsilon_x = \varepsilon_y = 0.0005$$

$$\varepsilon_\rho^L = \varepsilon_\rho^V = 0.0003 \text{ g/cm}^3$$

$$\varepsilon_{\gamma/\Delta\rho} = 0.04(\gamma/\Delta\rho)^{0.8}$$

$$\varepsilon_P = 1.0 \text{ psi}$$

Note that the above are measures of precision, rather than accuracy, of these measurements. As discussed earlier, the estimated inaccuracies are generally larger than these estimates of precision. Smoothed phase equilibria and interfacial tension data appear in Table VI. The regression procedure for obtaining the parameters in Table V was as follows. First, regressions were performed with all of the measured data points included and the results were analyzed. Next, any data point with a weighted deviation, $\Delta Y/\sigma_Y$, larger than 2.5 was discarded and the regressions were repeated. Weighted regressions were performed for phase densities, phase compositions and interfacial tensions at several values of the critical pressure, P_c. The optimum critical pressure was then chosen as the one that resulted in the minimum overall weighted root-mean-square error for all properties considered. Thus,

TABLE VI

SMOOTHED PHASE EQUILIBRIA AND INTERFACIAL TENSION DATA FOR CARBON DIOXIDE + N-DECANE AT 344.3 K (160 °F)

Pressure kPa	Pressure psia	Phase Compositions Mole Fraction CO_2 Liquid	Phase Compositions Mole Fraction CO_2 Vapor	Phase Densities (g/cm^3) Liquid	Phase Densities (g/cm^3) Vapor	Interfacial Tension mN/m
1379	200	0.1079	*	0.6923	0.0244	17.148
2068	300	0.1610	*	0.6946	0.0370	15.913
2758	400	0.2125	*	0.6966	0.0497	14.703
3447	500	0.2624	0.9941	0.6987	0.0629	13.515
4137	600	0.3110	0.9947	0.7009	0.0769	12.343
4826	700	0.3584	0.9953	0.7032	0.0918	11.187
5516	800	0.4046	0.9957	0.7054	0.1078	10.044
6205	900	0.4500	0.9958	0.7077	0.1251	8.917
6895	1000	0.4946	0.9956	0.7098	0.1438	7.804
7584	1100	0.5386	0.9952	0.7117	0.1643	6.707
8274	1200	0.5820	0.9945	0.7135	0.1870	5.630
8963	1300	0.6250	0.9938	0.7150	0.2126	4.576
9653	1400	0.6681	0.9929	0.7160	0.2420	3.551
10342	1500	0.7117	0.9917	0.7161	0.2768	2.564
11032	1600	0.7572	0.9897	0.7139	0.3195	1.634
11721	1700	0.8073	0.9854	0.7062	0.3755	0.797
12066	1750	0.8358	0.9813	0.6971	0.4125	0.437
12411	1800	0.8693	0.9739	0.6784	0.4626	0.146
12479	1810	0.8772	0.9716	0.6721	0.4758	0.099
12548	1820	0.8859	0.9685	0.6638	0.4912	0.059
12617	1830	0.8962	0.9642	0.6521	0.5105	0.026
12631	1832	0.8986	0.9631	0.6491	0.5151	0.021
12645	1834	0.9011	0.9618	0.6456	0.5202	0.016
12659	1836	0.9040	0.9602	0.6415	0.5259	(0.011)
12673	1838	0.9072	0.9583	0.6367	0.5325	(0.007)
12686	1840	0.9110	0.9558	(0.6306)	0.5404	(0.004)
12700	1842	(0.9162)**	0.9521	(0.6217)	0.5511	(0.001)
12714***	1844	(0.9349)	(0.9349)	(0.5875)	(0.5875)	(0.000)

* No vapor phase compositions were obtained below 500 psia so smoothed values are not extrapolated below this pressure.

** Numbers in parentheses are extrapolations beyond the highest measured pressures.

*** Estimated critical point (visual observations gave 1845 psia for the critical pressure).

the obtained critical pressure is the best estimate based on all experimental data simultaneously. The optimum critical pressure thus obtained (1844.0 psia) is in good agreement with visual observations of the equilibrium cell (1845 psia). This procedure resulted in the removal of five data points: two vapor densities (at 1768.1 psia and 508.4 psia), one vapor composition (at 1824.7 psia) and two $\gamma/\Delta\rho$ values (at 1831.4 and 1835.3 psia) as indicated in Tables II, III and IV. An estimated error bar is included on the highest pressure $\gamma/\Delta\rho$ point shown in Figure 12 to illustrate the large uncertainties in measured interfacial tensions near the critical point. Figures 13-15 show the weighted deviations of the final regressions for phase density, composition and interfacial tension data, respectively.

Comparison of Experimental Data

Several sources of previous experimental data exist for CO_2 + n-decane at 160 °F (7,19,20). This system was studied here to evaluate the abilities of the new automation systems discussed in Chapter III and to extend the range of previous data collected at Oklahoma State University (7). All data sources are included in Figures 10-12. However, the scale of these figures does not allow for detailed comparison of the data sets. Therefore, all data sets were fitted simultaneously to the smoothing functions described previously. Deviation plots showing the relative differences among the data sets are included in Figures 16-20 and the parameters obtained from regression of all available data are shown in Table VII. The data of Figures 16-20 are shown plotted against scaled pressure, $P^*=(P_c-P)/P_c$, where the critical pressure used is that determined as the optimum pressure to fit

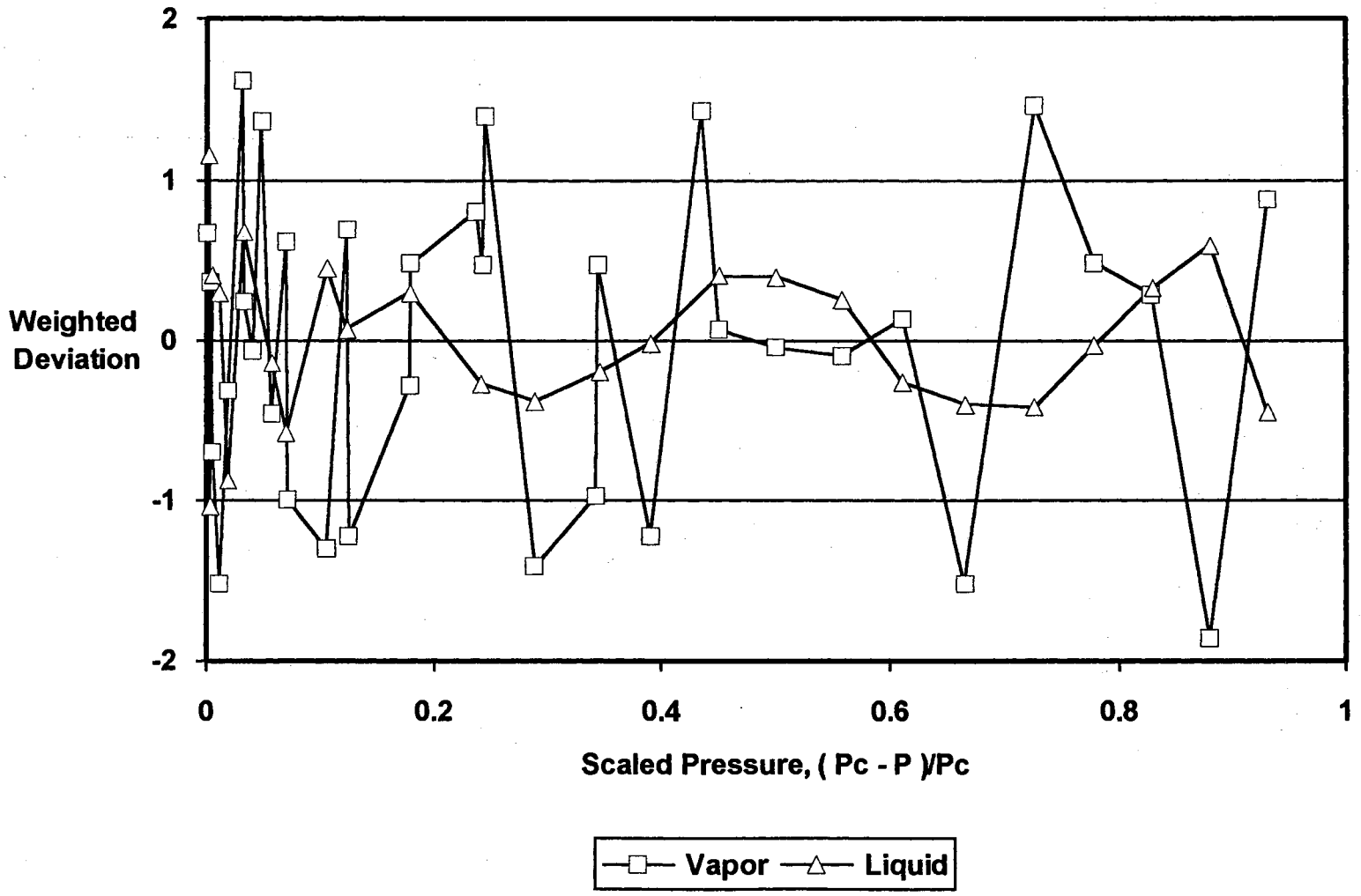

Figure 13. Extended Power Law Fit to Density Data for CO_2 + n-Decane at 344.3 K (160 °F)

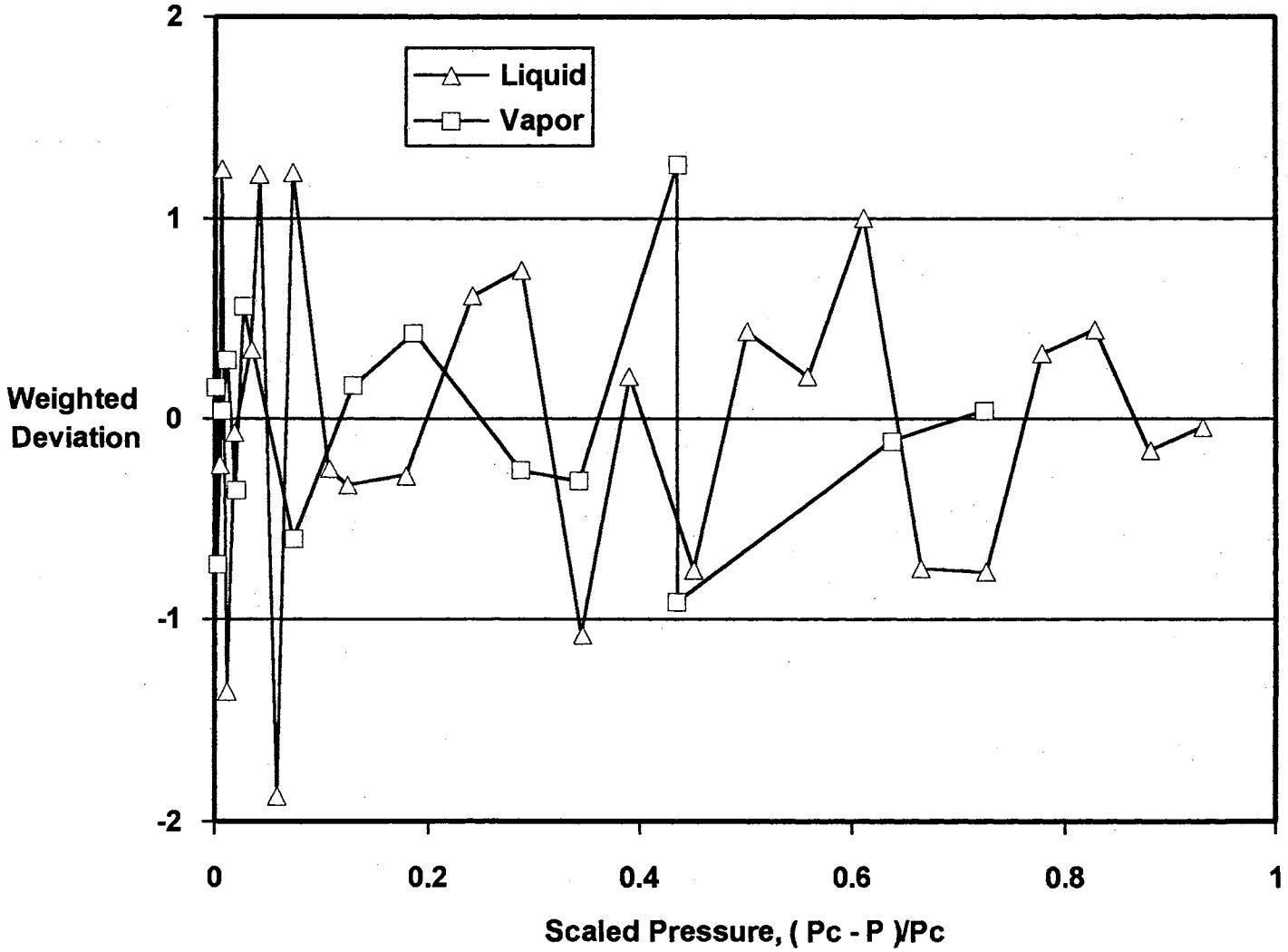

Figure 14. Extended Power Law Fit to Composition Data for CO_2 + n-Decane at 344.3 K (160 °F)

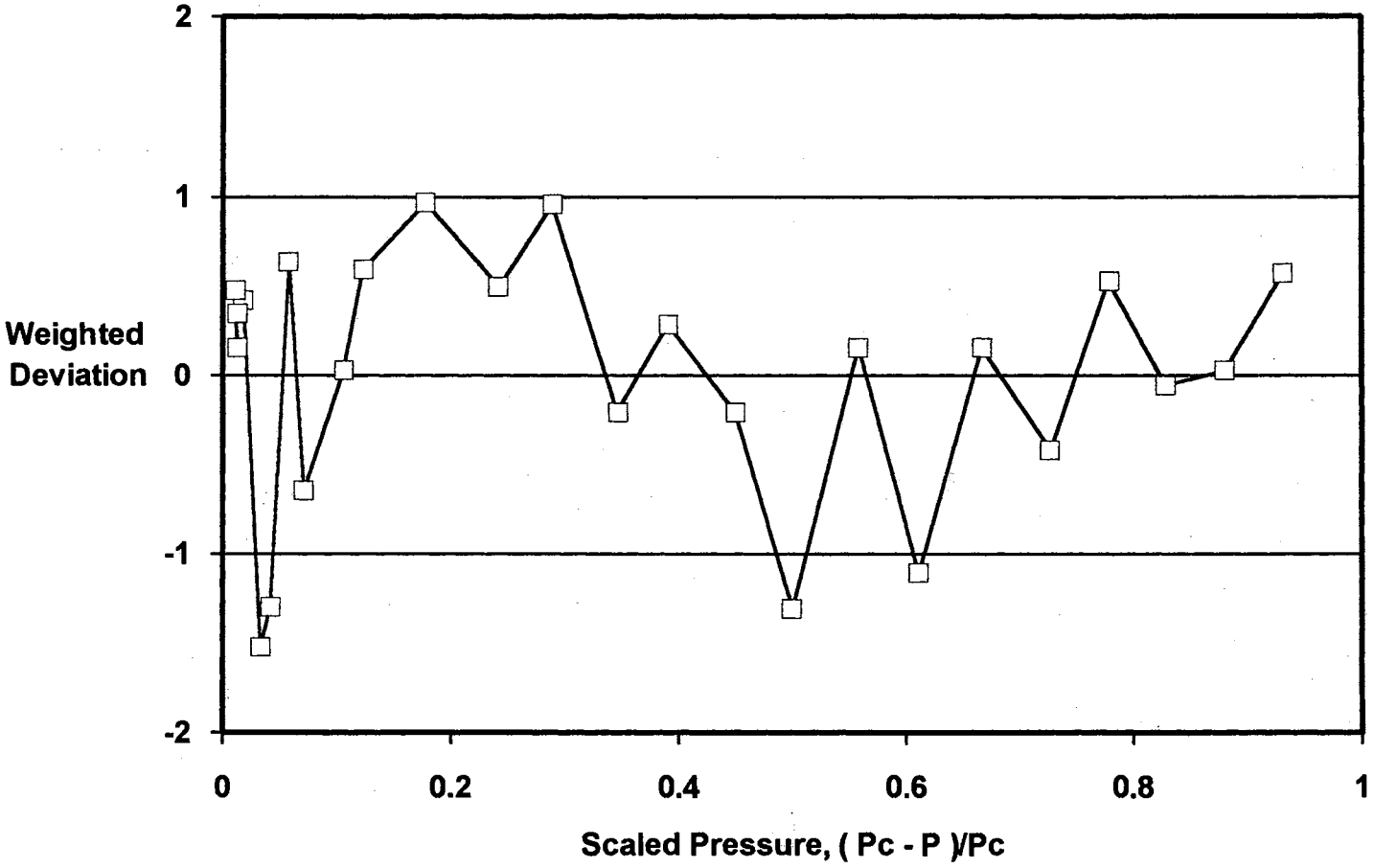

Figure 15. Extended Power Law Fit to Pendant Drop IFT Data for CO_2 + n-Decane at 344.3 K (160 °F)

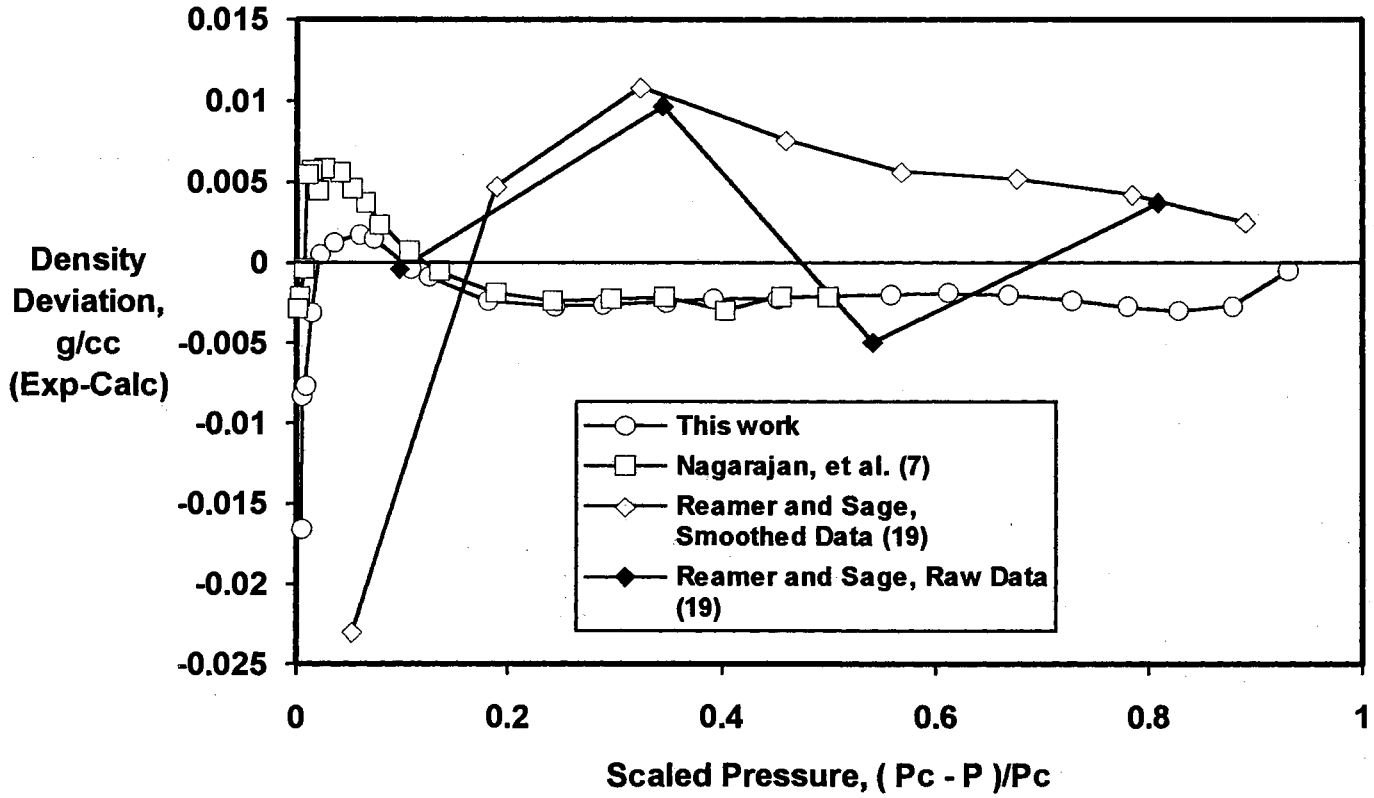

Figure 16. Deviations of Liquid Density Data from Extended Power Law Fit for all Data Sets of CO_2 + n-Decane at 344.3 K (160 °F)

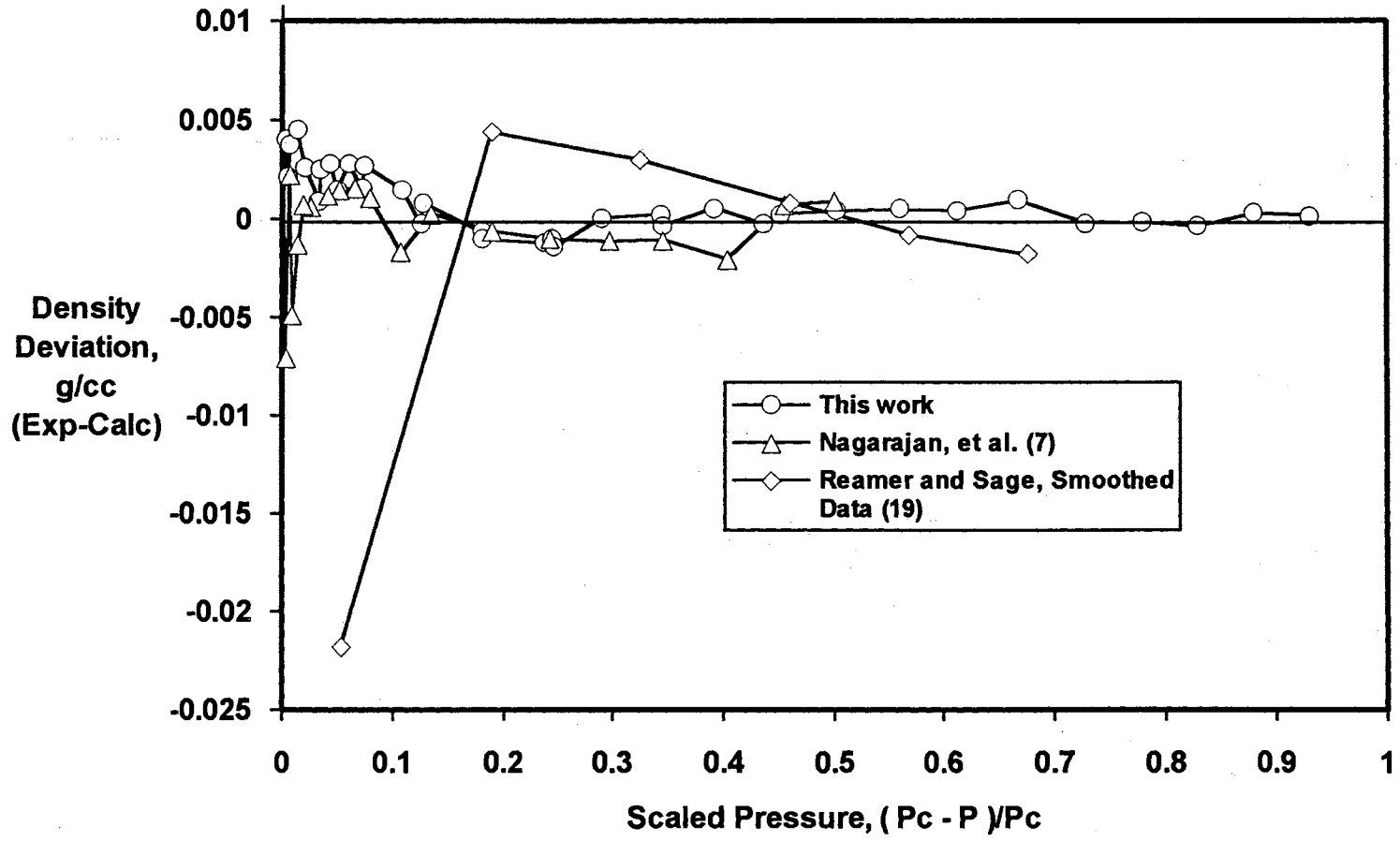

Figure 17. Deviations of Vapor Density Data from Extended Power Law Fit for all Data Sets of CO_2 + n-Decane at 344.3 K (160 °F)

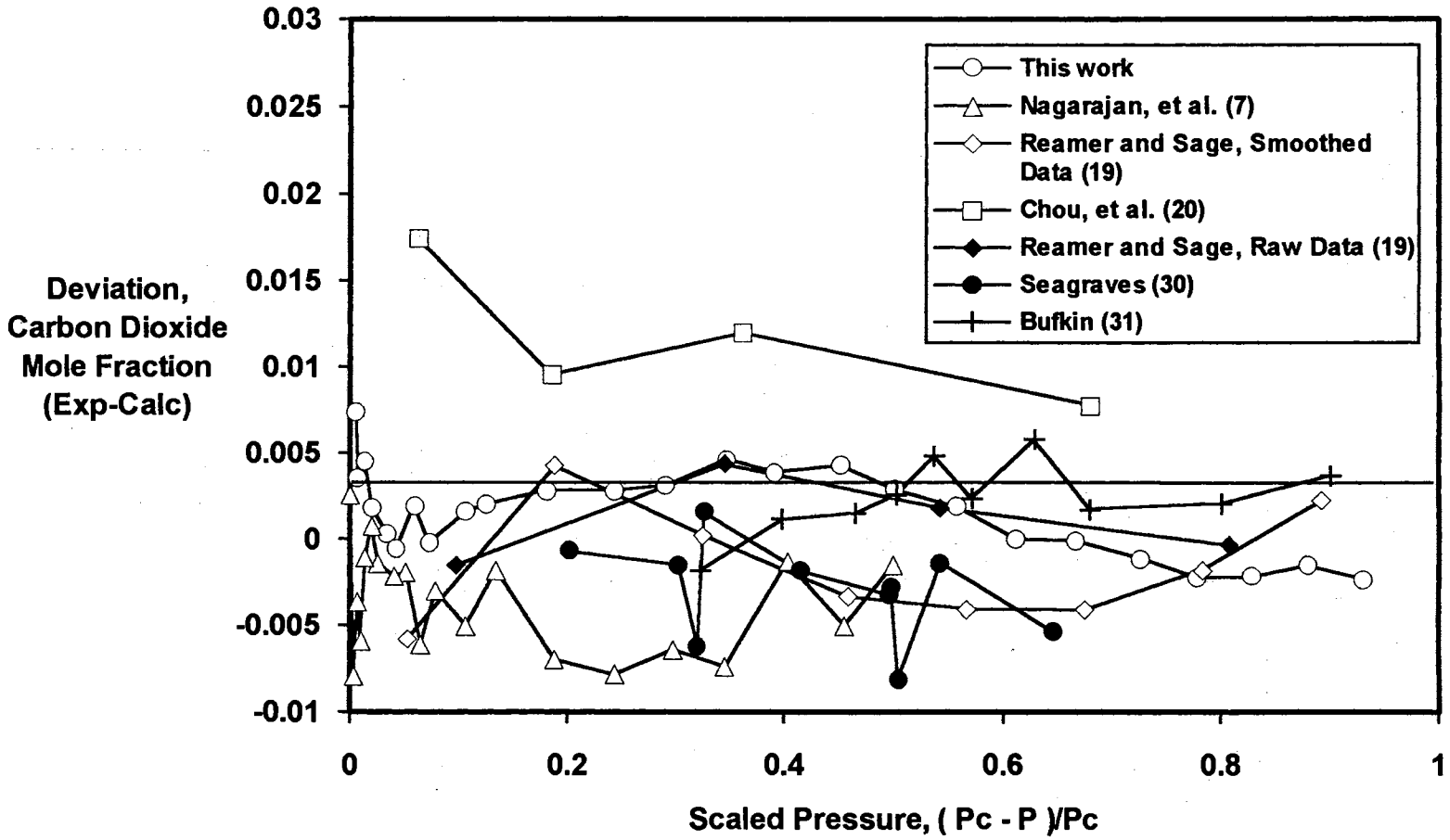

Figure 18. Deviations of Liquid Composition Data from Extended Power Law Fit for all Data Sets of CO_2 + n-Decane at 344.3 K (160 °F)

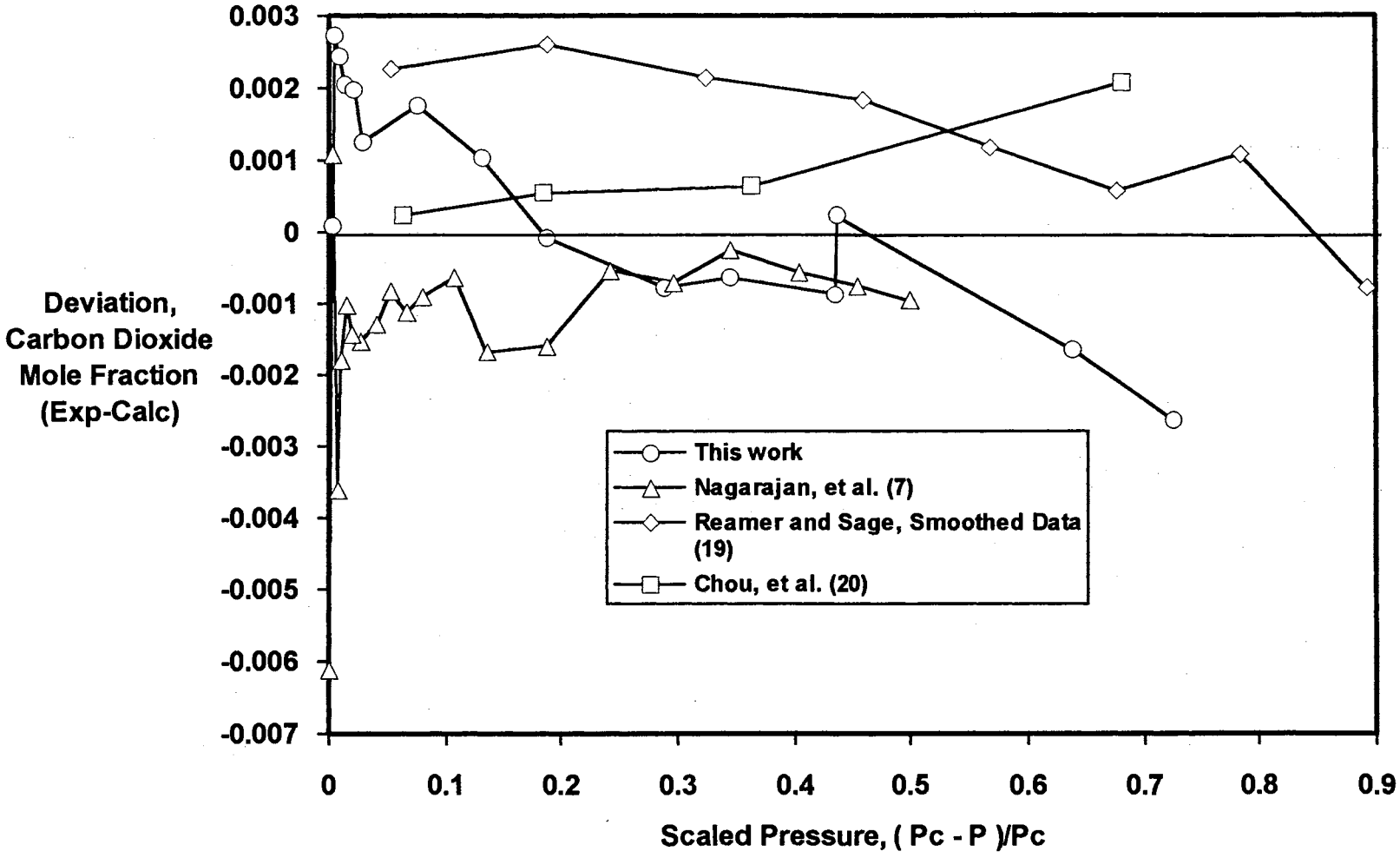

Figure 19. Deviations of Vapor Composition Data from Extended Power Law Fit for all Data Sets of CO_2 + n-Decane at 344.3 K (160 °F)

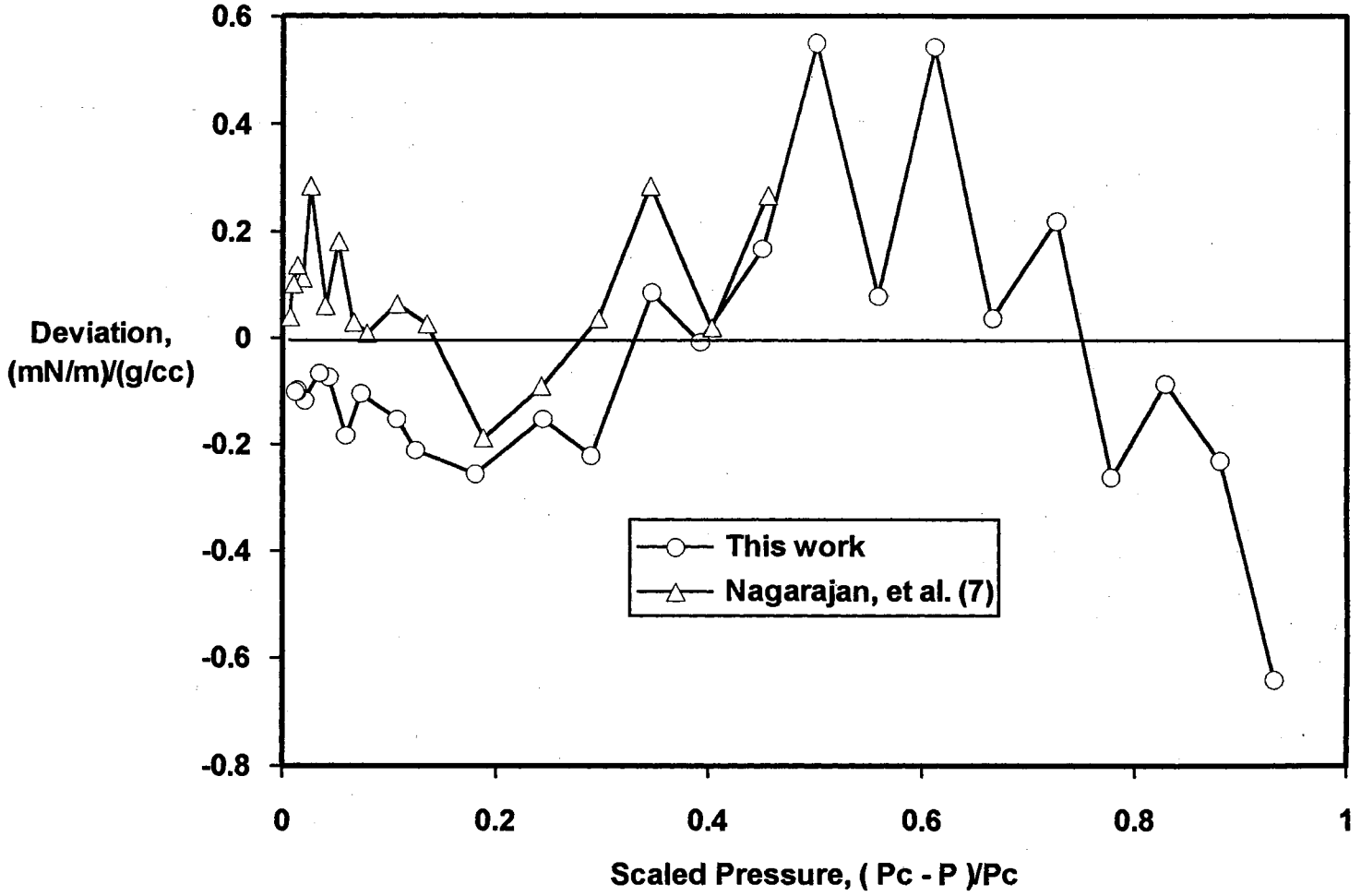

Figure 20. Deviations of Interfacial Tension Data from Extended Power Law Fit for all Data Sets of CO_2 + n-Decane at 344.3 K (160 °F)

all available equilibrium data simultaneously (1848 psia). Therefore, deviations shown near the critical point (at scaled pressures near zero) are exaggerated due to the different critical points of each individual data set. Figures 16 and 17 indicate excellent agreement between the phase densities measured in this work and those of Nagarajan, et al. (7). However, fairly large disagreement exists between these two data sets and that of Reamer and Sage (19). In general, the data of this work show lower liquid densities than that of Reamer and Sage at low pressures and higher densities near the critical point. The raw data of Reamer and Sage is included as an illustration of the spread in their experimental densities and as a contrast to their smoothed values. The observed critical pressure of the current work (1844 psia, 0.5875 g/cm^3) is in fair agreement with that of Nagarajan, et al. (7) (1848 psia, 0.5905 g/cm^3) but in disagreement with that reported by Reamer and Sage (1860 psia, 0.5122 g/cm^3). Two of their four experimental points shown in Figure 16 agree with the data of this work within 0.003 g/cm^3 while one data point (that at 1212 psia) disagrees by 0.012 g/cm^3. The vapor phase densities of this work and of Nagarajan are in excellent agreement as seen in Figure 17. Again, the data of Reamer and Sage is in disagreement near the critical point.

Figure 18 shows the deviation plot for liquid compositions of each data set included. In general, all data except that of Chou, et al. (20) agree to within 0.005 mole fraction CO_2 over the entire pressure range. Figure 19 indicates that the vapor phase compositions of this work are in good agreement with those of Nagarajan at lower pressures but differ by as much as 0.006 mole fraction CO_2 near the critical point. This can be attributed to the different observed critical

compositions for the two data sets (93.5% CO_2 for this work and 93.0% for Nagarajan, et al.). The data of both Reamer and Sage (19) and Chou, et al. (20) indicate higher vapor phase CO_2 mole fractions, differing by about 0.002.

Figure 20 indicates excellent agreement between the measured interfacial tensions of this work and those of Nagarajan, et al. (7). The previous work (7) measured interfacial tensions from a pressure of 1007 psia to the critical point. Therefore, the data of this work represent an extension of this data set down to a pressure of 130 psia and confirm the proper operation of the new digital video system for measurement of interfacial tensions using the pendant drop technique.

The regressed parameters given in Table VII were used to generate a smoothed data set based on all available data. This smoothed data is reported in Table VIII. This smoothed data set is now recommended as a comparison data set for the testing of new experimental apparatuses and procedures.

TABLE VII

PARAMETERS USED TO GENERATE SMOOTHED PROPERTIES FOR CARBON DIOXIDE + N-DECANE AT 344.3 K (160 °F) USING ALL AVAILABLE DATA

PHASE DENSITIES

Units: $(kg/m^3)x10^{-3}$ or g/cm^3

P_c	1848.000
ρ_c	0.5987550
AR_0	-2.462109
AR_1	2.795426
AR_2	-2.415809
AR_3	5.866611
AR_4	-8.679905
AR_5	6.804801
AR_6	-2.172137
BR_0	0.5808748
BR_1	1.578154
BR_2	-5.005240
BR_3	8.273842
BR_4	-8.360204
BR_5	4.833250
BR_6	-1.213362

PHASE COMPOSITIONS

Units: Mole Fraction CO_2

P_c	1848.000
z_c	0.9278876
AZ_0	1.110967
AZ_1	-2.119115
AZ_2	2.896111
AZ_3	-7.837561
AZ_4	12.39457
AZ_5	-10.17778
AZ_6	3.313047
BZ_0	0.3181489
BZ_1	-0.2091521
BZ_2	4.099096
BZ_3	-12.04934
BZ_4	19.08963
BZ_5	-14.93768
BZ_6	4.694137

IFT/DENSITY DIFFERENCE RATIO

Units: $[(mN/m)/(kg/m^3)]x10^{-3}$ or $[(mN/m)/(g/cm^3)]$

P_c	1848.000
G_0	173.5083
G_1	-180.5647
G_2	36.25067

TABLE VIII

SMOOTHED PHASE EQUILIBRIA AND INTERFACIAL TENSION DATA
FOR CARBON DIOXIDE + N-DECANE AT 344.3 K (160 °F)
BASED ON ALL AVAILABLE DATA

Pressure		Phase Compositions Mole Fraction CO_2		Phase Densities (g/cm^3)		Interfacial Tension
kPa	psia	Liquid	Vapor	Liquid	Vapor	mN/m
1379	200	0.1096	0.9962	0.6944	0.0246	17.353
2068	300	0.1628	0.9956	0.6975	0.0373	16.057
2758	400	0.2145	0.9961	0.6994	0.0497	14.789
3447	500	0.2641	0.9967	0.7012	0.0626	13.550
4137	600	0.3118	0.9969	0.7031	0.0764	12.339
4826	700	0.3579	0.9968	0.7051	0.0913	11.157
5516	800	0.4028	0.9964	0.7073	0.1073	10.003
6205	900	0.4471	0.9960	0.7096	0.1247	8.874
6895	1000	0.4909	0.9958	0.7118	0.1435	7.769
7584	1100	0.5346	0.9956	0.7139	0.1641	6.688
8274	1200	0.5781	0.9953	0.7159	0.1871	5.630
8963	1300	0.6214	0.9947	0.7177	0.2130	4.596
9653	1400	0.6648	0.9935	0.7188	0.2428	3.590
10342	1500	0.7090	0.9916	0.7184	0.2776	2.617
11032	1600	0.7553	0.9886	0.7151	0.3196	1.693
11721	1700	0.8064	0.9840	0.7051	0.3738	0.849
12066	1750	0.8353	0.9799	0.6952	0.4099	0.479
12411	1800	0.8681	0.9723	0.6777	0.4601	0.172
12479	1810	0.8755	0.9697	0.6724	0.4736	0.122
12548	1820	0.8833	0.9664	0.6658	0.4894	0.077
12617	1830	0.8918	0.9618	0.6572	0.5088	0.040
12631	1832	0.8937	0.9606	0.6551	0.5133	0.033
12645	1834	0.8957	0.9593	0.6528	0.5182	0.027
12659	1836	0.8977	0.9579	0.6502	0.5234	(0.022)
12673	1838	0.8999	0.9562	0.6473	0.5292	(0.016)
12686	1840	0.9023	0.9543	0.6440	0.5356	(0.012)
12700	1842	0.9049	0.9519	0.6400	0.5429	(0.007)
12714	1844	0.9080	0.9489	0.6350	0.5517	(0.004)
12728	1846	0.9122	0.9446	0.6277	0.5633	(0.001)
12741**	1848	(0.9279)*	(0.9279)	(0.5988)	(0.5988)	(0.000)

* Numbers in parentheses are extrapolations beyond the highest pressure used in regression of the smoothing function coefficients.

** Estimated critical point.

Ethane + 1-Methylnaphthalene at 160 °F

Experimental Data

No experimental data for mixtures of ethane + 1-methylnaphthalene at or near 160 °F were located in the literature. Therefore, this data set represents an addition to the literature of previously unavailable data. The raw data for this system appear in Tables IX through XI. Table IX includes the phase density data, Table X contains the phase composition data and Table XI contains the pendant drop interfacial tension data for this system. The estimated accuracy of the data is the same as reported earlier for the CO_2 + n-decane system. The experimental phase densities, phase compositions and interfacial tensions are shown in Figures 21-23. Figure 21 also shows vapor densities for pure ethane calculated from an NBS (33) equation of state. Since the vapor phase is predominantly ethane at lower pressures, the pure ethane density data is included to illustrate that the observed curvature in the saturated vapor density line should be expected.

During the collection of data for this system, the O-rings in the interfacial tension cell failed three times when the system pressure reached about 2000 psia. Attempts to alleviate this pressure limitation through the use of composite O-rings consisting of teflon-encapsulated viton were unsuccessful. Consequently, pendant drop data were only collected up to a pressure of 2014 psia as indicated in Table XI.

Smoothed Experimental Data

The experimental data for this system were evaluated using the same smoothing functions described previously for the CO_2 + n-decane

TABLE IX

COMPARISON OF EXPERIMENTAL AND CALCULATED PHASE DENSITIES
FOR ETHANE + 1-METHYLNAPHTHALENE AT 344.3 K (160 °F)

PRESSURE psia	PHASE DENSITIES (g/cm^3) Exp.	Calc.	ERROR IN CALCULATED DENSITY g/cm^3	% Dev.	Wt. Dev.	WEIGHTING FACTOR g/cm^3
			LIQUID PHASE			
2276.7	0.616114	0.616499	0.000385	0.062501	0.367046	0.001049
2266.6	0.625136	0.625381	0.000245	0.039125	0.293405	0.000834
2255.6	0.633904	0.633091	-0.000813	-0.128294	-1.157628	0.000703
2215.5	0.652478	0.652882	0.000404	0.061916	0.815718	0.000495
2164.8	0.669395	0.669481	0.000086	0.012829	0.210012	0.000409
2108.7	0.683793	0.683285	-0.000508	-0.074360	-1.364166	0.000373
2062.5	0.692649	0.692867	0.000218	0.031513	0.609523	0.000358
2014.9	0.701521	0.701725	0.000204	0.029035	0.584269	0.000349
1959.8	0.710871	0.711064	0.000193	0.027094	0.564861	0.000341
1917.7	0.717810	0.717679	-0.000131	-0.018185	-0.387877	0.000337
1914.2	0.718620	0.718212	-0.000408	-0.056789	-1.213840	0.000336
1865.6	0.725213	0.725359	0.000146	0.020191	0.440785	0.000332
1864.1	0.725456	0.725573	0.000117	0.016164	0.353110	0.000332
1815.1	0.732278	0.732367	0.000089	0.012142	0.270228	0.000329
1810.1	0.733106	0.733041	-0.000065	-0.008853	-0.197402	0.000329
1762.0	0.739442	0.739378	-0.000064	-0.008605	-0.194790	0.000327
1605.3	0.758872	0.758887	0.000015	0.002036	0.047711	0.000324
1506.2	0.770923	0.770943	0.000020	0.002592	0.061712	0.000324
1413.7	0.782301	0.782281	-0.000020	-0.002588	-0.062398	0.000325
1225.6	0.807419	0.807422	0.000003	0.000346	0.008282	0.000337
*1013.6	0.841356					
820.6	0.872732					
819.6	0.872736					
623.6	0.901914					
410.5	0.930204					
212.3	0.954310					
221.4	0.953199					
105.2	0.966209					

TABLE IX (Continued)

PRESSURE psia	PHASE DENSITIES (g/cm^3) Exp.	Calc.	ERROR IN CALCULATED DENSITY g/cm^3	% Dev.	Wt. Dev.	WEIGHTING FACTOR g/cm^3
			VAPOR PHASE			
2285.2	0.531456	0.530825	-0.000631	-0.118801	-0.422906	0.001493
2275.7	0.519639	0.519447	-0.000192	-0.036860	-0.181707	0.001054
2268.7	0.511999	0.512977	0.000978	0.191031	1.084863	0.000902
2254.6	0.502740	0.502460	-0.000280	-0.055627	-0.385381	0.000726
2217.0	0.482873	0.482597	-0.000276	-0.057162	-0.523958	0.000527
2165.8	0.463755	0.463963	0.000208	0.044882	0.479556	0.000434
2062.5	0.436236	0.436189	-0.000047	-0.010850	-0.122695	0.000386
2015.4	0.424974	0.425025	0.000051	0.011946	0.133745	0.000380
1960.8	0.412562	0.412515	-0.000047	-0.011364	-0.124771	0.000376
1914.7	0.402218	0.402164	-0.000054	-0.013431	-0.144510	0.000374
1910.7	0.401327	0.401272	-0.000055	-0.013647	-0.146559	0.000374
1866.1	0.391220	0.391378	0.000158	0.040319	0.423276	0.000373
1865.6	0.391447	0.391267	-0.000180	-0.045931	-0.482481	0.000373
1861.1	0.390443	0.390273	-0.000170	-0.043621	-0.457120	0.000373
1816.1	0.380207	0.380341	0.000134	0.035261	0.359953	0.000372
1812.6	0.379172	0.379568	0.000396	0.104559	1.064384	0.000372
1760.5	0.368153	0.368020	-0.000133	-0.036108	-0.355600	0.000374
1710.4	0.356781	0.356727	-0.000054	-0.015220	-0.144020	0.000377
1605.8	0.332010	0.331747	-0.000263	-0.079082	-0.669745	0.000392
1509.7	0.305541	0.305758	0.000217	0.071004	0.519028	0.000418
1507.2	0.304813	0.305029	0.000216	0.070804	0.515307	0.000419
1413.7	0.275782	0.275464	-0.000318	-0.115309	-0.699991	0.000454
1315.6	0.239417	0.239513	0.000096	0.040105	0.195341	0.000492
1225.6	0.203118	0.203394	0.000276	0.135699	0.545857	0.000505
1220.1	0.201433	0.201161	-0.000272	-0.134920	-0.538728	0.000504
*820.1	0.091904					
819.6	0.091494					
633.6	0.064345					
623.6	0.062529					
416.0	0.039529					
411.5	0.038798					
213.3	0.020907					
222.4	0.021977					
105.2	0.012302					

* Density data below 1200 psia were not included in the regressions of the extended power law equation. Below 1200 psia, only the raw data are reported here.

TABLE X

COMPARISON OF EXPERIMENTAL AND CALCULATED PHASE COMPOSITIONS FOR ETHANE + 1-METHYLNAPHTHALENE AT 344.3 K (160 °F)

PRESSURE psia	MOLE FRACTION ETHANE Exp.	Calc.	ERROR IN CALCULATED MOLE FRACTION Mol. Frac.	% Dev.	Wt.Dev.	WEIGHTING FACTOR Mol. Frac.
			LIQUID PHASE			
2285.2	0.7821	0.7852	0.003074	0.392983	1.445271	0.002127
2277.2	0.7707	0.7720	0.001250	0.162242	0.875805	0.001428
2267.1	0.7620	0.7609	-0.001099	-0.144203	-1.066651	0.001030
2255.6	0.7533	0.7522	-0.001107	-0.146903	-1.362643	0.000812
2216.0	0.7341	0.7347	0.000644	0.087685	1.080720	0.000596
2062.5	0.6948	0.6952	0.000363	0.052212	0.648362	0.000560
1960.3	0.6707	0.6698	-0.000874	-0.130332	-1.575458	0.000555
1914.7	0.6591	0.6591	0.000006	0.000846	0.010136	0.000550
1865.6	0.6483	0.6482	-0.000108	-0.016607	-0.197787	0.000544
1809.5	0.6370	0.6366	-0.000423	-0.066420	-0.786115	0.000538
1864.1	0.6486	0.6479	-0.000730	-0.112559	-1.341640	0.000544
1815.1	0.6366	0.6377	0.001096	0.172243	2.035177	0.000539
1761.5	0.6263	0.6273	0.001011	0.161345	1.892539	0.000534
1505.7	0.5828	0.5821	-0.000691	-0.118638	-1.296685	0.000533
1413.7	0.5639	0.5639	0.000047	0.008390	0.087144	0.000543
1315.6	0.5414	0.5414	-0.000026	-0.004739	-0.045894	0.000559
1225.6	0.5169	0.5171	0.000195	0.037715	0.337342	0.000578
820.6	0.3707	0.3709	0.000189	0.050903	0.293693	0.000642
623.6	0.2911	0.2909	-0.000222	-0.076246	-0.343337	0.000646
411.5	0.1969	0.1970	0.000076	0.038535	0.106208	0.000714
*1711.4	0.6158					

TABLE X (Continued)

PRESSURE psia	MOLE FRACTION ETHANE Exp.	Calc.	ERROR IN CALCULATED MOLE FRACTION Mol. Frac.	% Dev.	Wt.Dev.	WEIGHTING FACTOR Mol. Frac.
			-----VAPOR PHASE-----			
2285.2	0.8487	0.8475	-0.001230	-0.144875	-0.891595	0.001379
2276.2	0.8563	0.8568	0.000497	0.058019	0.502481	0.000989
2268.7	0.8626	0.8625	-0.000123	-0.014252	-0.146050	0.000842
2255.1	0.8701	0.8704	0.000281	0.032329	0.395513	0.000711
2217.0	0.8854	0.8856	0.000210	0.023752	0.350594	0.000600
2165.8	0.9009	0.9003	-0.000552	-0.061232	-0.982711	0.000561
2111.7	0.9128	0.9129	0.000059	0.006502	0.109461	0.000542
1912.7	0.9426	0.9434	0.000776	0.082287	1.514231	0.000512
1865.6	0.9484	0.9483	-0.000068	-0.007214	-0.134179	0.000510
1810.6	0.9537	0.9536	-0.000144	-0.015048	-0.282400	0.000508
1761.0	0.9582	0.9579	-0.000270	-0.028228	-0.533166	0.000507
1711.9	0.9624	0.9621	-0.000336	-0.034869	-0.662146	0.000507
1607.3	0.9709	0.9705	-0.000395	-0.040711	-0.780903	0.000506
1505.7	0.9779	0.9783	0.000356	0.036439	0.705142	0.000505
1413.7	0.9839	0.9846	0.000713	0.072499	1.415000	0.000504
1315.6	0.9902	0.9903	0.000060	0.006025	0.118725	0.000503
1013.6	0.9973	0.9977	0.000379	0.037979	0.757529	0.000500
1220.1	0.9950	0.9943	-0.000726	-0.072942	-1.448269	0.000501
820.1	0.9974	0.9971	-0.000318	-0.031922	-0.636764	0.000500
633.6	0.9975	0.9977	0.000199	0.019907	0.397064	0.000500
416.0	0.9976	0.9976	-0.000043	-0.004320	-0.085976	0.000501
*2014.9	0.9271					
*2062.0	0.9200					

* These data points were not included in the final regressions because they contained weighted deviations of greater than 2.5.

TABLE XI

COMPARISON OF EXPERIMENTAL AND CALCULATED IFT/DENSITY DIFFERENCE RATIOS FOR ETHANE + 1-METHYLNAPHTHALENE AT 344.3 K (160 °F)

PRESSURE psia	$\gamma/\Delta\rho$ (mN/m)/(g/cm^3) Exp.	Calc.	ERROR IN CALCULATED $\gamma/\Delta\rho$ (mN/m)/(g/cm^3)	% Dev.	Wt.Dev.	WEIGHTING FACTOR (mN/m)/(g/cm^3)
105.2	25.629	25.377	-0.251686	-0.982037	-0.511085	0.492455
622.5	14.184	13.975	-0.208681	-1.471223	-0.682688	0.305676
820.6	10.407	10.670	0.263317	2.530163	1.068797	0.246367
1413.7	3.8328	3.9524	0.119653	3.121828	1.074482	0.111359
1505.7	3.2034	3.2933	0.089938	2.807566	0.934514	0.096240
1604.8	2.6975	2.6826	-0.014922	-0.553173	-0.182695	0.081676
1713.9	2.1698	2.1174	-0.052414	-2.415634	-0.775450	0.067592
1761.0	1.9783	1.9048	-0.073515	-3.716073	-1.183689	0.062107
1815.0	1.7337	1.6810	-0.052679	-3.038534	-0.937353	0.056200
1864.1	1.5163	1.4949	-0.021402	-1.411459	-0.418272	0.051168
1917.7	1.3149	1.3074	-0.007548	-0.574038	-0.164192	0.045971
1960.3	1.1437	1.1678	0.024129	2.109762	0.574356	0.042011
2014.4	0.9484	0.9992	0.050765	5.352700	1.368285	0.037101
*1013.5	7.3429					

* This data point was not included in the final regressions because it contained a weighted deviation of greater than 2.5.

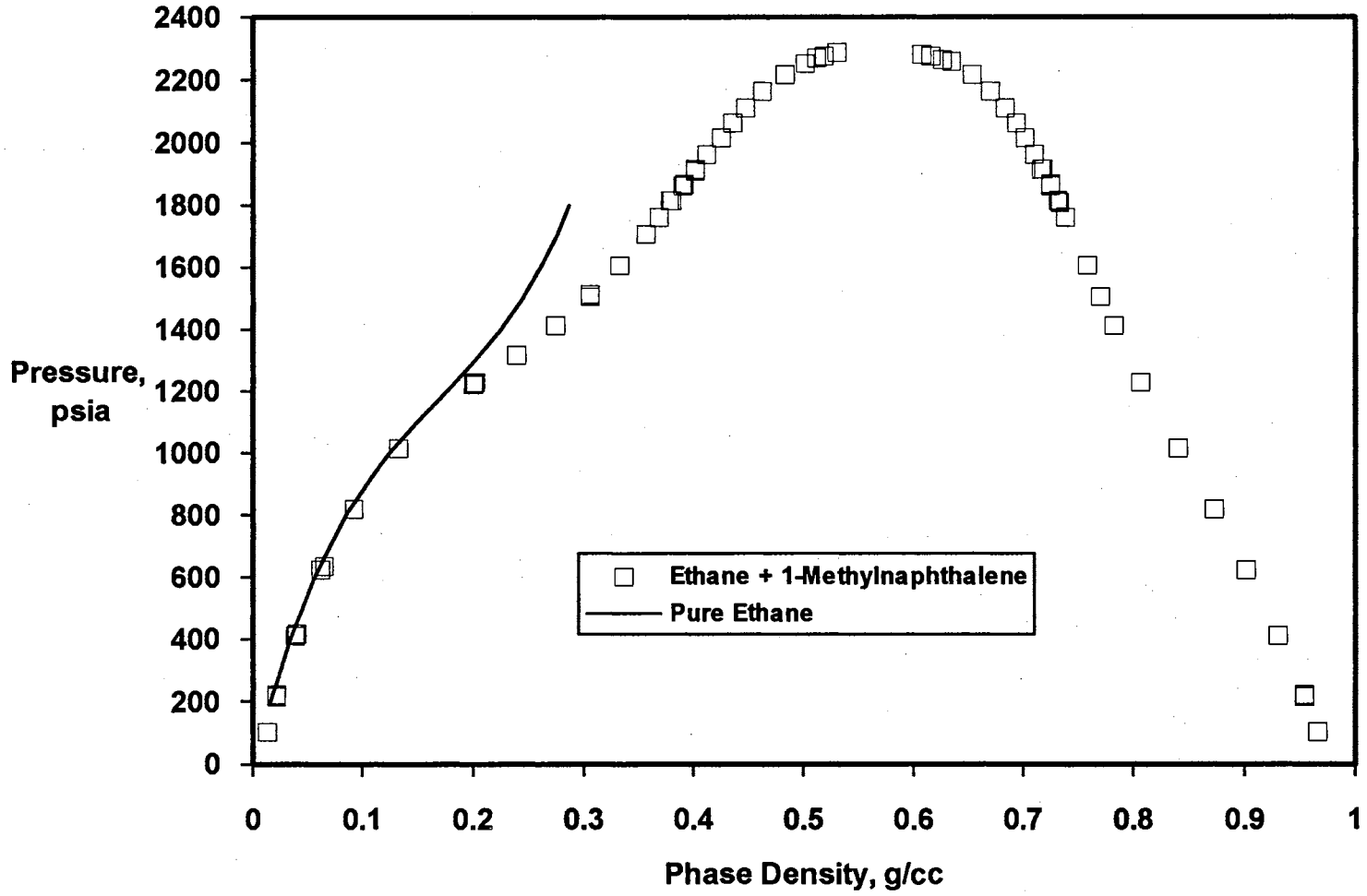

Figure 21. Phase Density Data for Ethane + 1-Methylnaphthalene at 344.3 K (160 °F)

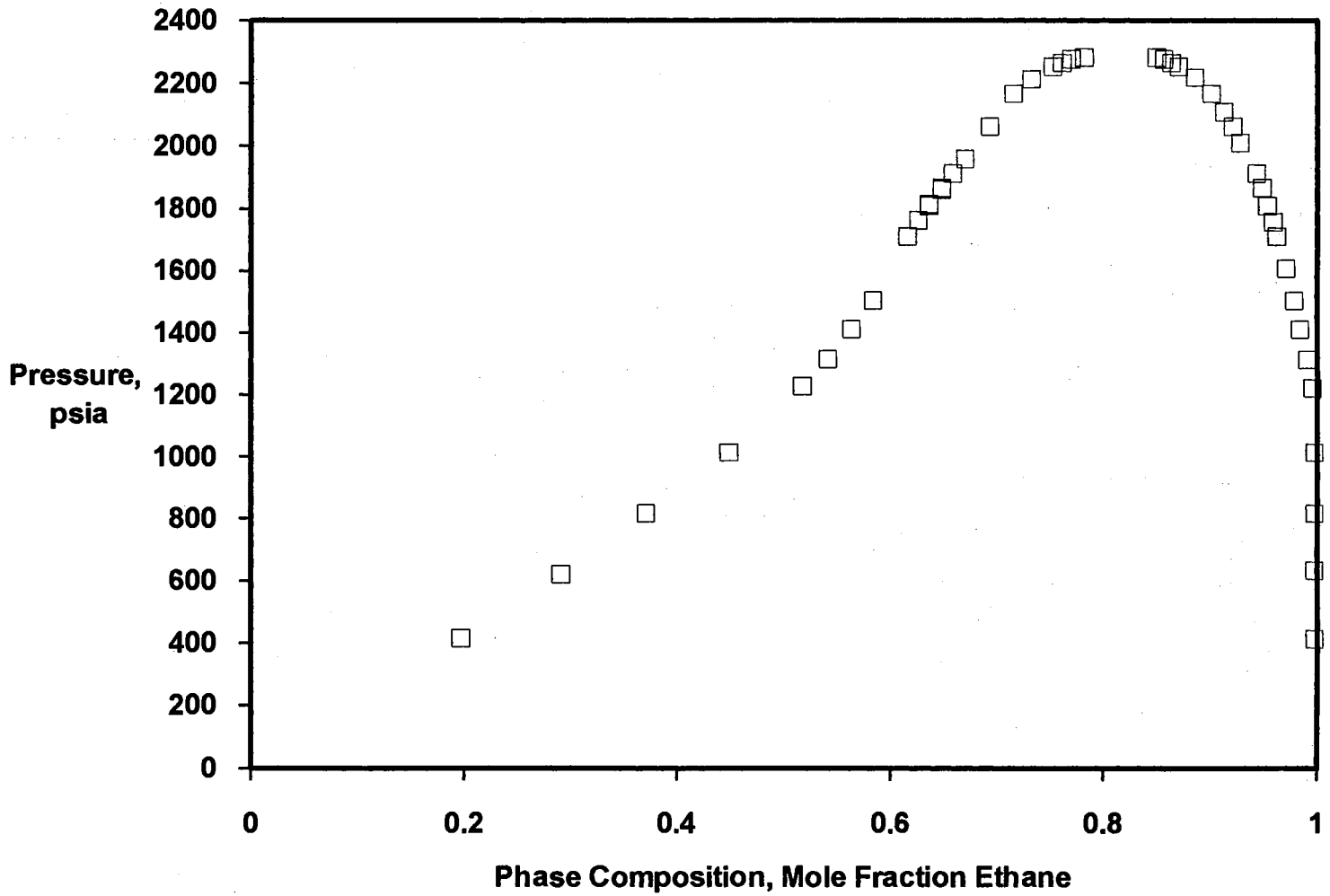

Figure 22. Phase Composition Data for Ethane + 1-Methylnaphthalene at 344.3 K (160 °F)

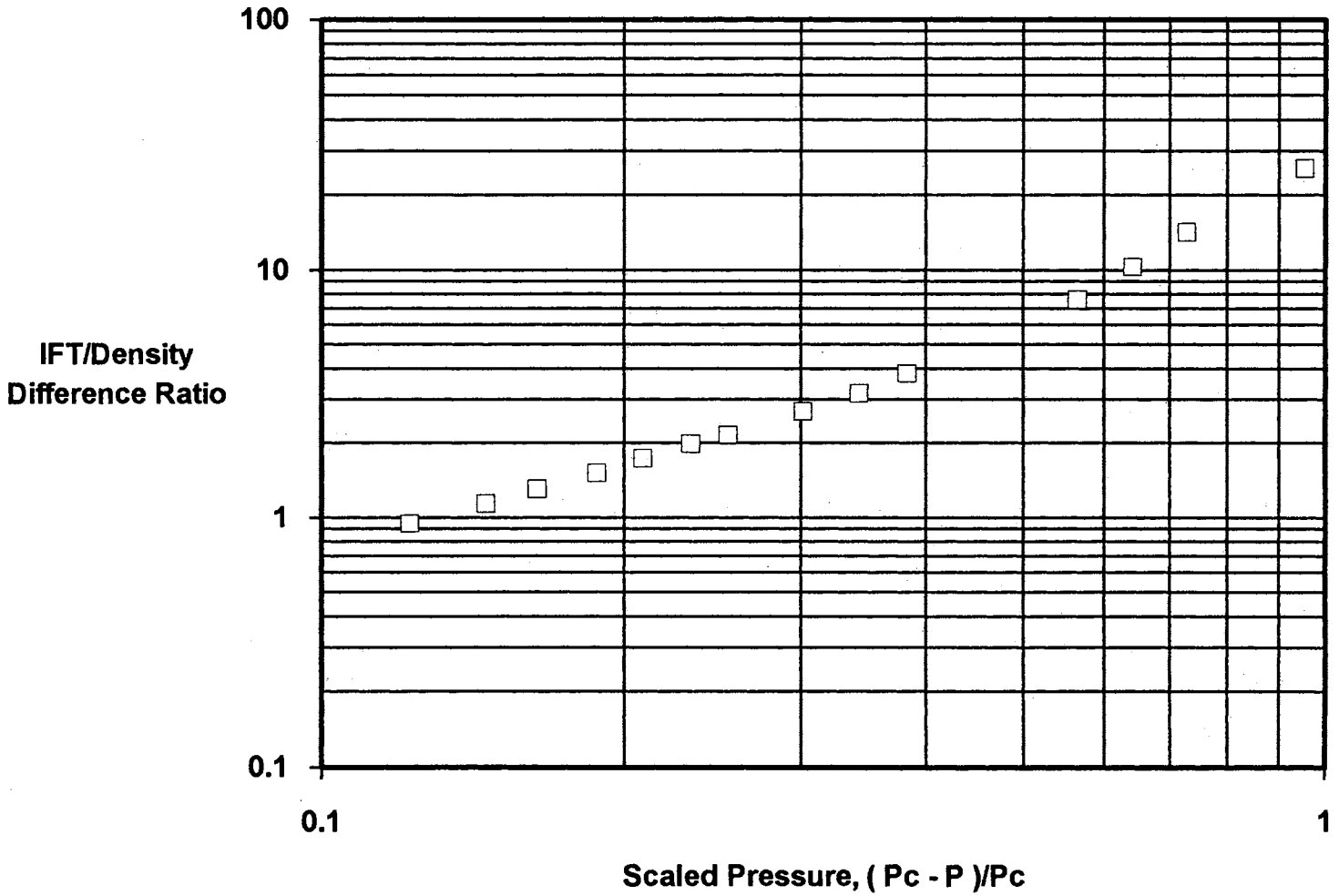

Figure 23. Pendant Drop IFT Data for Ethane + 1-Methylnaphthalene at 344.3 K (160 °F)

system. Equations (18) and (19) were used as smoothing functions with M=7 and N=7 of Equation (18) to account for the more demanding curvature of the phase density and composition lines. Due to difficulties in fitting phase densities over the entire pressure range, Equation (18) was fitted only to densities above a pressure of 1200 psia. This illustrates the problem of using the extended scaling equation (Equation (18)) for correlation of data with demanding curvature. The coefficients of Equation (18) are highly correlated and the parameters are not easily related to the physical properties of the compounds considered. This makes initial estimates difficult to obtain and results in inadequate regressions. Therefore, only the higher pressure density data were fitted to the smoothing function. The raw data below 1200 psia appear in Table IX.

Tables IX, X and XI document the ability of the extended power law equations to fit the experimental data considered. The parameters obtained from the data regressions are shown in Table XII. The results are based on the same weighted residual objective function reported earlier. As discussed earlier, any data points with weighted deviations of greater than 2.5 were discarded and the regressions were repeated. This procedure resulted in the removal of four experimental points: one liquid composition (at 1711.4 psia), two vapor compositions (at 2014.9 psia and at 2062.0 psia) and one interfacial tension measurement (at 1013.5 psia) as indicated in Tables IX through XI.

Weighted regressions were performed for phase densities, phase compositions and interfacial tensions at several values of the critical pressure, P_c. The optimum critical pressure was then chosen as the one that resulted in the minimum overall weighted root-mean-square error for

TABLE XII

PARAMETERS USED TO GENERATE SMOOTHED PROPERTIES
FOR ETHANE + 1-METHYLNAPHTHALENE
AT 344.3 K (160 °F)

PHASE DENSITIES
Units: $(kg/m^3)x10^{-3}$ or g/cm^3

P_c	2295.000
ρ_c	0.5687325
AR_0	0.0607289
AR_1	-0.1468330
AR_2	0.6470725
AR_3	-5.621772
AR_4	17.99530
AR_5	-17.38297
AR_6	-29.08099
AR_7	48.93671
BR_0	0.4484611
BR_1	-0.3631463
BR_2	15.73747
BR_3	-116.3427
BR_4	406.9592
BR_5	-747.3164
BR_6	697.5567
BR_7	-259.4943

PHASE COMPOSITIONS
Units: Mole Fraction Ethane

P_c	2295.000
z_c	0.8237590
AZ_0	-3.592932
AZ_1	5.409045
AZ_2	-10.53648
AZ_3	34.49362
AZ_4	-63.27367
AZ_5	54.53806
AZ_6	-14.63838
AZ_7	-2.957140
BZ_0	0.08061826
BZ_1	7.843290
BZ_2	-63.98587
BZ_3	265.8462
BZ_4	-601.7893
BZ_5	754.1407
BZ_6	-490.0994
BZ_7	129.0283

TABLE XII (Continued)

IFT/DENSITY DIFFERENCE RATIO Units: $[(mN/m)/(kg/m^3)]x10^{-3}$ or $[(mN/m)/(g/cm^3)]$	
P_c	2295.000
G_0	109.8250
G_1	-165.0155
G_2	83.39718

all properties considered. Thus, the regressed value of the critical pressure is an estimate based on all experimental data simultaneously. The optimum critical pressure thus obtained (2295.0 psia) is in good agreement with visual observations of the equilibrium cell (2291-2294 psia). Figures 24-26 show the weighted deviations of the final regressions for phase density, phase composition and interfacial tension data, respectively. Figures 24 and 25 indicate that the weighted deviations of density and composition data are well distributed and that the overall quality of fit of the extended power law equations is good for the range of data considered.

In order to provide data which is more convenient for future use, a smoothed data set based on the parameters given in Table XII is included in Table XIII.

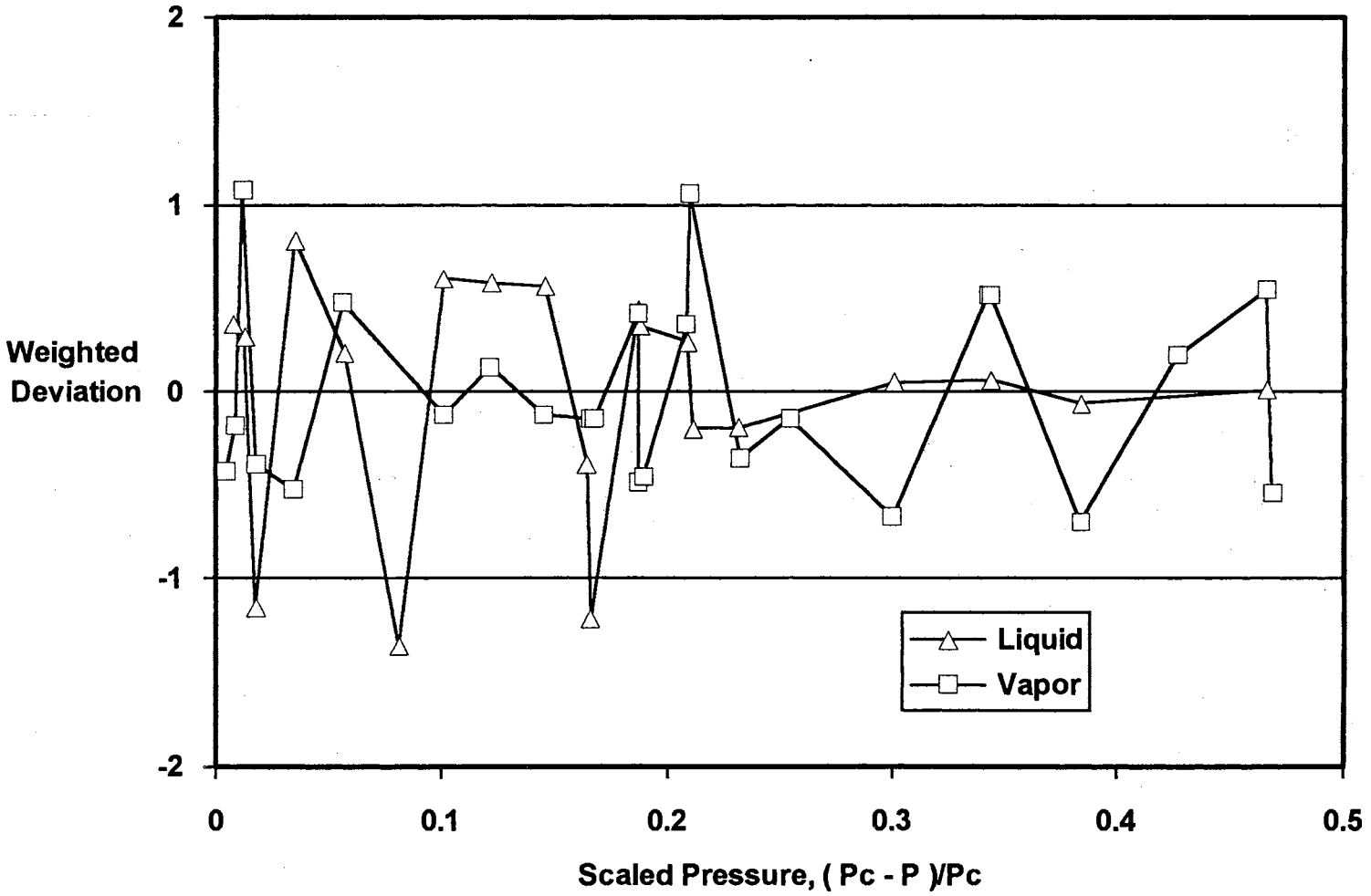

Figure 24. Extended Power Law Fit to Density Data for Ethane + 1-Methylnaphthalene at 344.3 K (160 °F)

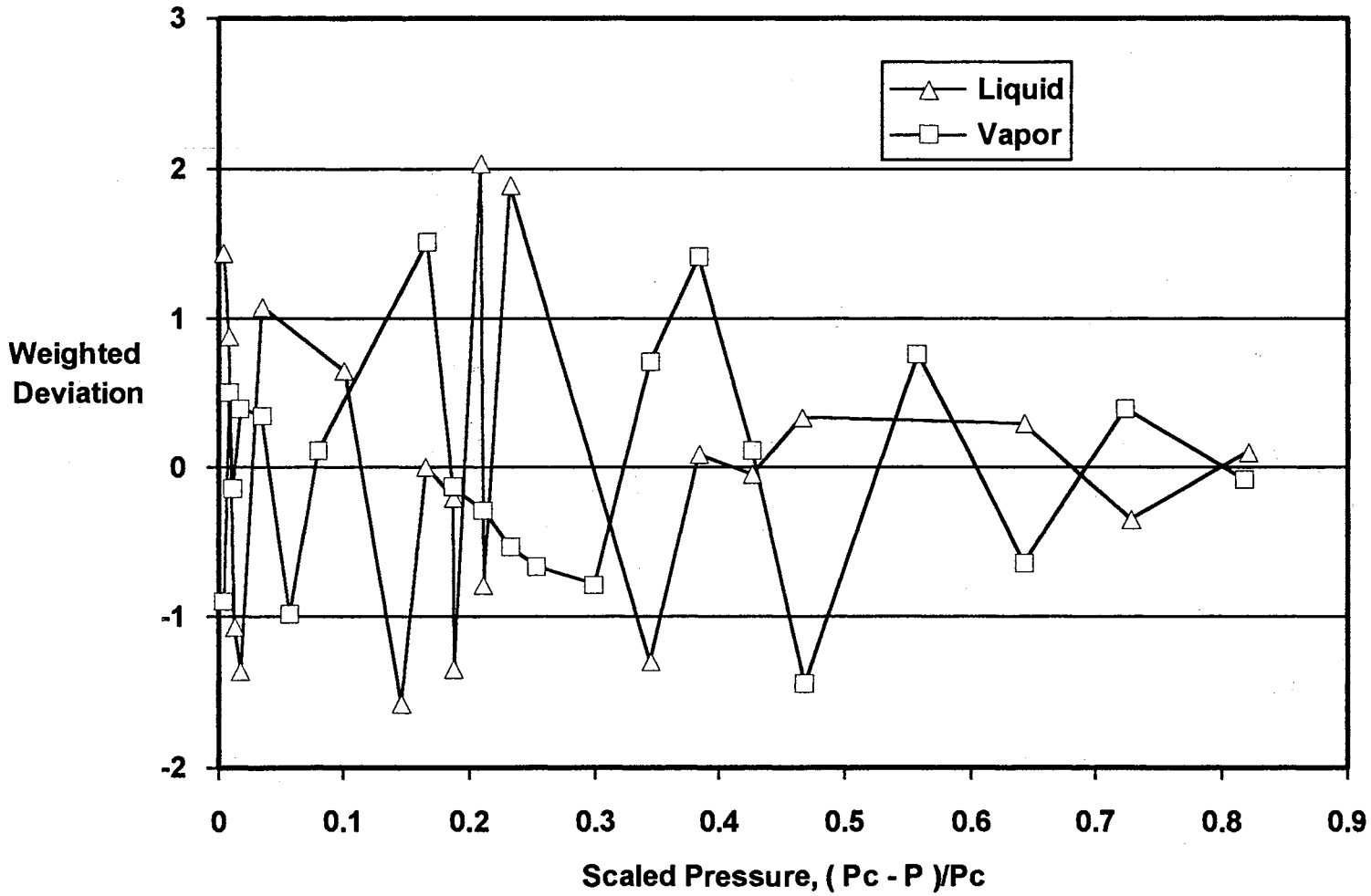

Figure 25. Extended Power Law Fit to Composition Data for Ethane + 1-Methylnaphthalene at 344.3 K (160 °F)

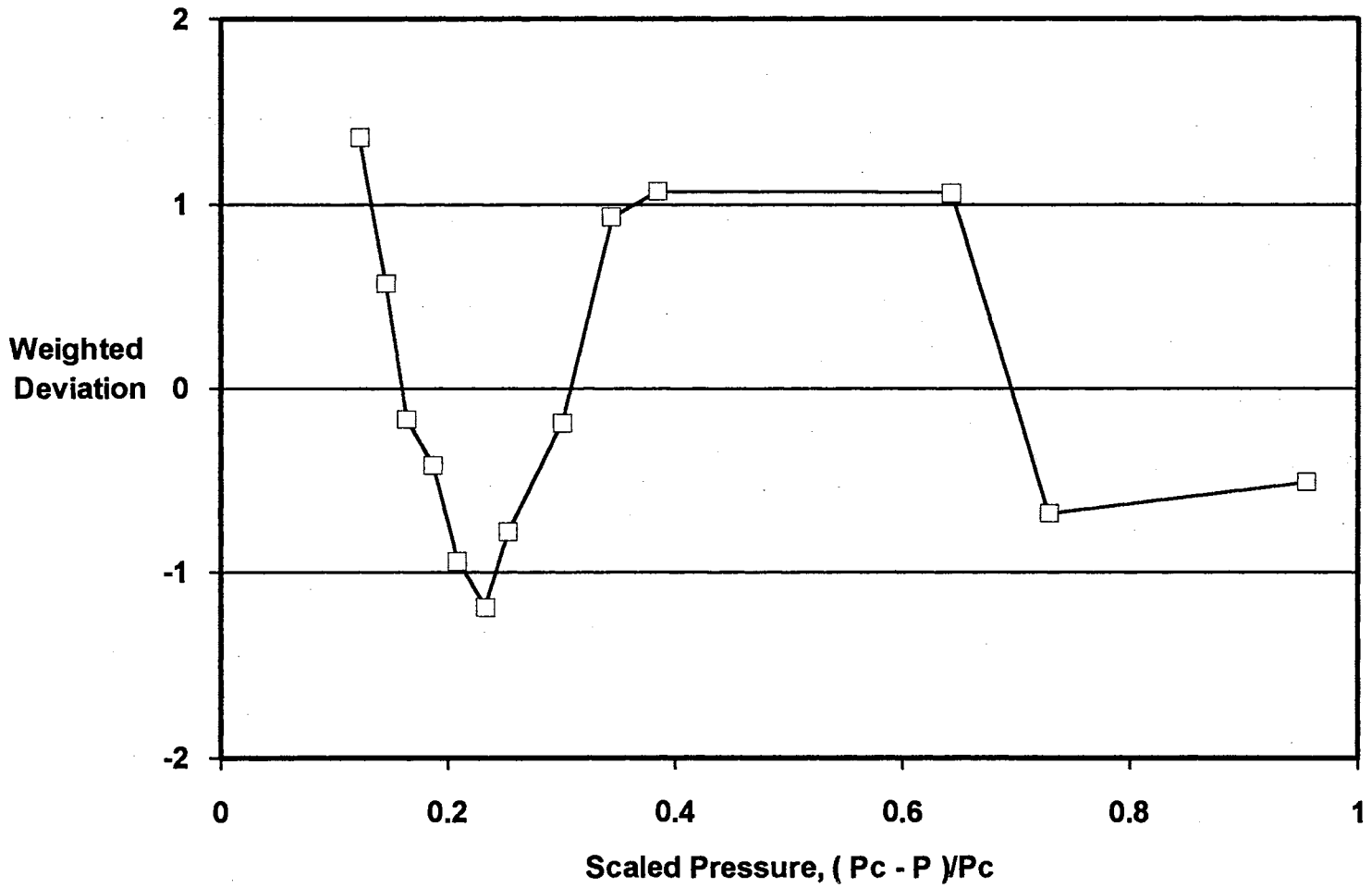

Figure 26. Power Law Fit to IFT Data for Ethane + 1-Methylnaphthalene at 344.3 K (160 °F)

TABLE XIII

SMOOTHED PHASE EQUILIBRIA AND INTERFACIAL TENSION DATA FOR ETHANE + 1-METHYLNAPHTHALENE AT 344.3 K (160 °F)

Pressure		Phase Compositions Mole Fraction Ethane		Phase Densities (g/cm^3)		Interfacial Tension
kPa	psia	Liquid	Vapor	Liquid	Vapor	mN/m
1379	200	0.0475	0.9607	*	*	*
2068	300	0.1311	0.9871	*	*	*
2758	400	0.1910	0.9969	*	*	*
3447	500	0.2387	0.9988	*	*	*
4137	600	0.2812	0.9981	*	*	*
4826	700	0.3220	0.9972	*	*	*
5516	800	0.3626	0.9970	*	*	*
6205	900	0.4027	0.9974	*	*	*
6895	1000	0.4413	0.9977	*	*	*
7584	1100	0.4773	0.9971	*	*	*
8274	1200	0.5095	0.9949	0.8115	0.1930	3.622
8963	1300	0.5374	0.9910	0.7968	0.2334	2.759
9653	1400	0.5610	0.9855	0.7840	0.2707	2.083
10342	1500	0.5810	0.9787	0.7717	0.3029	1.562
11032	1600	0.5989	0.9711	0.7595	0.3303	1.163
11721	1700	0.6162	0.9630	0.7472	0.3543	0.858
12411	1800	0.6347	0.9545	0.7344	0.3768	0.623
13100	1900	0.6558	0.9448	0.7203	0.3989	0.440
13789	2000	0.6795	0.9324	0.7043	0.4215	0.295
14479	2100	0.7045	0.9153	0.6852	0.4455	(0.177)
15168	2200	0.7299	0.8909	0.6586	0.4757	(0.075)
15513	2250	0.7488	0.8729	0.6365	0.4995	(0.029)
15582	2260	0.7552	0.8678	0.6302	0.5062	(0.021)
15651	2270	0.7636	0.8616	0.6226	0.5141	(0.013)
15720	2280	0.7760	0.8533	(0.6130)	0.5241	(0.007)
15754	2285	0.7848	0.8477	(0.6067)	0.5305	(0.004)
15789	2290	(0.7972)	(0.8401)**	(0.5982)	(0.5392)	(0.001)
15803	2292	(0.8041)	(0.8360)	(0.5934)	(0.5441)	(0.001)
15817	2294	(0.8137)	(0.8303)	(0.5857)	(0.5518)	(0.000)
15823***	2295	(0.8238)	(0.8238)	(0.5687)	(0.5687)	(0.000)

* Densities below 1200 psia were not included in the regressions of the smoothing function coefficients.

** Numbers in parentheses are extrapolations beyond the highest measured pressures.

*** Estimated critical point (visual observations gave 2291-2294 psia for the critical pressure).

Carbon Dioxide + *trans*-Decalin at 160 °F

Experimental Data

As mentioned in Chapter II, data for mixtures of CO_2 and *trans*-decalin at 160 °F were measured for two reasons. First, the phase densities, phase compositions and interfacial tensions reported by Gasem and Robinson (11) for this system remain questionable due to difficulties encountered during data collection (32). The vapor and liquid phase data were measured on separate experimental runs because of equipment problems, and the vapor phase compositions were suspected of being too lean in CO_2 mole fraction (32). Second, the liquid composition data reported by Tiffin (21) and Anderson (22) at 167 °F are in disagreement and new measurements were made to alleviate this discrepancy.

The raw data for this system appears in Tables XIV through XVI. Table XIV includes the phase density data, Table XV contains the phase composition data and Table XVI contains the pendant drop interfacial tension data for this system. The estimated accuracy of the data is the same as reported earlier for the CO_2 + n-decane system. The experimental phase densities, phase compositions and interfacial tensions are shown in Figures 27-29. Also included in Figures 27-29 is the previous data of Gasem and Robinson (11).

During the collection of data for this system, the O-rings in the IFT cell failed at a pressure of 1700 psia. Due to continued problems with the IFT cell at high pressures, no further interfacial tension measurements were attempted. Consequently, pendant drop data is only

TABLE XIV

COMPARISON OF EXPERIMENTAL AND CALCULATED PHASE DENSITIES
FOR CO_2 + TRANS-DECALIN AT 344.3 K (160 °F)

PRESSURE psia	PHASE DENSITIES (g/cm^3) Exp.	Calc.	ERROR IN CALCULATED DENSITY g/cm^3	% Dev.	Wt. Dev.	WEIGHTING FACTOR g/cm^3
			-----LIQUID PHASE-----			
2271.5	0.780091	0.779102	-0.000989	-0.126813	-0.935755	0.001057
2255.6	0.789588	0.790093	0.000505	0.063959	0.877335	0.000576
2236.1	0.797412	0.797440	0.000028	0.003556	0.067553	0.000420
2211.6	0.803356	0.803218	-0.000138	-0.017206	-0.388035	0.000356
2183.1	0.807831	0.807825	-0.000006	-0.000771	-0.018863	0.000330
2162.6	0.810441	0.810401	-0.000040	-0.004954	-0.124952	0.000321
2114.7	0.815054	0.815089	0.000035	0.004284	0.112081	0.000312
2066.7	0.818601	0.818639	0.000038	0.004606	0.122801	0.000307
2013.7	0.821687	0.821701	0.000014	0.001655	0.044689	0.000304
1915.7	0.825839	0.825828	-0.000011	-0.001314	-0.035923	0.000302
1809.7	0.828946	0.828973	0.000027	0.003224	0.088777	0.000301
1614.6	0.833056	0.832876	-0.000180	-0.021550	-0.597685	0.000300
1411.5	0.834515	0.834596	0.000081	0.009698	0.269749	0.000300
1412.5	0.834358	0.834593	0.000235	0.028222	0.784884	0.000300
1217.8	0.834762	0.834478	-0.000284	-0.033989	-0.945738	0.000300
1056.2	0.834726	0.834840	0.000114	0.013693	0.380902	0.000300
733.2	0.833729	0.833722	-0.000007	-0.000886	-0.024193	0.000305
			-----VAPOR PHASE-----			
2273.5	0.737442	0.740564	0.003122	0.423352	1.443880	0.002162
2256.6	0.716625	0.716097	-0.000528	-0.073669	-0.477786	0.001105
2236.6	0.699108	0.698431	-0.000677	-0.096894	-0.826946	0.000819
2211.6	0.681272	0.681030	-0.000242	-0.035453	-0.335509	0.000720
2184.1	0.663075	0.663413	0.000338	0.050967	0.480616	0.000703
2163.6	0.649599	0.650301	0.000702	0.108072	0.986938	0.000711
2116.7	0.618645	0.619220	0.000575	0.092995	0.773128	0.000744
2067.7	0.585358	0.585090	-0.000268	-0.045708	-0.347529	0.000770
2012.7	0.547238	0.545764	-0.001474	-0.269371	-1.897074	0.000777
1917.2	0.479435	0.478697	-0.000738	-0.153842	-0.994085	0.000742
1811.2	0.410398	0.411119	0.000721	0.175604	1.086107	0.000664
1811.2	0.409983	0.411119	0.001136	0.277006	1.711540	0.000664
1615.6	0.313497	0.312970	-0.000527	-0.168165	-1.026760	0.000513
1413.5	0.242231	0.242113	-0.000118	-0.048517	-0.278220	0.000422
1220.3	0.190404	0.190650	0.000246	0.129082	0.637918	0.000385
1056.7	0.153869	0.153759	-0.000110	-0.071247	-0.299709	0.000366
723.2	0.095068	0.095075	0.000007	0.006952	0.019549	0.000338

TABLE XV

COMPARISON OF EXPERIMENTAL AND CALCULATED PHASE COMPOSITIONS FOR CO_2 + TRANS-DECALIN AT 344.3 K (160 °F)

PRESSURE psia	MOLE FRACTION CO_2 Exp.	Calc.	ERROR IN CALCULATED MOLE FRACTION Mol. Frac.	% Dev.	Wt.Dev.	WEIGHTING FACTOR Mol. Frac.
			----------LIQUID PHASE----------			
2270.5	0.8369	0.8362	-0.000675	-0.080613	-0.399277	0.001690
2256.6	0.8192	0.8190	-0.000196	-0.023936	-0.174850	0.001121
2236.1	0.8010	0.8017	0.000731	0.091261	0.828897	0.000882
2211.6	0.7861	0.7859	-0.000221	-0.028173	-0.287845	0.000769
2162.6	0.7605	0.7606	0.000150	0.019698	0.219389	0.000683
2013.7	0.6982	0.6994	0.001212	0.173618	1.916781	0.000632
2066.7	0.7205	0.7202	-0.000346	-0.047957	-0.541187	0.000638
2114.2	0.7401	0.7394	-0.000658	-0.088935	-1.010196	0.000652
1915.7	0.6621	0.6618	-0.000340	-0.051357	-0.540081	0.000630
1712.2	0.5850	0.5845	-0.000502	-0.085847	-0.804143	0.000625
1601.6	0.5433	0.5437	0.000410	0.075440	0.663547	0.000618
1217.8	0.4127	0.4127	-0.000029	-0.007067	-0.048755	0.000598
1056.2	0.3591	0.3591	-0.000012	-0.003207	-0.019086	0.000603
733.2	0.2433	0.2433	0.000005	0.002184	0.008510	0.000624
*1412.5	0.4821					
			----------VAPOR PHASE----------			
2272.0	0.9016	0.9027	0.001062	0.117812	0.756310	0.001404
2256.6	0.9175	0.9167	-0.000826	-0.090076	-0.975173	0.000847
2234.6	0.9280	0.9288	0.000776	0.083583	1.147428	0.000676
2211.1	0.9389	0.9381	-0.000836	-0.088996	-1.373192	0.000608
2184.6	0.9460	0.9462	0.000243	0.025719	0.426016	0.000571
2115.7	0.9610	0.9614	0.000419	0.043571	0.789541	0.000530
2067.7	0.9689	0.9689	-0.000024	-0.002435	-0.045517	0.000518
2012.7	0.9755	0.9754	-0.000100	-0.010286	-0.196577	0.000510
1917.2	0.9838	0.9832	-0.000634	-0.064412	-1.257424	0.000504
1811.2	0.9877	0.9883	0.000571	0.057773	1.138357	0.000501
1615.6	0.9924	0.9925	0.000085	0.008527	0.169206	0.000500
1412.5	0.9944	0.9941	-0.000348	-0.034969	-0.695419	0.000500
1219.3	0.9946	0.9949	0.000253	0.025397	0.505183	0.000500
1056.7	0.9956	0.9955	-0.000069	-0.006896	-0.137303	0.000500

* This data point was not included in the final regressions because it contained a weighted deviation of greater than 2.5.

TABLE XVI

COMPARISON OF EXPERIMENTAL AND CALCULATED IFT/DENSITY DIFFERENCE RATIOS FOR CO_2 + TRANS-DECALIN AT 344.3 K (160 °F)

PRESSURE psia	$\gamma/\Delta\rho$ (mN/m)/(g/cm^3) Exp.	Calc.	ERROR IN CALCULATED $\gamma/\Delta\rho$ (mN/m)/(g/cm^3)	% Dev.	Wt.Dev.	WEIGHTING FACTOR (mN/m)/(g/cm^3)
733.2	16.548	16.578	0.029545	0.178542	0.084416	0.349993
1056.2	12.810	12.826	0.016216	0.126586	0.056872	0.285124
1217.8	10.930	10.968	0.038044	0.348071	0.151193	0.251624
1412.5	8.922	8.755	-0.167061	-1.872477	-0.794780	0.210197
1615.1	6.408	6.493	0.084307	1.315557	0.509042	0.165620

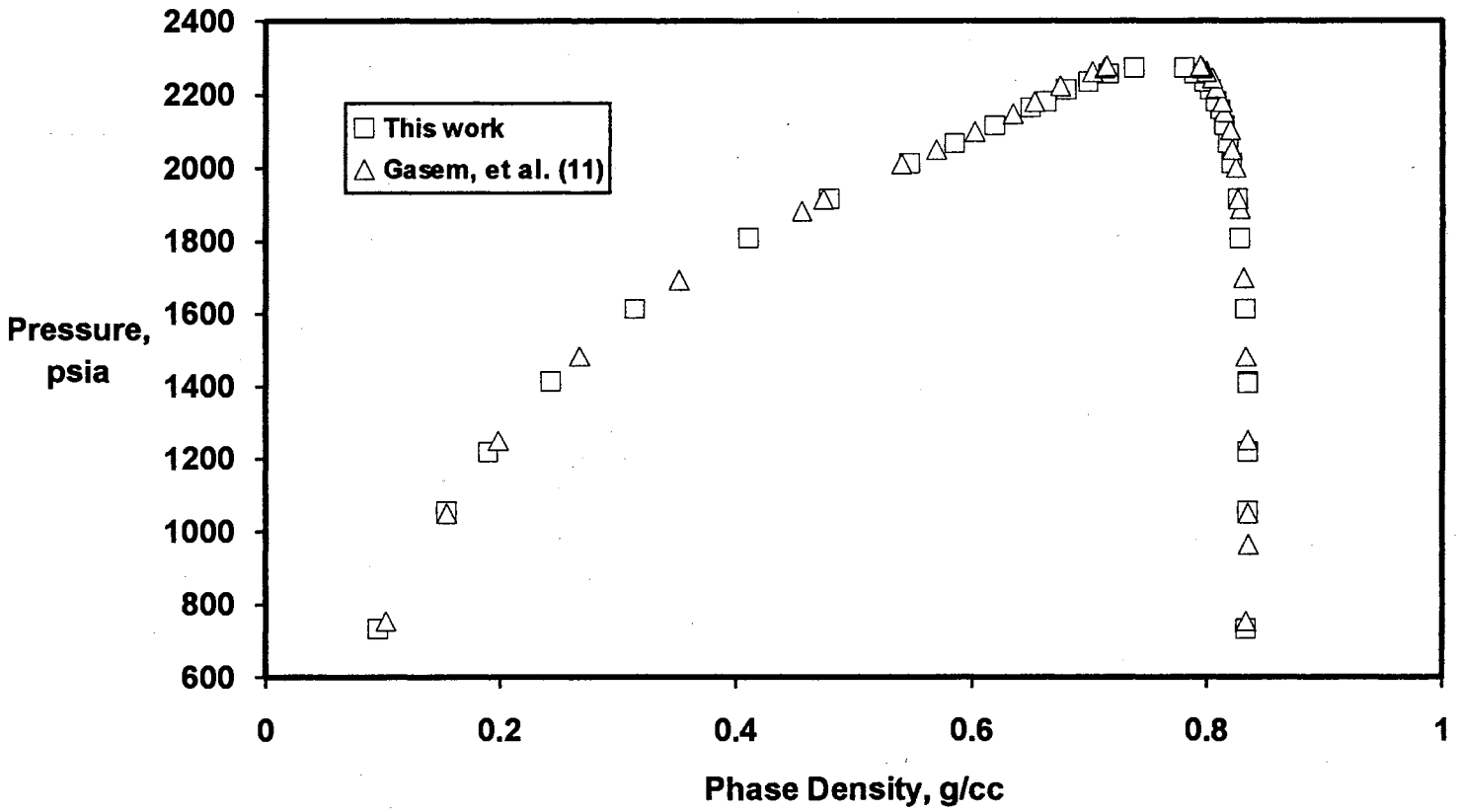

Figure 27. Phase Density Data for Carbon Dioxide + *trans*-Decalin at 344.3 K (160 °F)

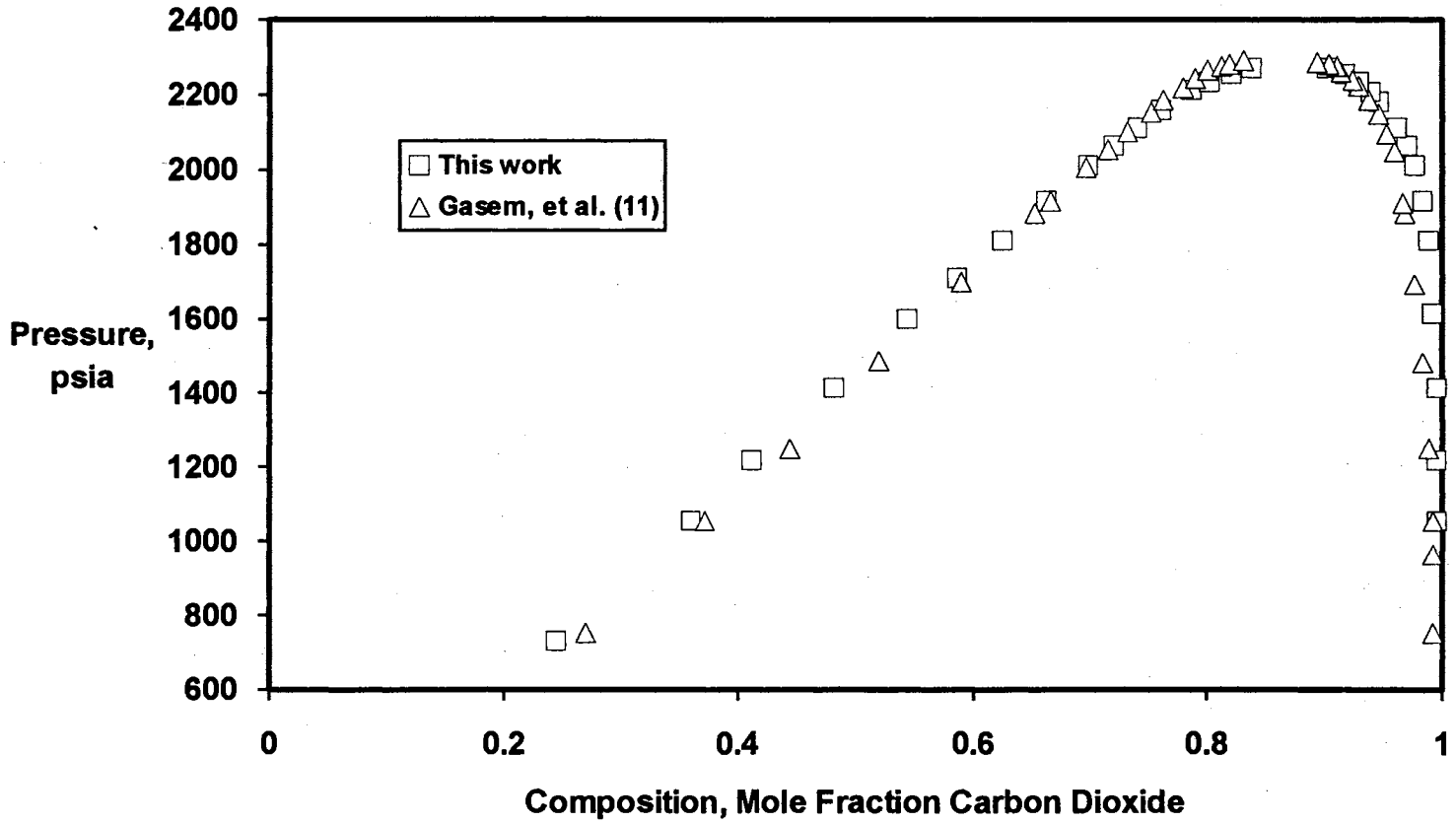

Figure 28. Phase Composition Data for Carbon Dioxide + *trans*-Decalin at 344.3 K (160 °F)

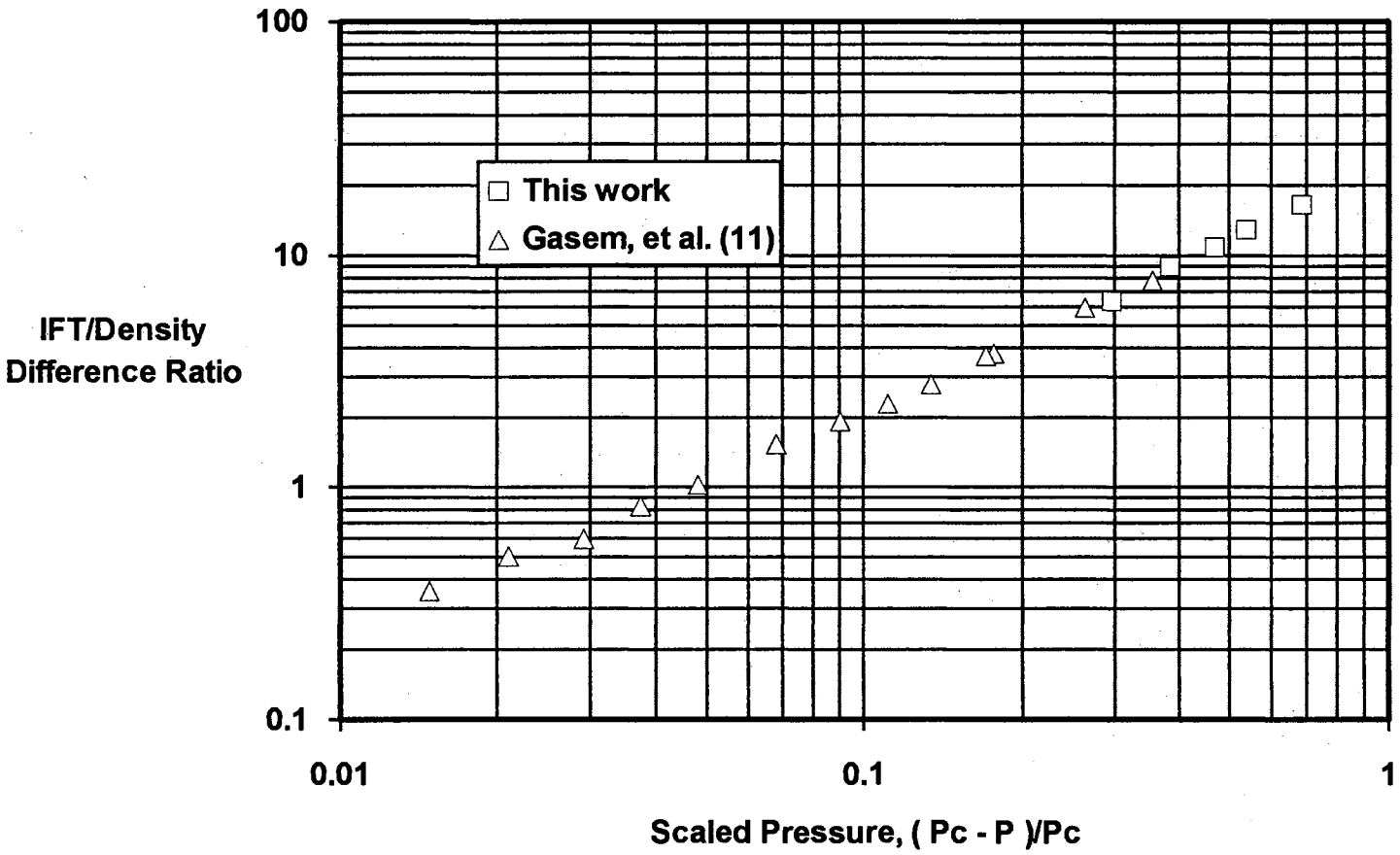

Figure 29. Pendant Drop IFT Data for CO_2 + *trans*-Decalin at 344.3 K (160 °F)

reported up to the highest pressure successfully achieved with the IFT cell (1615 psia) as indicated in Table XVI.

Smoothed Experimental Data

The experimental data for this system were evaluated using the same smoothing functions described previously for the CO_2 + n-decane system. Equations (18) and (19) were used as smoothing functions with M=6 and N=6 of Equation (18). Tables XIV, XV and XVI document the ability of the extended power law equations to fit the experimental data. The parameters obtained from the data regressions are shown in Table XVII. The results are based on the same weighted residual objective function reported earlier. As discussed previously, any data point with a weighted deviation of greater than 2.5 was discarded and the regressions were repeated. This procedure resulted in the removal of only one experimental point: a liquid composition at 1412.5 psia as indicated in Table XV.

Weighted regressions were performed for phase densities, phase compositions and interfacial tensions at several values of the critical pressure, P_c. The optimum critical pressure was then chosen as the one that resulted in the minimum overall weighted root-mean-square error for both phase densities and compositions. Thus, the regressed value for the critical pressure is an estimate based on all experimental data simultaneously. The optimum critical pressure thus obtained (2280.0 psia) is in excellent agreement with visual observations of the equilibrium cell (2277-2280 psia). Figures 30 and 31 show the weighted deviations of the final regressions for phase densities and phase compositions, respectively. The two figures indicate that the weighted

TABLE XVII

PARAMETERS USED TO GENERATE SMOOTHED PROPERTIES
FOR CO_2 + TRANS-DECALIN
AT 344.3 K (160 °F)

PHASE DENSITIES
Units: $(kg/m^3)x10^{-3}$ or g/cm^3

P_c	2280.000
ρ_c	0.7634975
AR_0	-2.300272
AR_1	3.148662
AR_2	-11.09429
AR_3	44.12156
AR_4	-89.21637
AR_5	90.33094
AR_6	-36.40653
BR_0	0.04515076
BR_1	5.799941
BR_2	-42.45178
BR_3	164.0457
BR_4	-305.6112
BR_5	270.6657
BR_6	-92.23288

PHASE COMPOSITIONS
Units: Mole Fraction CO_2

P_c	2280.000
z_c	0.8732287
AZ_0	-0.7987379
AZ_1	0.9067279
AZ_2	-1.576433
AZ_3	0.3994586
AZ_4	7.526417
AZ_5	-14.57439
AZ_6	8.271577
BZ_0	0.3713194
BZ_1	0.9152074
BZ_2	-1.344305
BZ_3	-2.163994
BZ_4	16.09525
BZ_5	-24.78127
BZ_6	12.33464

IFT/DENSITY DIFFERENCE RATIO
Units: $[(mN)/(kg/m^3)]x10^{-3}$ or $[(mN)/(g/cm^3)]$

P_c	2280.000
G_0	54.79339
G_1	-29.61820
G_2	0.0

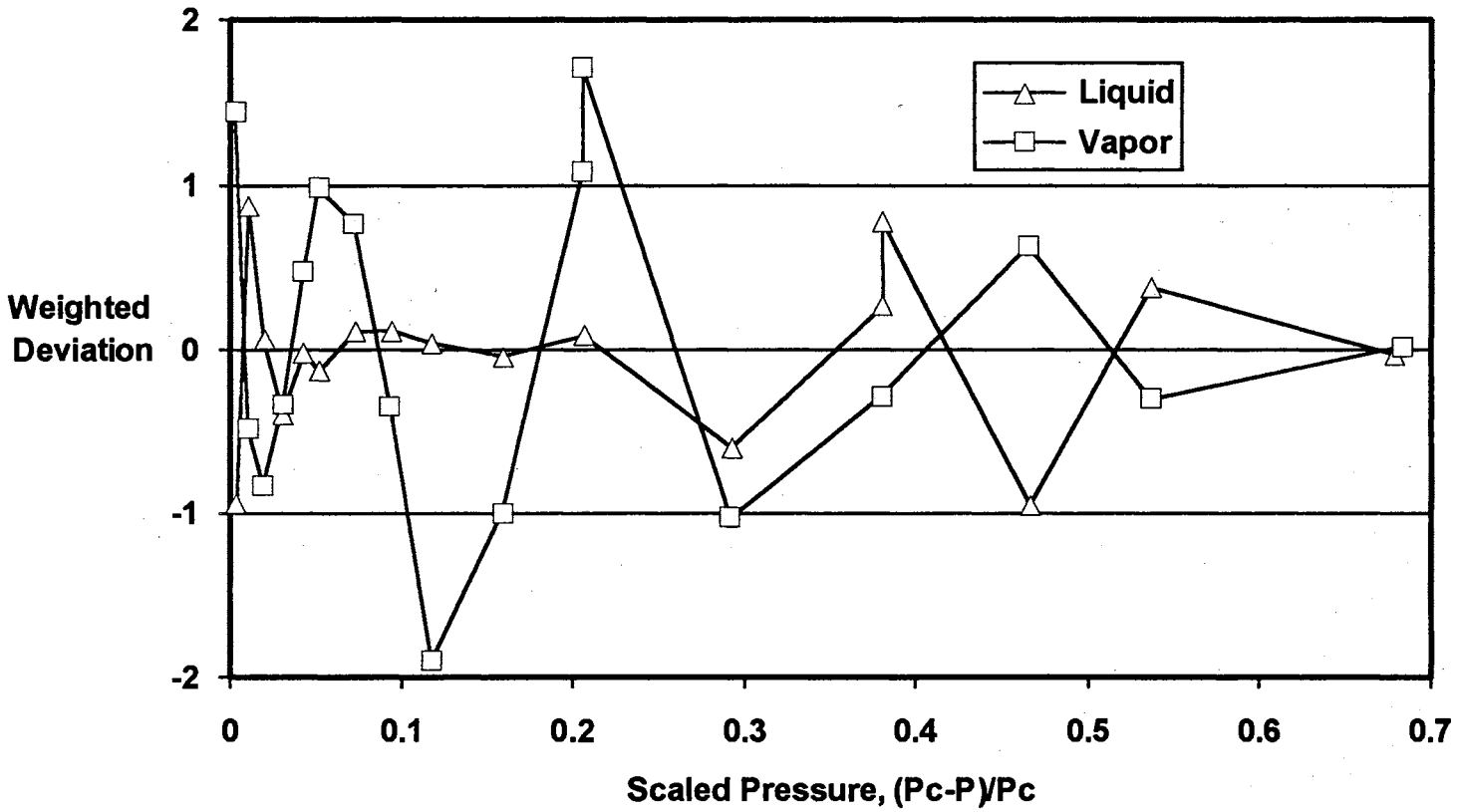

Figure 30. Extended Power Law Fit to Density Data for CO_2 + *trans*-Decalin at 344.3 K (160 °F)

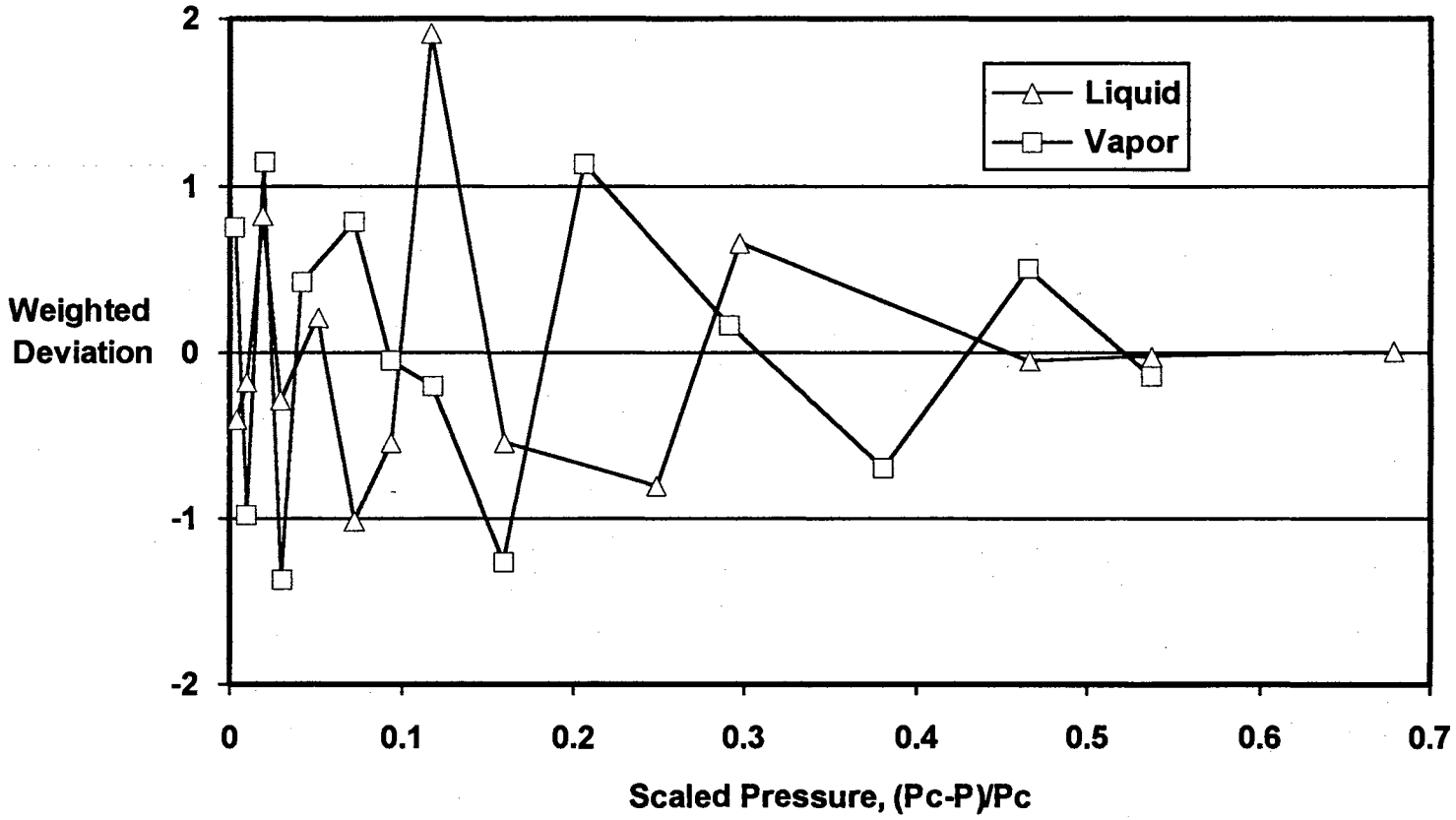

Figure 31. Extended Power Law Fit to Composition Data for CO_2 + *trans*-Decalin at 344.3 K (160 °F)

deviations of density and composition data are well distributed and that the overall quality of fit of the extended power law equations is good. In order to provide data which is more convenient for future use, a smoothed data set based on the parameters given in Table XVII is included in Table XVIII. Since no interfacial tension was successfully obtained above 1615 psia, smoothed values for $\gamma/\Delta\rho$ are not extrapolated beyond the measured range.

TABLE XVIII

SMOOTHED PHASE EQUILIBRIA AND INTERFACIAL TENSION DATA FOR CARBON DIOXIDE + TRANS-DECALIN AT 344.3 K (160 °F)

Pressure kPa	Pressure psia	Phase compositions Mole Fraction CO_2 Liquid	Phase compositions Mole Fraction CO_2 Vapor	Phase Densities (g/cm^3) Liquid	Phase Densities (g/cm^3) Vapor	Interfacial Tension mN/m
4826	700	0.2309	***	0.8313	0.0914	12.553
5516	800	0.2682	***	0.8361	0.1070	11.518
6205	900	0.3048	***	0.8363	0.1236	10.431
6895	1000	0.3399	0.9960	0.8353	0.1422	9.340
7584	1100	0.3738	0.9953	0.8346	0.1630	8.275
8274	1200	0.4068	0.9949	0.8345	0.1858	7.247
8963	1300	0.4397	0.9946	0.8346	0.2106	6.258
9653	1400	0.4731	0.9941	0.8346	0.2381	5.306
10342	1500	0.5075	0.9935	0.8342	0.2695	4.388
11032	1600	0.5431	0.9927	0.8331	0.3066	3.506
11721	1700	0.5799	0.9912	0.8314	0.3511	****
12411	1800	0.6176	0.9887	0.8292	0.4045	****
13100	1900	0.6558	0.9842	0.8264	0.4671	****
13789	2000	0.6941	0.9767	0.8224	0.5367	****
14479	2100	0.7336	0.9641	0.8163	0.6077	****
14824	2150	0.7549	0.9547	0.8118	0.6415	****
15168	2200	0.7793	0.9417	0.8053	0.6735	****
15237	2210	0.7849	0.9384	0.8035	0.6800	****
15375	2230	0.7974	0.9308	0.7991	0.6936	****
15444	2240	0.8046	0.9262	0.7962	0.7011	****
15513	2250	0.8128	0.9209	0.7926	0.7096	****
15582	2260	0.8226	0.9142	0.7878	0.7199	****
15617	2265	0.8284	0.9101	0.7846	0.7262	****
15651	2270	0.8354	0.9051	0.7806	0.7339	****
15665	2272	(0.8388)	0.9027	0.7786	0.7375	****
15679	2274	(0.8426)	(0.8998)	(0.7763)	0.7417	****
15692	2276	(0.8472)	(0.8963)	(0.7736)	(0.7465)	****
15706	2278	(0.8533)	(0.8913)	(0.7702)	(0.7526)	****
15720**	2280	(0.8732)*	(0.8732)	(0.7635)	(0.7635)	****

* Numbers in parentheses are extrapolations beyond the highest pressure used in regression of the smoothing function coefficients.

** Estimated critical point.

*** Vapor compositions are not extrapolated below the lowest pressure data measured.

**** Interfacial tension data is not extrapolated beyond the measured range.

Comparison of Experimental Data

Several sources of previous experimental data exist for mixtures of CO_2 + *trans*-decalin at or near 160 °F (11,21,22). The data of Gasem, et al. (11) is a complete data set collected at Oklahoma State University consisting of phase densities, phase compositions and interfacial tensions at 160 °F at pressures from 750 psia up to the mixture critical point. This data set is included in Figures 27, 28 and 29. Tiffin (21) and Anderson (22) both report solubilities of CO_2 in *trans*-decalin at 167 °F. Two types of comparisons are made with the data of this work. The first is a comparison of the full data set of Gasem, et al. (11) and this work using the same procedure described earlier in the experimental comparisons section for the CO_2 + n-decane system. The second is a comparison of the liquid phase compositions below 1700 psia using the Peng-Robinson equation of state. Each comparison is discussed in detail below.

For comparison purposes, the data of Gasem, et al. (11) and this work were simultaneously fit to Equations (18) and (19). The deviations of the experimental data from the best fit equation are shown in Figures 32-35. Figures 32 and 33 indicate excellent agreement in phase densities for the two data sets at scaled pressures above 0.2. However, drastic differences are seen near the mixture critical point because of differences in the observed critical points of the two data sets. The critical point of the current data was found to be 0.7635 g/cm^3 at 2280.0 psia while that of the older data was determined as 0.7658 g/cm^3 at 2297.0 psia. Such a large difference in the observed critical point can possibly be attributed to one of several factors including an incorrect calibration of the pressure transducer, an incorrect

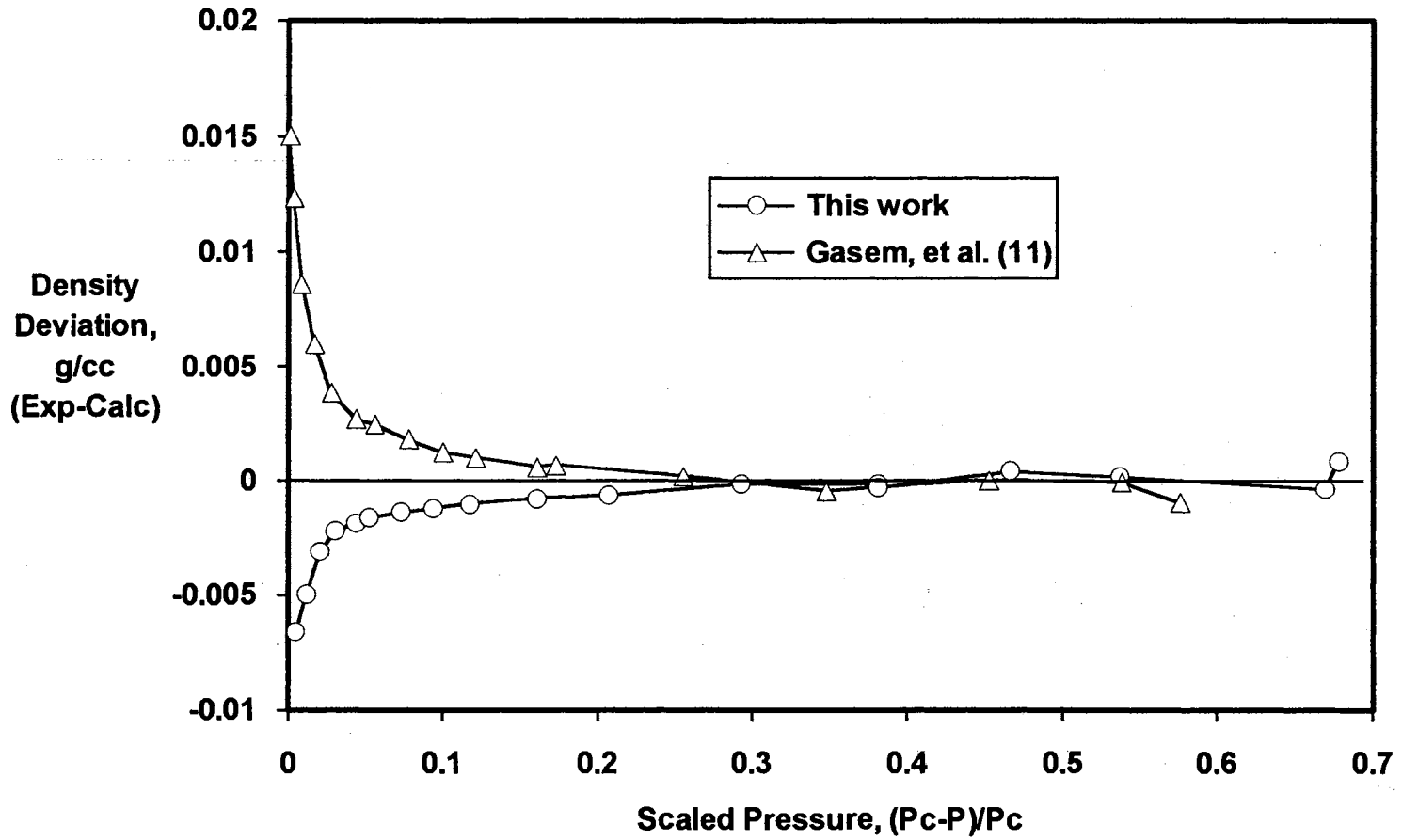

Figure 32. Deviations of Liquid Density Data from Extended Power Law Fit for CO_2 + *trans*-Decalin at 344.3 K (160 °F)

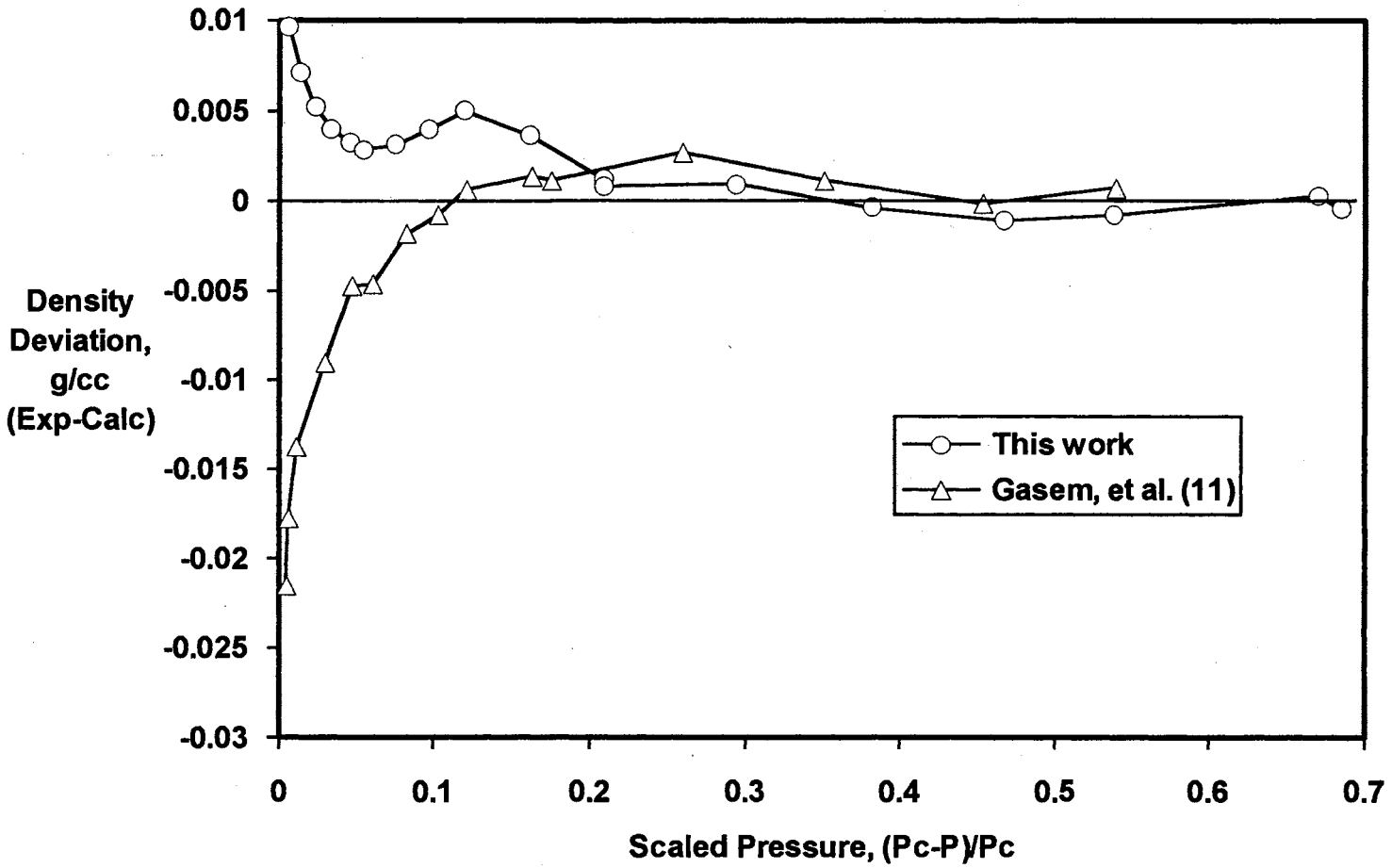

Figure 33. Deviations of Vapor Density Data from Extended Power Law Fit for CO_2 + *trans*-Decalin at 344.3 K (160 °F)

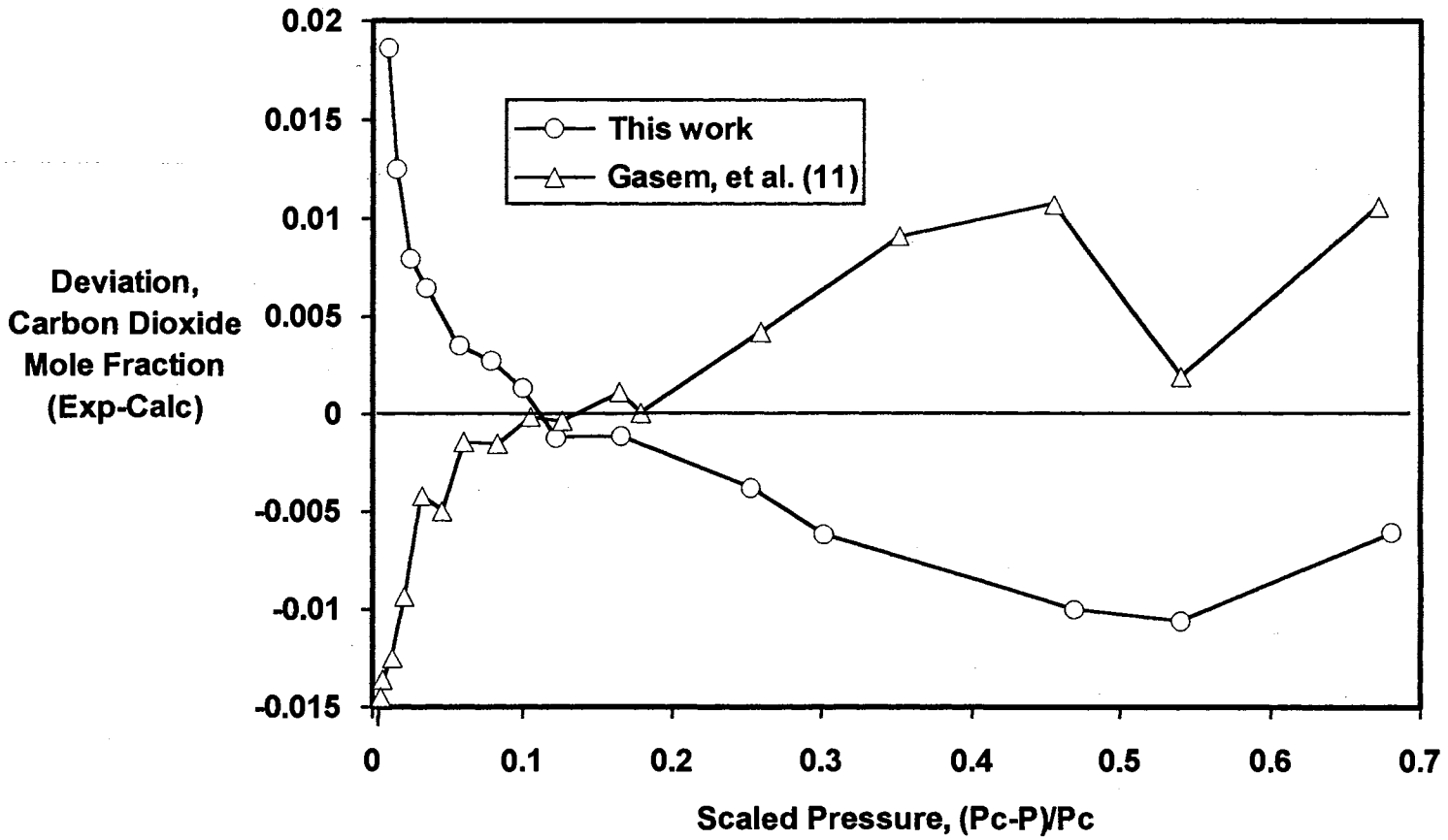

Figure 34. Deviations of Liquid Composition Data from Extended Power Law Fit for CO_2 + *trans*-Decalin at 344.3 K (160 °F)

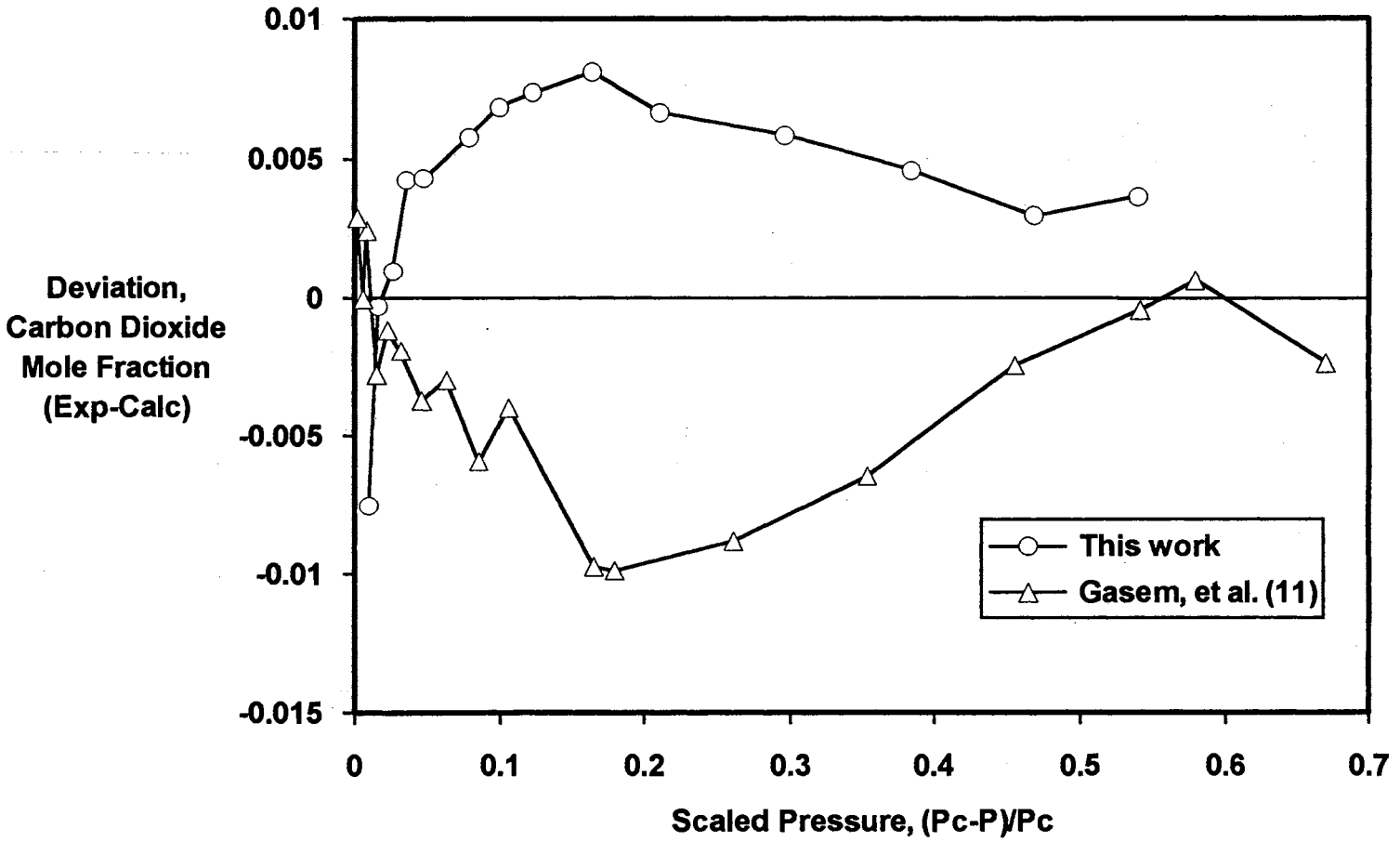

Figure 35. Deviations of Vapor Composition Data from Extended Power Law Fit for CO_2 + *trans*-Decalin at 344.3 K (160 °F)

calibration of the temperature probes or an impurity in either the solute or solvent used. Following the current experimental run, the pressure transducer was checked against the same Ruska dead weight tester used in the initial calibration and results showed that the pressure transducer was properly operating. In addition, all thermocouple and RTD calibrations were verified by a calibration check against the Minco platinum resistance thermometer. No major impurities are believed to have been present since the chemicals used during this experiment were from the same suppliers and of the same reported purity as those used in the earlier work (11) and no indication of impurities were detected during gas chromatograph sampling.

Figures 34 and 35 show the deviations of liquid and vapor compositions from the extended power law equations for both sets of data. Composition data of the two data sets are in disagreement over the entire range of pressure studied. The difference is not, however, a systematic shift in one direction. At lower pressures the liquid phase compositions of this work are leaner in CO_2 than the previous data, and as expected vapor compositions are richer in CO_2 than the previous data. The new sampling valve position discussed in Chapter III is believed to provide more reliable vapor phase compositions than past work. As with the phase densities, Figures 34 and 35 indicate large disagreements in phase compositions near the critical point (at low values of scaled pressure). This is again attributed to the differences in the observed critical points (87.3% CO_2 for this work and 86.2% CO_2 for the earlier work).

The above comparisons shown in Figures 32-35 represent a compromised fit for both data sets and, consequently, the proper scaling

behavior near the critical point is distorted. To further investigate the difference in the observed critical points of the two data sets, the comparisons for densities and compositions done above were repeated with a different procedure. The two data sets were compared at equal values of reduced pressures. This was done by using the coefficients obtained from regression of the current data (shown in Table XVII) along with the corresponding observed critical pressure for each system. Figures showing the results of this comparison are shown in Appendix B. The figures and discussion in Appendix B indicate that the difference between the two data sets is not simply due to differences in pressure calibrations or to impurities. In consideration of this comparison and those discussed above, no clear explanation is available for the observed differences.

Liquid phase compositions below 1700 psia were compared to those of Gasem et al. (11) and to the solubility measurements of Anderson (22) and Tiffin (21) at 167 °F. The comparison was done by fitting two interaction parameters (C_{ij} and D_{ij}) in the Peng-Robinson equation of state to the bubble point pressures of the current work below 1700 psia. The equation of state was then used to predict the bubble point pressures of the various data sets at the reported liquid phase compositions. The results (with C_{ij}=0.1065 and D_{ij}=0.0441) are shown in Figure 36. The data of Gasem, et al. (11) and Anderson, et al. (22) appear to agree with one another, and that of this work and Tiffin (21) appear to agree with one another. However, the discrepancy between the two apparent trends cannot be explained.

Figure 37 displays the deviations of experimental $\gamma/\Delta\rho$ from the extended power law equation for both data sets. Although pressure

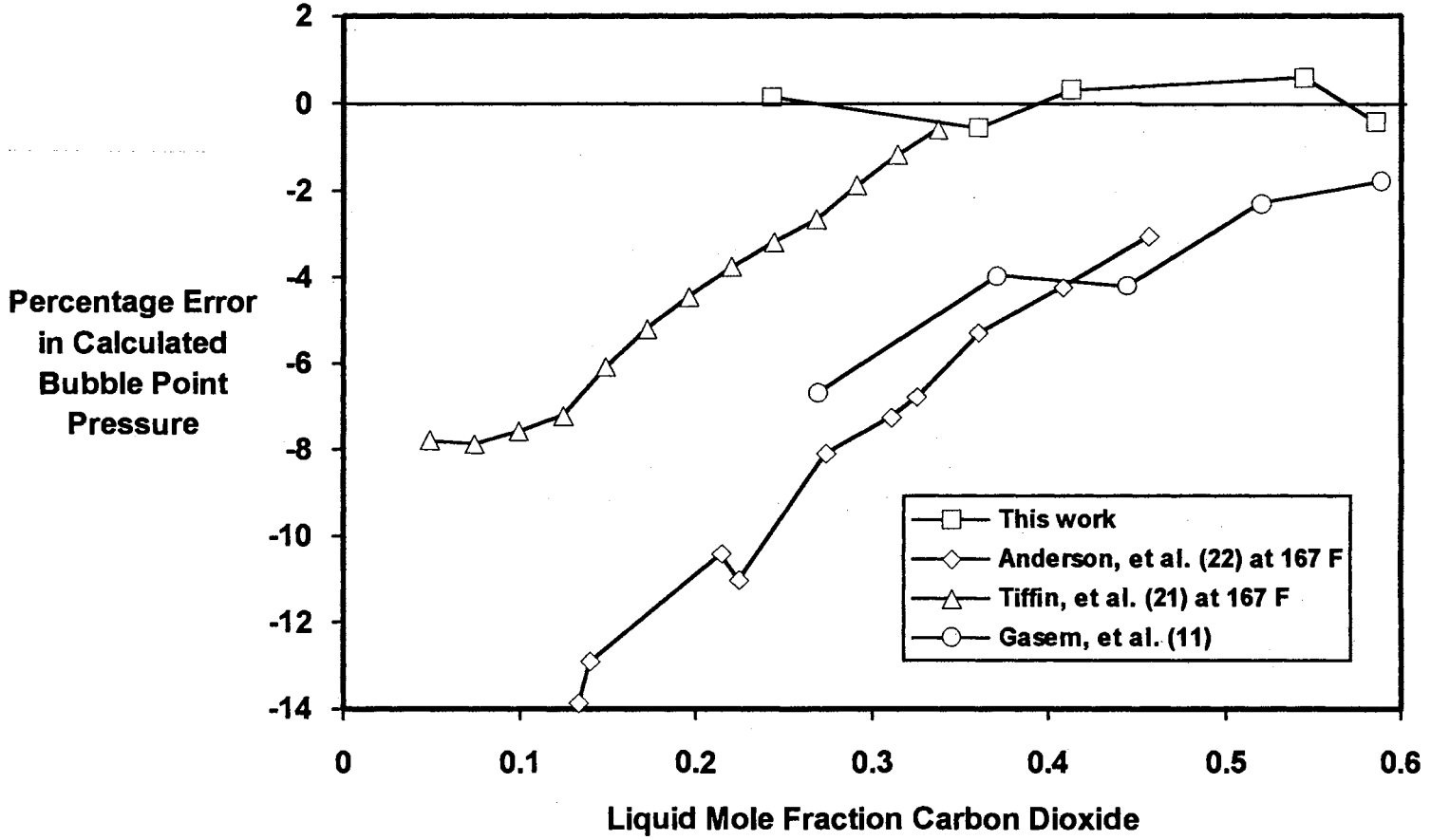

Figure 36. Comparison of Liquid Phase Composition Data for CO_2 + *trans*-Decalin Using the Peng-Robinson Equation of State

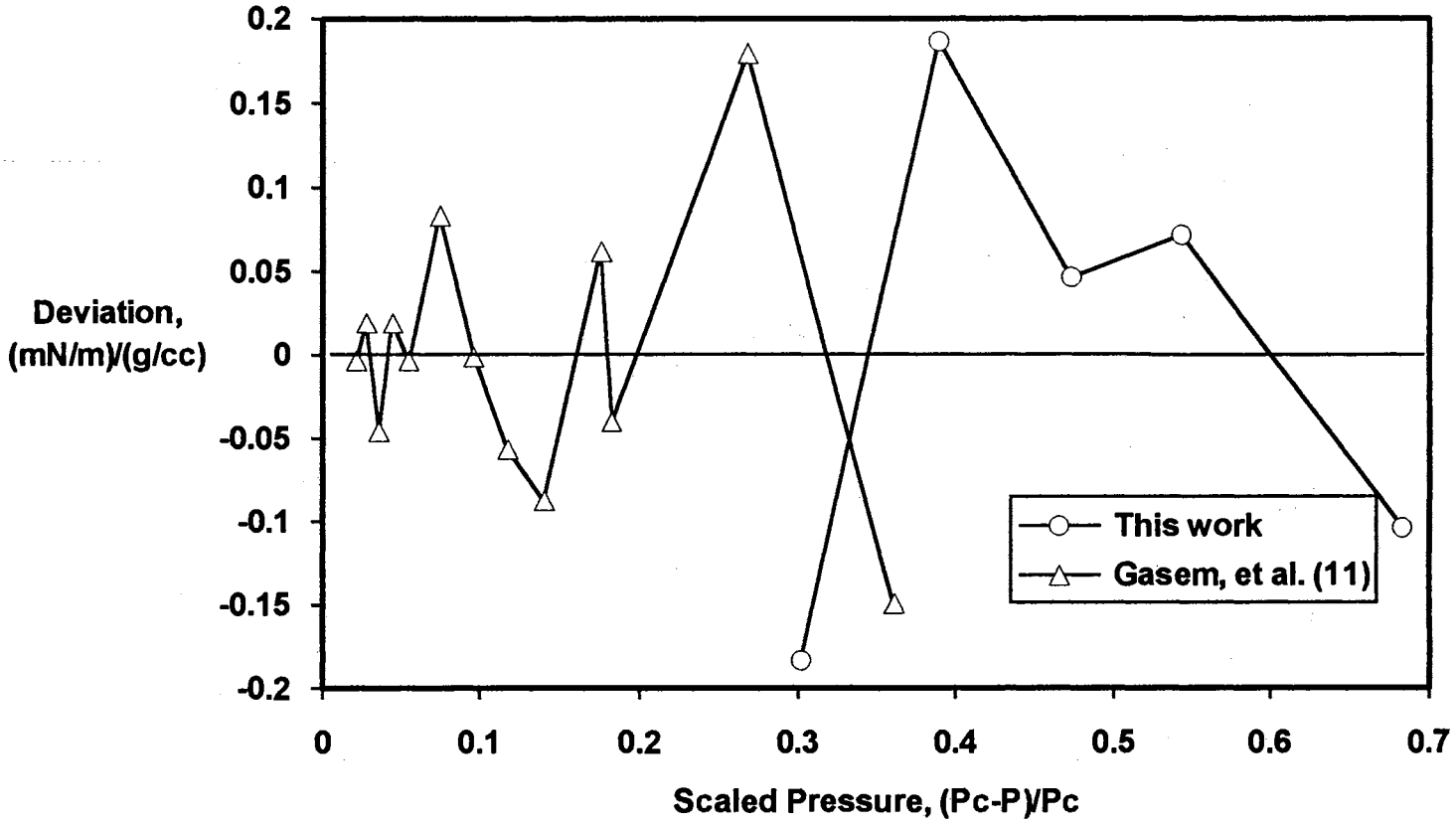

Figure 37. Deviations of Interfacial Tension Data from Extended Power Law Fit for CO_2 + *trans*-Decalin at 344.3 K (160 °F)

limitations of the interfacial tension cell restricted the range of data collected in this work, the two data sets appear to be in fair agreement. The new data represents an extension of the range of IFT measurements covered by the previous data.

CHAPTER V

CONCLUSIONS AND RECOMMENDATIONS

A recently automated experimental apparatus was used to measure liquid and vapor phase equilibrium properties (liquid and vapor phase densities and compositions and interfacial tensions). Several further modifications were made to the apparatus during this work. Where possible, the newly acquired measurements were compared to existing literature data. Following are specific conclusions and recommendations which can be made based on this work.

Conclusions

1. Additional modifications to the apparatus have been undertaken including: positioning the gas chromatograph sampling valve at a higher inverted location to improve vapor phase composition analysis, addition of a stream switching valve upstream of the interfacial tension cell to allow for convenient selection of needle size for the measurement of interfacial tensions using the pendant drop technique, and addition of an externally driven circulation fan for the main oven to improve temperature control.
2. A computer program has been developed for the convenient acquisition of experimental data. The computer program records all raw data received by the ACRO Systems computer interface module and applies all equipment calibrations to the collected

data. The program also contains graphing routines to allow for real-time observation of data gathering and generation of the phase envelope.

3. Experimental data have been collected for three systems: CO_2 + n-decane at 160 °F, ethane + 1-methylnaphthalene at 160 °F, and CO_2 + *trans*-decahydronaphthalene (*trans*-decalin) at 160 °F. The experimental precision of the data is comparable to previous studies (5-17). The consistency of the data is due in part to the fact that all measured properties ($x, y, \rho^L, \rho^V, \gamma/\Delta\rho$) were obtained simultaneously from the same apparatus.
4. The experimental data for the CO_2 + n-decane system at 160 °F represent an extension of the range of previous data collected at Oklahoma State University (7) and demonstrates the viability of new computer automation systems and of the new digitized imaging procedure for measurement of interfacial tensions. The data were compared to those of five different sources. Excellent agreement was observed for the phase densities of this work and those of Nagarajan, et al. (7). Reasonable agreement exists for all liquid phase compositions (within 0.005 mole fraction CO_2) except for those of Chou, et al. (20). Vapor phase compositions of all data sets agree to within 0.005 mole fraction CO_2. A smoothed data set based on all available data was produced from extended scaling law equations. The smoothed data set is recommended as a comparison data set for the testing of new experimental equipment and procedures.
5. The experimental data for the ethane + 1-methylnaphthalene system at 160 °F represent an addition to the literature of previously

unavailable data. Pressure limitations of the interfacial tension cell restricted measurements of interfacial tensions to pressure less than 2000 psia. The weighted deviations of the data from the extended scaling law equations are well distributed over the entire pressure range studied and give no indication of systematic errors.

6. The experimental data for the CO_2 + *trans*-decalin system at 160 °F were compared to several previous data sets (11,21,22). Low pressure liquid phase compositions of this work agree well with those of Tiffin (21) but disagree with those of Anderson, et al. (22) and Gasem, et al. (11). This disagreement could not be explained. The observed mixture critical point (2280 psia) is considerably lower than that reported by Gasem, et al. (2297 psia) (11). Comparisons between the data of this work and of Gasem, et al. indicate that the two data sets exhibit different behavior in the near-critical region. This discrepancy could not be fully explained.

Recommendations

1. The interfacial tension cell is limited to pressures below 2000 psia. This is due to failure of the O-rings that seal pressure against the high pressure cell windows. Several types of O-rings have been tested with the most successful being a composite O-ring consisting of viton encapsulated by teflon. Further modification of the cell is required to achieve higher working pressures. The grooves which hold the O-rings in place should be deepened

slightly to reduce the gap remaining between the cell body and window to reduce extrusion of the O-rings at high pressures.

2. Analysis of vapor compositions is difficult at pressures below 1000 psia. This is due to contamination of vapor samples with liquid. One possible remedy may be the installation of separate sampling valves for vapor and liquid phases.

3. Additional bubble point measurements at pressures below 1000 psia for the CO_2 + *trans*-decalin system at 160 °F may help elucidate the observed differences in the data of this work and others (11,21,22).

LITERATURE CITED

1. Gasem, K. A. M. and R. L. Robinson, Jr., "Evaluation of the Simplified Perturbed Hard Chain Theory (SPHCT) for Prediction of Phase Behavior of n-Paraffins and Mixtures of n-Paraffins with Ethane," Fluid Phase Equilibria, 58, 13-33 (1990).

2. Ponce-Ramirez, L., C. Lira-Galeana, and C. Tapia-Medina, "Application of the SPHCT Model to the Prediction of Phase Equilibria in CO_2-Hydrocarbon Systems," Fluid Phase Equilibria, 70, 1-18 (1991).

3. van Pelt, A., C. J. Peters and J. de Swaan Arons, "Application of the Simplified-Perturbed-Hard-Chain Theory for Pure Components Near the Critical Point," Fluid Phase Equilibria, 74, 67-83 (1992).

4. Roush, K. V., "Automated Phase Densities and Interfacial Tension Measurements," M. S. Thesis, Oklahoma State University, Stillwater, Oklahoma (1991).

5. Dulcamara, P. B., "Interfacial Tensions for Carbon Dioxide or Light Hydrocarbons in Hydrocarbon Solvents: Experimental Data and Correlations," M. S. Thesis, Oklahoma State University, Stillwater, Oklahoma (1987).

6. Hsu, J. C., N. Nagarajan and R. L. Robinson, Jr., "Equilibrium Phase Compositions, Phase Densities, and Interfacial Tensions for CO_2 + Hydrocarbon Systems. 1. CO_2 + n-Butane," Journal of Chemical and Engineering Data, 30, 485-491 (1985).

7. Nagarajan, N. and R. L. Robinson, Jr., "Equilibrium Phase Compositions, Phase Densities, and Interfacial Tensions for CO_2 + Hydrocarbon Systems. 2. CO_2 + n-Decane," Journal of Chemical and Engineering Data, 31, 168-171 (1986).

8. Gasem, K. A. M., K. B. Dickson, P. B. Dulcamara, N. Nagarajan and R. L. Robinson, Jr., "Equilibrium Phase Compositions, Phase Densities, and Interfacial Tensions for CO_2 + Hydrocarbon Systems. 5. CO_2 + n-Tetradecane," Journal of Chemical and Engineering Data, 34, 191-195 (1989).

9. Nagarajan, N. and R. L. Robinson, Jr., "Equilibrium Phase Compositions, Phase Densities, and Interfacial Tensions for CO_2 + Hydrocarbon Systems. 3. CO_2 + Cyclohexane. 4. CO_2 + Benzene," Journal of Chemical and Engineering Data, 32, 369-371 (1989).

10. Nagarajan, N., Y. K. Chen, and R. L. Robinson, Jr., "Interfacial Tensions in Carbon Dioxide-Hydrocarbon Systems: Development of Experimental Facilities and Acquisition of Experimental Data. Experimental Data for CO_2 + Benzene," Technical Progress Report (June 15, 1984).

11. Gasem, K. A. M., and R. L. Robinson, Jr., "Interfacial Tensions in Carbon Dioxide-Hydrocarbon Systems: Development of Experimental Facilities and Acquisition of Experimental Data. Experimental Data for CO_2 + trans-Decalin," Technical Progress Report (October 10, 1986).

12. Gasem, K. A. M., and R. L. Robinson, Jr., "Interfacial Tensions in Ethane-Hydrocarbon Systems: Development of Experimental Facilities and Acquisition of Experimental Data. Experimental Data for Ethane + n-Decane," Technical Progress Report (September 25, 1985).

13. Gasem, K. A. M., P. B. Dulcamara, and R. L. Robinson, Jr., "Interfacial Tensions in Ethane-Hydrocarbon Systems: Acquisition of Experimental Data. Experimental Data for Ethane + Benzene," Technical Progress Report (July 24, 1987).

14. Nagarajan, N., K. A. M. Gasem and R. L. Robinson, Jr., "Equilibrium Phase Compositions, Phase Densities, and Interfacial Tensions for CO2 + Hydrocarbon Systems. 6. CO2 + n-Butane + n-Decane," Journal of Chemical and Engineering Data, 35(3), 228-231 (1990).

15. Gasem, K. A. M., K. B. Dickson, and R. L. Robinson, Jr., "Interfacial Tensions in Carbon Dioxide-Hydrocarbon Systems: Development of Experimental Facilities and Acquisition of Experimental Data. Experimental Data for Carbon Dioxide + a Recombined Reservoir Oil," Technical Progress Report (March 28, 1986).

16. Gasem, K. A. M., R. D. Shaver, and R. L. Robinson, Jr., "Interfacial Tensions in Carbon Dioxide-Hydrocarbon Systems: Acquisition of Experimental Data for CO_2 + a Synthetic Oil," Progress Report (November 12, 1987).

17. Gasem, K. A. M., R. D. Shaver, K. V. Roush, and R. L. Robinson, Jr., "Interfacial Tensions in CO_2-Hydrocarbon Systems: Acquisition of Experimental Data. Experimental Data for Selected Hydrocarbon Solvents," Department of Energy Report (January, 1988).

18. Jennings, J. W., and N. R. Pallas, "An Efficient Method for the Determination of Interfacial Tensions from Drop Profiles," Langmuir, 4(4), 959-967 (1988).

19. Reamer, H. H. and B. H. Sage, "Phase Equilibria in Hydrocarbon Systems. Volumetric and Phase Behavior of the n-Decane-CO_2 System," Journal of Chemical and Engineering Data, 8(4), 508-513 (1963).

20. Chou, G. F., R. R. Forbert and J. M. Prausnitz, "High-Pressure Vapor-Liquid Equilibria for CO_2/n-Decane, CO_2/Tetralin, and CO_2/n-Decane/Tetralin at 71.1 and 104.4 °C," Journal of Chemical and Engineering Data, 35(1), 26-29 (1990).

21. Tiffin, D. L., A. L. DeVera, K. D. Luks and J. P. Kohn, "Phase-Equilibria Behavior of the Binary Systems Carbon Dioxide-n-Butylbenzene and Carbon Dioxide-*trans*-Decalin," Journal of Chemical and Engineering Data, 23(1), 45-47 (1978).

22. Anderson, J. M., M. W. Barrick and R. L. Robinson, Jr., "Solubilities of Carbon Dioxide in Cyclohexane and *trans*-Decalin at Pressures to 10.7 MPa and Temperatures from 323 to 423 K," Journal of Chemical and Engineering Data, 31(2), 172-175 (1986).

23. Rotenburg, Y., L. Boruvka, and A. W. Neuman, "Determination of Surface Tension and Contact Angle from the Shapes of Axisymmetric Fluid Interfaces," Journal of Colloid Interface Science, 93(1), (1983).

24. Robinson, R. L., Jr., "Interfacial Tensions in Carbon Dioxide-Hydrocarbon Systems: Development of Data Correlation, Final Technical Report," Submitted to Amoco Production Company (1983).

25. Levelt-Sengers, J. M. H., Greer, W. L., and J. V. Sengers, Journal of Physical and Chemical Reference Data, 5(1) (1976).

26. Le Gillou, J. C., and J. Zinn-Hustin, "Critical Exponents from Field Theory," Physical Review, B 21, 3976-3998 (1980).

27. Wichterle, I., Chappelear, P. S., and R. Kobayashi, "Determination of Critical Exponents from Measurements of Binary Vapor-Liquid Equilibrium in the Neighborhood of the Critical Line," Journal of Computational Physics, 7, 606-620 (1971).

28. Charoensombut-amon, T., and R. Kobayashi, "Application of the Wilson-Wegner Expansion to Represent Vapor-Liquid Equilibrium Surfaces of Binary and Ternary Systems from the Critical Locus to the Vapor Pressure of the Heavier Component," Fluid Phase Equilibria, 31, 23-34 (1986).

29. Wegner, F. J., "Corrections to Scaling Laws," Physical Review, B 5, 4529-4536 (1972).

30. Seagraves, T. P., "Experimental Determination of Crude Oil Phase Behaviors," M. S. Thesis, Oklahoma State University, Stillwater, Oklahoma (1993).

31. Bufkin, B., "High Pressure Solubilities of Carbon Dioxide and Ethane in Selected Paraffinic, Naphthenic and Aromatic Solvents," M. S. Thesis, Oklahoma State University, Stillwater, Oklahoma (1983).

32. Gasem, K. A. M., Private Communication, Oklahoma State University, Stillwater, Oklahoma (1992).

33. Goodwin, R. D., H. M. Roder and G. C. Straty, "Thermophysical Properties of Ethane from 90 to 600 K at Pressures to 700 Bars," National Bureau of Standards (1976).

APPENDIX A

COMPUTER PROGRAMS USED

This appendix contains the source code listings for two of the computer programs used in this work. The first program (TRANS.FOR) is one originally written by Roush (4) and later modified for this work. The input to this program is a listing of (x,y) pixel values for the edge trace of a pendant drop photographed with the Javelin CCTV camera. The input data is supplied by an ASCII file generated by the edge-tracing function of Jandel Scientific's JAVA software. TRANS.FOR scales the data to the units of centimeters and produces the data file needed as input for the program developed by Pallas (18) for determining interfacial tensions. The program also provides an estimate of $\gamma/\Delta\rho$ using a two point method described in detail by Roush (4). TRANS.FOR has been modified to allow more flexibility in defining the parameters required for the measurement of very low interfacial tensions.

The second program (SYSTEM.FOR) is used to record data during an experimental run. The program records all raw data as well as that converted to the desired units through the system calibration equations. Data recorded include the current temperatures of all thermocouples and RTD's, the raw and calibrated pressure, the density meter period, the GC area ratio, and the calculated density and composition. SYSTEM.FOR also provides graphs of phase densities and compositions for real-time monitoring of data gathering and generation of the phase envelope.

Both programs are included here for the benefit of future users of this or a similar apparatus. Source listings for other programs used during this work are quite lengthy and were, therefore, not included here.

```
C*****************************************************************
C
C     PROGRAM TRANS.FOR
C
C     KURTIS V. ROUSH
C     OKLAHOMA STATE UNIVERSITY
C
C     MODIFIED BY R. D. SHAVER 8/1/92
C
C     LOCATE APEX, XMIN, XMAX, CALCULATE De AND Ds FROM
C     DROP PROFILE DATA, AND ESTIMATE IFT
C
C     THE PROGRAM ASSUMES THAT THE EDGE IS TRACED STARTING FROM THE
C     LEFT SIDE.  THE RIGHT SIDE MUST EXTEND HIGHER OR EVEN TO THE
C     LEFT SIDE.  THE PROGRAM ASSUMES THAT THE MONITOR IS TURNED ON
C     END.
C
C     VARIABLES:
C
C     X -       X COORDINATE
C     Y -       Y COORDINATE
C     DIAXL -   X COORDINATE OF LEFT SIDE OF NEEDLE
C     DIAXR -   X COORDINATE OF ROGHT SIDE OF NEEDLE
C     DIAMAG -  DIAMETER OF MAGNIFIED NEEDLE IN PIXELS
C     APEX -    INTEGER VALUE REPRESENTING ARRAY VALUE OF THE APEX
C     APEXX -   X COORDINATE OF THE APEX
C     APEXY -   Y COORDINATE OF THE APEX
C     XMIN -    FAR LEFT X VALUE
C     XMAX -    FAR RIGHT X VALUE
C     DE -      MAXIMUM WIDTH OF DROP
C     DSL -     X COORDINATE ON LEFT SIDE OF DROP A DISTANCE DE FROM
C               THE APEX
C     DSR -     X COORDINATE ON RIGHT SIDE OF DROP A DISTANCE DE FROM
C               THE APEX
C     DS -      THE WIDTH OF THE DROP A DISTANCE DE FROM THE APEX
C     NDIA -    ACTUAL NEEDLE DIAMETER IN INCHES
C     DELROE -  DIFFERENCE IN LIQUID AND VAPOR DENSITY
C     S -       RATIO DE/DS
C     H -       FACTOR DEPENDENT ON S
C     IFT -     CALCULATED IFT USING DISCRETE POINT METHOD
C
C*****************************************************************
C
      IMPLICIT REAL (A-Z)
      DOUBLE PRECISION X(2000),Y(2000)
      INTEGER N,NPTS,APEX,START,END
      CHARACTER*28 FILE1,FILE2
      CHARACTER*11 FIL
C
      WRITE(*,*) 'INPUT DATA FILE NAME: '
      READ(*,*) FILE1
      WRITE(*,*) 'OUTPUT FILE NAME: '
      READ(*,*) FILE2
      WRITE(*,*) 'INPUT DELTA RHO IN G/CC: '
      READ (*,*) DELRHO
C
      WRITE(*,*) 'INPUT NEEDLE DIAMETER IN INCHES: '
      READ (*,*) NDIA
C
      WRITE(*,*) 'ENTER THE NUMBER OF INITIAL DATA POINTS TO DISCARD: '
```

```
      READ(*,*) NDISCARD
C
      WRITE(*,*) 'ENTER THE PIXEL TOLERANCE FOR DETECTION OF NEEDLE',
     & ' TIP: '
      READ(*,*) PIXTOL
C
      WRITE(*,*) 'ENTER THE NUMBER OF DATA POINTS TO INCREMENT FOR',
     & ' CREATING PALLAS FILE (1-4): '
      READ(*,*) NSKIP
C
      OPEN(UNIT=8, FILE=FILE1, STATUS='OLD')
      OPEN(UNIT=9, FILE=FILE2, STATUS='UNKNOWN')
C
C ******* DELETE FIRST 'NDISCARD' POINTS DUE TO ERROR IN ESTIMATING EDGE
C
      DO 100 N=1,NDISCARD
         READ(8,*)
  100 CONTINUE
C
C ******* READ REST OF DATA POINTS AND CORRECT FOR IMAGE BEING SIDEWAYS
C
      N=0
   20 CONTINUE
      N=N+1
      READ(8,*,END=30) Y(N),X(N)
      Y(N)= -Y(N) + 1000.0
      GOTO 20
C
   30 NPTS=N-1
C
C ******** DELETE RIGHT SIDE OF TRACE ABOVE LEFT SIDE
C
      N=NPTS
   40 IF(Y(N).LE.Y(1))THEN
        NPTS=N
        GOTO 50
      ENDIF
      N=N-1
      GOTO 40
C
   50 CONTINUE
C
C ******** CALCULATE MAGNIFIED DIAMETER USING AVERAGE OF TOP 10 LEFT
C          AND TOP 10 RIGHT X COORDINATES
C
      DIAXL=0.0
      DO 110 N=1,10
         DIAXL=DIAXL+X(N)
  110 CONTINUE
      DIAXL=DIAXL/10.0
C
      DIAXR=0.0
      DO 120 N=NPTS,NPTS-9,-1
         DIAXR=DIAXR+X(N)
  120 CONTINUE
      DIAXR=DIAXR/10.0
C
      DIAMAG=DIAXR-DIAXL
C
C ********  LOCATE APEX
```

```
C
      YMIN2Q=1000.00
      DO 130 N=1,NPTS
         IF(Y(N).LT.YMIN2Q) THEN
           YMIN2Q=Y(N)
           Y2Q=N
         ENDIF
         IF(Y(N).EQ.YMIN2Q) THEN
           YMIN3Q=Y(N)
           Y3Q=N
         ENDIF
  130 CONTINUE
C
      APEX=INT((Y3Q+Y2Q)/2)
      APEXX=X(APEX)
      APEXY=Y(APEX)
C
C     TRANSFORMS COORDINATES RELATIVE TO THE APEX (0,0)
C
      DO 135 N=1,NPTS
         X(N)=X(N)-APEXX
         Y(N)=Y(N)-APEXY
CREM          WRITE(9,133) x(n), y(n)
  133    FORMAT(10x,F10.4,10x,F10.4)
  135 CONTINUE
C
C ********  LOCATE MINIMUM X
C
      XMIN=1000
      DO 140 N=1,APEX
         IF(X(N).LT.XMIN) THEN
           XMIN=X(N)
         ENDIF
  140 CONTINUE
C
C ********  LOCATE MAXIMUM X
C
      XMAX=0.0
      DO 150 N=APEX,NPTS
         IF(X(N).GT.XMAX) THEN
           XMAX=X(N)
         ENDIF
  150 CONTINUE
C
C ********  CALCULATE De AND Ds
C
      DE=XMAX-XMIN
      YS=Y(APEX)+DE
      N=0
  160 N=N+1
      IF(Y(N).LE.YS) THEN
        DSL=X(N)
        GOTO 161
      ENDIF
      GOTO 160
  161 CONTINUE
      N=NPTS
  170 N=N-1
      IF(Y(N).LE.YS) THEN
        DSR=X(N)
```

```
        GOTO 171
      ENDIF
      GOTO 170
  171 CONTINUE
      DS=DSR-DSL
C
C     ESTIMATE GAMMA/DELTA RHO (dyne-cm)/(g/cc)
C
      DE=DE*NDIA/DIAMAG
      DS=DS*NDIA/DIAMAG
      DE=DE/39.37
      DS=DS/39.37
C
      S=DS/DE
      H=1/(0.31470 * S**(-2.62529))
C
      IFT=1.0E6*(9.79777*DE**2.0)/H
      WRITE(*,1000) IFT
 1000 FORMAT(2X,'GAMMA/DELTA RHO = ',F7.3,' (dyne-cm)/(g/cc)')
      IFT=IFT*DELRHO
      WRITE(*,1010) IFT
 1010 FORMAT(2X,'GAMMA = ',F7.3,' (dyne-cm)')
C
C     PREPARE DATA FILE FOR PALLAS PROGRAM
C
C     REMOVE DATA ENCOMPASSING NEEDLE
C
      I=2
  200 IF(ABS(X(1)-X(I)).LE.PIXTOL) THEN
        I=I+1
        GOTO 200
      ENDIF
      START=I
C
      I=NPTS-1
  210 IF(Y(I).GE.Y(START)) THEN
        I=I-1
        GOTO 210
      ENDIF
      END=I
C
C     TRANSLATE THE DATA SO Y(1), THE HIGHEST POINT, IS AT X,0
C
      YORIGIN=Y(START)
      DO 300, I=START,END
         Y(I)=Y(I)-YORIGIN
 300  CONTINUE
C
C     CONVERT DATA FROM PIXELS TO CENTIMETERS
C
      NDIA=NDIA*30.48/12.0
      DO 400, I=START,END
         X(I)=X(I)*NDIA/DIAMAG
         Y(I)=Y(I)*NDIA/DIAMAG
 400  CONTINUE
C
C     REDUCE DATA SET BY 75% AND SET HEADERS AND FOOTERS
C
      WRITE(9,401) FILE1
 401  FORMAT(A30)
```

```
      WRITE(9,402)
402   FORMAT('00:00:00')
      I=START
403   IF(I.GT.END) GOTO 450
      WRITE(9,470) X(I), Y(I)
      I=I+NSKIP
      GOTO 403
450   CONTINUE
      WRITE(9,451) FILE1
451   FORMAT(A30)
      WRITE(9,452)
452   FORMAT('00:00:00')
470   FORMAT(10X,F10.6,10X,F10.6)
      STOP
      END
```

```
C*****************************************************************
C
C     PROGRAM SYSTEM.FOR
C
C     CODED BY RONALD D. SHAVER
C     OKLAHOMA STATE UNIVERSITY
C     STILLWATER, OK
C
C*****************************************************************
C
        IMPLICIT REAL*8 (A-Z)
        INTEGER TYPE,OPT
        CHARACTER*30 FILE1,FILE2,FILE3,FILE4,FILE5,FILE6
        CHARACTER*30 CDATE,CTIME
        CHARACTER*10 DATE
        CHARACTER*12 TIME
        CHARACTER*2 TYPEC
        FILE1='A:\RAW.TMP'
        FILE2='A:\CALIB.PAR'
        FILE4='A:\DATE'
        FILE5='A:\TIME'
        FILE6='A:\TICK'
        CDATE='>A:\DATE DATE'
        CTIME='>A:\TIME TIME'
        CALL PLOTS(0,0,0)
        CALL TITLE
        AR=0.0
        X=0.0
C
C     GIVE THE OPTION TO ENTER A NEW DATA POINT OR TO PLOT EXISTING
C     DATA
C
 5      CALL GTEXT(12,5,'CHOOSE ONE OF THE FOLLOWING OPTIONS:')
        CALL GTEXT(13,5,'  (1)  Enter a new data point')
        CALL GTEXT(14,5,'  (2)  Plot existing data')
        CALL GTEXT(16,5,'CHOICE:  ')
        READ(*,*) DUMMY
        IF(DUMMY.LT.1.OR.DUMMY.GT.2) GOTO 5
C
C     INPUT THE FILE NAMES FOR STORING RAW DATA AND CALIBRATED DATA
C
        CALL GTEXT(12,5,'                                          ')
        CALL GTEXT(13,5,'                                          ')
        CALL GTEXT(14,5,'                                          ')
        CALL GTEXT(16,5,'                                          ')
        CALL GTEXT(12,5,'ENTER THE SUMMARY DATA FILE NAME:  ')
        READ(*,*) FILE3
        IF(DUMMY.EQ.2) GOTO 100
C
C     OPEN THE REQUIRED FILES
C
        OPEN(UNIT=8, FILE=FILE1, ACTION='READ,DENYNONE', STATUS='OLD')
        OPEN(UNIT=9, FILE=FILE2, STATUS='OLD')
        OPEN(UNIT=10, FILE=FILE3, STATUS='UNKNOWN', POSITION='APPEND')
C
C     READ IN THE CALIBRATION CONSTANTS
C
        READ(9,*)
        READ(9,*)
        READ(9,*) A1,A2,A3,A4
```

```
        READ(9,*)
        READ(9,*) W1,W2,W3,W4
        READ(9,*)
        READ(9,*) TAL1,TAL2,TAL3,TAL4
        READ(9,*)
        READ(9,*) TAV1,TAV2,TAV3,TAV4
        READ(9,*)
        READ(9,*) TWL1,TWL2,TWL3,TWL4
        READ(9,*)
        READ(9,*) TWV1,TWV2,TWV3,TWV4
        READ(9,*)
        READ(9,*) P1,P2,P3,P4
        READ(9,*)
        READ(9,*) C1,C2
C
C     INPUT THE TYPE OF DATA BEING RECORDED
C
 10     CALL GTEXT(12,5,'ENTER THE TYPE OF DATA BEING RECORDED:')
        CALL GTEXT(12,43, '                                    ')
        CALL GTEXT(13,5,'  (1)  Liquid density')
        CALL GTEXT(14,5,'  (2)  Liquid composition')
        CALL GTEXT(15,5,'  (3)  Vapor density')
        CALL GTEXT(16,5,'  (4)  Vapor composition')
        CALL GTEXT(18,5,'CHOICE:  ')
        READ(*,*) TYPE
        IF(TYPE.LT.1.OR.TYPE.GT.4) GOTO 10
        IF(TYPE.EQ.1) TYPEC='LD'
        IF(TYPE.EQ.2) TYPEC='LC'
        IF(TYPE.EQ.3) TYPEC='VD'
        IF(TYPE.EQ.4) TYPEC='VC'
C
C     RETRIEVE THE RAW DATA FROM THE LTC LOG FILE AND INPUT
C     ANY ADDITIONAL DATA.
C
        READ(8,*)
        READ(8,*)
        READ(8,*) TPVT,RPVT,TIFT,RIFT,TVDMA,RVDMA,TLDMA,RLDMA,
     &  TIFTV,RIFTV,P,DMA
        CALL GTEXT(12,5,'                                          ')
        CALL GTEXT(13,5,'                                          ')
        CALL GTEXT(14,5,'                                          ')
        CALL GTEXT(15,5,'                                          ')
        CALL GTEXT(16,5,'                                          ')
        CALL GTEXT(18,5,'                                          ')
        CALL GTEXT(12,5,'ENTER THE PRESSURE FROM THE SENSOTEC GAGE ')
        CALL GTEXT(12,47,'(IN PSIG):  ')
        READ(*,*) P
        CALL GTEXT(12,5,'                                              ')
        CALL GTEXT(12,47,'                                          ')
        CALL GTEXT(13,5,'                                          ')
        CALL GTEXT(14,5,'                                          ')
        CALL GTEXT(12,5,'ENTER THE ATMOSPHERIC PRESSURE (in mm Hg):  ')
        READ(*,*) PATM
        PATM = PATM/760.0*14.696
        IF(TYPE.EQ.2.OR.TYPE.EQ.4) THEN
          CALL GTEXT(12,5,'                                            ')
          CALL GTEXT(12,40,'                          ')
          CALL GTEXT(12,5,'ENTER THE AVERAGED GC AREA RATIO:  ')
          READ(*,*) AR
        ENDIF
```

```
        CALL GTEXT(12,5,'                                                  ')
        CALL GTEXT(12,40,'                                  ')
        CALL GTEXT(12,5,'DO YOU WANT TO MANUALLY ENTER THE DMA COUNT?')
        CALL GTEXT(13,5,'  (1) Yes')
        CALL GTEXT(14,5,'  (2) No')
        CALL GTEXT(16,5,'CHOICE:  ')
        READ(*,*) DUMMY
        CALL GTEXT(12,5,'                                                  ')
        CALL GTEXT(12,40,'                            ')
        CALL GTEXT(13,5,'                                                  ')
        CALL GTEXT(14,5,'                                                  ')
        CALL GTEXT(16,5,'                                                  ')
        IF(DUMMY.EQ.1) THEN
          CALL GTEXT(12,5,'ENTER THE DMA COUNT:  ')
          READ(*,*) DMA
        ENDIF
C
C     GET THE CURRENT DATE AND TIME
C
        CALL GTEXT(12,5,'PRESS <ENTER> TO RETRIEVE THE CURRENT DATE')
        CALL SYSTEM(CDATE)
        OPEN(UNIT=11, FILE=FILE4, STATUS='OLD')
        READ(11,20) DATE
 20     FORMAT(20X,A10)
        CLOSE(11)
        CALL GTEXT(13,5,DATE)
C
        CALL GTEXT(14,5,'PRESS <ENTER> TO RETRIEVE THE CURRENT TIME')
        CALL SYSTEM(CTIME)
        OPEN(UNIT=12, FILE=FILE5, STATUS='OLD')
        READ(12,30) TIME
 30     FORMAT(16X,A12)
        CLOSE(12)
        CALL GTEXT(15,5,TIME)
C
C     ADJUST THE PRESSURE BY THE CALIBRATION
C
        PRESS = P1 + P2*P + P3*P**2 + P4*P**3 + PATM
C
C     CALCULATE THE PROPER DENSITY
C
        IF(TYPE.EQ.1.OR.TYPE.EQ.2) THEN
         TAUAIR = TAL1 + TAL2*PRESS + TAL3*PRESS**2.0 + TAL4*PRESS**3.0
         TAUWAT = TWL1 + TWL2*PRESS + TWL3*PRESS**2.0 + TWL4*PRESS**3.0
        ENDIF
C
        IF(TYPE.EQ.3.OR.TYPE.EQ.4) THEN
         TAUAIR = TAV1 + TAV2*PRESS + TAV3*PRESS**2.0 + TAV4*PRESS**3.0
         TAUWAT = TWV1 + TWV2*PRESS + TWV3*PRESS**2.0 + TWV4*PRESS**3.0
        ENDIF
C
        DENAIR = A1 + A2*PRESS + A3*PRESS**2.0 + A4*PRESS**3.0
        DENWAT = W1 + W2*PRESS + W3*PRESS**2.0 + W4*PRESS**3.0
        K=(DENAIR-DENWAT)/(TAUAIR**2.0-TAUWAT**2.0)
        DEN=K*(DMA**2.0-TAUWAT**2.0) + DENWAT
C
C     CALCULATE THE PHASE COMPOSITION IF REQUIRED
C
        IF(TYPE.EQ.1.OR.TYPE.EQ.3) GOTO 50
        A = C2/AR
```

```
        B = (C1/AR + 1.0)
        C = -1.0
        X = -B+(B**2.0-4.0*A*C)**0.5
        X = X/(2.0*A)
 50     CONTINUE
C
C     RECORD THE DATA IN THE SUMMARY DATA FILE
C
        WRITE(10,*)
        WRITE(10,60) DATE,TPVT,TIFT,TVDMA,TLDMA,TIFTV
        WRITE(10,70) TIME,RPVT,RIFT,RVDMA,RLDMA,RIFTV
        WRITE(10,80) TYPEC,P,DMA,AR
        WRITE(10,90) PRESS,DEN,X
 60     FORMAT(2X,A10,2X,5F9.2)
 70     FORMAT(A12,2X,5F9.2)
 80     FORMAT(10X,A2,6X,F9.1,4X,F10.6,2X,F10.4)
 90     FORMAT(18X,F9.1,4X,F10.6,2X,F10.4)
C
C     PROVIDE OPTIONS FOR PLOTTING
C
 100    CALL GTEXT(18,5,'CHOOSE ONE OF THE FOLLOWING OPTIONS:')
        CALL GTEXT(19,5,'  (1)  Plot liquid densities versus pressure')
        CALL GTEXT(20,5,'  (2)  Plot vapor densities versus pressure')
        CALL GTEXT(21,5,'  (3)  Plot both liquid and vapor densities')
        CALL GTEXT(21,48,' versus pressure')
        CALL GTEXT(22,5,'  (4)  Plot liquid compositions versus')
        CALL GTEXT(22,43,' pressure')
        CALL GTEXT(23,5,'  (5)  Plot vapor compositions versus')
        CALL GTEXT(23,42,' pressure')
        CALL GTEXT(24,5,'  (6)  Plot both liquid and vapor')
        CALL GTEXT(24,38,' compositions versus pressure')
        CALL GTEXT(25,5,'  (7)  End the program')
        CALL GTEXT(27,5,'CHOICE:  ')
        READ(*,*) OPT
        IF(OPT.LT.1.OR.OPT.GT.7) GOTO 100
        IF(OPT.EQ.7) GOTO 200
C
C     CLOSE ALL FILES
C
        CLOSE(8)
        CLOSE(9)
        CLOSE(10)
C
C     CALL THE PLOTTING ROUTINE AND PLOT THE DESIRED DATA
C
        CALL GRAPH(OPT,FILE3,FILE6)
        GOTO 100
C
 200    CALL PLOT(0,0,999)
        STOP
        END
C
C*************************************************************************
C
C     SUBROUTINE TITLE
C
C*************************************************************************
C
        SUBROUTINE TITLE
C
```

```
        CALL SYSTEM('CLS')
        CALL NEWPEN(3)
        CALL PLOT(2.0,8.0,3)
        CALL PLOT(2.0,6.0,2)
        CALL PLOT(9.0,6.0,2)
        CALL PLOT(9.0,8.0,2)
        CALL PLOT(2.0,8.0,2)
        CALL GTEXT(3,29,'PHASE EQUILIBRIUM DATA')
        CALL GTEXT(5,31,'ACQUISITION SYSTEM')
        CALL GTEXT(7,27,'OKLAHOMA STATE UNIVERSITY')
        RETURN
        END
C
C*************************************************************************
C
C     SUBROUTINE GRAPH
C
C*************************************************************************
C
        SUBROUTINE GRAPH(OPT,FILE3,FILE6)
        INTEGER OPT,I,J,DELX,DELY
        CHARACTER*30 FILE3,FILE6
        CHARACTER*2 TYPE(200)
        CHARACTER*6 CYTICK,CXTICK
        LOGICAL YES
        REAL*8 P(200),DMA(200),AR(200),PRESS(200),DEN(200),COMP(200),
     &  X(200),Y(200)
        REAL*4 XPLOT(200),YPLOT(200)
C
        YES=.FALSE.
        I=0
        J=1
        OPEN(UNIT=8, FILE=FILE3, STATUS='OLD')
        OPEN(UNIT=9, FILE=FILE6, STATUS='UNKNOWN')
  5     I=I+1
        READ(8,10,END=20) TYPE(I),P(I),DMA(I),AR(I),PRESS(I),DEN(I),
     &  COMP(I)
 10     FORMAT(///10X,A2,6X,F10.1,5X,F10.6,4X,F10.4,/,18X,
     &  F10.1,5X,F10.6,4X,F10.4)
C
        IF(OPT.EQ.1.AND.TYPE(I).EQ.'LD') YES=.TRUE.
        IF(OPT.EQ.3.AND.TYPE(I).EQ.'LD') YES=.TRUE.
        IF(OPT.EQ.2.AND.TYPE(I).EQ.'VD') YES=.TRUE.
        IF(OPT.EQ.3.AND.TYPE(I).EQ.'VD') YES=.TRUE.
C
        IF(YES) THEN
          X(J)=DEN(I)
          Y(J)=PRESS(I)
          J=J+1
          YES=.FALSE.
        ENDIF
C
        IF(OPT.EQ.4.AND.TYPE(I).EQ.'LC') YES=.TRUE.
        IF(OPT.EQ.6.AND.TYPE(I).EQ.'LC') YES=.TRUE.
        IF(OPT.EQ.5.AND.TYPE(I).EQ.'VC') YES=.TRUE.
        IF(OPT.EQ.6.AND.TYPE(I).EQ.'VC') YES=.TRUE.
C
        IF(YES) THEN
          X(J)=COMP(I)
          Y(J)=PRESS(I)
```

```
          J=J+1
          YES=.FALSE.
        ENDIF
C
        GOTO 5
 20     CONTINUE
        NPTS=J-1
        IF(NPTS.LE.1) THEN
          CALL GTEXT(27,5,'THERE IS NOT SUFFICIENT DATA - ')
          CALL GTEXT(27,36,'CANNOT PRODUCE PLOT')
          GOTO 110
        ENDIF
C
C     FIND THE MINIMUM AND MAXIMUM X AND Y VALUES TO BE PLOTTED
C
        XMIN=X(1)
        XMAX=X(1)
        YMIN=Y(1)
        YMAX=Y(1)
        DO 30 I=2,NPTS
          IF(X(I).LT.XMIN) XMIN=X(I)
          IF(X(I).GT.XMAX) XMAX=X(I)
          IF(Y(I).LT.YMIN) YMIN=Y(I)
          IF(Y(I).GT.YMAX) YMAX=Y(I)
 30     CONTINUE
C
C     FIND THE PROPER AXIS SCALING
C
        XRIGHT = XMAX + 0.05*(XMAX-XMIN)
        XLEFT = XMIN - 0.05*(XMAX-XMIN)
        XRANGE = XRIGHT - XLEFT
C
        YTOP = YMAX + 0.05*(YMAX-YMIN)
        YBOT = YMIN - 0.05*(YMAX-YMIN)
        IF(YBOT.LT.0.0) YBOT=0.0
        YRANGE = YTOP - YBOT
C
C     ADJUST X AND Y VALUES
C
        DO 50 I=1,NPTS
          XPLOT(I) = 1.5 + 9.0*(X(I)-XLEFT)/XRANGE
          YPLOT(I) = 1.5 + 7.0*(Y(I)-YBOT)/YRANGE
 50     CONTINUE
C
        CALL SYSTEM('CLS')
        CALL NEWPEN(2)
C
C     NUMBER TICK MARKS
C
        DO 80 I=0,3
        YTICK=YBOT+I*(YRANGE/3.0)
        XTICK=XLEFT+I*(XRANGE/3.0)
        WRITE(9,70) YTICK,XTICK
  70    FORMAT(F5.0,F6.4)
  80    CONTINUE
        CLOSE(9)
C
        OPEN(UNIT=9, FILE=FILE6, STATUS='UNKNOWN')
        DELX=22
        DELY=8
```

```
        DO 90 I=0,3
        READ(9,85) CYTICK, CXTICK
 85     FORMAT(A4,1X,A6)
        CALL GTEXT(26,(8+I*DELX),CXTICK)
        CALL GTEXT((24-I*DELY),5,CYTICK)
 90     CONTINUE
C
C     DRAW GRAPH BORDER AND TICK MARKS
C
        CALL PLOT(1.5, 1.5, 3)
        CALL PLOT(10.5, 1.5, 2)
        CALL PLOT(10.5, 8.5, 2)
        CALL PLOT(1.5, 8.5, 2)
        CALL PLOT(1.5, 1.5, 2)
C
        CALL PLOT(1.5,1.5,3)
        CALL PLOT(1.5,1.4,2)
        CALL PLOT(4.5,1.5,3)
        CALL PLOT(4.5,1.4,2)
        CALL PLOT(7.5,1.5,3)
        CALL PLOT(7.5,1.4,2)
        CALL PLOT(10.5,1.5,3)
        CALL PLOT(10.5,1.4,2)
C
        CALL PLOT(1.5,1.5,3)
        CALL PLOT(1.4,1.5,2)
        CALL PLOT(1.5,3.833,3)
        CALL PLOT(1.4,3.833,2)
        CALL PLOT(1.5,6.167,3)
        CALL PLOT(1.4,6.167,2)
        CALL PLOT(1.5,8.5,3)
        CALL PLOT(1.4,8.5,2)
C
C     LABEL AXES
C
        CALL GTEXT(11,0,'PRESSURE')
        CALL GTEXT(13,2,'psia')
C
        IF(OPT.EQ.1) THEN
          CALL GTEXT(27,37,'LIQUID DENSITY')
        ENDIF
C
        IF(OPT.EQ.2) THEN
          CALL GTEXT(27,38,'VAPOR DENSITY')
        ENDIF
C
        IF(OPT.EQ.3) THEN
          CALL GTEXT(27,36,'PHASE DENSITIES')
        ENDIF
C
        IF(OPT.EQ.4) THEN
          CALL GTEXT(27,35,'LIQUID COMPOSITION')
        ENDIF
C
        IF(OPT.EQ.5) THEN
          CALL GTEXT(27,35,'VAPOR COMPOSITION')
        ENDIF
C
        IF(OPT.EQ.6) THEN
          CALL GTEXT(27,35,'PHASE COMPOSITIONS')
```

```
        ENDIF
C
C     PLOT THE DATA POINTS
C
        DO 100 I=1,NPTS
          CALL CIRCLE(XPLOT(I),YPLOT(I),0.05)
 100    CONTINUE
C
 110    CALL GTEXT(29,31,'(Press any key to continue)')
        IX = IXKEY()
C
        CALL SYSTEM('CLS')
        CALL TITLE
        RETURN
        END
```

APPENDIX B

ADDITIONAL COMPARISONS FOR CARBON DIOXIDE + TRANS-DECALIN PHASE DENSITIES AND COMPOSITIONS

The comparisons of the data of this work and those of Gasem, et al. (11) for CO_2 + *trans*-decalin mixtures at 344.3 K (160 °F) described in Chapter IV were repeated here using a different procedure to investigate the behavior of the two data sets in the near-critical region. The comparisons shown in Figures 32-35 were done by fitting both data sets simultaneously to the extended scaling equation (Equation (18)). The resulting smoothing function represents a compromised fit for both data sets and may distort comparisons in the near-critical region. The coefficients given in Table XVII based on the data of this work were used for a second comparison given here.

The deviations of each data set from Equation (18) are shown in Figures B.1 through B.4 where the value for the critical pressure used for each data set is the one determined as optimum for that data set (2280 psia for the data of this work and 2297 for that of Gasem, et al.). Figure B.1 indicates that the liquid densities for the two data sets exhibit different scaling behavior near the critical region. Vapor phase densities shown in Figure B.2 show similar behavior for both data sets. As with the liquid densities, the liquid compositions shown in Figure B.3 indicate different behavior as the critical point is approached. Figure B.4 illustrates the magnitude of the difference in vapor phase compositions of the two data sets. As discussed previously, modifications have been made to the sampling valve system which provide more reliable vapor phase compositions than past work. This may explain the observed difference in vapor phase compositions.

Figures B.1 through B.4 provide further evidence that the observed differences in the two data sets are more than that caused by the measurement of different critical pressures. The old data was collected

with an interfacial tension cell which contained several Viton O-rings. During testing done after the older data was collected, discoloration of the *trans*-decalin was observed due to the presence of these O-rings (32) which may represent a source of contamination. The experimental system of this work contained only teflon O-rings to eliminate this contamination problem.

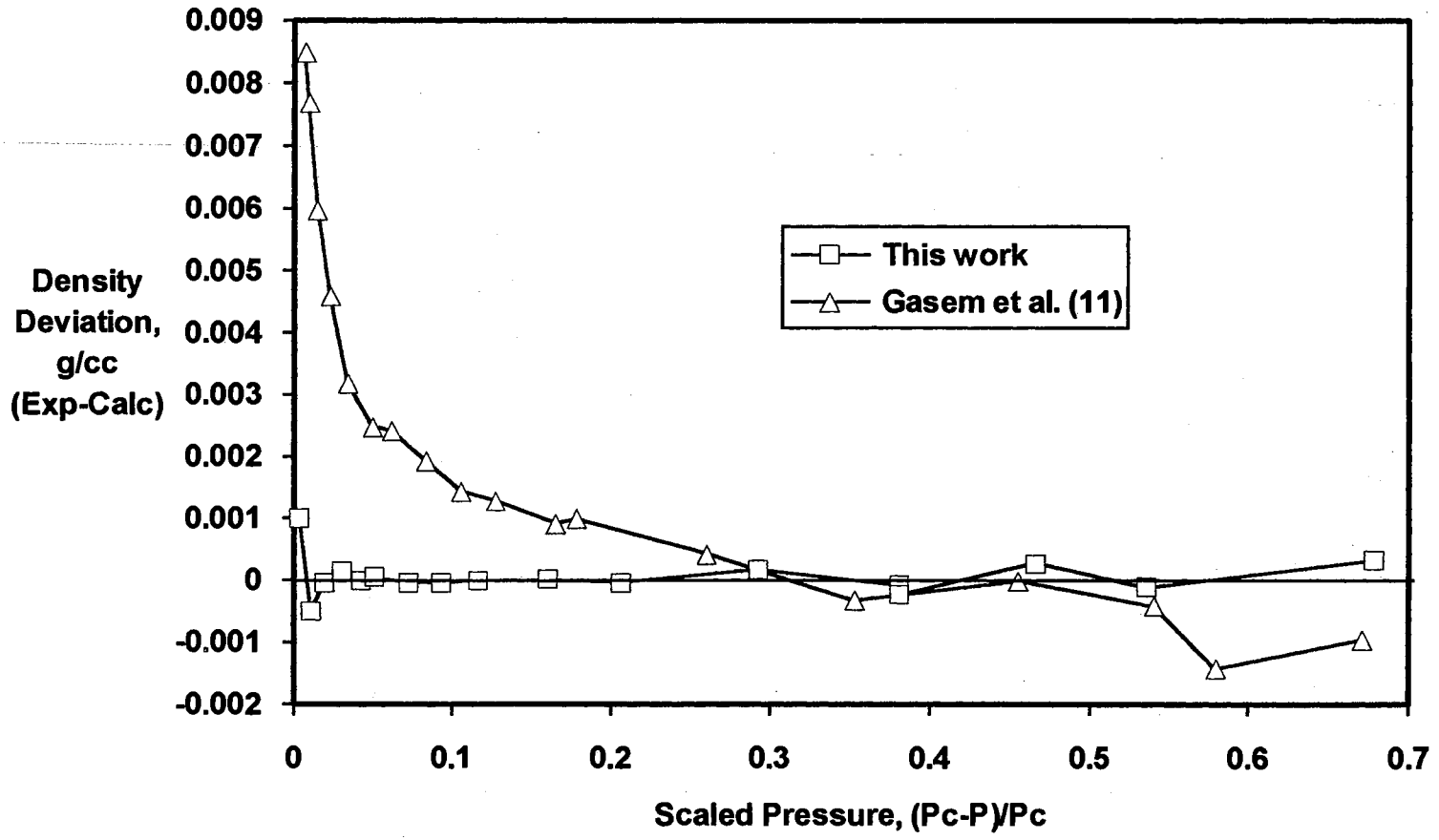

Figure B.1. Comparison of Liquid Phase Density Data for CO_2 + *trans*-Decalin Shown at Equal Values of Scaled Pressures

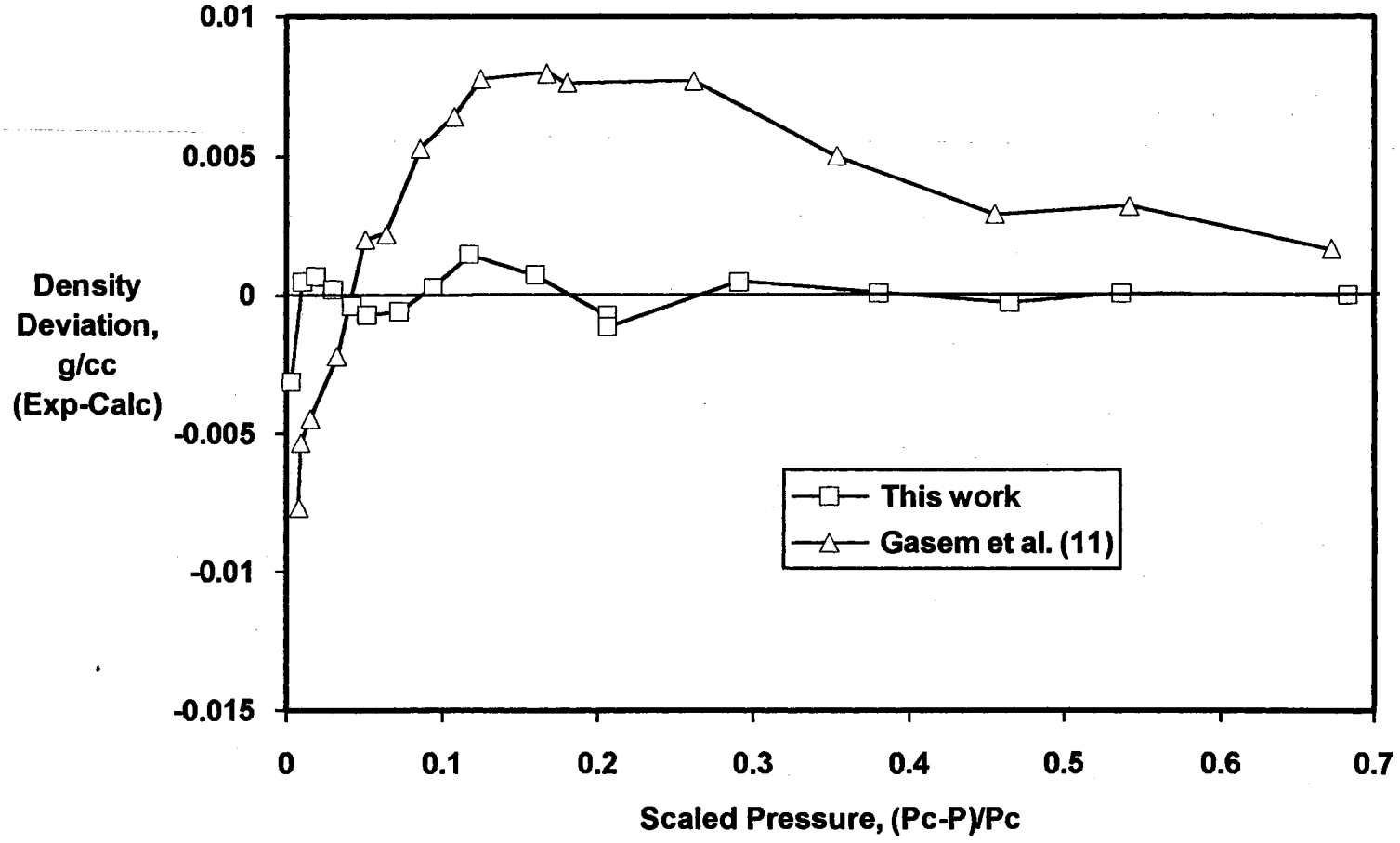

Figure B.2. Comparison of Vapor Phase Density Data for CO_2 + *trans*-Decalin Shown at Equal Values of Scaled Pressures

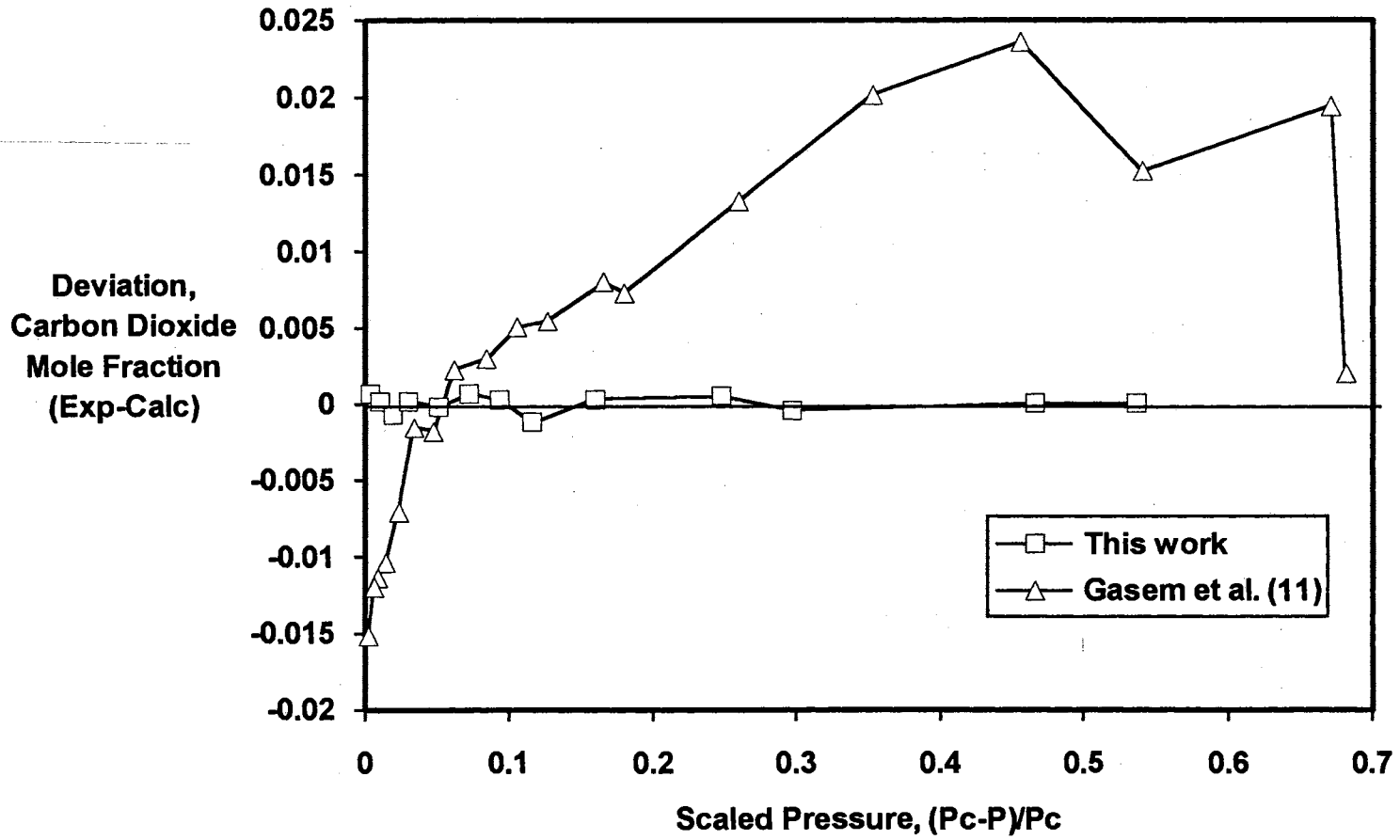

Figure B.3. Comparison of Liquid Phase Composition Data for CO_2 + *trans*-Decalin Shown at Equal Values of Scaled Pressures

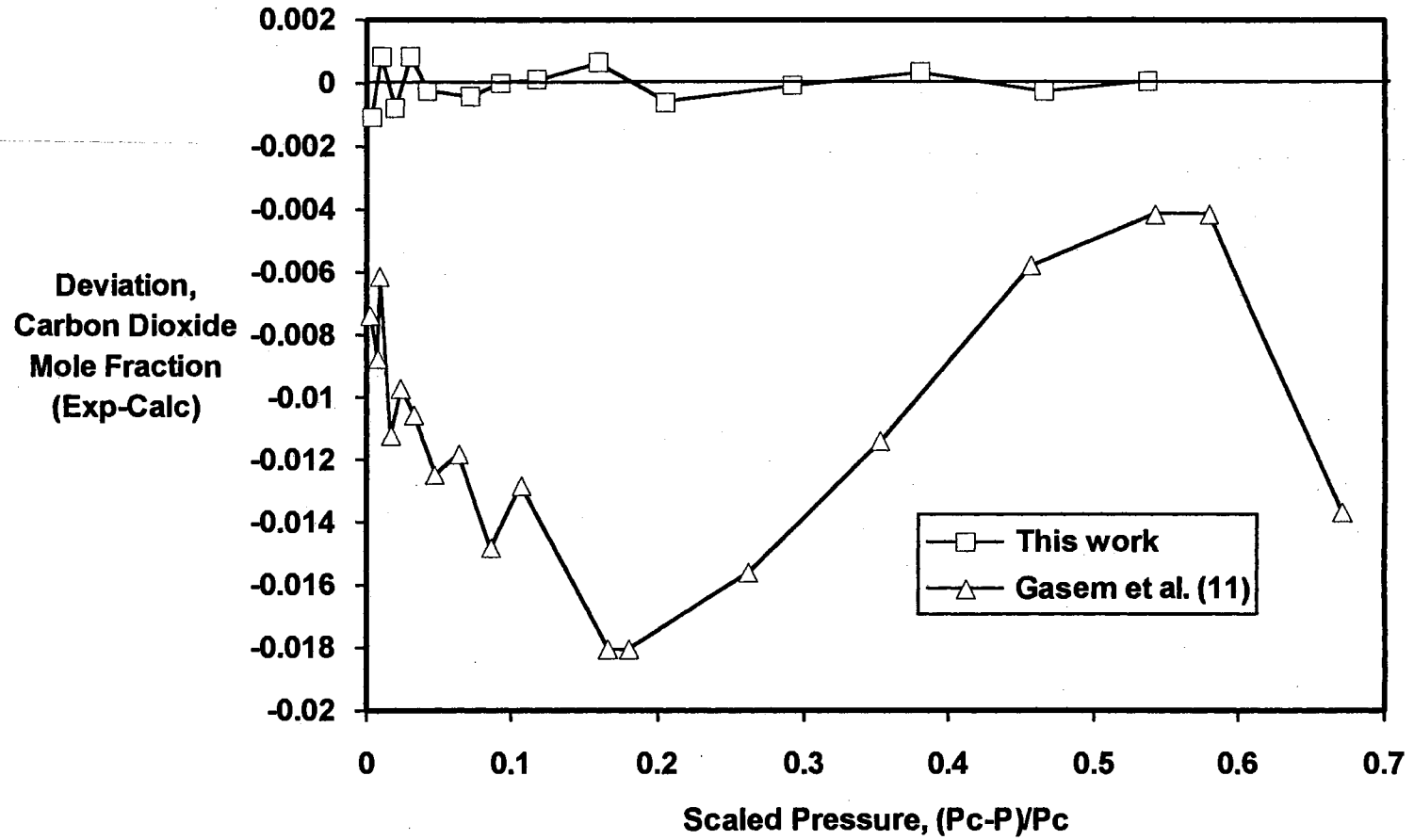

Figure B.4. Comparison of Vapor Phase Composition Data for CO_2 + *trans*-Decalin Shown at Equal Values of Scaled Pressures

SECTION 2 - EQUATION OF STATE MODIFICATIONS

CHAPTER I

INTRODUCTION

The accurate prediction of thermodynamic properties is essential in nearly every area of chemical engineering. The most convenient form for representation of equilibrium phase behavior for process design and optimization calculations has long been recognized as that of analytic equations of state (1-3). Historically, the most commonly used equations of state are the cubic van der Waals type equations such as the Peng-Robinson (PR) and the Soave-Redlich-Kwong (SRK) equations. While cubic equations are capable of representing the essential qualitative features of vapor-liquid systems, their largely empirical nature limits the interpretation that can be placed upon their equation parameters. These commonly used cubic equations suffer from several shortcomings including the inability to describe mixtures containing molecules with large variation in size, the inability to adequately describe mixtures of polar and associating molecules, the inability to properly handle mixtures of polymeric compounds, and the restricted range of use due to improper limiting behavior at high temperatures (4).

In order to overcome some of these deficiencies and to develop a theoretically based equation of state capable of representing both vapor and liquid phases, Beret and Prausnitz (5) and Donohue and Prausnitz (6) developed the perturbed-hard-chain theory (PHCT). The PHCT helps to

bridge the gap between conventional equations of state and those used for representation of polymeric liquids. Since the development of the original PHCT equation, a number of similar equations based on the same theoretical structure have been proposed and tested (7-14,28). The most widely used and studied is the one proposed by Kim, et al. (7) known as the simplified-perturbed-hard-chain theory (SPHCT) equation of state. The SPHCT equation of state has two main advantages over the cubic equations. First, its foundation in statistical thermodynamics makes the assumptions made during its development clear in terms of molecular behavior. Second, molecular interactions are modeled as segment-segment interactions rather than the simpler molecule-molecule interactions of the cubic equations.

Aside from its expected limitations of addressing only normal fluids, the SPHCT equation suffers from several disadvantages which hinder its use in engineering calculations. Although the equation of state parameters represent specific molecular characteristics, they are not directly related to any physical properties. This makes them obtainable only from regression of experimental data and the values thus obtained are highly dependent upon the method used for generating them. This poor parameterization coupled with the fact that the equation of state is fifth-order in volume makes numerical implementation of equilibrium calculations difficult. Like most analytic equations of state, the equation is not constrained to predict the proper behavior near the vapor-liquid critical point, thus resulting in excessive errors in calculated vapor pressures and saturated densities in the near-critical region.

The goal of this work was to address these limitations of the SPHCT equation and to explore possible modifications to the equation to improve its performance. The specific objectives were as follows:

1. Investigate the sensitivity of calculated properties to the equation of state parameters. This is done to identify which parameters have the largest influence on calculated properties and to investigate the possibility of introducing temperature and/or density dependence to the parameters or altering the functional form of the equation to better describe experimental data.
2. Investigate the results of applying the critical point constraints to the SPHCT equation to improve near-critical property predictions and to define some (or all) of the equation of state parameters in terms of critical point constants.
3. Investigate various strategies of volume translation to improve saturated density predictions over the entire range of the saturation curve.
4. Demonstrate the usefulness of the proposed changes to the SPHCT equation through the prediction of pure fluid saturation properties and determine the extent to which the proposed modifications can be used to represent mixture equilibrium and volumetric properties.

Chapter II of this section presents a review of the historical development of the SPHCT equation of state, a review of the derivation of the form of the equation and a review of various volume translation strategies. Chapter III contains discussions of the modifications of the SPHCT equation that were investigated. Chapter IV presents the

results and comparisons of the various EOS modifications studied for both pure fluids and mixtures, and Chapter V contains conclusions and recommendations for the current EOS work.

CHAPTER II

LITERATURE REVIEW

Review of SPHCT Development

The most convenient form for representation of equilibrium phase behavior for process design and optimization calculations has long been recognized as that of analytic equations of state (1-3). In general, equations of state can be classified as either empirical or theoretical, although some equations based partially in theory are sometimes referred to as semiempirical or semitheoretical (5). While there are many empirical equations of state (15-16) there are relatively few which have a firm basis in theory. Probably the best known theoretical equation is the virial equation of state (17) which has limited engineering use since it is applicable only to low to moderate density vapors.

The development of most other theoretically based equations has essentially occurred on one of two paths. The first approach has dealt mostly with simple nonpolar fluids such as argon which can be described as nonattracting rigid spheres (18). Equations developed from these theories that are capable of describing more realistic fluid behavior are referred to as perturbed-hard-sphere equations (19). The other approach has been developed by physical and polymer chemists to describe the behavior of very large molecules at liquid densities. The most well known work in this area is that done by Prigogine (20) and Flory (21). Most of these types of equations incorporate the simplifying assumption

first proposed by Prigogine that density dependent degrees of freedom can be treated as equivalent translational degrees of freedom at high densities although others have developed similar equations using different arguments (31). Although these models have proven very useful for describing liquids, some (such as the one proposed by Flory (21)) are qualitatively incorrect at low densities since they do not correctly approach the ideal-gas law at zero density (5).

In the mid-1970's, Beret and Prausnitz developed the perturbed-hard-chain theory (PHCT) to bridge the gap between these two types of equations. Later, Donohue and Prausnitz (6) extended the PHCT for the prediction of multicomponent mixture properties. The PHCT equation is applicable to both liquid and gas phases for compounds ranging in structural complexity from methane to heavy hydrocarbons and polymers. Its utility has been demonstrated by several researchers. Kaul and coworkers (22) showed that Henry's constants can be predicted with the PHCT equation with small values for binary interaction parameters, and Liu and Prausnitz (23) demonstrated that the solubilities of gases in liquid polymers where the gas is a supercritical component can be predicted using the PHCT equation.

One drawback of the PHCT equation is that the partition function used to derive the equation is quite complex. This is because the attractive term of the PHCT equation uses the molecular dynamics results of Alder (24) for square-well molecules. The resulting expression for pressure is a series expansion in both density and inverse temperature making computer calculations cumbersome. In 1986, Kim (25) proposed a simplification to the PHCT equation by replacing the attractive portion of the partition function with the model of Lee, Lombardo and Sandler

(26). Kim's equation results in an attractive term with a much simpler density and temperature dependence than the original PHCT equation making it more convenient for engineering calculations.

Since its introduction, the simplified-perturbed-hard-chain theory (SPHCT) equation of state has been studied by several investigators (1-4). Georgeton and Teja (27) developed a group contribution equation of state based on the SPHCT equation which can predict multicomponent phase equilibria using group contribution interaction parameters. Ponce-Ramirez, et al. (2) applied the SPHCT equation to the prediction of phase equilibria of CO_2-hydrocarbon systems and showed that bubble point pressures can be predicted for these systems with average errors of less than 5%. Gasem and Robinson (1) evaluated the SPHCT equation for the prediction of phase behavior of n-paraffins and mixtures of n-paraffins with ethane and showed that comparable predictions of phase compositions can be obtained from the SPHCT and the SRK equations, with the SPHCT equation providing better results for the heavier n-paraffins. Similarly, Garcia-Sanchez, et al. (29) showed that the SPHCT equation can be used for the prediction of critical points for reservoir fluid systems.

Through the work of other investigators, several difficulties in using the SPHCT equation can be stated. First, optimization schemes used in obtaining the pure fluid equation of state parameters are very sensitive to the initial estimates of the equation parameters. Ponce-Ramirez, et al. (2) describe a procedure which utilizes two conditions at the fluid critical point and the reference pressure defining the acentric factor to obtain initial parameter estimates for their optimizations. Second, systematic errors have been observed for vapor

pressure and liquid density predictions for pure fluids near both the triple point and the critical temperatures (1). Such errors have been attributed in part to poor characterization of the equation of state parameters, and tend to make optimization of EOS parameters difficult. Lastly, implementation of the equation is difficult because liquid roots for the equation are hard to obtain. Thus, a robust solution algorithm is required for obtaining the correct vapor and liquid roots for reliable operation, especially when EOS parameters are being optimized or when modifications to the equation are being investigated. All of these difficulties are addressed in the chapters that follow.

The SPHCT Equation of State

The necessary equations for relating the canonical partition function of statistical thermodynamics to classical thermodynamics are as follows (19):

$$A = -kT \ln(Q) \tag{1}$$

$$P = -\left(\frac{\partial A}{\partial V}\right)_{T,N} = kT\left(\frac{\partial \ln(Q)}{\partial V}\right)_{T,N} \tag{2}$$

$$U = kT^2\left(\frac{\partial \ln(Q)}{\partial T}\right)_{N,V} \tag{3}$$

where Q is the canonical partition function, A is the Helmoltz energy, k is Boltzmann's constant, T is absolute temperature, V is total volume, N is the number of molecules, P is pressure and U is internal energy. The partition function can be written as a sum over all possible energy states for a collection of N molecules as

$$Q(N, V, T) = \sum_i e^{-E_i(N,V)/kT} \tag{4}$$

Assuming that the different modes of molecular energy can be separated, the partition function for a pure fluid can be written as

$$Q = \frac{1}{N!}(q_t)^N(q_{rep})^N(q_{att})^N(q_{r,v})^N f(T) \tag{5}$$

where q_t represents the molecular translation contribution to the partition function, q_{rep} represents the contribution due to molecular repulsions, q_{att} represents the contribution due to molecular attractions and $q_{r,v}$ is that due to molecular rotations and vibrations.

The function f(T) includes all other forms of molecular energies (such as electronic and nuclear spin energies) which are functions only of temperature and which do not contribute to the equation of state as indicated by Equation (2). The translational portion of the partition function, q_t, can be shown (30) to be

$$q_t = \left(\frac{1}{\Lambda^3}\right) \tag{6}$$

where Λ is the de Broglie wavelength given by

$$\Lambda = \frac{h}{\sqrt{2\pi mkT}} \tag{7}$$

The repulsive portion of the partition function, q_{rep}, is dominated by the infinite intermolecular potential energy at small molecular separations and is given by

$$q_{rep} = V_f \tag{8}$$

where V_f is the free volume that is available to the center of a molecule as it moves among all other molecules in a container. The attractive portion of the partition function is

$$q_{att} = \exp\left(\frac{-\phi}{2kT}\right) \tag{9}$$

where $\phi/2$ is the intermolecular potential energy of a single molecule due to the presence of all other molecules. Combining all of the terms, the partition function can be written as

$$Q = \frac{1}{N!}\left(\frac{V}{\Lambda^3}\right)^N\left(\frac{V_f}{V}\right)^N\left(\exp\frac{-\phi}{2kT}\right)^N\left(q_{r,v}\right)^N f(T) \tag{10}$$

For a polyatomic molecule, some of the rotational and vibrational degrees of freedom are dependent upon density as well as temperature so the $q_{r,v}$ term is factored as

$$q_{r,v} = (q_{r,v})_{ext}(q_{r,v})_{int} \tag{11}$$

where $(q_{r,v})_{ext}$ represents the external (density dependent) terms and $(q_{r,v})_{int}$ represents the internal (density independent) terms. Following Prigogine and others (5-10,20) the assumption is made that the contributions to the partition function for external rotational and vibrational degrees of freedom can be treated as equivalent translational motions. Since there are three translational degrees of freedom, each degree of freedom contributes

$$\left(\frac{V_f}{V}\right)^{1/3} \tag{12}$$

to the free volume expression of the partition function. Defining 3c as the total number of degrees of freedom that are density dependent and that affect the free volume expression of a polyatomic molecule, $(q_{r,v})_{ext}$ can be expressed as

$$(q_{r,v}) = \left(\frac{V_f}{V}\right)^{\frac{3c-3}{3}} = \left(\frac{V_f}{V}\right)^{c-1} \tag{13}$$

The $(q_{r,v})_{int}$ term is a function of temperature only and is therefore included in f(T). The partition function can now be written as

$$Q = \left(\frac{1}{N!}\right)\left(\frac{V}{\Lambda^3}\right)^N\left(\frac{V_f}{V}\right)^{Nc}\left(\exp\frac{-\phi}{2kT}\right)^N f(T) \tag{14}$$

Combining the attractive term with the free volume term and eliminating f(T) since it does not contribute to the equation of state, the canonical ensemble partition function for chain-like molecules used by Kim et al. (7,25) can be produced.

$$Q = \left(\frac{1}{N!}\right)\left(\frac{V}{\Lambda^3}\right)^N \left(\frac{V_f}{V} \exp\frac{-\phi}{2ckT}\right)^{Nc} \tag{15}$$

At this point some mention of the different interpretations of the parameter c is worthwhile. As shown here, the original developers of the perturbed-hard-chain theories viewed 3c as the total degrees of freedom that can be represented as translational motions (5-7). This interpretation requires that for a spherical molecule such as argon or methane (with no external rotational or vibrational degrees of freedom) c should be equal to one. Hall and coworkers (31-33) have derived continuous-space analogs of the Flory lattice theory in which c represents the ratio of the excluded volume of the molecule to the excluded volume of one molecular segment ($v_e(n)/v_e(1)$). Again, in this interpretation c is one for spherical molecules which contain only one segment. A possible advantage to this view is that c can be estimated by geometrical considerations alone (13,31). Both interpretations agree that c should equal one for spherical molecules, should be greater than one for all other molecules and should be proportional to the number of molecular segments comprising a single molecule.

The expression used for the free volume term in the partition function is the Carnahan-Starling (18) equation:

$$\ln\left(\frac{V_f}{V}\right) = \frac{3(\tau\tilde{\rho})^2 - 4(\tau\tilde{\rho})}{(1-\tau\tilde{\rho})^2} \tag{16}$$

with

$$\tau = \frac{\pi\sqrt{2}}{6} = 0.7405 \tag{17}$$

$$\tilde{\rho} = \frac{v^*}{v} \tag{18}$$

where τ is a geometrical constant, v^* is a characteristic volume defined as

$$v^* = \frac{N_a s_i \sigma_{ii}^3}{\sqrt{2}} \tag{19}$$

in which N_a is Avogodro's number, s_i is the number of molecular segments in a single molecule and σ_{ii} is the hard-core diameter of a segment.

In the original PHCT equation, the molecular dynamics results of Alder for square-well molecules (24) were used for the attractive term, $\phi/2ckT$. Alder's equation is an expansion in both inverse temperature and in density, thus making computations cumbersome. In 1986, Kim (25) proposed a simplification to the PHCT equation by using the simpler model of Lee, Lombardo and Sandler (26) for the attractive term. Kim (25) showed that an expression for the attractive portion of the partition function can be written in terms of the coordination number, N_c as

$$\frac{-\phi}{2ckT} = \int_{T=\infty}^{T} \frac{E^{CONF}}{kT^2}\,dT = \frac{1}{2}\int_{\frac{1}{\tilde{T}}=0}^{\frac{1}{\tilde{T}}} N_c(\rho, T)\,d\left(\frac{1}{\tilde{T}}\right) \tag{20}$$

with

$$\tilde{T} = \frac{T}{T^*} = \frac{ckT}{\varepsilon q} \tag{21}$$

where T* is a characteristic temperature, ε is a characteristic intermolecular interaction energy per unit external surface area and q is the external surface area of the molecule. N_c is the number of segments within the interaction range of a given segment of a molecule.

For a square-well potential model this interaction range is between σ and Rσ and is given by

$$N_c = \frac{N}{V} \int_{\sigma}^{R\sigma} g(r;\rho,T) s 4\pi r^2 dr \tag{22}$$

in which g(r) is the molecular radial distribution function which is a function of both temperature and density. An approximate expression for the coordination number, N_c, is obtained by considering the lattice model of Lee, et al. (26) and Kim (25). The lattice is imagined to contain two components: square-well molecular segments (labeled 1) and holes (labeled 0). As shown by Bokis et al. (34), the distribution of the two components about a central segment can be given by the local composition model

$$\frac{N_{01}}{N_{11}} = \frac{N_0}{N_1} \frac{\sigma_{01}^3}{\sigma_{11}^3} \frac{\int_1^{R_{01}} g_{01} 4\pi\tilde{r}^2 d\tilde{r}}{\int_1^{R_{11}} g_{11} 4\pi\tilde{r}^2 d\tilde{r}} \tag{23}$$

where N_{ij} is the number of segments of species i surrounding a central segment of species j, N_i is the total number of segments of species i, $\tilde{r} = r / \sigma$ and σ_{ij} is the hard core diameter for a species i interacting with species j. A maximum coordination number can be defined as

$$N_{11} + N_{01} = Z_M \tag{24}$$

Recognizing that N_{11} is the same as N_c, the coordination number can then be written as (34)

$$N_c \equiv N_{11} = \frac{Z_M}{1 + \frac{N_0}{N_1}\Psi} \tag{25}$$

where Ψ is given by

$$\Psi = \frac{\sigma_{01}^3}{\sigma_{11}^3} \frac{\int_1^{R_{01}} g_{01}\, 4\pi\tilde{r}^2 d\tilde{r}}{\int_1^{R_{11}} g_{11}\, 4\pi\tilde{r}^2 d\tilde{r}} \tag{26}$$

Lee, et al. (26) and Kim (25) assumed that

$$g_{ij} = g_{ij}^0 e^{-\varepsilon q/2ckT} \tag{27}$$

where g_{ij}^0 is the hard-core radial distribution function. They also assumed that the density dependence of the ratio of the integrals in the above equation cancel out. Since for a lattice model $\sigma_{01} = \sigma_{11}$ the equation they arrived at was

$$\Psi = \exp\left(\frac{-\varepsilon q}{2ckT}\right) \tag{28}$$

The close-packed molar volume, v*, defined earlier can be used to relate the ratio of N_0 to N_1 as

$$\frac{N_0}{N_1} = \frac{v - v^*}{v^*} \tag{29}$$

and, thus the coordination number is found to be

$$N_c = \frac{Z_M v^*(Y+1)}{v + v^* Y} \tag{30}$$

where

$$Y = \exp\left(\frac{\varepsilon q}{2ckT}\right) - 1 \tag{31}$$

Combining Equation (30) with Equation (20) to produce an expression for the attractive portion of the partition function, the equation of state obtained is

$$z = 1 + c(z^{rep} + z^{att}) \tag{32}$$

where

$$z = \frac{Pv}{RT} \tag{33}$$

$$z^{rep} = \frac{4(\tau\tilde{\rho}) - 2(\tau\tilde{\rho})^2}{(1-\tau\tilde{\rho})^3} \tag{34}$$

$$z^{att} = -\frac{Z_M c v^* Y}{cv + cv^* Y} \tag{35}$$

$$Y = \exp\left(\frac{1}{2\tilde{T}}\right) - 1 \tag{36}$$

For mixtures, the same pure fluid partition function is used and pseudo-pure compounds are defined by the following mixing rules:

$$\langle c \rangle = \sum_i x_i c_i \tag{37}$$

$$\left\langle v^* \right\rangle = \sum_i x_i v_i^* \tag{38}$$

$$\left\langle cv^* Y \right\rangle = \sum_i \sum_j x_i x_j c_i \left[\exp\left(\frac{\varepsilon_{ij} q_i}{2 c_i kT} \right) - 1 \right] \frac{s_j \sigma_{ij}^3}{\sqrt{2}} \tag{39}$$

$$\varepsilon_{ij} = \sqrt{(\varepsilon_{ii} \varepsilon_{jj})}(1 - C_{ij}) \tag{40}$$

$$\sigma_{ij} = \frac{\sigma_{ii} + \sigma_{jj}}{2} \tag{41}$$

where C_{ij} is a binary interaction parameter.

Volume Translation Strategies

In general, equations of state can be applied to vapor and liquid phases to calculate both equilibrium and volumetric properties. However, most equations of state show moderate success in calculation of phase densities without additional EOS tuning (36). As first pointed out by Martin (15), certain translations can be done along the volume axis which leave the predicted equilibrium conditions unchanged. Peneloux, et al. (37) proposed a simple correction for the SRK equation which vastly improves volume estimations except near the vapor-liquid critical point. Chou and Prausnitz (38) introduced a more complicated phenomenological correction for volumetric predictions of the SRK equation which can be used near the vapor-liquid critical point. Sudibandriyo (36) extended a scaled-variable-reduced-coordinate correlation framework (78) for the prediction of CO_2 + hydrocarbon phase densities and developed a volume translation strategy that properly obeys scaling laws in the near-critical region.

As shown by Peneloux (37), any translation in volume which is only a function of temperature and which translates the vapor and liquid phase volumes by the same amount does not affect the EOS equilibrium calculations. Equilibrium conditions are found by determining the conditions under which component fugacities in each phase are equal. An expression for the fugacity coefficient is given by

$$\ln \phi_i = \int_0^P \left(\frac{v_i}{RT} - \frac{1}{P} \right) dP \qquad (42)$$

where v_i is the partial molar volume,

$$v_i = \left(\frac{\partial V}{\partial n_i}\right)_{T,P,n_j} \tag{43}$$

The condition of equal component fugacities at equilibrium is given by

$$x_i'\phi_i' = x_i''\phi_i'' \tag{44}$$

where ' and " represent two different phases. Any translation in volume such as

$$V = V_{EOS} + \sum_i c_i n_i \tag{45}$$

in which V_{EOS} is the volume calculated from the untranslated equation of state and c_i is a function only of temperature will not affect the equilibrium calculations. The partial molar volume as calculated from the above equation is

$$\tilde{v}_i = v_i + c_i \tag{46}$$

and the fugacity coefficient is given by

$$\ln \tilde{\phi}_i = \int_0^P \left(\frac{\tilde{v}_i}{RT} - \frac{1}{P}\right) dP = \ln \phi_i + c_i \frac{P}{RT} \tag{47}$$

Thus, the equal fugacity expression becomes

$$x_i'\phi_i' \exp\left(\frac{c_i P}{RT}\right) = x_i''\phi_i'' \exp\left(\frac{c_i P}{RT}\right) \tag{48}$$

and the translation term cancels out. The translations used by Martin (15) and Peneloux (37) are done with the c_i's obtained from a correlation with the Rackett compressibility factor, Z_{RA} (37). Chou and Prausnitz (38) proposed a more complicated translation which still

satisfies the above equilibrium conditions. In their approach, a dimensionless distance parameter is defined as

$$d = \frac{1}{RT_c}\left(\frac{\partial p^{EOS}}{\partial \rho}\right)_T \tag{49}$$

and volume translations are done according to

$$\tilde{v} = v - c - \delta_c\left(\frac{\eta}{\eta + d}\right) \tag{50}$$

in which

$$\delta_c = \frac{RT_c}{P_c}(z_c^{EOS} - z_c) \tag{51}$$

and η is a universal constant determined from the regression of pure fluid density data. This type of translation forces the equation of state to correctly predict the experimental critical point and allows for a volume translation which is implicitly a function density. Chou and Prausnitz (38) also included a near-critical correction to flatten the coexistence curve near the critical point. They assumed that the residual Helmoltz energy can be expressed as the sum of a classical contribution and a non-classical contribution as

$$A^r = A^c + A^{nc} \tag{52}$$

where the classical portion, A^c, is obtained from the original EOS and the non-classical portion, A^{nc}, is obtained from the expression

$$\frac{A^{nc}}{RT_c} = A_m^{nc}\exp\left(-wD^2\right) \tag{53}$$

where A_m^{nc} and w are constants obtained from regression of pure fluid data and D is obtained by dividing d of Equation (49) by the reduced density, ρ/ρ_c,

$$D = \frac{1}{\rho}\left(\frac{\partial P^{EOS}}{\partial \rho}\right)_T\left(\frac{\rho_c}{RT_c}\right) \tag{54}$$

Chou and Prausnitz (38) showed that the resulting volumetric predictions are improved significantly using this approach. They also extended their approach for the prediction of mixture properties and demonstrated considerable improvement in mixture volumetric property predictions.

CHAPTER III

EQUATION OF STATE MODIFICATIONS

The simplified-perturbed-hard-chain theory (SPHCT) equation of state described in Chapter II of Section 2 has been shown to be useful for engineering applications (1-3,25). However, the SPHCT EOS suffers from several disadvantages. First, like all analytic equations of state, vapor pressure and saturated density predictions near the vapor-liquid critical point are poor (5). Although the SPHCT has been used for prediction of vapor pressures near the critical point (3), previous work was limited to pure components in the reduced temperature range $0.75<T/T_c<1$ and did not address the deficiencies of predicted saturated vapor and liquid densities in this region. The SPHCT equation has also been shown to be capable of predicting critical points for reservoir oil fluid systems (29) with results comparable to those of the SRK equation. Second, the SPHCT equation has been shown, in general, to be less accurate than the SRK equation for the prediction of pure fluid vapor pressures (1). The goal of the current work was to improve the vapor pressure and saturated density predictions of the SPHCT equation both near and far from the vapor-liquid critical point for both pure fluid and mixture calculations.

The strategy for EOS modifications consisted of five steps. As discussed earlier, a robust solution algorithm is required for obtaining the proper vapor and liquid roots during parameter regressions.

Therefore, the first step was to develop a reliable EOS solution strategy. Second, a study of the existing EOS parameters was done to lend insight into the sensitivity of EOS calculations to parameter values and to perform a preliminary investigation of the temperature dependence of the model parameters. Third, the effect of constraining the SPHCT equation at the critical point using the classical requirements of setting the first and second derivatives of pressure with respect to volume equal to zero at the critical point along the critical isotherm was investigated. Fourth, volume translation strategies of the type described in Chapter II were tested to develop a viable approach for improving saturated vapor and liquid density predictions. Finally, knowledge gained from the first three steps was used to propose a modification to the temperature-dependent portion of the attractive term in the SPHCT equation. The results of the proposed EOS modifications were then compared to the original SPHCT equation and to the Peng-Robinson equation for 23 pure fluids and a number of mixtures comprising ethane + n-paraffin and CO_2 + n-paraffin systems. Following are sections describing each phase of the study described above and results of the proposed EOS changes.

Equation of State Solution Algorithm

In order to successfully investigate the behavior of the SPHCT equation of state and any modifications thereof, a robust routine was required for obtaining the proper vapor and liquid roots at a given temperature and pressure. As mentioned by other workers (2), optimization of the SPHCT parameters is quite sensitive to the EOS parameters and a reliable solution algorithm is essential. The

conventional method for obtaining the proper vapor and liquid volumes of an equation of state is to express the equation in terms of compressibility factor and define a function such that the proper roots correspond to a function value of zero (52,53). For the Soave-Redlich-Kwong (SRK) equation the equation of state and function F1(z) are given as

$$P = \frac{RT}{v - b} - \frac{a\alpha}{v(v + b)} \tag{55}$$

and

$$F1(z) = z^3 - z^2 + z(A - B - B^2) - AB \tag{56}$$

where $A = \frac{aP}{RT^2}$ $\quad B = \frac{bP}{RT}$

and a and b are equation of state parameters. Sudibandriyo (36) discusses several commonly used solution algorithms for determining the proper roots of Equation (56) and provides helpful information on how to properly define the feasible solution domain.

The SPHCT equation can be expressed in a similar fashion in the form

$$F1(z) = z^5 + Az^4 + Bz^3 + Cz^2 + Dz + E = 0 \tag{57}$$

where A, B, C, D and E are coefficients dependent only on the EOS parameters and the temperature and pressure. Figure 1 shows the function F1(z) for both the SRK and the SPHCT equations for methane at 150 K. The proper vapor root is obvious at a compressibility near 1.0. However, the scale must be expanded to reveal the liquid roots for the two equations. Figure 2 shows an enlarged view of the lower range of

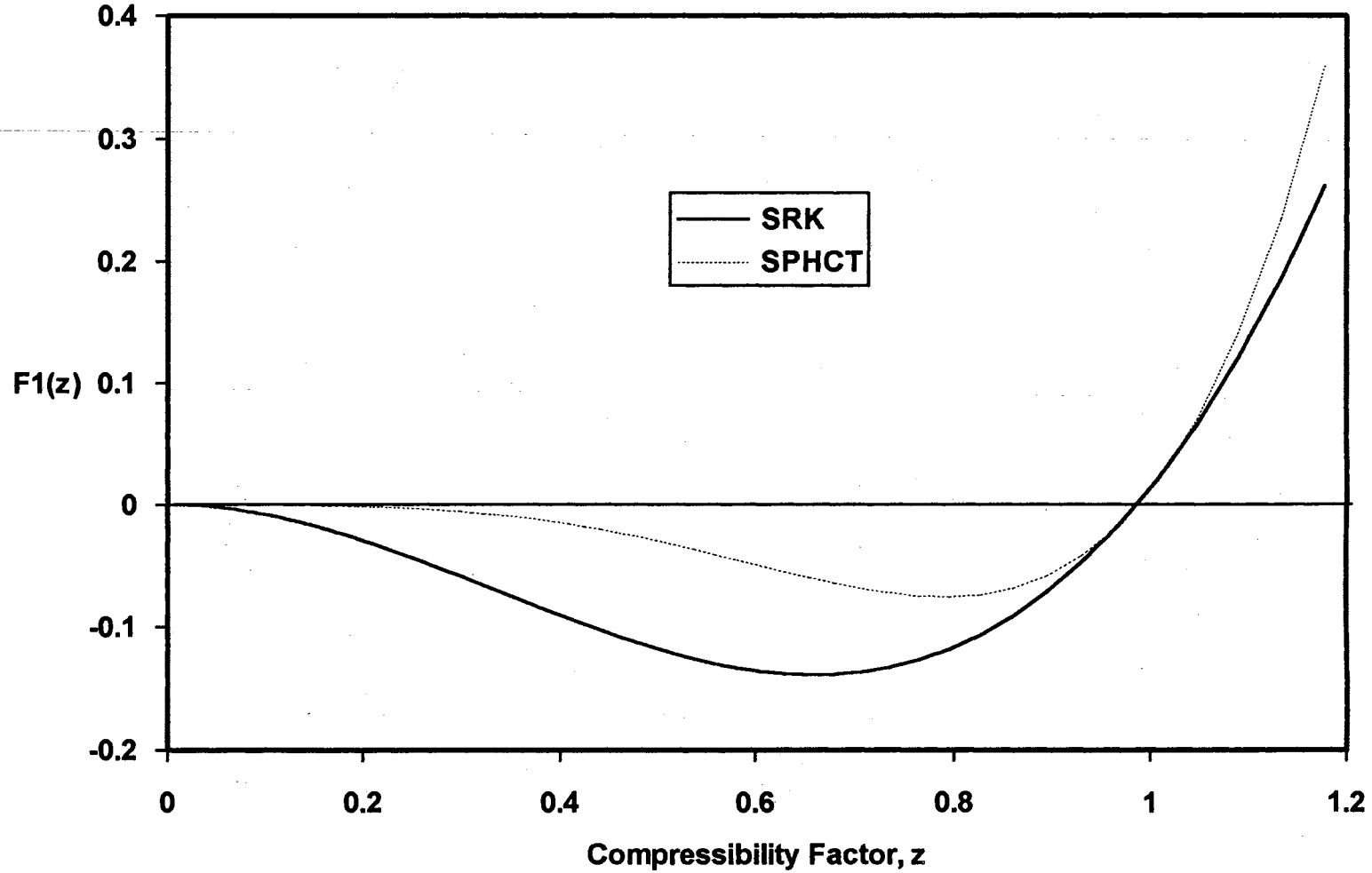

Figure 1. Example of Function F1(Z) for Solution of Vapor and Liquid Roots of SRK and SPHCT Equations

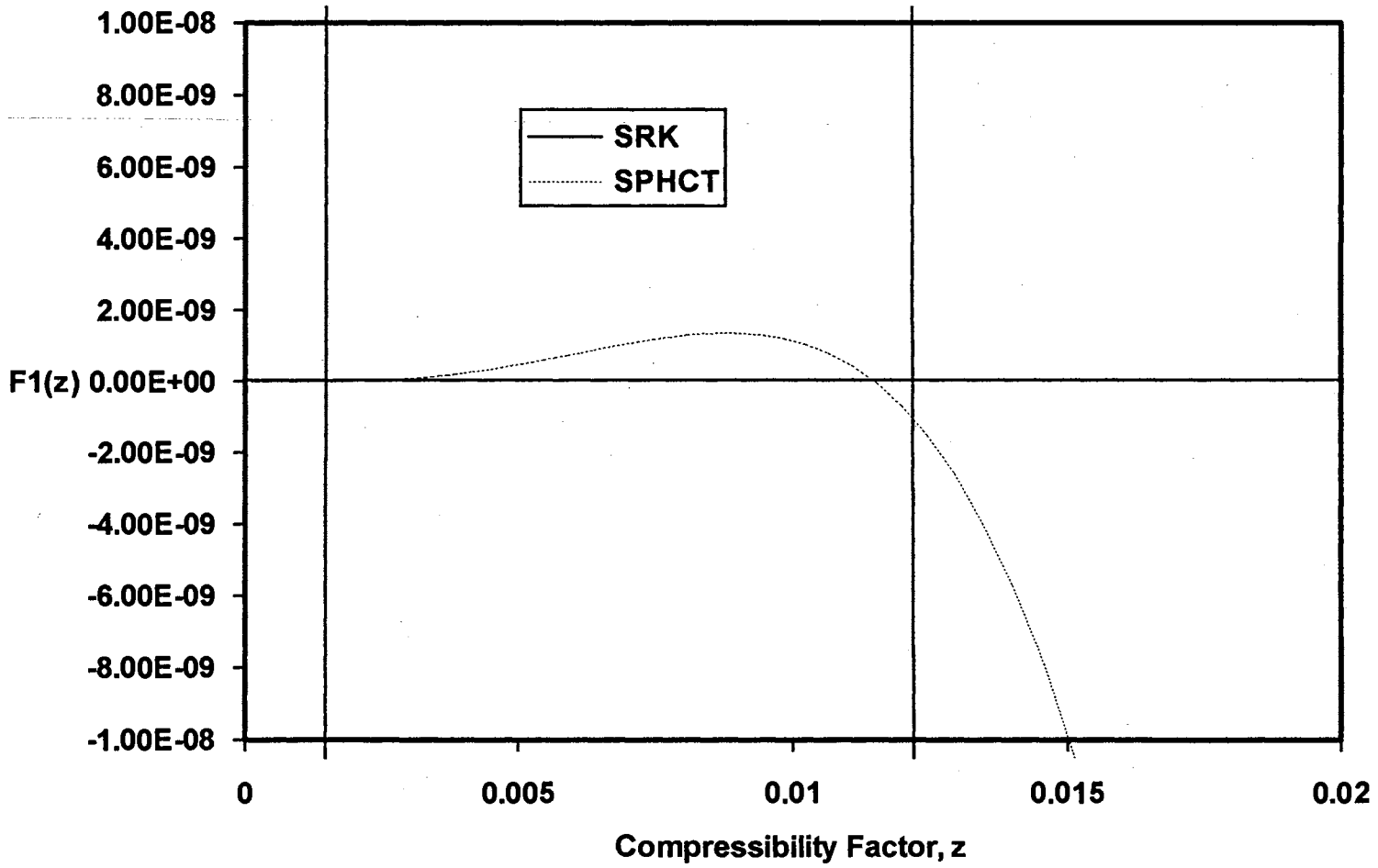

Figure 2. Enlarged View of the Lower Range of Figure 1

Figure 1. On this much expanded scale the difficulty associated with solution of the SPHCT equation is readily apparent. Extremely small values of F1(z) are seen in the vicinity of the liquid root. This creates several difficulties in locating the proper liquid root. First, the magnitude of F1(z) is on the order of 10^{-10} which results in difficulties in defining a reliable convergence tolerance. Second, the function is very flat in this region which can result in large errors in calculated liquid compressibility if the convergence tolerance is too large. Finally, the shape of the F1(z) function is quite sensitive to the EOS parameters and minor changes in the parameter values can cause the liquid root to disappear altogether. Such behavior of the F1(z) function makes parameter regressions quite difficult and, therefore, a different solution strategy was developed.

A function, F2(z), can be defined for the SPHCT equation as

$$F2(z) = z - \left(1 + cz^{rep} + cz^{att}\right) \tag{58}$$

in which the term in parentheses is the SPHCT equation and the desired vapor and liquid roots are found at the points where F2(z)=0. A similar equation for the SRK equation can be developed as

$$F2(z) = z - \left[1 + \frac{b}{\frac{zRT}{P} - b} - \frac{a\alpha RT}{\frac{zRT}{P} + b}\right] \tag{59}$$

A graph of the function F2(z) for typical conditions is shown in Figure 3 for the SRK and SPHCT equations. The function F2(z) is much better behaved than F1(z) for several reasons. First, the relative magnitude of the function F2(z) is the same over the entire range of

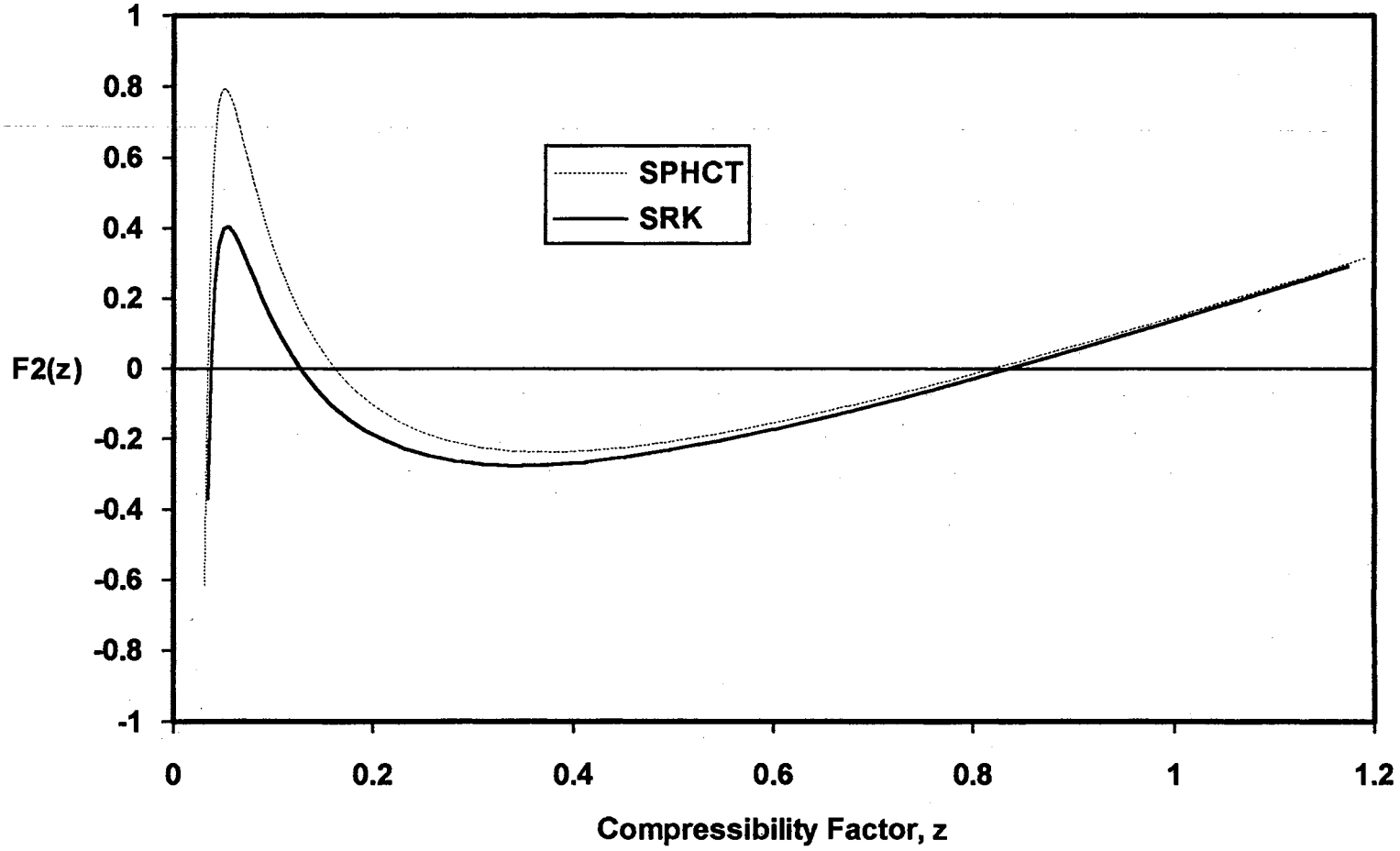

Figure 3. Example of Function F2(Z) for Solution of Vapor and Liquid Roots of SRK and SPHCT Equations

compressibilities of interest eliminating problems associated with convergence tolerances. Second, the slope of F2(z) is very steep at the proper liquid root allowing tighter convergence of this root. Finally, the function has a lower limit for the compressibility below which the equation is not used. The minimum value of z occurs at the point where the denominator of the repulsive term of the equation of state approaches zero. For the SPHCT equation this minimum z is given by

$$z_{min} = \frac{\tau v^* P}{RT} \tag{60}$$

and for the SRK equation by

$$z_{min} = \frac{bP}{RT} \tag{61}$$

The procedure for obtaining liquid and vapor roots is then as follows. For liquid roots the initial estimate for z_L, the liquid compressibility factor, is $1.05z_{min}$. F2(z) is calculated and checked to determine if it is positive or negative. Z_L is then increased by 5% and F2(z) is calculated again. At the point where F2(z) becomes positive, z_L is reduced to its value from the previous iteration and the solution is continued using a simple Newton-Raphson routine. When convergence is obtained the sign of the derivative of F2(z) with respect to z is checked to make sure the intermediate false root was not obtained for z_L. Although this procedure is time-consuming computationally (requiring 5-10 times as much computation time as the Peng-Robinson equation), the routine has proven to be very robust and no problems of obtaining the improper liquid root have been observed. The vapor root

is found by initializing z_V, the vapor compressibility, as 2.0 and using a simple Newton-Raphson method to locate the correct root.

SPHCT Parameter Study

The next step in modifying the SPHCT equation of state was a study of the EOS parameters. This study was done (a) to gain insight into the sensitivity of property predictions (vapor pressures and saturated densities) to EOS parameter values and (b) to investigate the behavior of the EOS parameters when optimized to produce accurate vapor pressures and saturated densities over the full saturation range. The parameter study was performed on four selected pure fluids: methane, carbon dioxide, benzene and water. As shown in Chapter II, for pure fluids the SPHCT equation contains three parameters: T*, v* and c. During this parameter study, the maximum coordination number, Z_M, (which is related to the interaction distance of the square-well potential model used) was treated as a fourth parameter.

The sensitivity of calculated properties (vapor pressures and saturated vapor and liquid densities) to each of the four EOS parameters was determined from the triple point to the critical point for the four compounds mentioned above. The parameter sensitivity is defined as

$$\frac{A}{X}\left(\frac{\partial X}{\partial A}\right) \tag{62}$$

where X is the calculated property (vapor pressure, vapor density or liquid density) and A is one of the EOS parameters. Thus, the sensitivity represents the fractional change in the calculated property per fractional change in the parameter value. Figures 4-6 show the

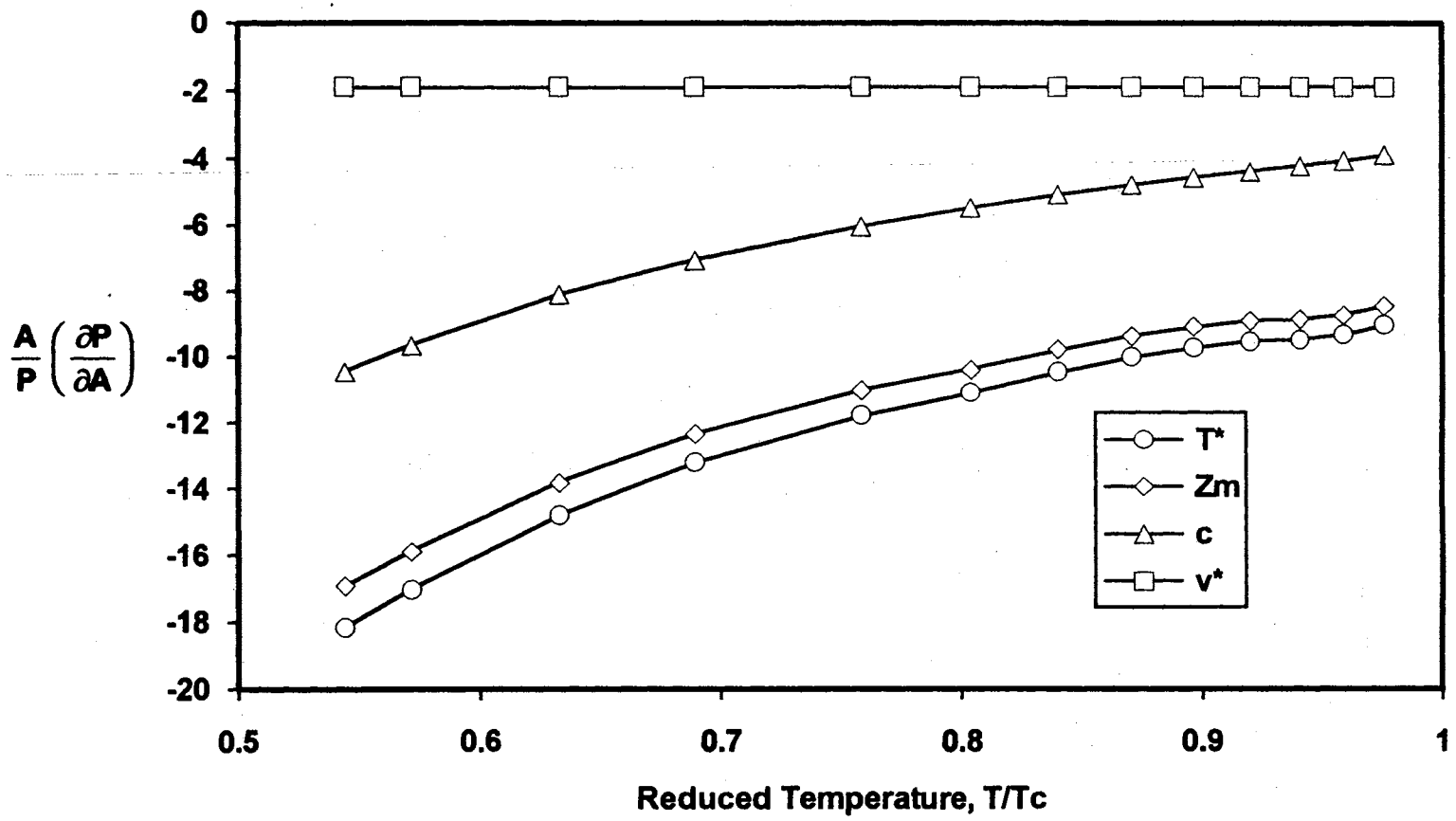

Figure 4. Effect of Reduced Temperature on Vapor Pressure Sensitivity for Saturated Methane

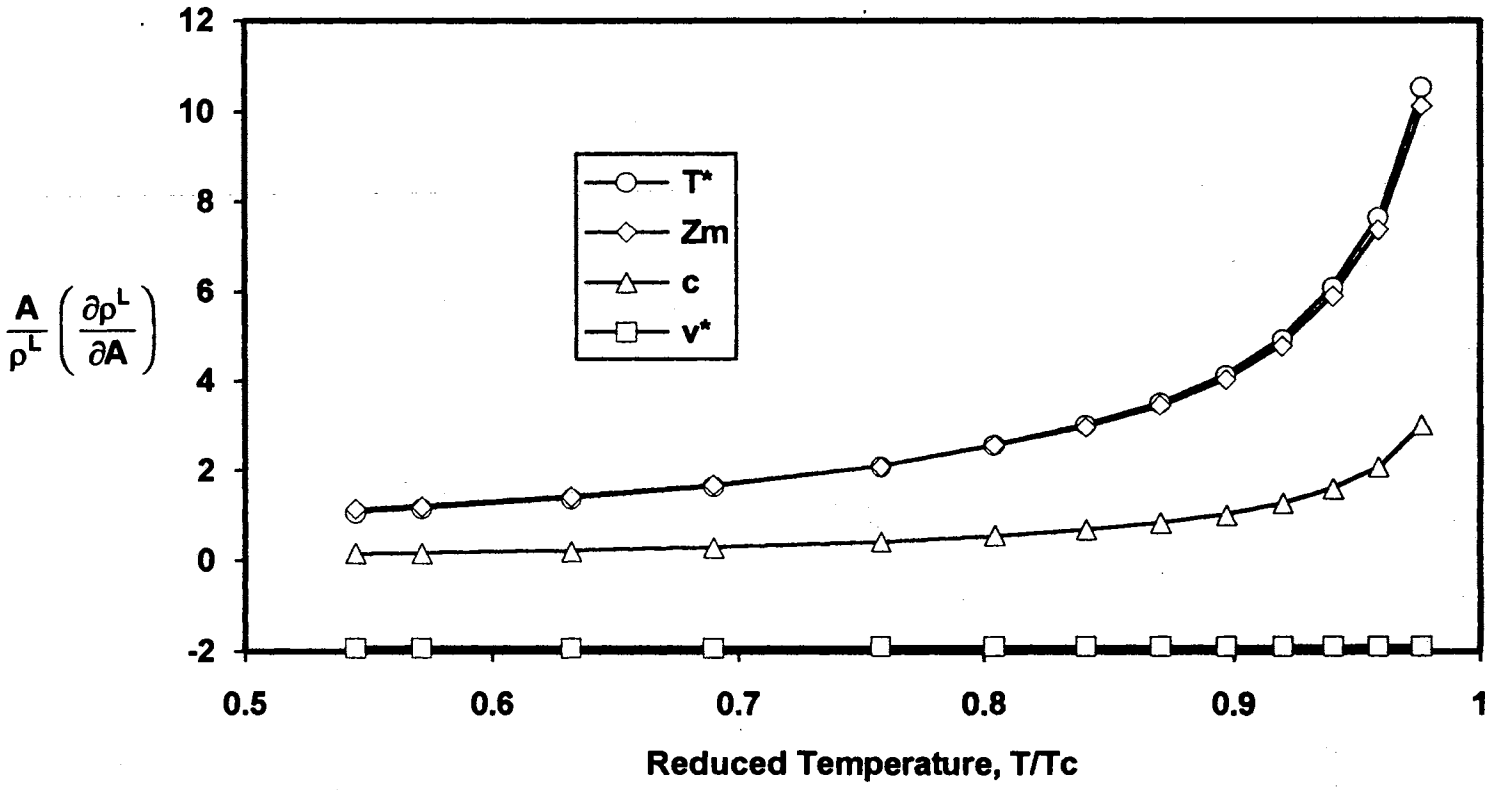

Figure 5. Effect of Reduced Temperature on Liquid Density Sensitivity for Saturated Methane

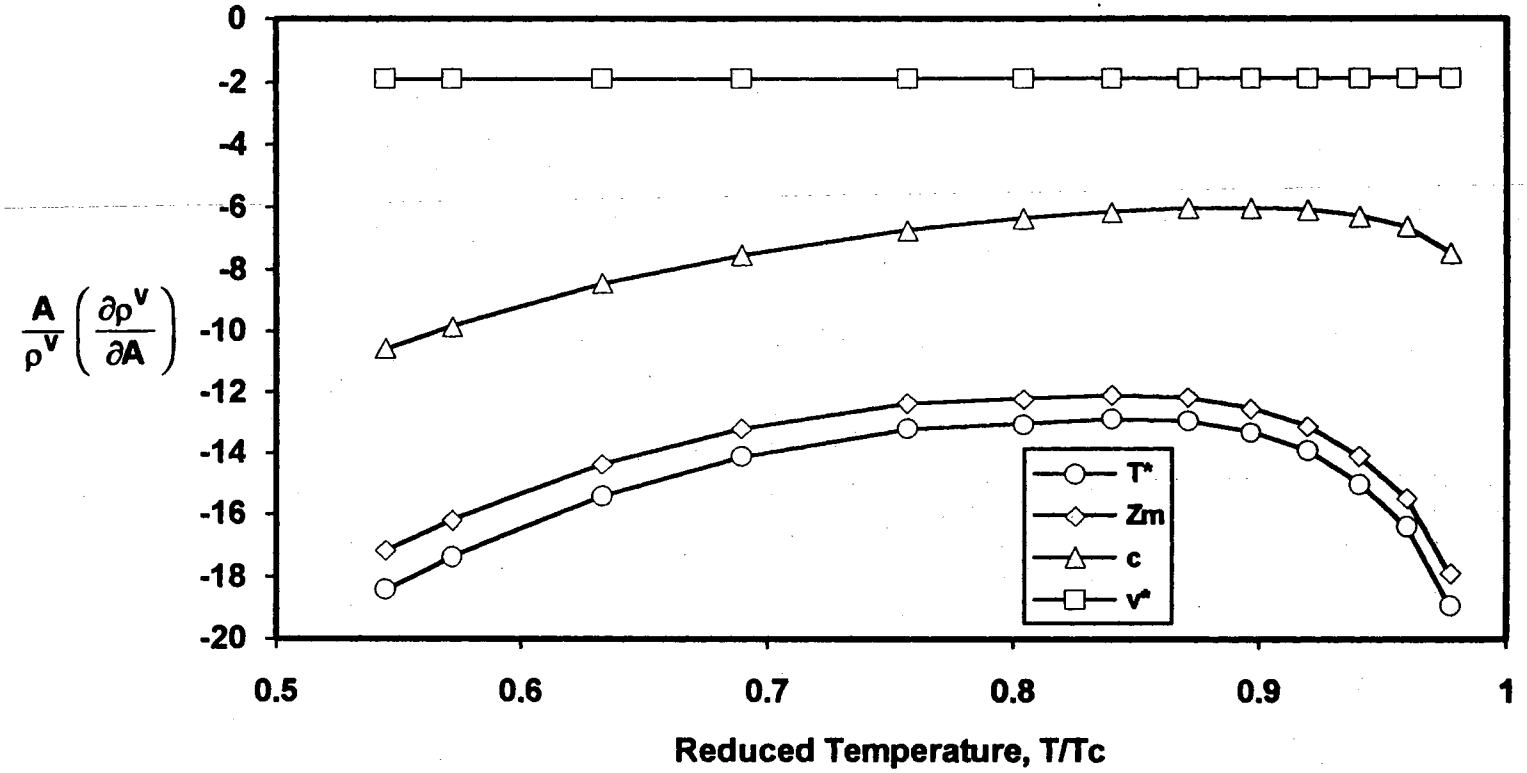

Figure 6. Effect of Reduced Temperature on Vapor Density Sensitivity for Saturated Methane

sensitivity to calculated vapor pressure, saturated liquid density and saturated vapor density, respectively, for each of the four parameters for prediction of methane properties. These figures reveal several important aspects of the SPHCT equation. First, the sensitivity for v* is nearly constant over the entire temperature range and is the least sensitive parameter for calculation of vapor pressure and vapor density. Second, all property calculations are extremely sensitive to the parameters T* and Z_M. Figures showing similar results for calculating the saturated properties of benzene, carbon dioxide and water are included in Appendix A.

The parameter behavior study was done by optimizing the four EOS parameters (T*, v*, c and Z_M) to provide accurate predictions for vapor pressures and saturated vapor and liquid densities simultaneously at three levels of temperature. For example, the four parameters were fit to vapor pressures and densities at reduced temperatures of 0.5, 0.55 and 0.6 with the optimized parameters obtained assigned to a reduced temperature of 0.55. The procedure was then repeated using data at reduced temperatures of 0.55, 0.6 and 0.65 with the results assigned to a reduced temperature of 0.6. This "sliding window" procedure was repeated for the four compounds listed above over temperature ranges from the triple point to the critical point. The results for the optimized parameters thus obtained are shown for methane in Figures 7-10. Figures showing the results for the other compounds studied are included in Appendix A. These figures suggest several characteristics of the SPHCT equation. First, there appears to be a fairly strong dependence of v* with temperature as shown in Figure 8. However, as shown earlier, v* has the least amount of influence on the calculated

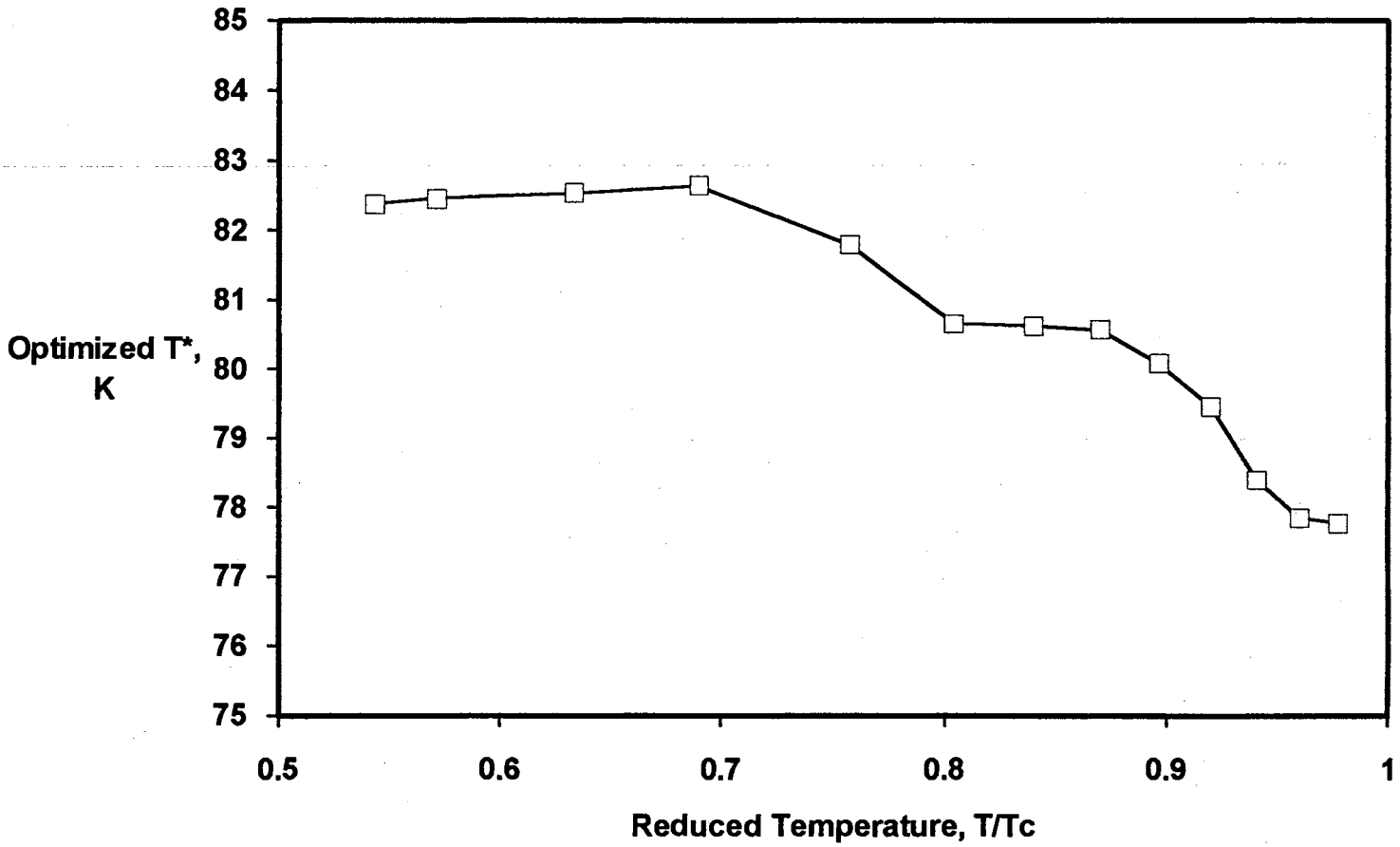

Figure 7. Effect of Reduced Temperature on Optimized T* for Saturated Methane

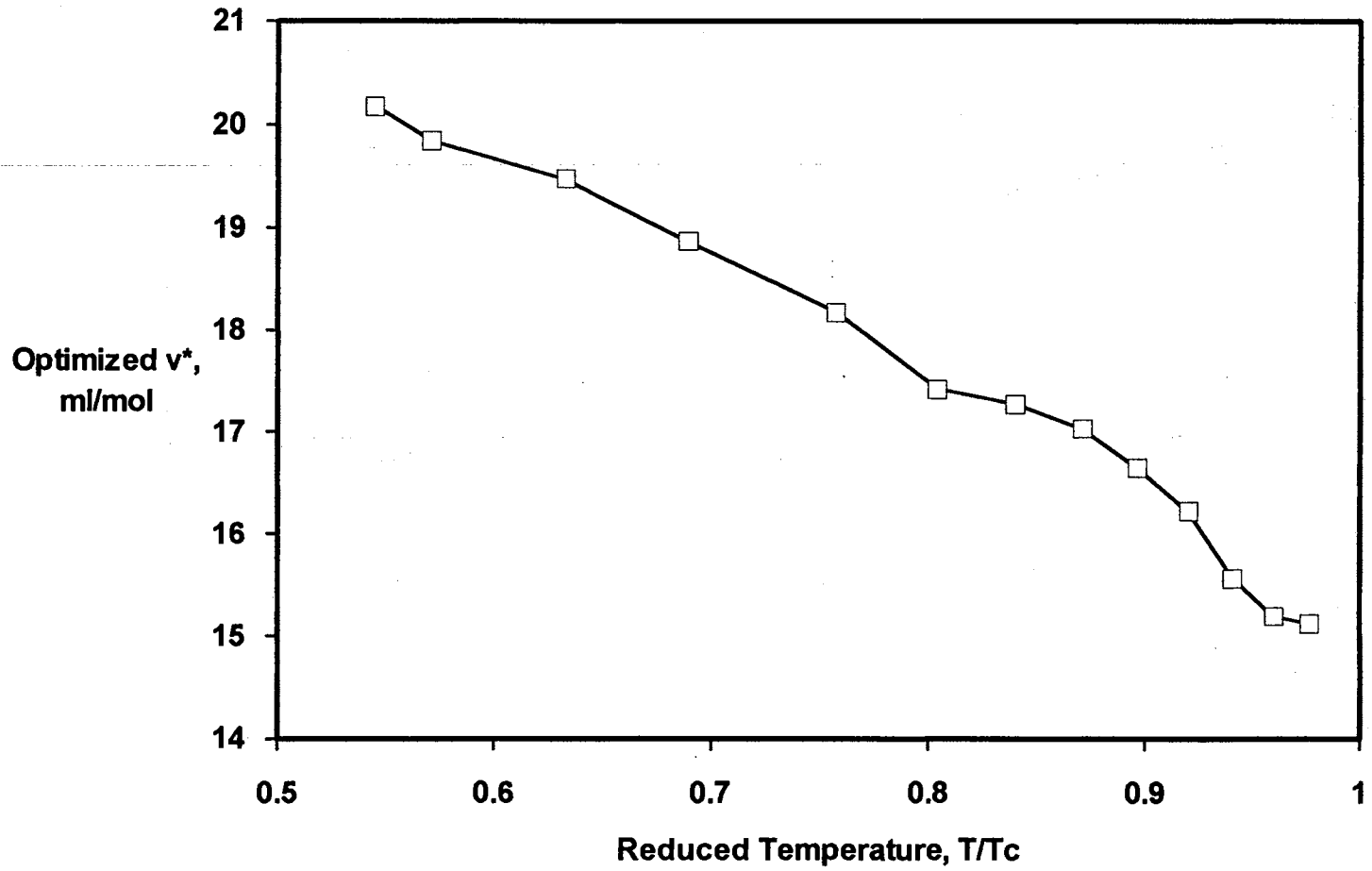

Figure 8. Effect of Reduced Temperature on Optimized v* for Saturated Methane

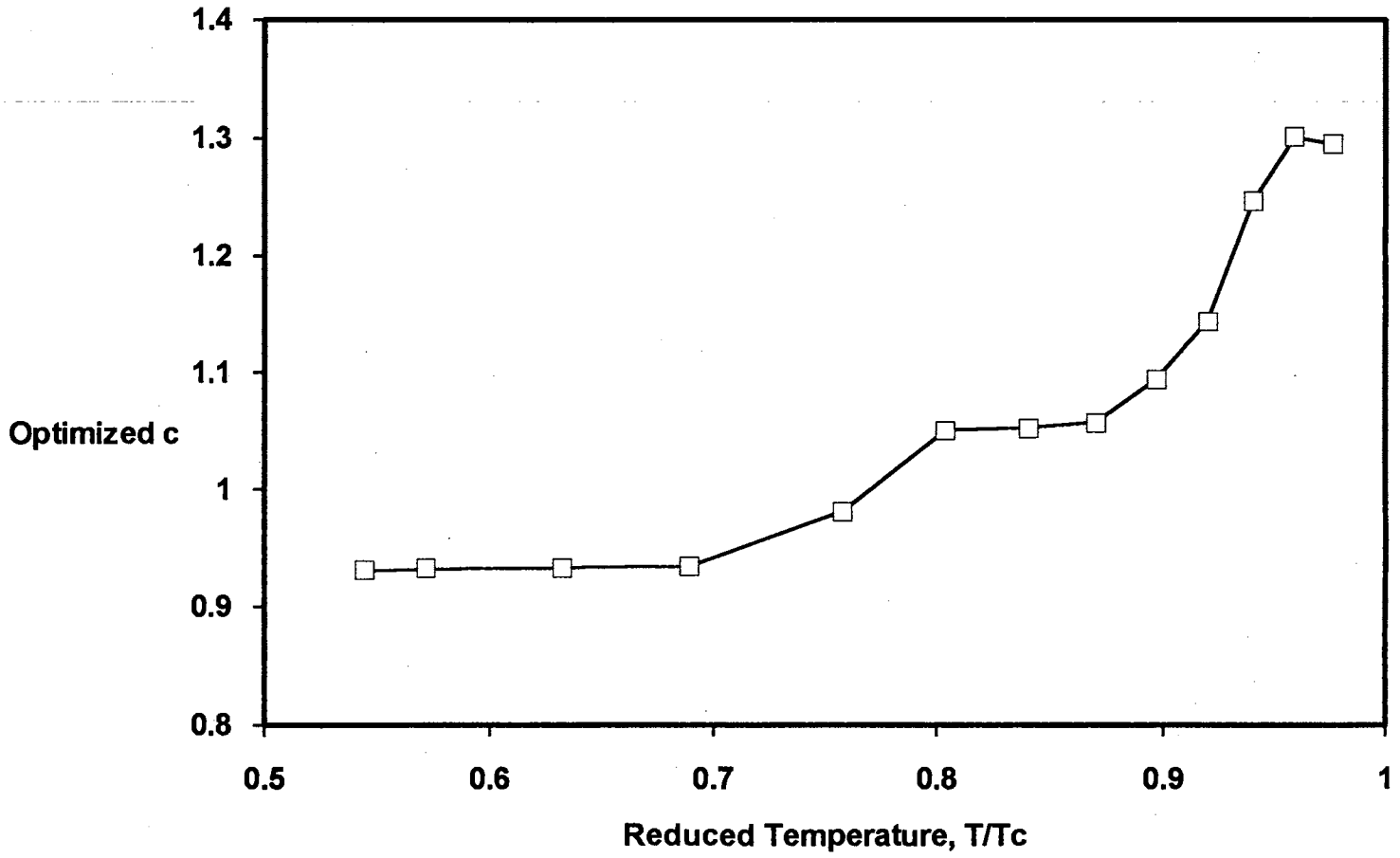

Figure 9. Effect of Reduced Temperature on Optimized c for Saturated Methane

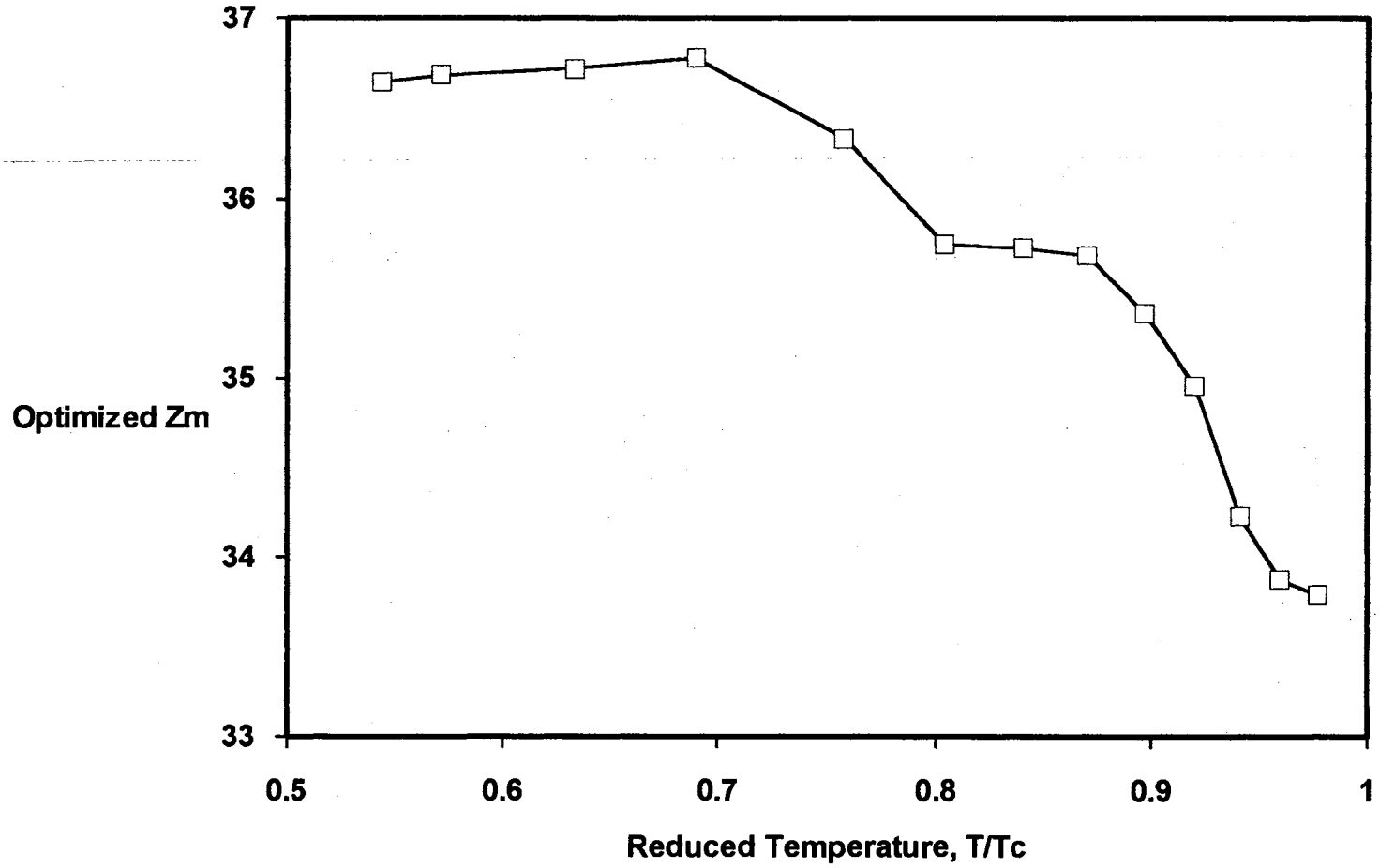

Figure 10. Effect of Reduced Temperature on Optimized Z_M for Saturated Methane

parameters indicating poor equation of state parameterization. If v* is made a linear function of temperature while restricting the other three parameters to remain constant over the entire temperature range, only very minor improvements in predictions are obtained. For example, the average absolute percent deviation (AAPD) for vapor pressure calculations obtained when all four parameters are regressed to fit vapor pressures and saturated densities of methane is 3.8%. The AAPD of the same data regressed with v* treated as a linear function of temperature is 3.7%. Therefore, it appears that to take advantage of the observed temperature dependence of v*, temperature dependencies for T*, Z_M and c would also need to be included. However, as shown in Figures 7-10 the temperature dependence of these parameters are not simple linear functions. The temperature dependence of v* and the extreme sensitivity of T* and Z_M coupled with their nonlinear temperature dependence suggests that the temperature functionality of the attractive term of the SPHCT equation is inadequate. Attention was therefore focused on improving this function as described in later sections.

Critical Point Constraints

The second phase for modifying the SPHCT equation was examining the effect of constraining the equation using the classical critical point constraints. For a pure fluid at its critical point the following two conditions should be satisfied:

$$\left(\frac{\partial P}{\partial v}\right)_{T=T_c} = 0 \qquad (63)$$

$$\left(\frac{\partial^2 P}{\partial v^2}\right)_{T=T_c} = 0 \tag{64}$$

In addition, the equation of state should satisfy the requirement that

$$P(v_c, T_c) = P_c \tag{65}$$

When Z_M is fixed at its theoretical value of 18.0 (for a square-well fluid with the interaction range R=1.5σ), a pure fluid has three parameters (T*, v* and c) which can be determined from the above three equations. However, doing so does not leave any flexibility for fitting the parameters to experimental data and results in unrealistic values for the model parameters and poor predictions at temperatures outside the immediate vicinity of the critical point. For example, the parameters thus obtained for methane are c=0.105, T*=561 K and v*=2.3 ml/mol. Recalling that the parameter c should be near 1.0 for methane, the value from the critical point constraints is unacceptable. More reasonable parameter values can be obtained from the constraints by treating the critical volume, v_c, as an adjustable parameter as done by van Pelt, et al. (3). In this way, one of the equation of state parameters can be fitted to experimental data with the other two parameters and the critical volume obtained from the three equations shown above. This is identical to the traditional method of satisfying Equations (63) and (64) at the experimental T_c and P_c and obtaining the predicted volume at the critical point from the equation of state.

As evident from the equations shown for the SPHCT EOS in Chapter II, the above equations are nonlinear in the parameters and cannot be

solved analytically. The two constraints were reformulated as done by Ponce-Ramirez, et al. (2) as

$$z + \eta\left(\frac{\partial z}{\partial \eta}\right)_{T=T_c} = 0 \tag{66}$$

$$2\left(\frac{\partial z}{\partial \eta}\right)_{T=T_c} + \eta\left(\frac{\partial^2 z}{\partial \eta^2}\right)_{T=T_c} = 0 \tag{67}$$

where

$$\eta = \frac{v^* \tau}{v} \tag{68}$$

Equations (66-68) were solved numerically using a Marquart nonlinear regression routine (35) as described in Appendix B. The numerical routine was then embedded within the regressions routine used for fitting parameters to experimental data to provide for a constrained optimization.

Simple correlations were developed to relate T* and v* to c subject to the constraints shown above. These correlations are included in Appendix B and should enable others to apply the critical point constraints in future work without having to solve the cumbersome equations that result from Equations (66) and (67). Use of these correlations to satisfy the critical point constraints during parameter optimizations significantly reduces computation time and greatly reduces the complexity necessary for implementation of the constraints. The effect of the critical point constraints on the SPHCT EOS predictions are shown along with the other EOS modifications studied in a later section.

Modification of the Attractive Term

As discussed in Chapter II, the attractive term of the SPHCT equation contains several assumptions which simplify its temperature and density dependence. This fact, along with the high sensitivity of calculated properties to T* and Z_M discussed earlier, suggest that improvements in EOS predictions can be achieved by modifying the temperature and/or structural dependence of the attractive term. Several investigators (1,34,79) have suggested possible improvements for the SPHCT equation through the addition of temperature or density dependence to the maximum coordination number of the attractive portion of the equation of state, and Ciocca, et al. (80) have suggested a density dependence for the degrees of freedom parameter, c. Therefore, possible modifications to the equation can be realized by removing some of the simplifying assumptions present in the initial EOS derivation.

By returning to the expression for the ratio of species coordination numbers (Equation (26)) and relaxing the simplifying assumptions, a more general expression can be inferred for the attractive term. A more general form for the radial distribution function of Equation (27) can be assumed as

$$g_{ij} = g_{ij}^{0} e^{-F_t} \tag{69}$$

where

$$F_t = F_t(T_{ij}^{*}, T) \tag{70}$$

and

$$T_{ij}^{*} = \frac{\varepsilon_{ij} q_i}{c_i k} \tag{71}$$

In this way Equation (26) can be written as

$$\Psi = F_g e^{-F_t} \tag{72}$$

where F_g represents the portion of the structural and temperature dependence of the integrals of Equation (26) that can be factored out. Although this type of treatment is essentially empirical, the more general form of Equation (72) can be used to investigate modifications of the attractive term of the SPHCT equation while (a) maintaining the mathematical form of the original equation and (b) providing some insight into the empirical changes that are investigated. By combining Equation (72) with a temperature and/or structurally dependent maximum coordination number, Z_M, the attractive term of the SPHCT equation can be written as

$$Z^{att} = -\frac{Z_M^* cv^* \left(F_g e^{F_t} - 1\right)}{cv + cv^* \left(F_g e^{F_t} - 1\right)} \tag{73}$$

where the asterisk on Z_M indicates that Z_M is a function of temperature and/or structural parameters.

Various functions for F_t, F_g and Z_M^* were studied using vapor pressure data for the pure paraffins methane, propane, n-decane and n-tetradecane. Following is a list of the types of functions investigated:

$$F_t = \sum_{i=1}^{k} b_i \left(\frac{1}{2\bar{T}}\right)^{\frac{i}{2}} \tag{74}$$

$$F_g = 1 + \sum_{i=1}^{k} b_i \left(T^*\right)^i \tag{75}$$

$$Z_M^* = \sum_{i=1}^{k} b_i \tilde{T}^{i-1} \qquad (76)$$

Each function was evaluated by optimizing the function parameters and the values of c for each of the compounds listed above simultaneously while subject to the critical point constraints discussed earlier. Regression of pure fluid data resulted in equivalent quality of fit with Z_M equal to either its commonly used value 36 or its theoretical value of 18 (26). The functions F_t and F_g were therefore studied with Z_M set equal to 18.

Results for several cases studied are shown in Table I. As shown in Table I, the function F_t provides the best results when only one of the functions is utilized. When used alone, the function F_g results in values of the parameter c that are highly non-linear with carbon number. In fact, the values obtained for c in these cases contain a maximum at a carbon number of 10, and extrapolations to higher molecular weight n-paraffins would result in negative c values. When used alone, the function Z_M^* results in low values for the maximum coordination number ranging from about 9 to 11. Using either F_g or Z_M^* in addition to F_t does not provide any significant improvement in vapor pressure predictions over the use of F_t alone. Therefore, further work was restricted to the use of only F_t, and the optimized coefficients for the function F_t are included in Table II.

The effect of introducing the modifying function F_t on the quantity (cv*Y) of the attractive term can be seen in Figure 11. Here values of (cv*Y) are shown relative to the values obtained from regression of experimental data for methane. The values of (cv*Y)

TABLE I

EVALUATION OF MODIFYING FUNCTIONS FOR THE ATTRACTIVE PORTION OF THE CONSTRAINED SPHCT EQUATION

Function Included	Number of Terms (k)	Ave. % Dev. for Vapor Pressure Predictions
F_t	4	1.26
F_g	2	4.87*
F_g	4	4.80*
Z_M^*	2	7.11**
F_t F_g	4 2	0.96
F_t Z_M^*	4 2	1.20

* The cases containing only F_g results in c values non-linear with carbon number.

** The case with only Z_M^* results in very small values of Z_M (b_1=8.97, b_2=0.237).

obtained from the original expression of Equation (36) show considerable deviation from the regressed values while those obtained using the function F_t show much improved results. Detailed evaluations of this modification to the attractive term of the constrained SPHCT equation

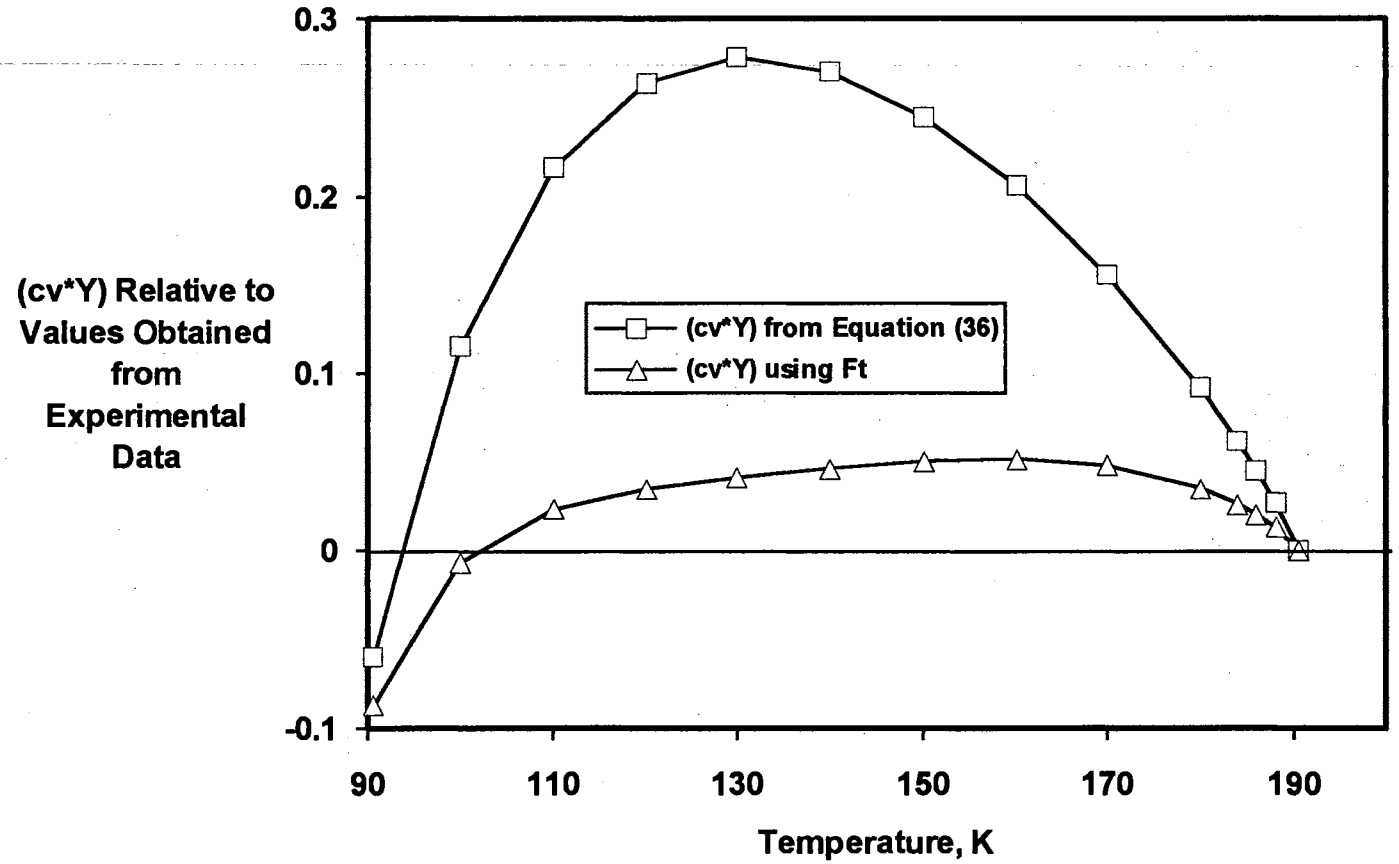

Figure 11. Comparison of Calculated and Regressed Values of (cv*Y) for Methane

for both pure fluid and mixture calculations are included in the next chapter.

TABLE II

COEFFICIENTS FOR THE MODIFYING FUNCTION F_t FOR THE CONSTRAINED SPHCT EQUATION

Coefficient	Value
b_1	-1.1803
b_2	7.0000
b_3	-8.0419
b_4	3.9106

Mixing Rules and Mixture Calculations

Extension of the SPHCT equation for pure fluids (shown in Chapter II) requires the introduction of mixing rules for the various equation of state parameters. The mixing rules listed in Equations (37)-(41) are the ones originally used by Kim, et al. (7). However, these are not the only mixing rules that have been proposed for the types of parameters encountered in the SPHCT equation. Donohue and Prausnitz (6) used more complicated mixing rules for T* in which powers of T* are given separate mixing rules. In their work, each mixing rule for T^{*n} contains a ratio of two quadratic mixing terms. For example, their mixing rule for $\langle T^* \rangle^2$ would be written as

$$\langle T^* \rangle^2 = \frac{\sum_i \sum_j x_i x_j q_i \frac{\varepsilon_{ij} q_i}{c_i k} s_j \sigma_{ji}^3}{\sum_i \sum_j x_i x_j q_i s_j \sigma_{ji}^3} \tag{77}$$

Vimalchand (14) used similar mixing rules for his perturbed anisotropic chain theory equation of state for multi-polar molecules. Use of these types of mixing rules within the exponential term of Equation (73) would result in very cumbersome expressions for the component fugacities and makes their use undesirable. Moreover, a closer inspection of the expressions for species coordination numbers and the configurational energy for mixtures (detailed in Appendix C) indicates that the type of mixing for <cv*Y> used by Kim, et al. (7) is justifiable. This simpler type of mixing was therefore adopted with $\tilde{T}$ in the function F_t defined for mixtures as

$$\tilde{T} = \frac{T}{T_{ij}^*} \tag{78}$$

where

$$T_{ij}^* = \frac{\varepsilon_{ij} q_i}{c_i k} \tag{79}$$

The simple linear mixing for <c> and <v*> given in Equations (37) and (38) are also extended to quadratic mixing to allow for the introduction of interaction parameters to account for nonidealities in mixing for the parameters <c> and <v*>. The new mixing rules lend additional flexibility to the equation and are given as

$$\langle c \rangle = \sum_i \sum_j x_i x_j c_{ij} \tag{80}$$

$$\text{with} \quad c_{ij} = \frac{\left(c_i + c_j\right)}{2}\left(1 + E_{ij}\right) \tag{81}$$

and

$$\left\langle v^* \right\rangle = \sum_i \sum_j x_i x_j v^*_{ij} \tag{82}$$

$$\text{with} \quad v^*_{ij} = \frac{s_j \sigma^3_{ij}}{\sqrt{2}} \tag{83}$$

$$\text{and} \quad \sigma_{ij} = \frac{\left(\sigma_{ii} + \sigma_{jj}\right)}{2}\left(1 + D_{ij}\right) \tag{84}$$

in which D_{ij} and E_{ij} are binary interaction parameters. The necessary changes to the fugacity coefficient expression for each of these types of mixing is included in Appendix D.

Volume Translations

As discussed in Chapter II, volumetric properties predicted by equations of state can be improved by certain translations along the volume axis which leave the predicted equilibrium conditions unchanged (15). The simple volume translation procedure proposed by Peneloux (37) (represented by Equation (45)) is inadequate for improvement in saturated density predictions of the SPHCT equation. This is because the untranslated volumes of the SPHCT equation are not shifted by the same amount over the full saturation range. This is illustrated in Figure 12 where the errors in predicted vapor and liquid volumes are shown for methane using the SPHCT equation with the EOS parameters obtained to satisfy the critical point constraints of Equations (66) and

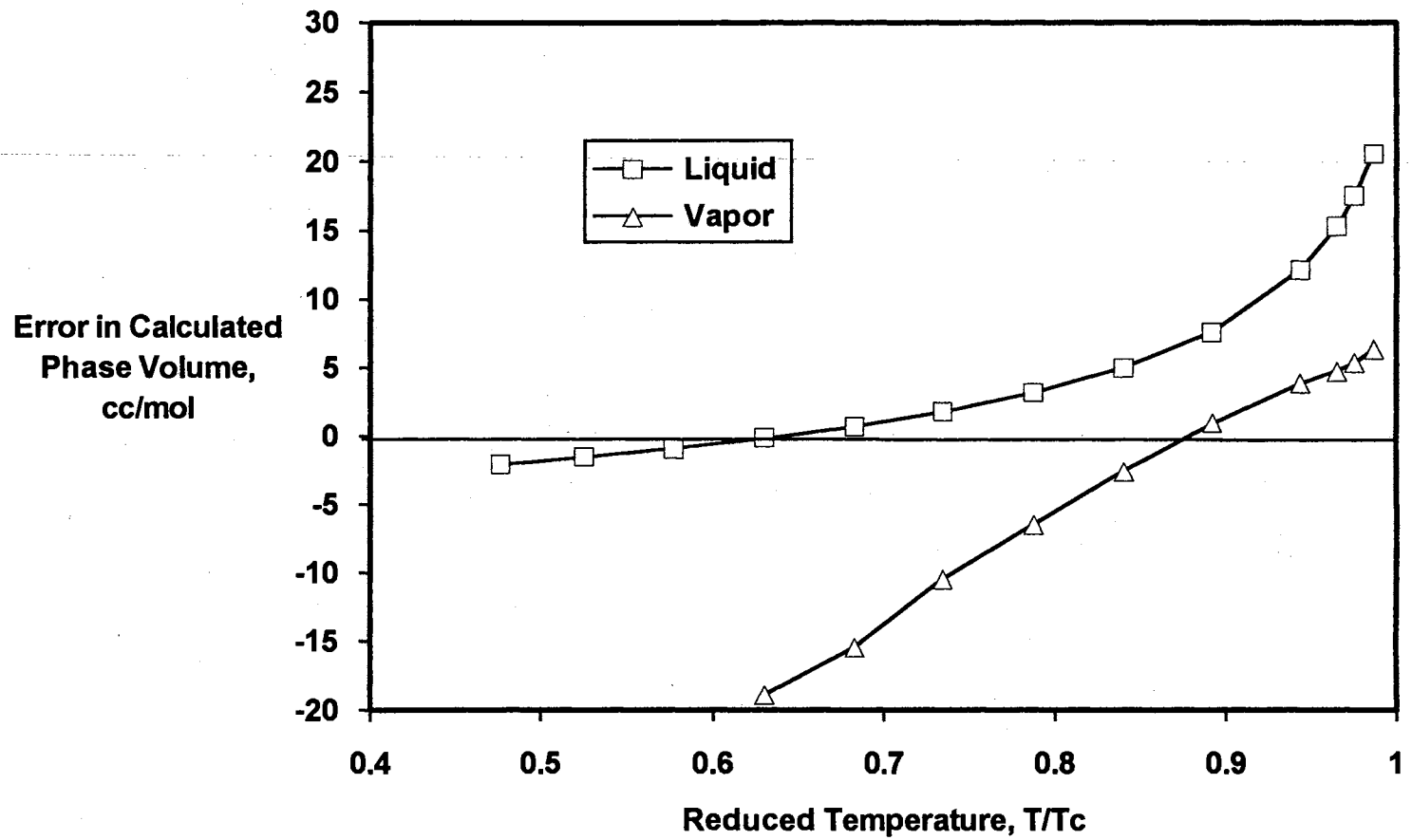

Figure 12. Errors in Calculated Saturated Vapor and Liquid Volumes Using the Untranslated Constrained SPHCT Equation

(67). Clearly, a simple volume translation as given by Equation (45) is insufficient. Accordingly, a phenomenological volume translation similar to that of Chou and Prausnitz (38) discussed in Chapter II is proposed.

The dimensionless distance parameter defined by Chou and Prausnitz (38) is used to determine the amount of volume translation at a given temperature:

$$d = \frac{1}{RT_c}\left(\frac{\partial P^{EOS}}{\partial \rho}\right)_T \tag{85}$$

Volume translations are then done according to

$$v = v_{EOS} + \delta_c\left(1 - S^{c_1} - S^{c_2}\right) \tag{86}$$

where,

$$\delta_c = \frac{RT_c}{P_c}(z_c^{EOS} - z_c) \tag{87}$$

$$S = \frac{1}{1 + d} \tag{88}$$

The correlating variable, d, is evaluated at the saturated liquid condition and c_1 and c_2 are volume translation parameters. Thus, the volume translation technique studied in this work contains two parameters (c_1 and c_2). The results for volumetric predictions using the above equations with two substance-specific parameters and results with one or both of the parameters generalized are shown in Chapter IV.

CHAPTER IV

RESULTS AND DISCUSSION

The equation of state modifications discussed in the previous chapter were investigated using a database of 23 pure fluids and a number of binary mixtures comprised of ethane + n-paraffins and CO_2 + hydrocarbons. Following are detailed descriptions of the cases studied for pure fluids and mixtures and comparisons made with the original SPHCT equation and the Peng-Robinson (PR) equation.

Pure Fluid Database Used

The effects of the various modifications discussed in Chapter III were studied using a database of 23 pure compounds. The sources and ranges of saturated data used for pure fluids are shown in Table E.I of Appendix E. The compounds were chosen to represent several classes of organic chemicals (n-alkanes, 1-alkenes, cycloparaffins and aromatics) as well as CO_2, argon and water. Where available, data were included for vapor pressures and both saturated liquid and vapor densities at temperatures from the triple point to reduced temperatures of 0.95 or greater but not including the critical point itself. The critical point was not included because of the expected difficulty in calculating vapor pressures at the point where all of the equation of state roots converge. For several compounds only limited saturated liquid density data were available, and for six of the compounds only vapor pressures

were available as indicated in Table E.I of Appendix E. As seen in previous studies (1), vapor pressure predictions using the SPHCT equation at very low vapor pressures are poor. Consequently, a lower limit of 0.1 psia was imposed on all comparisons following the recommendation of Gasem and Robinson (1).

Results for Pure Fluids

The equation of state modifications discussed in Chapter III were evaluated by studying five different cases involving the application of the critical point constraints, the modified form for the attractive portion of the equation of state and the proposed volume translation strategy. The five cases are listed in Table III. Case 1 is the SPHCT equation with Z_M=18 subjected to the critical point constraints of Equations (63-65). In this case, the parameter c was optimized to minimize percentage errors in calculated vapor pressures with the other parameters (T*, v*, and the adjusted critical volume, v_c) obtained from the solution of Equations (63-65). In Case 2, the same procedure was used in obtaining the pure fluid parameters as in Case 1. The difference is the inclusion of the modifying function, F_t, given by Equation (74) for the temperature dependence of the attractive portion of the SPHCT equation. Cases 3-5 are identical to Case 2 with respect to the procedure for obtaining the EOS parameters and calculation of vapor pressure. Cases 3-5 represent investigation of the proposed volume translation strategy. In Case 3, the two parameters of Equation (86) (c_1 and c_2) are regressed for each compound to minimize percentage errors in both liquid and vapor density predictions (or only liquid densities for the compounds for which vapor density data were

TABLE III

DESCRIPTIONS OF EACH CASE STUDIED DURING EVALUATION OF SPHCT MODIFICATIONS FOR PURE FLUIDS

Case	Description
1	SPHCT equation of state with Z_M=18 including critical point constraints (Equations 63-65). One parameter (c) is optimized to fit vapor pressures.
2	SPHCT equation of state with Z_M=18 including critical point constraints (Equations 63-65) and the modified attractive term (Equation 74). One parameter (c) is optimized to fit vapor pressures.
3	Same as Case 2 with the addition of volume translation given by Equation 86. c_1 and c_2 are optimized as substance-specific parameters.
4	Same as Case 2 with the addition of volume translation given by Equation 86. c_1 is fixed at 0.04 and c_2 is optimized as a single substance-specific parameter.
5	Same as Case 2 with the addition of volume translation given by Equation 86. c_1 is fixed at 0.04 and c_2 is fixed at 1.5 for all compounds.

unavailable). In Case 4, c_1 is fixed at a value of 0.04 for all compounds, and c_2 is regressed as a system-specific parameter to fit the phase densities. Case 5 represents a generalized volume translation in which both parameters of Equation (86) (c_1 and c_2) are fixed at the universal values of c_1=0.04 and c_2=1.5.

The five cases described in Table III were compared to the Peng-Robinson (PR) equation and the original SPHCT equation treated as follows. The PR equation was used strictly in a predictive mode. That is, no tuning of the EOS input variables (T_c, P_c, ω) was done. The parameters for the original form of the SPHCT equation (T*, v*, c) were regressed to minimize the following objective function for both vapor pressures and phase densities:

$$SS = \sum_{i=1}^{n}\left[\left(\frac{P_{calc} - P_{exp}}{P_{exp}}\right)_i^2 + \left(\frac{\rho^L_{calc} - \rho^L_{exp}}{\rho^L_{exp}}\right)_i^2 + \left(\frac{\rho^V_{calc} - \rho^V_{exp}}{\rho^V_{exp}}\right)_i^2\right] \qquad (89)$$

For the compounds for which vapor densities were not available, the three parameters were fit only to vapor pressures and liquid densities. For those compounds for which neither phase density data was available the three parameters were fit only to vapor pressures. Consequently, the compounds studied without density data show favored vapor pressure predictions using the original SPHCT equation. The equation of state parameters thus obtained for the original SPHCT equation as well as those of Cases 1-5 are included in Appendix F.

Table IV shows the results for the vapor pressure predictions of Cases 1 and 2 as well as the results obtained from the PR and original SPHCT equations. The results for Case 1 indicate that constraining the

TABLE IV

EVALUATION OF PURE FLUID VAPOR PRESSURE PREDICTIONS

	Peng-Robinson		Original SPHCT		Case 1		Cases 2-5*	
Component	RMSE, bar	%AAD	RMSE, bar	%AAD	RMSE, bar	%AAD	RMSE, bar	%AAD
Methane	0.162	1.57	0.444	3.81	0.665	4.79	0.239	1.30
Ethane	0.075	3.52	0.721	4.40	0.767	7.12	0.056	0.51
Propane	0.074	5.76	0.721	3.73	0.633	7.26	0.101	0.94
n-Butane	0.094	1.72	0.764	4.49	0.653	8.13	0.167	0.88
n-Octane	0.050	2.00	0.408	4.16	0.463	7.79	0.128	1.68
n-Decane	0.063	3.90	0.489	3.60	0.258	6.93	0.115	1.05
n-Tetradecane	0.030	7.26	0.021	1.26	0.140	8.34	0.027	1.24
n-Eicosane	0.036	8.17	0.005	0.68	0.049	6.61	0.004	0.80
Ethene	0.056	2.77	0.923	4.08	0.741	7.23	0.134	0.48
Propene	0.053	1.22	0.655	3.97	0.691	6.15	0.143	0.72
1-Butene	0.052	10.34	0.685	3.28	0.702	7.72	0.158	0.83
1-Hexene	0.039	1.12	0.227	0.85	0.570	8.10	0.117	1.09
Cyclopropane	0.072	1.57	0.384	0.96	0.889	7.41	0.188	0.51
Cyclobutane	0.061	0.52	0.378	1.16	0.865	8.78	0.199	1.21
Cyclohexane	0.029	2.09	0.668	2.15	0.560	5.55	0.083	1.21
Cyclooctane	0.176	7.34	1.029	3.95	0.380	5.54	0.220	2.12
trans-Decalin	0.049	11.86	0.009	0.84	0.092	7.72	0.006	1.21
Benzene	0.082	2.10	0.447	3.79	0.685	4.99	0.156	1.25
Toluene	0.056	1.75	1.105	4.13	0.609	8.12	0.141	1.10
1-Methylnaphthalene	0.080	19.32	0.010	0.68	0.100	8.03	0.006	1.20
Argon	0.110	0.39	0.338	2.32	0.618	3.52	0.216	0.74
Carbon Dioxide	0.344	2.21	0.651	2.96	0.625	1.94	0.212	0.45
Water	0.829	4.69	3.763	6.97	4.925	11.43	1.968	2.79
Overall	0.223	3.76	1.032	3.03	1.231	6.85	0.457	1.12

* Vapor pressure predictions for Cases 2-5 are identical.

SPHCT equation with Equations (63-65) results in poor vapor pressure predictions. This is because the constrained equation is not capable of adequately describing the entire range of temperatures considered. However, work by van Pelt, et al. (3) has shown reasonable results for this approach when limited to temperatures in the reduced temperature range $0.75<T_r<1.0$. The results for Case 2 in which the modified attractive term has been included show significant improvement in vapor pressure predictions. The overall percent average absolute deviations (%AAD) of this case (1.12%) is less than half of that observed for either the PR or original SPHCT equations (3.76% and 3.03%, respectively).

Tables V through VIII show the results for volumetric predictions of the five cases and the PR and original SPHCT equations. Table V indicates the PR and the original SPHCT equations provide comparable saturated liquid density predictions. Table VI indicates that Cases 1 and 2, which did not include volume translation, produce poor liquid density predictions (10.65% and 10.00%, respectively). However, Case 3 (2-constant volume translation) results in significant improvement in liquid density predictions (1.28%) with less than 1/4 of the %AAD of either the PR or original SPHCT equations (6.74% and 6.82%, respectively). Fixing one or both of the volume translation parameters at universal values results in only slight deterioration of the quality of saturated liquid density predictions (1.89 %AAD for Case 4 and 2.66 %AAD for Case 5). Table VII shows the performance of the PR (3.14%) and original SPHCT (6.01%) equations in predicting saturated vapor densities. The evaluations given indicate that the PR equation results in about half of the %AAD of the original SPHCT equation. The results

TABLE V

EVALUATION OF PURE FLUID LIQUID DENSITY PREDICTIONS
FOR PENG-ROBINSON AND ORIGINAL SPHCT EQUATIONS

	Peng-Robinson		Original SPHCT	
Component	RMSE, g/cm^3	%AAD	RMSE, g/cm^3	%AAD
Methane	0.036	8.75	0.028	6.97
Ethane	0.030	5.45	0.045	7.82
Propane	0.032	5.56	0.047	7.79
n-Butane	0.029	5.04	0.049	7.88
n-Octane	0.030	5.19	0.062	9.88
n-Decane	0.043	7.14	0.068	11.48
n-Tetradecane	0.079	8.83	0.002	0.25
n-Eicosane	0.144	20.43	0.001	0.02
Ethene	0.041	7.10	0.037	7.35
Propene	0.041	6.60	0.039	7.55
1-Butene	0.024	3.90	0.024	3.72
Cyclohexane	0.018	2.60	0.029	4.10
Benzene	0.038	5.56	0.072	9.28
Toluene	0.027	2.89	0.060	7.24
Argon	0.145	9.99	0.077	5.93
Carbon Dioxide	0.047	4.36	0.051	4.49
Water	0.156	19.54	0.077	8.28
Overall	0.063	6.74	0.052	6.82

TABLE VI

EVALUATION OF PURE FLUID LIQUID DENSITY
PREDICTIONS FOR THIS WORK

	Case 1		Case 2		Case 3		Case 4		Case 5	
Component	RMSE, g/cm^3	%AAD	RMSE, g/cm^3	%AAD	RMSE, g/cm^3	%AAD	RMSE, g/cm^3	%AAD	RMSE, g/cm^3	%AAD
Methane	0.036	10.64	0.034	9.88	0.003	0.78	0.003	0.81	0.007	1.82
Ethane	0.052	10.96	0.047	9.82	0.003	0.50	0.003	0.56	0.010	1.86
Propane	0.053	9.34	0.046	8.12	0.005	0.83	0.005	0.83	0.005	0.83
n-Butane	0.057	10.06	0.049	8.75	0.006	1.01	0.006	0.97	0.007	0.95
n-Octane	0.068	11.57	0.058	9.88	0.014	2.35	0.021	3.64	0.024	3.66
n-Decane	0.084	15.33	0.073	12.84	0.034	4.86	0.036	5.14	0.059	9.23
n-Tetradecane	0.021	3.16	0.013	1.93	0.000	0.00	0.000	0.00	0.015	2.30
n-Eicosane	0.034	4.88	0.022	3.16	0.000	0.00	0.000	0.00	0.061	8.68
Ethene	0.048	9.10	0.043	8.14	0.004	0.83	0.004	0.81	0.005	0.92
Propene	0.051	9.44	0.045	8.31	0.006	1.08	0.006	1.09	0.009	1.62
1-Butene	0.057	10.85	0.053	10.03	0.004	0.66	0.004	0.73	0.004	0.71
Cyclohexane	0.066	10.31	0.064	10.27	0.003	0.36	0.005	0.80	0.010	1.35
Benzene	0.084	12.88	0.077	11.78	0.010	1.17	0.010	1.23	0.015	2.35
Toluene	0.073	9.58	0.064	8.34	0.014	1.73	0.020	2.73	0.020	2.63
Argon	0.092	7.66	0.084	6.96	0.006	0.47	0.010	0.63	0.011	0.79
Carbon Dioxide	0.101	9.31	0.109	10.73	0.005	0.32	0.006	0.48	0.006	0.49
Water	0.168	20.68	0.172	21.58	0.043	4.89	0.087	10.13	0.136	13.78
Overall	0.079	10.65	0.077	10.00	0.015	1.28	0.026	1.89	0.041	2.66

Case 1: Constrained SPHCT equation without volume translation.
Case 2: Constrained SPHCT equation including the modified attractive term, no volume translation.
Case 3: Constrained SPHCT equation including the modified attractive term, 2 constant volume translation.
Case 4: Constrained SPHCT equation including the modified attractive term, 1 constant volume translation.
Case 5: Constrained SPHCT equation including the modified attractive term, generalized volume translation.

TABLE VII

EVALUATION OF PURE FLUID VAPOR DENSITY PREDICTIONS
FOR PENG-ROBINSON AND ORIGINAL SPHCT EQUATIONS

	Peng-Robinson		Original SPHCT	
Component	RMSE, g/cm^3	%AAD	RMSE, g/cm^3	%AAD
Methane	0.002	3.14	0.007	6.61
Ethane	0.001	4.01	0.006	7.05
Propane	0.001	6.12	0.006	5.26
n-Butane	0.001	2.12	0.010	6.53
n-Octane	0.001	2.25	0.009	8.11
Ethene	0.001	2.88	0.008	6.52
Propene	0.000	1.56	0.009	6.11
Benzene	0.002	2.78	0.014	7.13
Toluene	0.004	4.04	0.009	5.12
Argon	0.003	1.36	0.014	3.98
Carbon Dioxide	0.001	2.64	0.015	4.64
Water	0.003	5.99	0.017	11.29
Overall	0.002	3.14	0.011	6.01

TABLE VIII

EVALUATION OF PURE FLUID VAPOR DENSITY
PREDICTIONS FOR THIS WORK

	Case 1		Case 2		Case 3		Case 4		Case 5	
Component	$\overline{RMSE}_\rho$ g/cm^3	%AAD	$\overline{RMSE}_\rho$ g/cm^3	%AAD	$\overline{RMSE}_\rho$ g/cm^3	%AAD	$\overline{RMSE}_\rho$ g/cm^3	%AAD	$\overline{RMSE}_\rho$ g/cm^3	%AAD
Methane	0.001	4.42	0.001	1.39	0.003	2.41	0.003	2.40	0.003	2.25
Ethane	0.001	6.58	0.002	1.80	0.001	0.97	0.001	0.96	0.001	0.95
Propane	0.001	6.60	0.002	2.23	0.001	1.92	0.001	1.92	0.001	1.92
n-Butane	0.002	7.61	0.003	1.92	0.003	1.78	0.003	1.78	0.003	1.81
n-Octane	0.002	7.22	0.003	4.48	0.001	3.04	0.001	3.04	0.001	3.00
Ethene	0.001	7.37	0.002	2.01	0.002	1.90	0.002	1.91	0.002	1.90
Propene	0.002	5.60	0.003	2.58	0.002	1.75	0.002	1.75	0.002	1.76
Benzene	0.004	4.70	0.005	3.76	0.003	2.90	0.003	2.89	0.003	2.86
Toluene	0.003	7.38	0.001	2.35	0.006	3.91	0.006	4.00	0.006	4.01
Argon	0.004	3.55	0.005	1.33	0.002	0.95	0.002	0.91	0.002	0.88
Carbon Dioxide	0.004	2.23	0.005	2.72	0.002	1.59	0.002	1.60	0.002	1.60
Water	0.005	10.29	0.006	3.29	0.002	1.43	0.002	1.75	0.002	1.36
Overall	0.003	5.61	0.003	2.25	0.003	1.87	0.003	1.91	0.003	1.85

Case 1: Constrained SPHCT equation without volume translation.
Case 2: Constrained SPHCT equation including the modified attractive term, no volume translation.
Case 3: Constrained SPHCT equation including the modified attractive term, 2 constant volume translation.
Case 4: Constrained SPHCT equation including the modified attractive term, 1 constant volume translation.
Case 5: Constrained SPHCT equation including the modified attractive term, generalized volume translation.

for vapor density predictions of Cases 1-5 are shown in Table VIII. Cases 1 and 2 which contain no volume translation show similar results to the PR and the original SPHCT equations. With the addition of volume translation, vapor density predictions are improved as indicated by Cases 3-5. The generalization of the volume translation parameters (Cases 4 and 5) indicate that there is minimal loss in accuracy for the vapor density predictions over the two-parameter volume translation of Case 3.

Case 3 represents a three-parameter equation in which c was fit to vapor pressures (with T* and v* obtained from the critical point constraints) and c_1 and c_2 simultaneously fit to saturated liquid and vapor densities. Consequently, a direct comparison can be made between this case and the original three-parameter (T*, v*, c) SPHCT equation. As shown in Tables IV-VIII, Case 3 (same as Case 2 for vapor pressure predictions) is significantly better than the original SPHCT equation for vapor pressure predictions (1.12 %AAD versus 3.03 %AAD), saturated liquid density predictions (1.28 %AAD versus 6.82 %AAD) and saturated vapor density predictions (1.87 %AAD versus 6.01 %AAD).

To determine how the original intent of the SPHCT equation and its parameters as discussed in Chapter II are affected by the modifications made, the parameters of the original SPHCT equation were compared to those obtained for Case 2. Figure 13 shows the values of the parameter c for n-paraffins as a function of carbon number. As required by the theory, c is near 1.0 for methane and increasing with increasing number of segments. The modified equation results in parameters with a slope slightly less than the original equation indicating less incremental

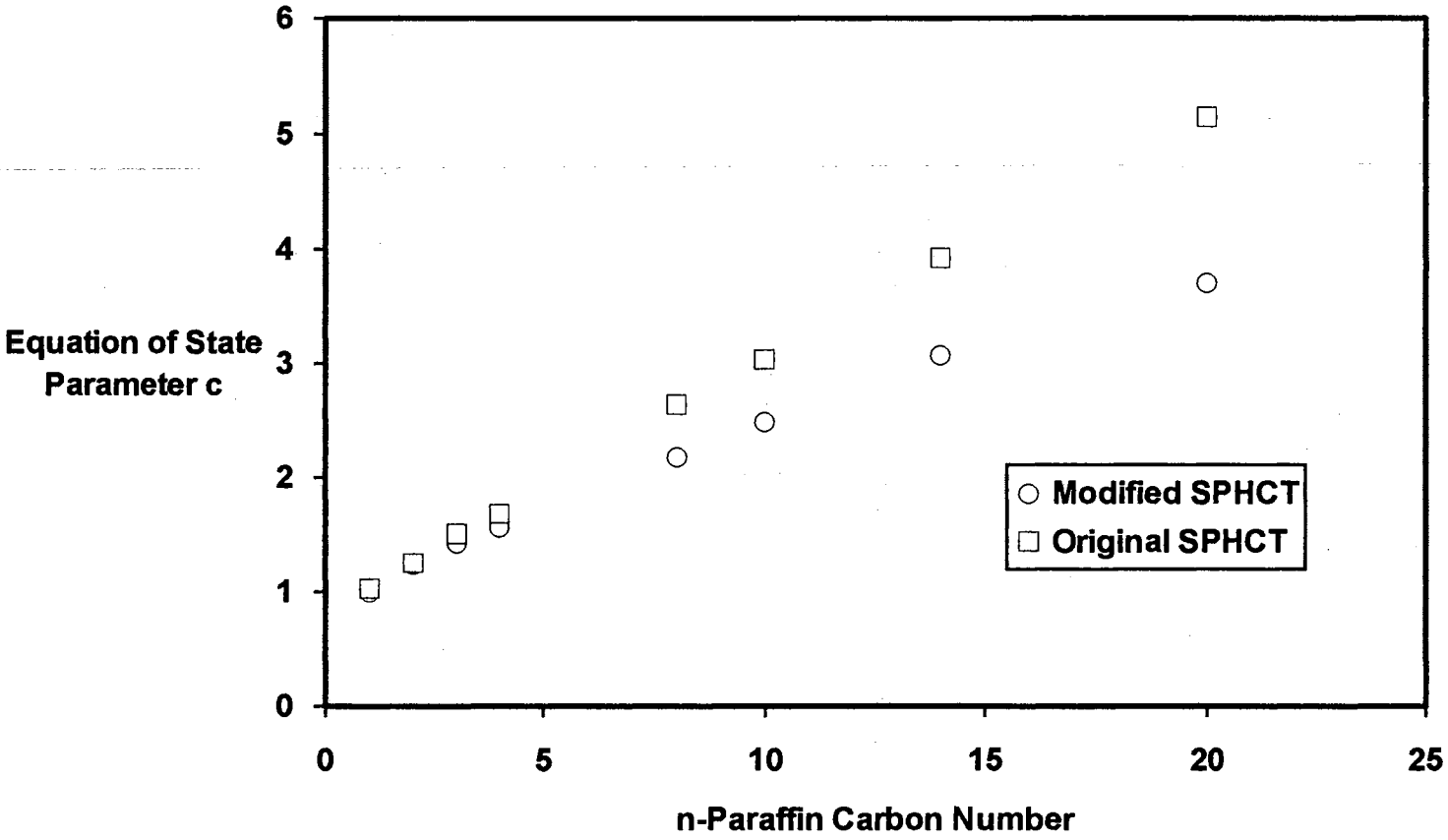

Figure 13. SPHCT Degree of Freedom Parameter for n-Paraffins

change in the number of translationally equivalent degrees of freedom. Figure 14 shows the values of the characteristic volumes (v*) for n-paraffins as a function of carbon number. The parameters are nearly the same for the original SPHCT equation and that of Case 2. The slope of the original parameters yields a value of $\frac{N_a\sigma^3}{\sqrt{2}}$ of 8.249 mL/mol while that of the modified equation is 8.622 mL/mol. Both values are comparable to that observed by Kim, et al. (7) (8.667 mL/mol). The characteristic temperatures (T*) of the original equation and that of Case 2 are shown in Figure 15. The values of T* for Case 2 are about 20-30% larger than those of the original equation. Overall, the original meaning of the equation of state parameters has been maintained.

The poor parameterization of the original SPHCT equation discussed previously can be seen in the regressed parameter values shown in Table F.I of Appendix F. Notice that the parameters for members of homologous series (such and the alkenes and cycloparaffins) are not easily related to the number of segments. This is because the parameters for most of these compounds were obtained through the regression of vapor pressure data only (or vapor pressure and liquid density data only) as indicated in Appendix E. This emphasizes the need for both equilibrium and volumetric data for generation of the original SPHCT parameters and the difficulty in obtaining consistent and reliable parameters for this equation.

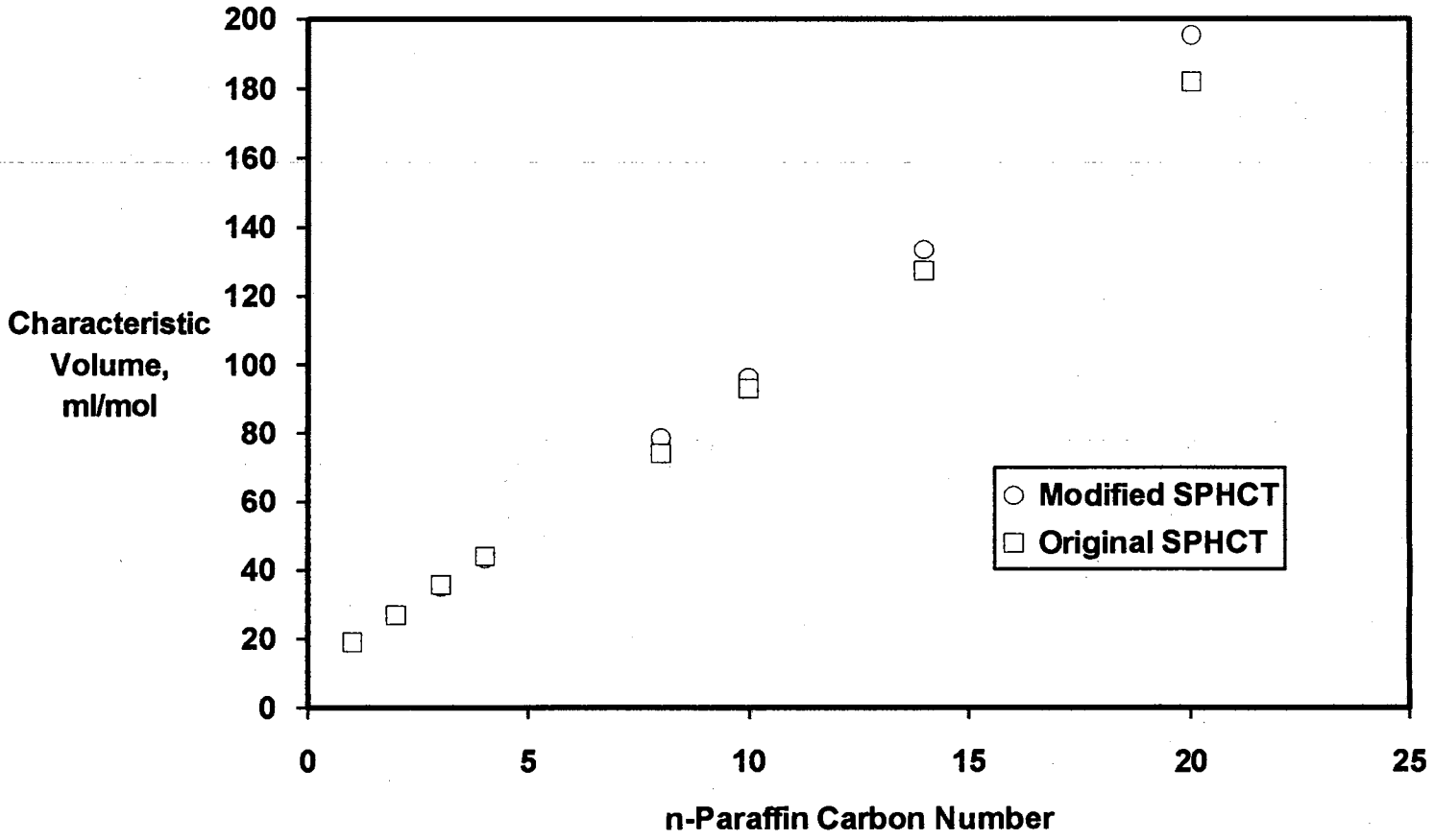

Figure 14. SPHCT Characteristic Volumes for n-Paraffins

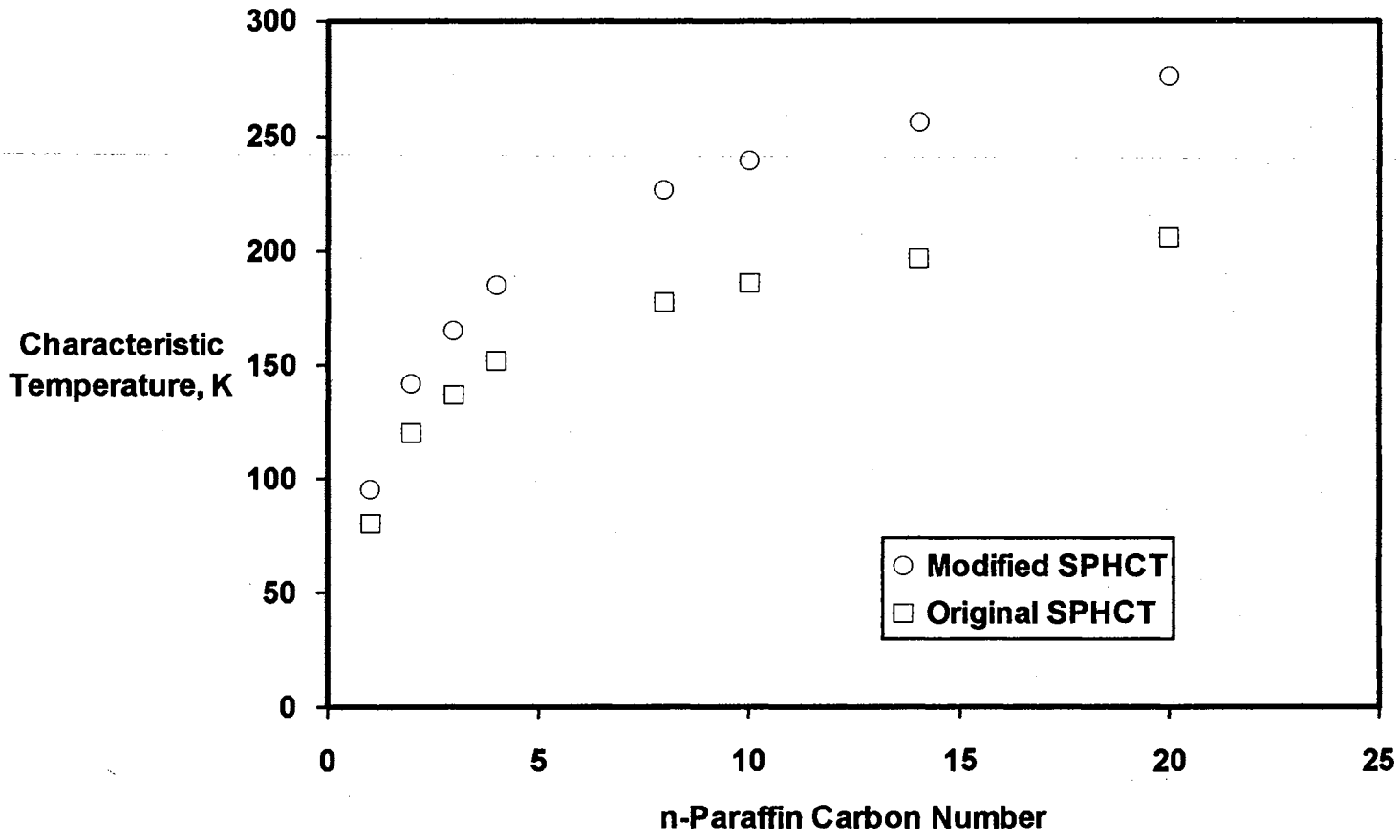

Figure 15. SPHCT Characteristic Temperatures for n-Paraffins

Mixture Database Used

The equation of state modifications discussed in Chapter III and evaluated for pure fluids above were further evaluated for the prediction of binary mixture bubble point pressures, compositions and phase densities. The database used in these evaluations consisted of three databases previously compiled at Oklahoma State University (1,36,71) and expanded by the data of this work. Table E.II of Appendix E lists the database containing solubility data for ethane + n-paraffin systems used in earlier evaluations of the SPHCT equation by Gasem, et al. (1). The database consists of bubble point pressures and liquid phase compositions for binary mixtures of ethane and n-paraffins ranging in molecular weight from n-C_4 to n-C_{44}. Table E.III lists a similar database previously used in the evaluation of the SRK and PR equations (71) consisting of bubble point pressures and liquid phase compositions for binary mixtures of CO_2 + n-paraffins from n-C_4 to n-C_{44}. Tables E.IV and E.V list the third database consisting of vapor and liquid phase compositions and vapor and liquid phase densities for binary mixtures at pressures up to and including the mixture critical points.

Results for Solubility Data

The modified SPHCT equation of state, consisting of the constrained form of the equation and the modifying function F_t described in Chapter III, was first evaluated for the prediction of bubble point pressures of ethane + n-paraffin binary mixtures and CO_2 + n-paraffin binary mixtures. The modified equation was evaluated using the six cases listed in Table IX and compared to the performance of the original SPHCT and Peng-Robinson (PR) equations. The cases listed in Table IX

TABLE IX

SPECIFIC CASES USED IN EQUATION OF STATE EVALUATIONS

Case	Parameters Regressed	Description
1	$C_{ij}=0$	The 'raw predictive ability' of the equation of state.
2	C_{ij}	A single value of C_{ij} is determined for application to all binary systems for each solute studied.
3	$C_{ij}(CN)$	A separate value of C_{ij} is determined for each binary system, independent of temperature. This is the most commonly used equation of state representation.
4	$C_{ij}(T)$	A separate value of C_{ij} is determined for each binary system at each temperature.
5	$C_{ij}(T), D_{ij}(T)$	A separate value of C_{ij} and D_{ij} is determined for each binary system at each temperature. This case represents the correlative capability of the equation of state with two interaction parameters.
6	$C_{ij}(T), E_{ij}(T)$	A separate value of C_{ij} and E_{ij} is determined for each binary system at each temperature. This case represents the correlative capability of the equation of state with two interaction parameters.

represent an increasing degree of complexity for the interaction parameters used. Case 1 with no interaction parameter (C_{ij}=0) represents the 'raw predictive ability' of the equation of state to represent bubble point pressures. Case 2 illustrates the performance of the equation when a single value of the interaction parameter, C_{ij}, is used for every n-paraffin studied. Case 3 is the most commonly used equation of state representation used in the literature in which a separate C_{ij} is used for each binary mixture independent of temperature.

Cases 4-6 illustrate the ultimate correlative capability of the equation where interaction parameters are obtained for each temperature of each binary mixture. Cases 5 and 6 are included to demonstrate the maximum correlative capability of the equation when two interaction parameters are obtained for each temperature of each mixture. In Case 5 D_{ij} (introduced in Equations (82-84)) is included and in Case 6 E_{ij} (introduced in Equations (80-81)) is included in addition to C_{ij} for each temperature of each mixture. For the PR equation with two interaction parameters, only Case 5 was considered with D_{ij} representing a second interaction parameter used in the co-volume mixing rules in the usual way (70).

In all evaluations of the bubble point databases, the following objective function was used in regression of experimental data to obtain the interaction parameters

$$SS = \sum_{i=1}^{n} \left[\frac{\left(P_{calc} - P_{exp}\right)}{P_{exp}} \right]_i^2 \qquad (90)$$

where P_{exp} is the experimental bubble point pressure and P_{calc} is the calculated bubble point pressure. This is one of the more commonly used types of objective functions used for obtaining equation of state parameters from regression of experimental data (2,3,29) and results in an even distribution of percentage errors over the pressure range of the data.

Results for the modified SPHCT, the original SPHCT and the PR equations for the six cases studied are discussed below. Results are presented for both ethane + n-paraffin and CO_2 + n-paraffin systems.

Ethane + n-Paraffin Systems

A summary of the results for the six cases described above is presented in Table X and detailed tables containing the complete statistics for each isotherm of each case are included in Appendix G. Inspection of Table X reveals that the modified SPHCT equation is comparable to the PR equation in the *a priori* predictive case (Case 1) and provides about half of the average error of the original SPHCT equation for this case. However, the addition of the binary interaction parameter, C_{ij}, does not result in as much improvement for the modified equation as for the original form. This is seen in the results for Cases 2-4 in which the modified equation shows less improvement with each progressively more complex case than the original equation but is still comparable to the PR equation. In the most correlative cases (Cases 5 and 6) the modified equation is slightly better than the original equation. These two cases illustrate the benefit that can be obtained for both the original and the modified SPHCT equations through the addition of the second interaction parameters used to account for

TABLE X

SUMMARY OF RESULTS FOR REPRESENTATION OF
BUBBLE POINT PRESSURES OF ETHANE + N-PARAFFIN SYSTEMS

Case Number	Bubble Point Pressure RMSE (bar)	BIAS (bar)	AAD (bar)	%AAD
PENG-ROBINSON				
1	1.68	0.24	1.24	6.49
2	1.85	-0.56	1.51	7.26
3	1.51	-0.50	0.84	3.23
4	1.42	-0.45	0.74	2.85
5	0.29	-0.04	0.17	0.69
ORIGINAL SPHCT				
1	4.28	-3.46	3.46	13.68
2	1.73	-0.57	1.29	5.37
3	1.45	-0.54	0.95	3.38
4	0.82	-0.17	0.46	1.58
5	0.48	-0.07	0.24	0.89
6	0.49	-0.07	0.25	0.90
MODIFIED SPHCT				
1	1.82	-0.92	1.32	6.27
2	1.96	0.28	1.37	5.53
3	2.09	0.35	1.26	4.54
4	1.03	0.20	0.66	2.35
5	0.34	-0.01	0.19	0.74
6	0.30	-0.01	0.18	0.71

nonidealities in the mixing rules for v* and c as introduced in the previous chapter.

Figure 16 shows the effect of carbon number on the optimum interaction parameter of Case 3. The figure indicates that both the modified and original SPHCT equations result in fairly constant interaction parameters with increasing carbon number as compared to those of the PR equation. This is as expected since the equations were developed to represent segment-segment interactions rather than molecule-molecule interactions. The interaction parameters of the modified equation are about half as large as those of the original SPHCT equation and show excellent extrapolative capability for heavier molecular weight compounds.

The effect of temperature on the interaction parameter can be seen in Figures 17-19 in which the C_{ij}'s of Case 4 are shown for the modified SPHCT equation, the original SPHCT equation and the PR equation, respectively. The apparant temperature dependence for n-C_7 is due to limited data for ethane + n-C_7 mixtures (only one data point is available for each isotherm). Figure 17 indicates a strong temperature dependence for the interaction parameters of the heavier components of the modified equation. This temperature dependence of C_{ij} for the modified equation can be explained as an inadequacy of the mixing rules used. As discussed in Chapter III the mixing rules used for F_t in the attractive portion of the equation of state remain questionable. While more complicated mixing rules such as those used by Donohue (6) and Vimalchand (14) may lessen the temperature dependence of C_{ij}, their additional complexity would make the equation of state quite cumbersome and would not be practical for engineering calculations. Figure 18 and

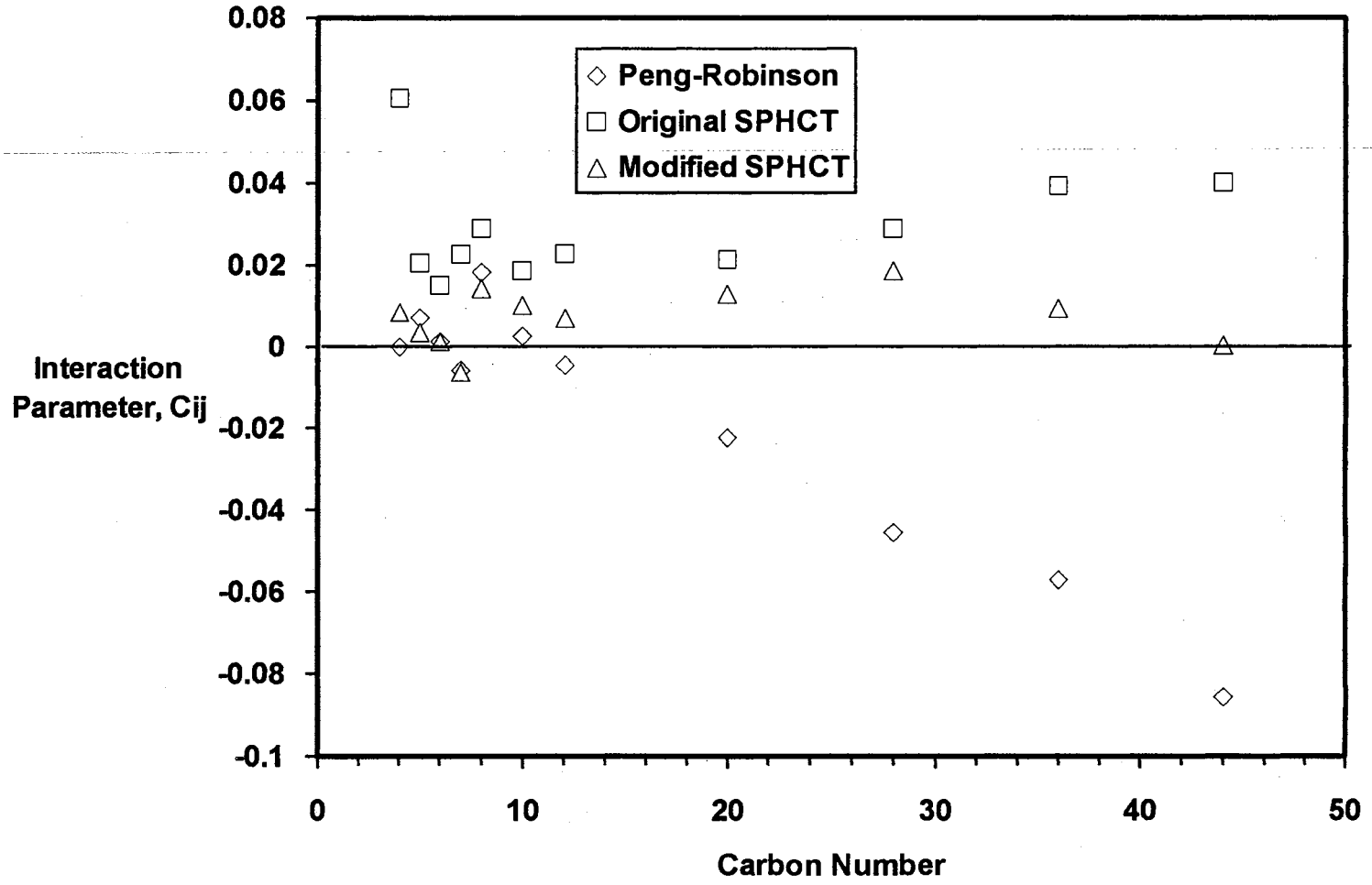

Figure 16. Equation of State Interaction Parameters, C_{ij}, for the Ethane + n-Paraffin Systems

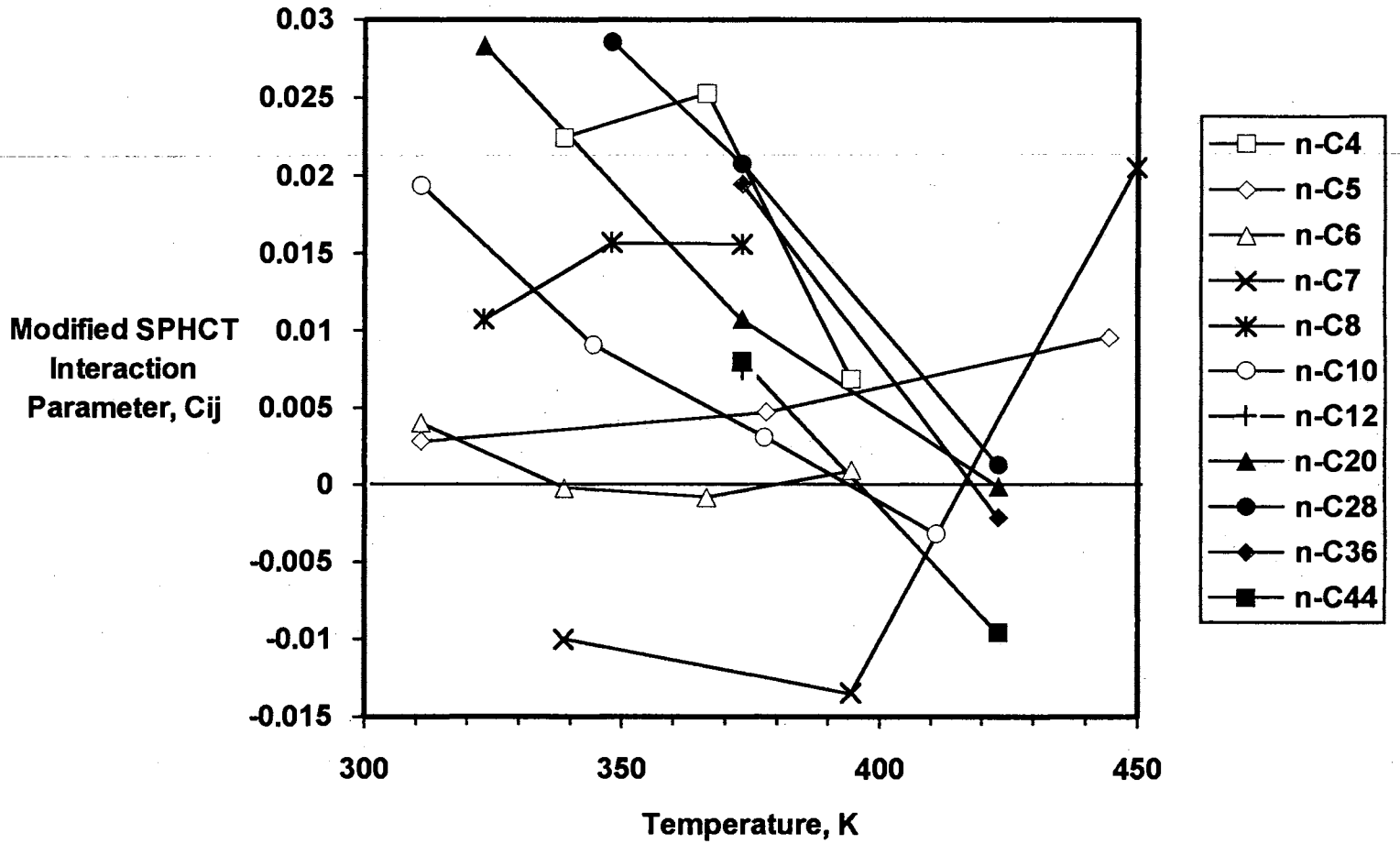

Figure 17. Modified SPHCT Interaction Parameter, C_{ij}, Temperature and Carbon Number Dependence for Ethane + n-Paraffin Systems

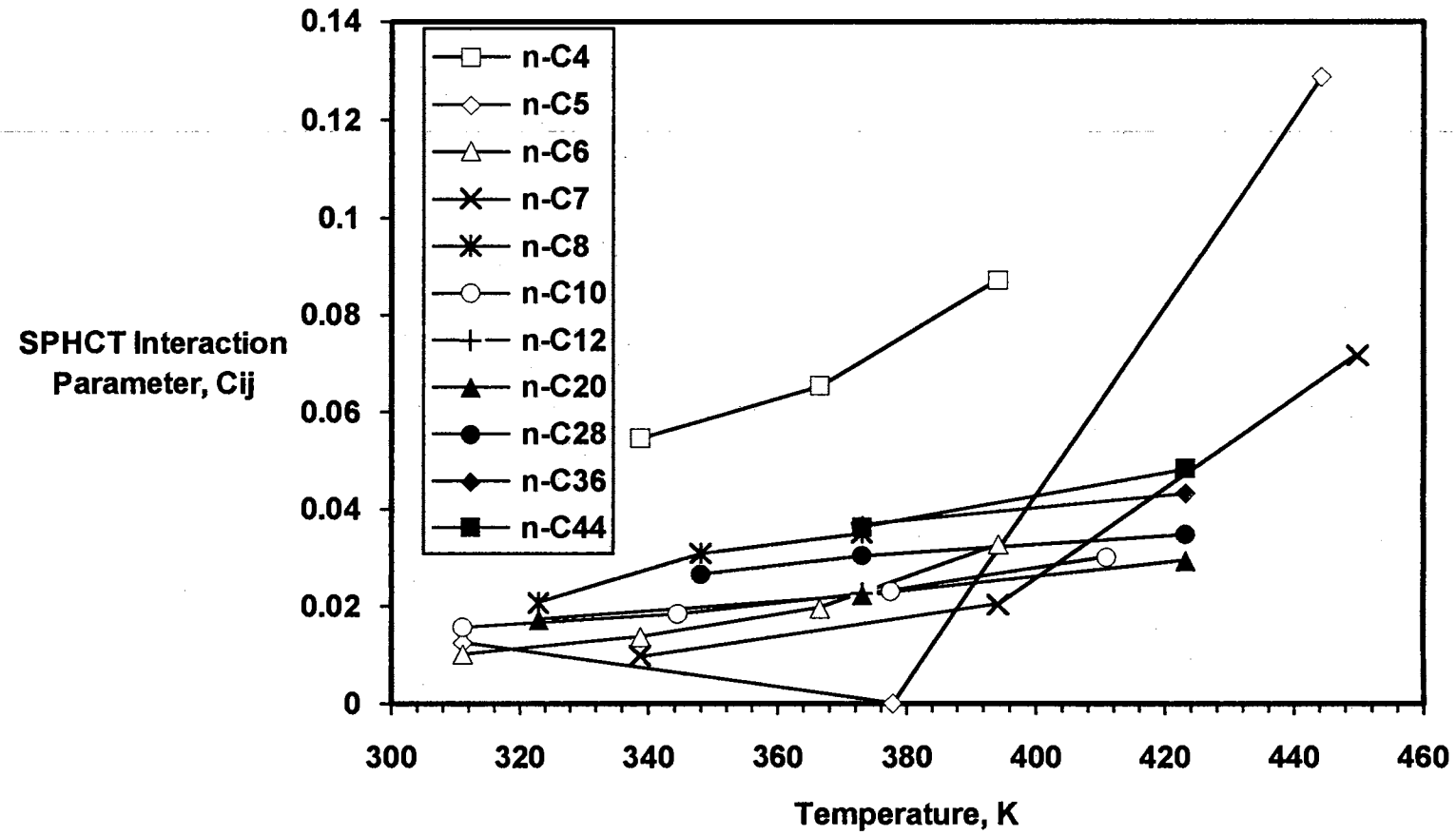

Figure 18. SPHCT Interaction Parameter, C_{ij}, Temperature and Carbon Number Dependence for Ethane + n-Paraffin Systems

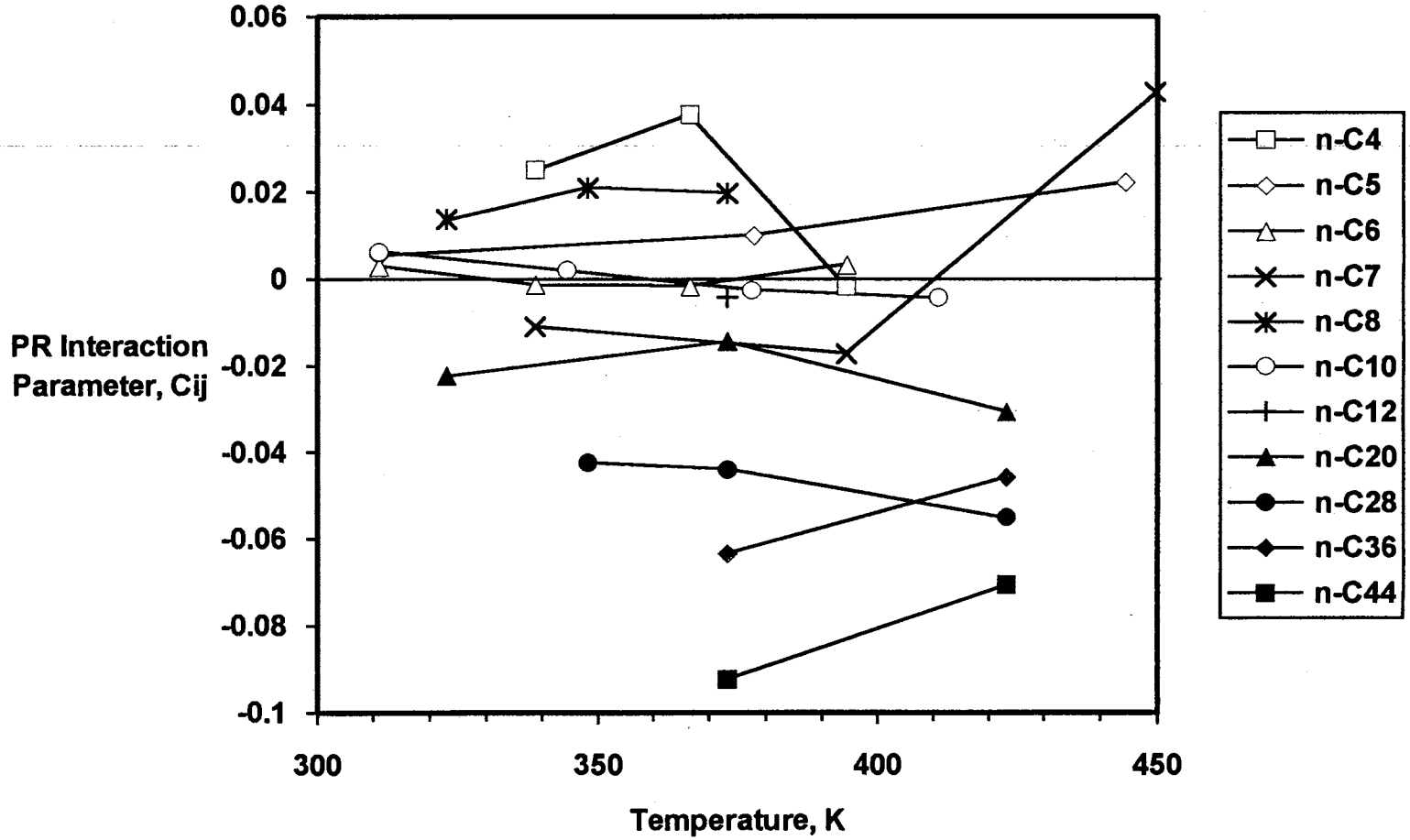

Figure 19. PR Interaction Parameter, C_{ij}, Temperature and Carbon Number Dependence for Ethane + n-Paraffin Systems

19 indicate that the C_{ij}'s of the original SPHCT and PR equations exhibit only a weak dependence on temperature.

Figures 20 through 22 illustrate the performance of each equation for the cases considered where the RMSPE in calculated bubble point pressure is shown versus carbon number. Comparison of Figures 20 and 21 indicate that the modified equation provides superior results in the predictive case (Case 1) and comparable results in the correlative cases (Cases 5 and 6) but is less flexible in the intermediate cases due largely to the strong temperature dependence of C_{ij} mentioned above. Figure 22 indicates that the PR equation exhibits only minor improvement in the progression from Case 1 to Case 4 with significant improvement requiring the addition of a second interaction parameter (Case 5) as recognized by Gasem, et al. (71).

The behavior of the interaction parameters in Cases 5 and 6 can be seen in Figures 23 and 24 in which the interaction parameters are shown for each carbon number for the modified SPHCT equation. In both cases the second interaction parameter is small and shows only a weak temperature dependence while the values for C_{ij} continue to show considerable spread for different temperatures. In Case 6 the values for C_{ij} and E_{ij} are highly correlated resulting in substantial scatter in the regressed values at low carbon numbers. The original SPHCT equation exhibits similar behavior for these two cases.

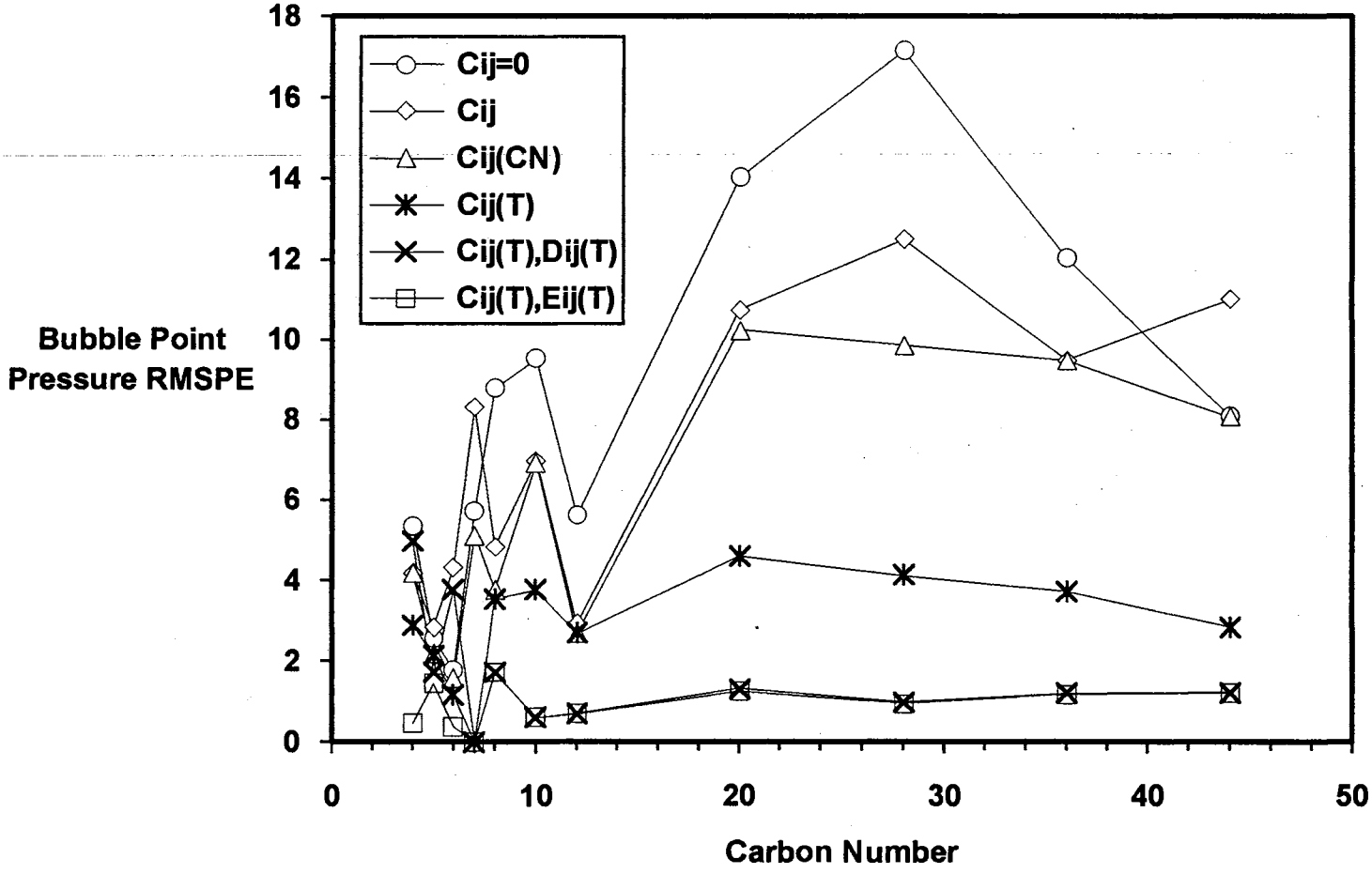

Figure 20. Effect of Carbon Number on Modified SPHCT Predictions for Ethane + n-Paraffin Systems

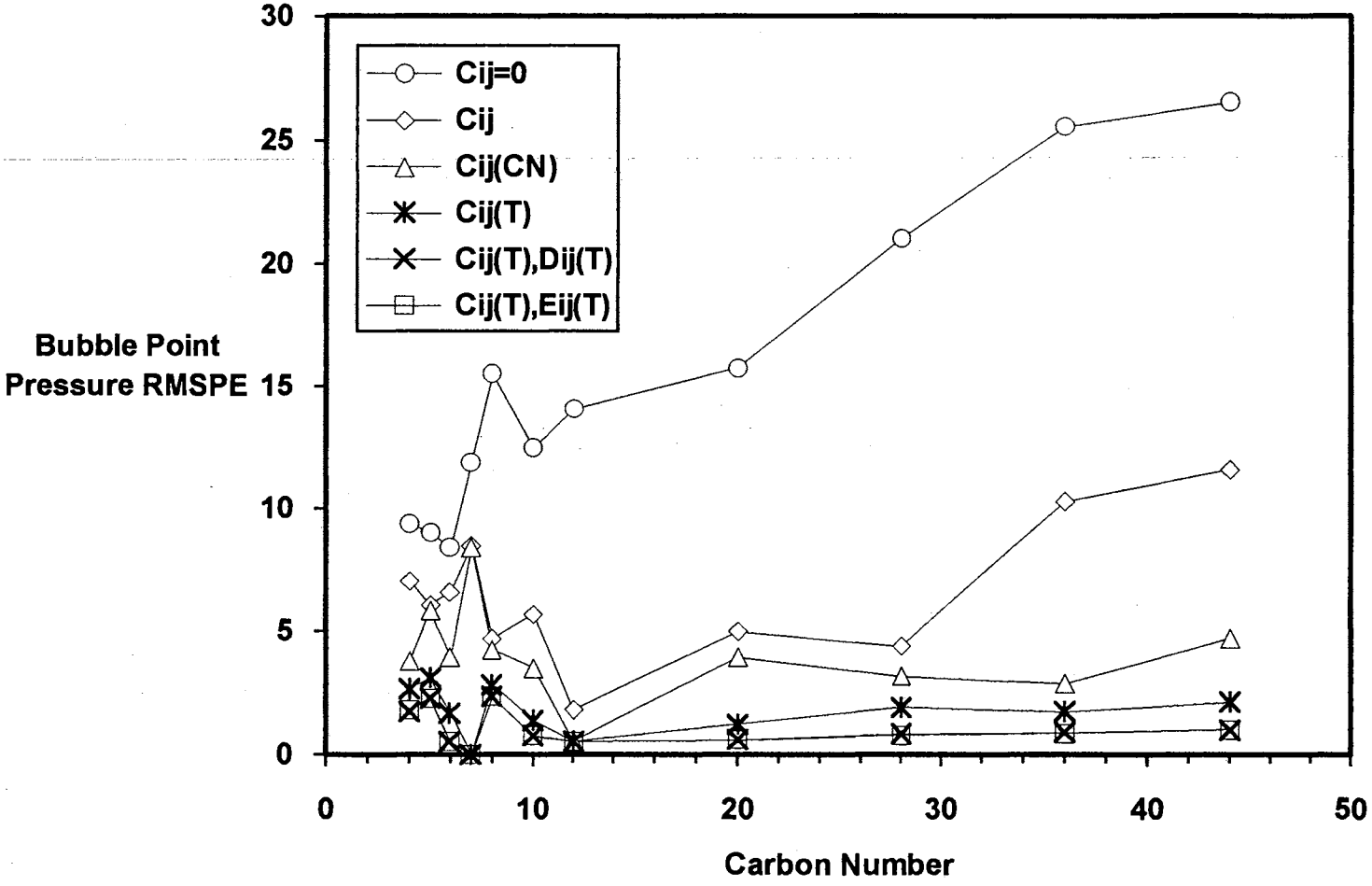

Figure 21. Effect of Carbon Number on SPHCT Predictions for Ethane + n-Paraffin Systems

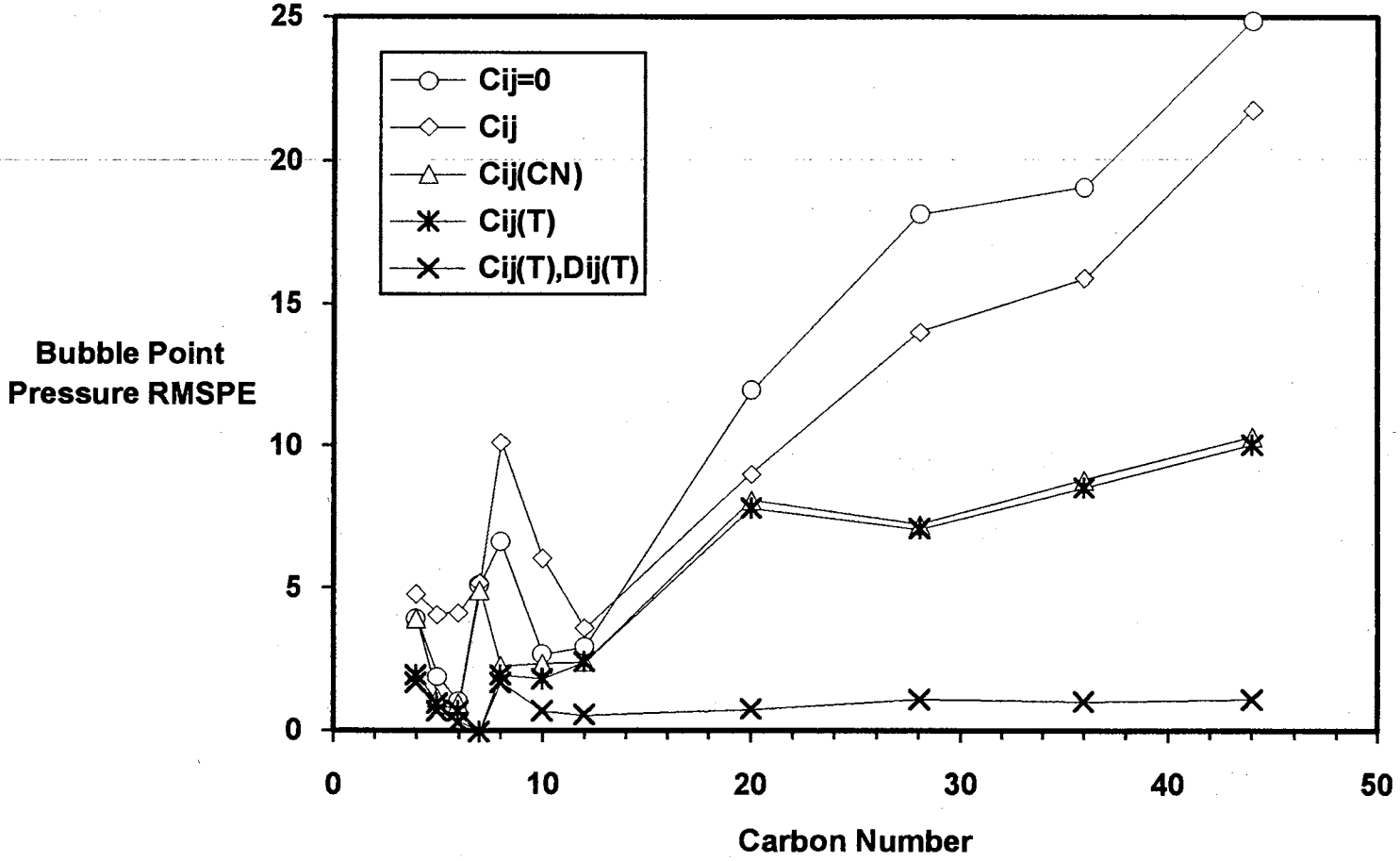

Figure 22. Effect of Carbon Number on PR Predictions for Ethane + n-Paraffin Systems

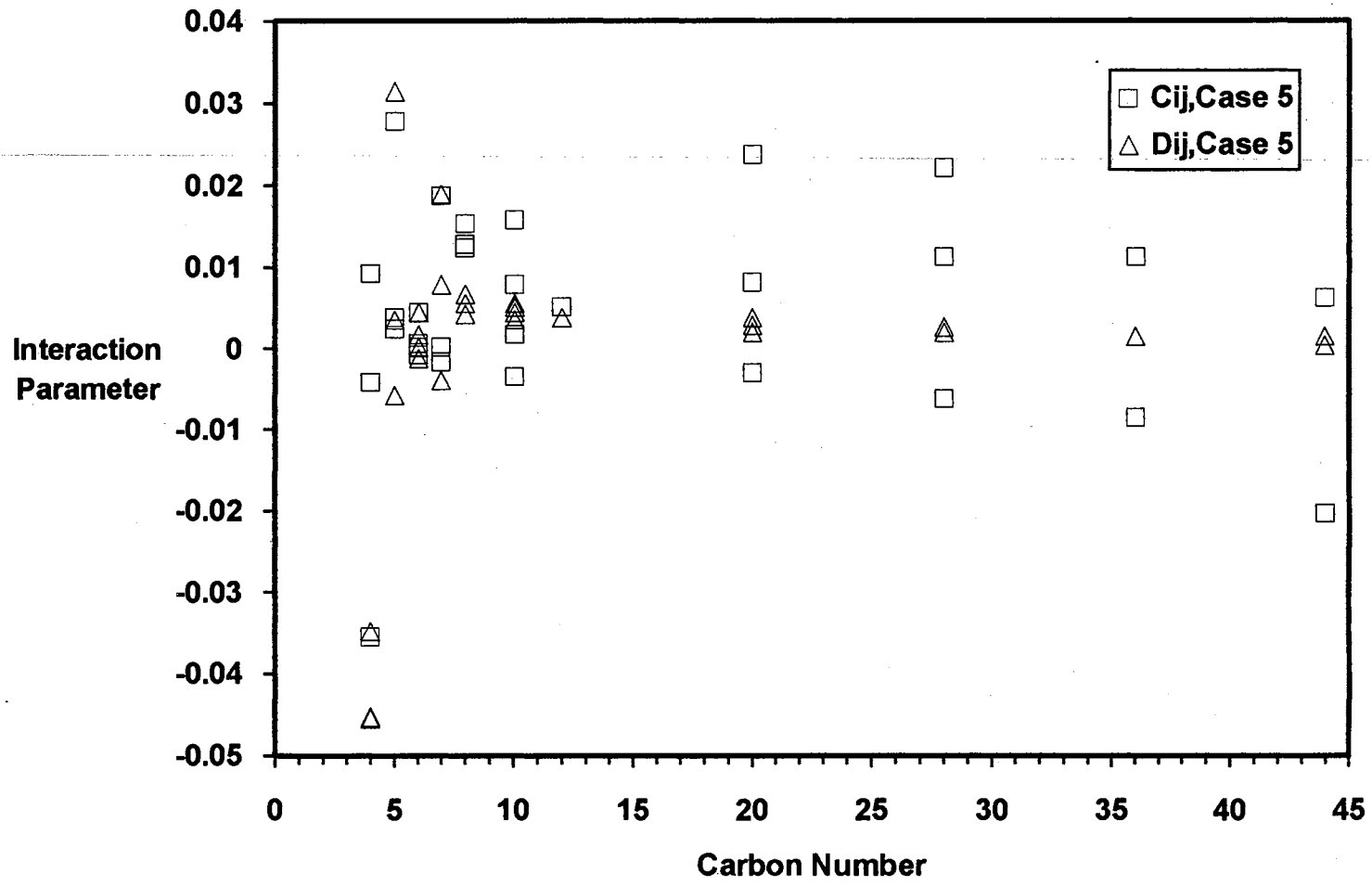

Figure 23. Effect of Carbon Number on C_{ij} and D_{ij} of the Modified SPHCT Equation for Predictions for Ethane + n-Paraffin Systems

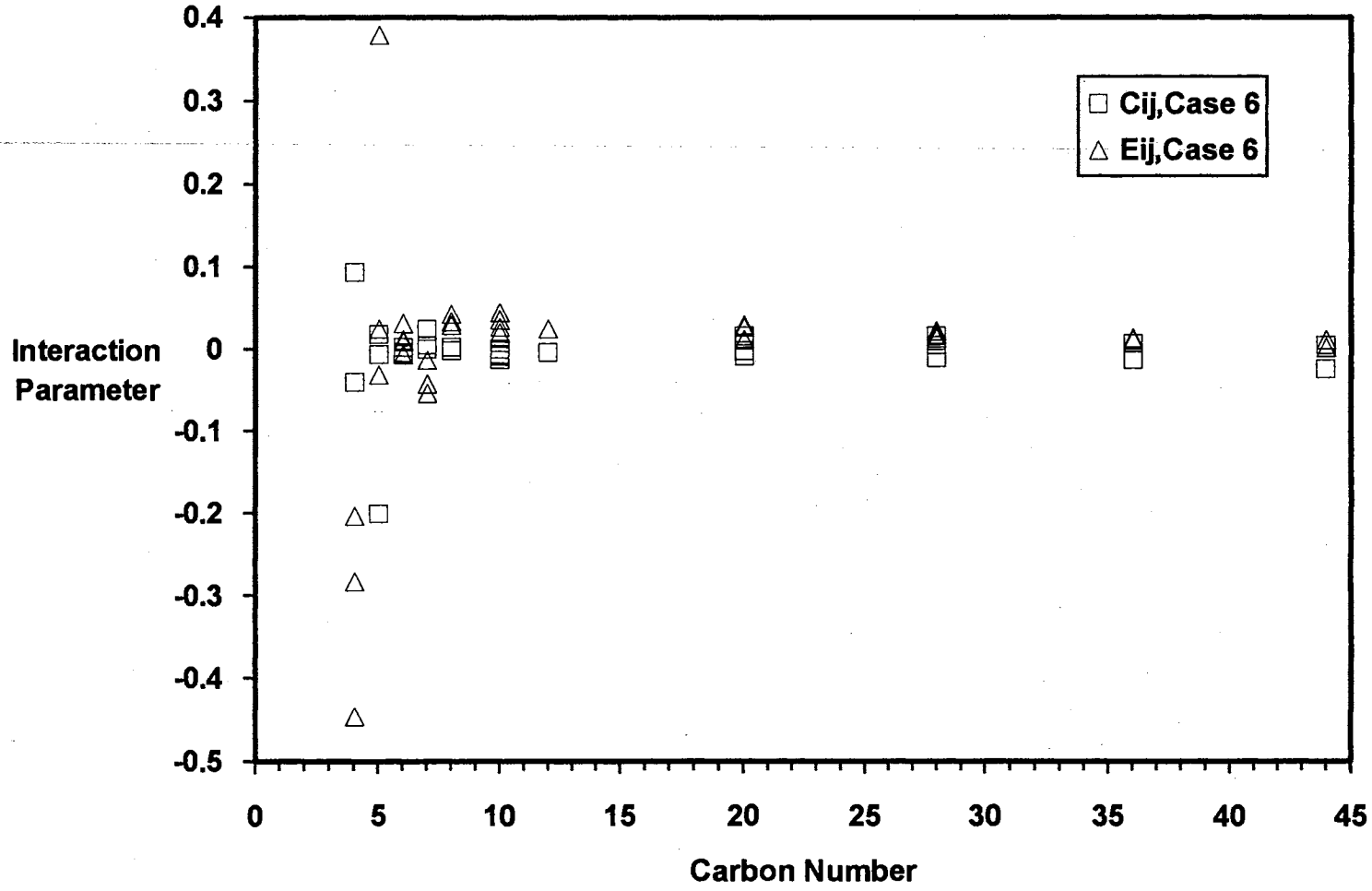

Figure 24. Effect of Carbon Number on C_{ij} and E_{ij} of the Modified SPHCT Equation for Predictions for Ethane + n-Paraffin Systems

Carbon Dioxide + n-Paraffin Systems

A summary of the results for the six cases described in Table IX are shown in Table XI for the prediction of bubble point pressures of CO_2 + n-paraffin binary mixtures. Table XI indicates that all three equations (modified SPHCT, SPHCT, and PR) are very poor in the *a priori* predictive case (Case 1). The predictions for both the modified SPHCT and the original SPHCT contained phase behavior convergence problems in that no two phase region exists for many of the higher pressure data points. This emphasizes the danger of using these equations with no interaction parameters for demanding molecular interactions such as those produced by the presence of CO_2. As with the ethane + n-paraffin systems, the modified SPHCT is comparable to the original SPHCT and PR equations for the predictive and correlative cases and less accurate for Cases 2 and 3.

The inadequacy of the modified SPHCT equation for representation of CO_2 systems can be attributed to the fact that the original equation was derived for non-polar compounds. Other workers (13,14) have addressed this problem by including additional terms in the partition function to account for dipolar and quadrupolar effects. Vimalchand (14) showed that his perturbed-anisotropic-chain theory (PACT) equation of state provides significantly better predictions of K-values for CO_2 + ethane mixtures than the PHCT equation of Donohue and Prausnitz (6). This inherent deficiency in the SPHCT equation of state framework coupled with the loss of empirical flexibility due to the critical point constraints helps to explain the observed results.

TABLE XI

SUMMARY OF RESULTS FOR REPRESENTATION OF BUBBLE POINT PRESSURES OF CO_2 + N-PARAFFIN SYSTEMS

Case Number	Bubble Point Pressure RMSE (bar)	BIAS (bar)	AAD (bar)	%AAD
PENG-ROBINSON				
1	12.08	-9.01	9.01	20.17
2	2.59	-0.70	2.09	5.53
3	2.25	-0.25	1.38	3.15
4	1.79	-0.27	1.07	2.44
5	0.88	-0.11	0.51	1.09
ORIGINAL SPHCT				
1	13.93	-11.31	11.31	26.51*
2	5.11	-0.36	3.64	7.48
3	3.39	-0.83	2.34	4.80
4	2.95	-0.91	1.56	2.66
5	1.13	-0.23	0.63	1.29
6	1.38	-0.29	0.74	1.44
MODIFIED SPHCT				
1	13.35	-10.44	10.50	26.50*
2	11.39	1.22	6.77	14.37
3	7.66	1.31	4.78	10.55
4	3.87	0.73	2.16	4.98
5	0.90	-0.06	0.60	1.28
6	0.87	-0.07	0.57	1.21

* In the predictive case, approximately 1/4 of the higher pressure data points were predicted as being single phase.

Figure 25 shows the effect of carbon number on the optimum interaction parameter of Case 3. As with the ethane systems, both the modified and original SPHCT equations contain smaller interaction parameters than the PR equation. However, there is more scatter in the C_{ij} values making extrapolations to heavier molecular weight compounds for the CO_2 systems less reliable.

The effect of temperature on the interaction parameter can be seen in Figures 26-28 in which the C_{ij}'s of Case 4 are shown for the modified SPHCT equation, the original SPHCT equation and the PR equation, respectively. Figure 26 indicates a strong temperature dependence for the interaction parameters of the modified equation. Figures 27 and 28 indicate temperature dependencies for the original SPHCT and PR equations which also appear to be weak functions of carbon number. However, the magnitude of the temperature dependence for these equations is less than that of the modified equation allowing the use of temperature independent C_{ij}'s (Case 3) to provide reasonable results. As with the ethane systems, the strong temperature dependence of the modified equation can be partially attributed to the inadequacy and uncertainty of the mixing rules as discussed in Chapter III.

Figures 29 through 31 illustrate the performance of each equation for the cases considered where the RMSPE in calculated bubble point pressure is shown versus carbon number. Comparison of Figures 29-31 indicate that the modified equation provides comparable results to both the original SPHCT and PR equations in the correlative cases (Cases 5 and 6).

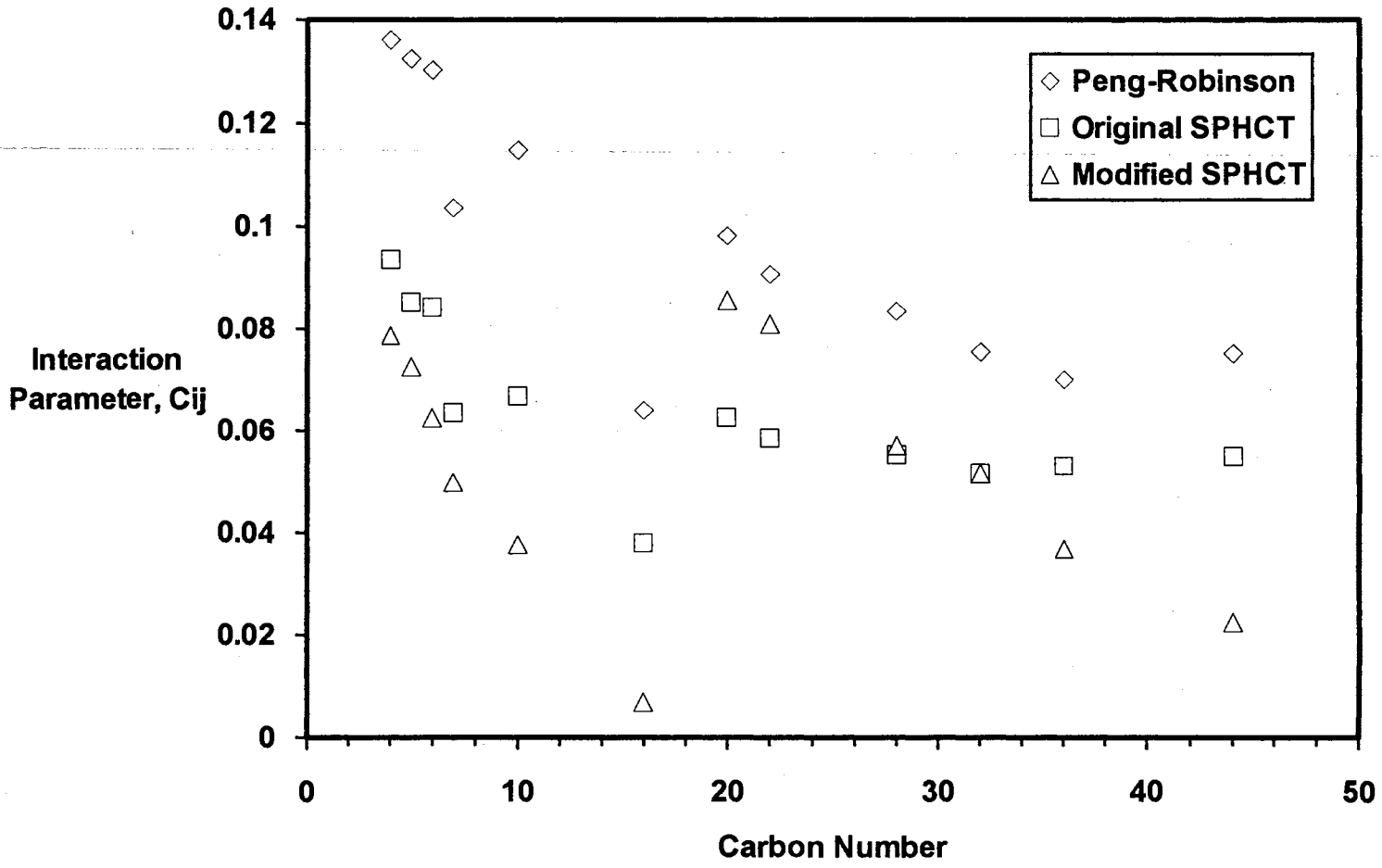

Figure 25. Equation of State Interaction Parameters, C_{ij}, for the CO_2 + n-Paraffin Systems

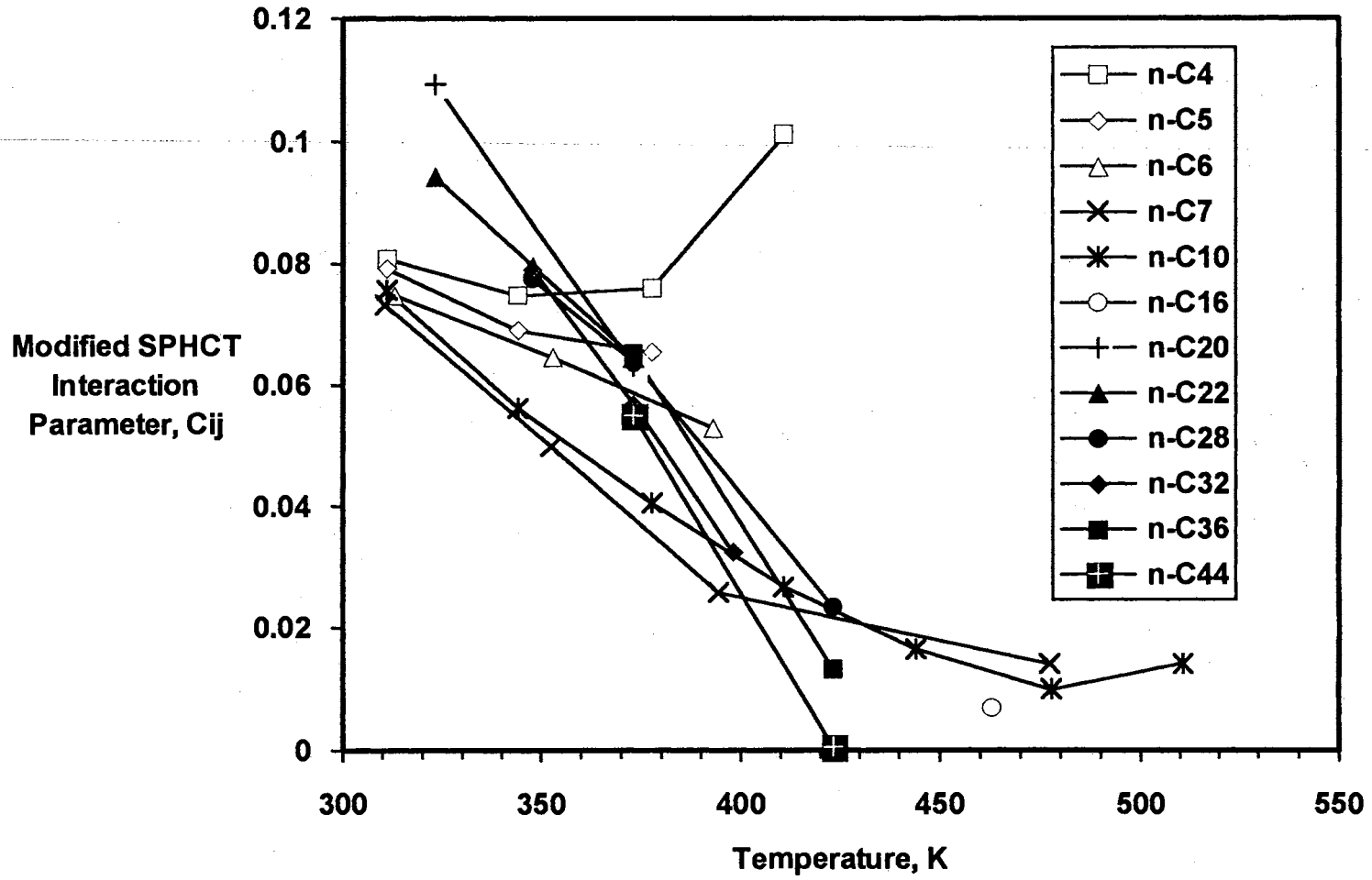

Figure 26. Modified SPHCT Interaction Parameter, C_{ij}, Temperature and Carbon Number Dependence for CO_2 + n-Paraffin Systems

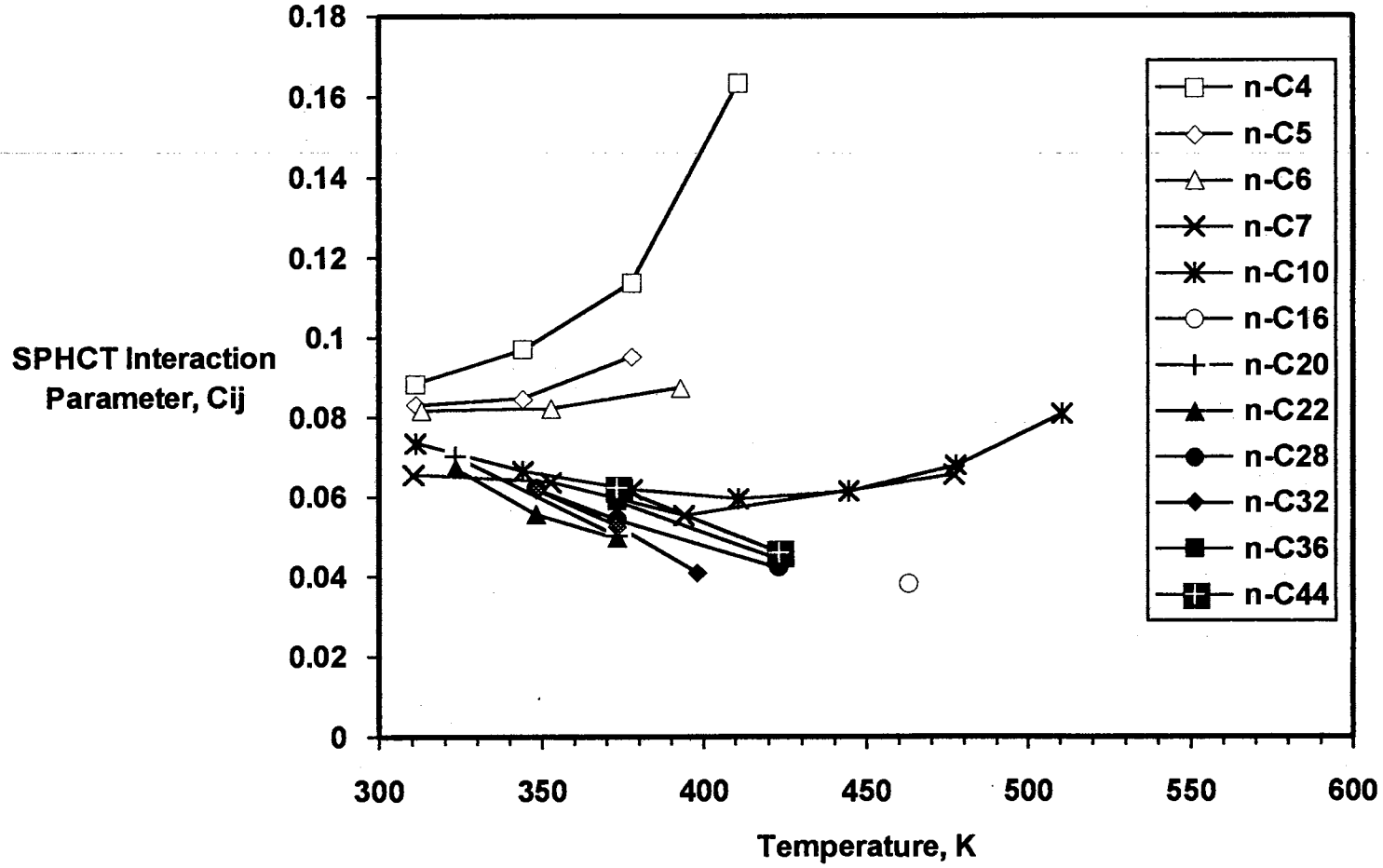

Figure 27. SPHCT Interaction Parameter, C_{ij}, Temperature and Carbon Number Dependence for CO_2 + n-Paraffin Systems

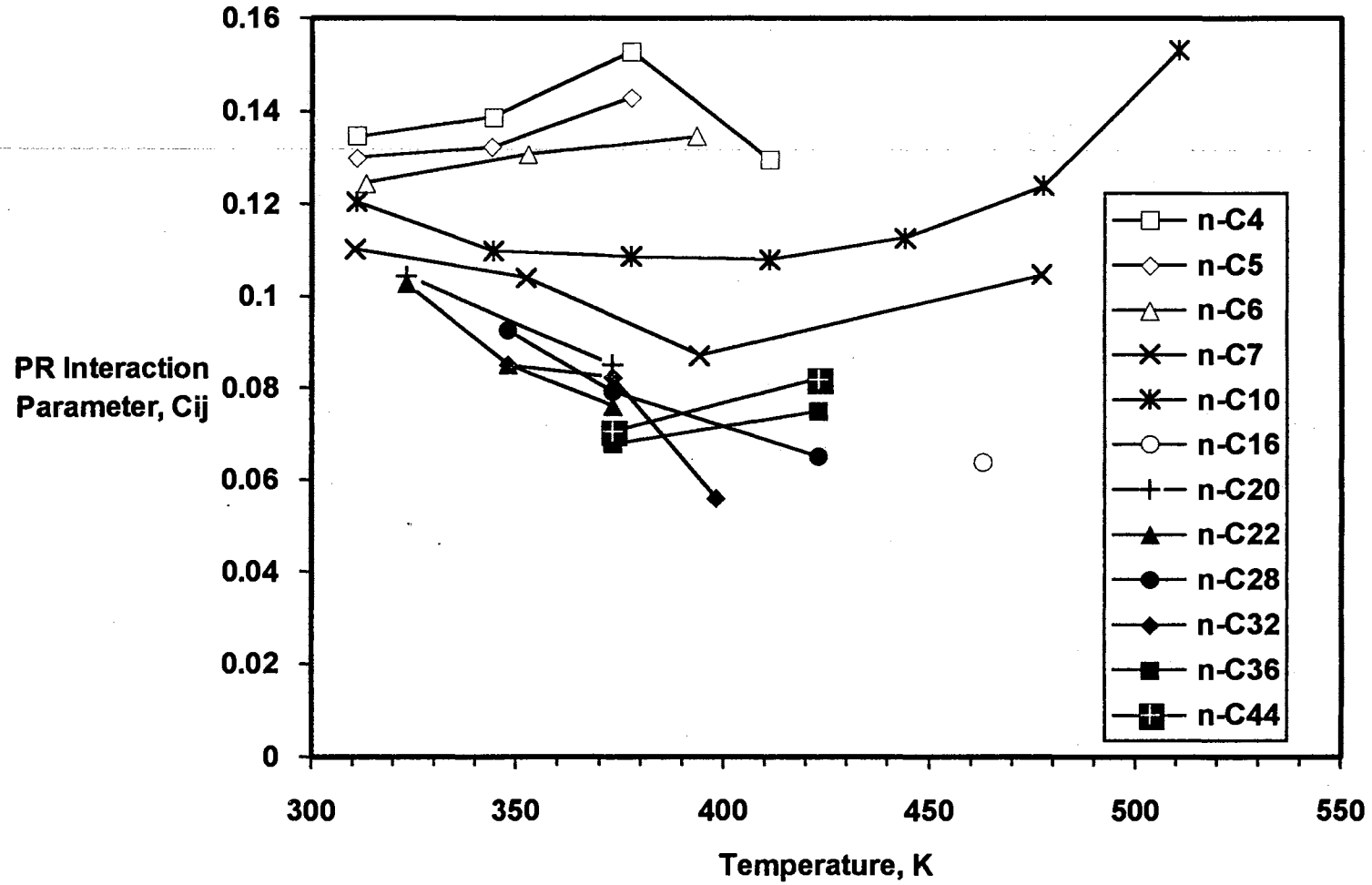

Figure 28. PR Interaction Parameter, C_{ij}, Temperature and Carbon Number Dependence for CO_2 + n-Paraffin Systems

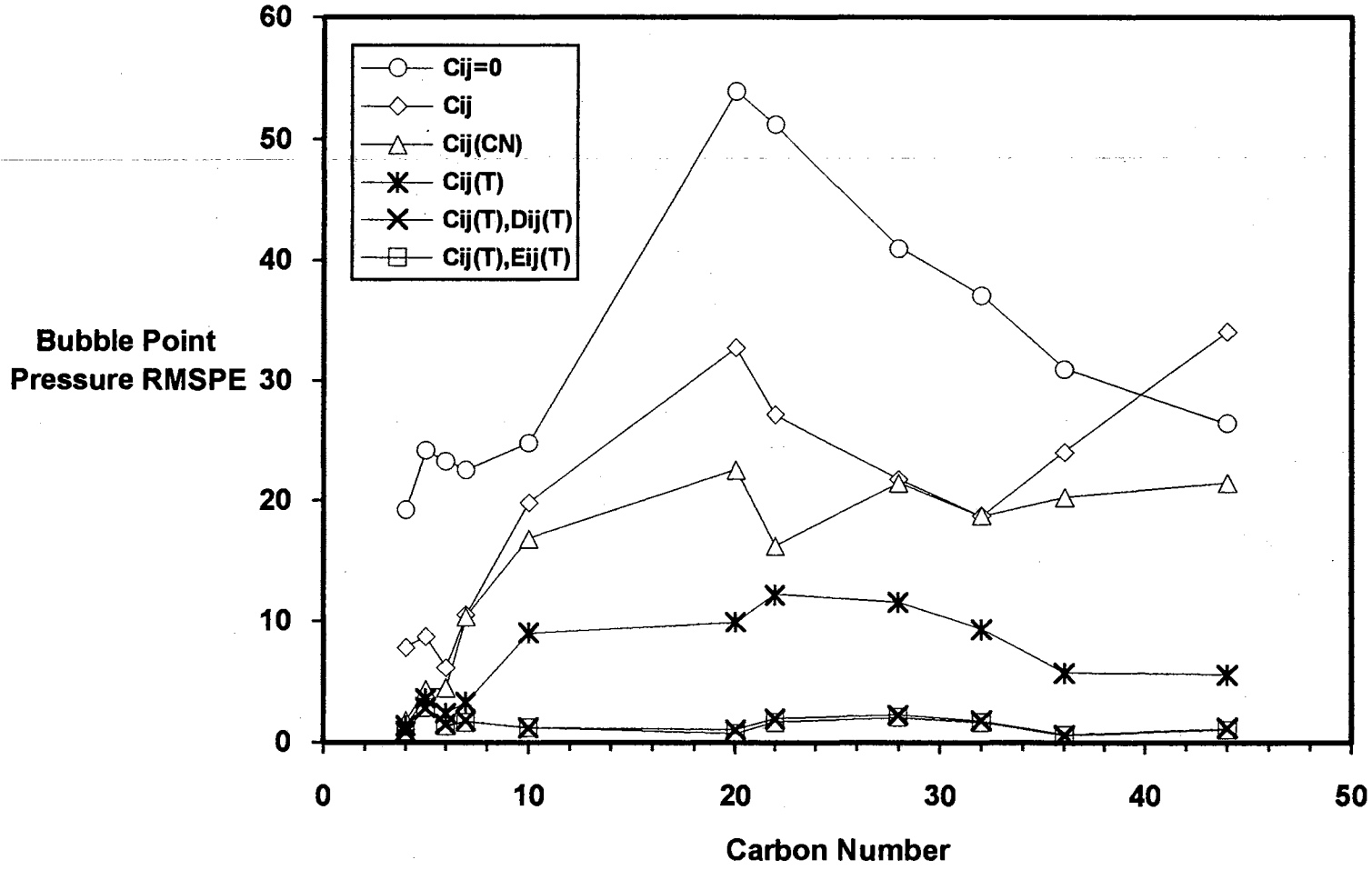

Figure 29. Effect of Carbon Number on Modified SPHCT Predictions for CO_2 + n-Paraffin Systems

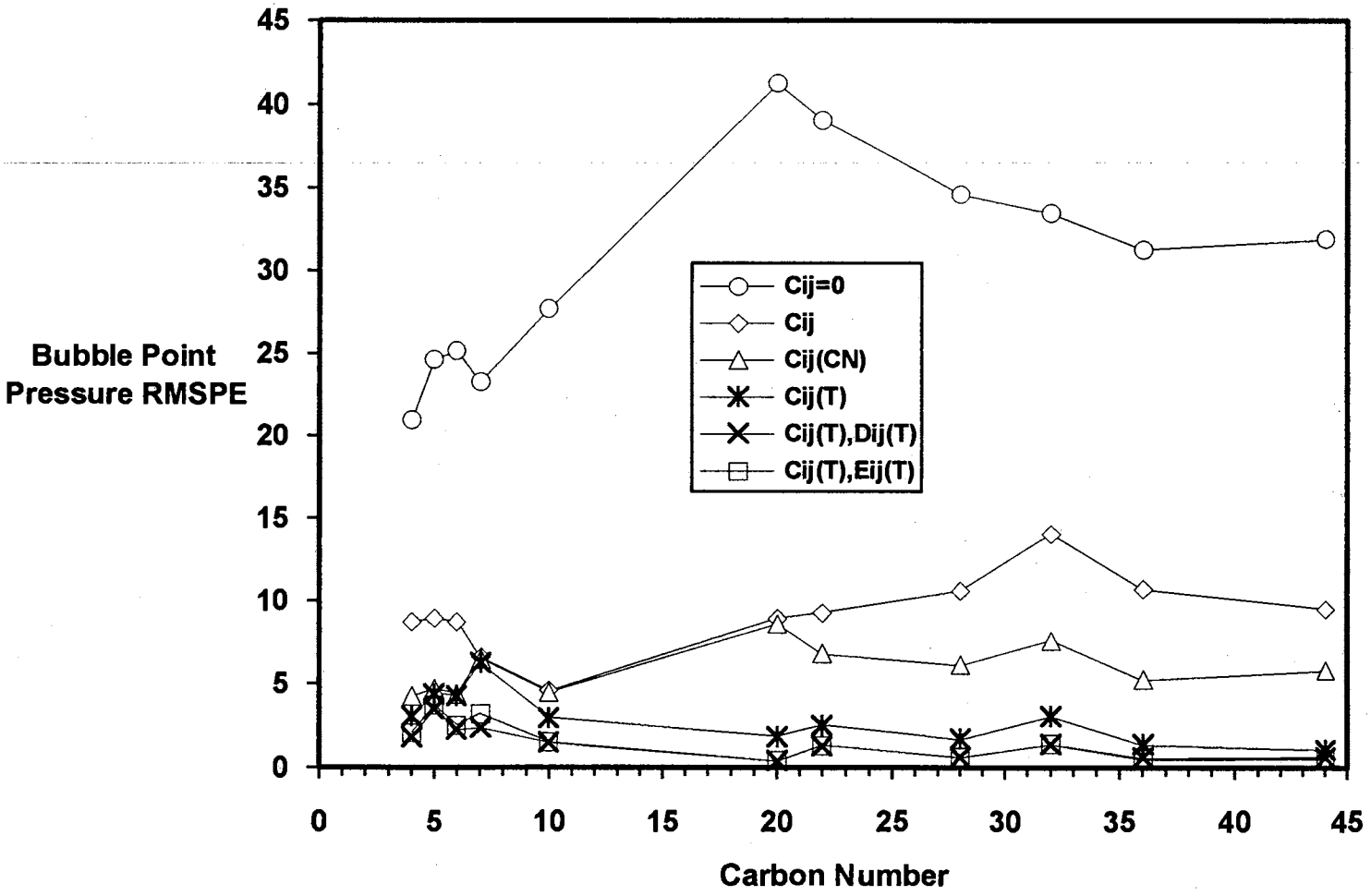

Figure 30. Effect of Carbon Number on SPHCT Predictions for CO_2 + n-Paraffin Systems

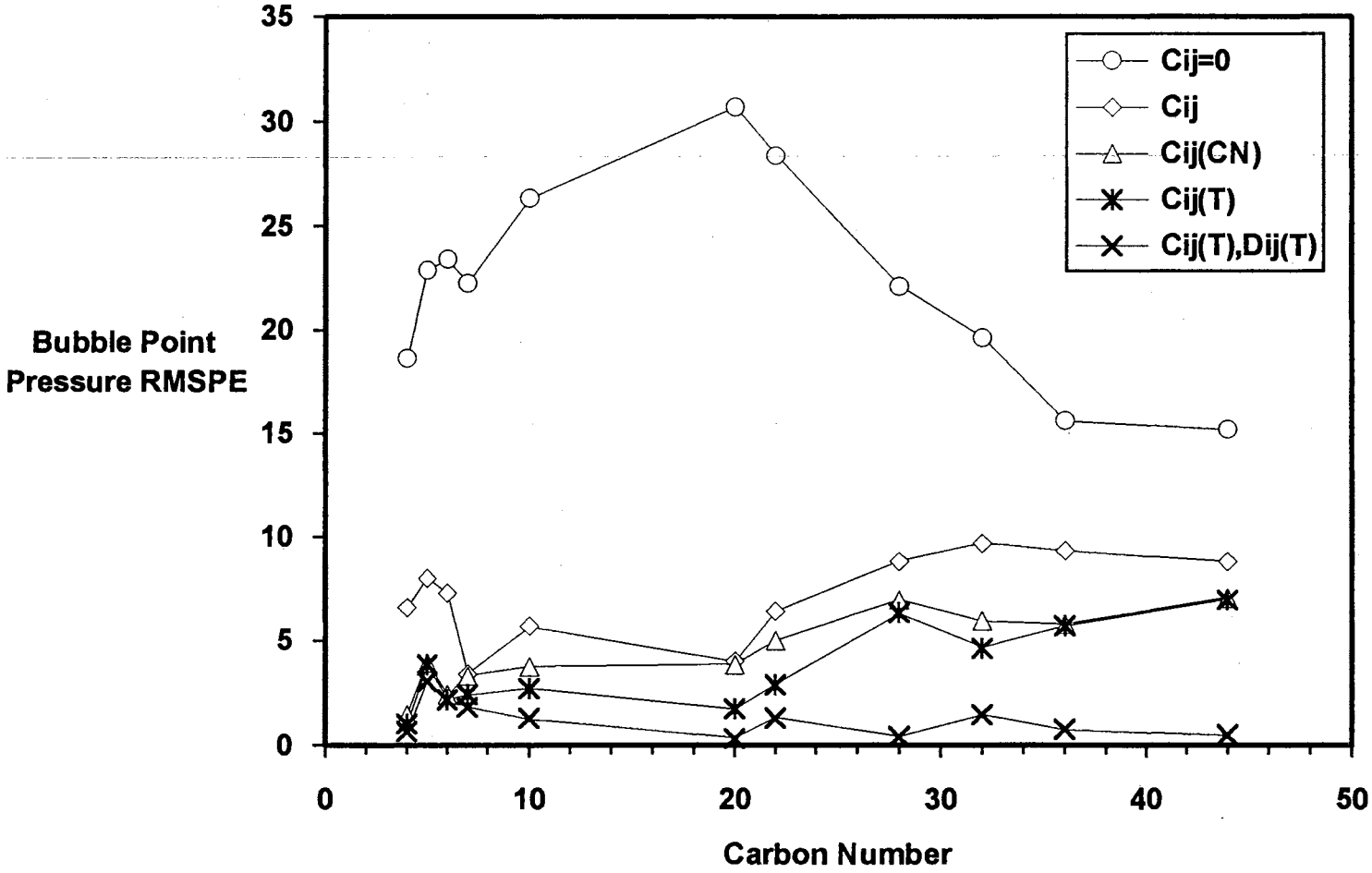

Figure 31. Effect of Carbon Number on PR Predictions for CO_2 + n-Paraffin Systems

Results for Data Containing Phase Densities and Compositions

The modified form of the SPHCT equation discussed in Chapter III and evaluated for the prediction of bubble point pressures of ethane + n-paraffin and CO_2 + n-paraffin systems in Chapter IV was further evaluated using a database containing both vapor and liquid phase compositions and densities. This evaluation was done for two reasons: (1) to demonstrate the ability of the modified equation to predict vapor phase compositions and phase densities over the full saturation range and (2) to demonstrate the application of the volume translation proposed in Chapter III for mixture calculations. The database used for these evaluations is included in Tables E.IV and E.V of Appendix E.

Four specific cases were studied as listed in Table XII. Case 1 represents the raw predictive ability of the equation in *a priori* predictions using no interaction parameters (C_{ij}=0). Since the evaluations using the two solubility databases showed that the modified equation performs best in the correlative cases, only these cases (Cases 2-4) were evaluated with this density-composition database. In Case 2, a separate value of C_{ij} is determined for each isotherm of each binary mixture. Cases 3 and 4 represent the ultimate correlative capability of the equation in which two interaction parameters are determined for each isotherm of each mixture. In Case 3, the second interaction parameter, D_{ij}, introduced in Chapter III is included in addition to C_{ij}. In Case 4, the second interaction parameter, E_{ij}, also introduced in Chapter III is included along with C_{ij}. Cases 3 and 4 were evaluated both with and without the volume translation proposed in Equations (85)-(88). The generalized form of volume translation was used with c_1=0.04 and c_2=1.5, and with δ_c treated as a system-specific parameter. The values for δ_c

TABLE XII

SPECIFIC CASES USED IN EQUATION OF STATE EVALUATIONS
USING THE DATABASE WITH PHASE COMPOSITIONS AND DENSITIES

Case	Parameters Regressed	Description
1	$C_{ij}=0$	The 'raw predictive ability' of the equation of state.
2	$C_{ij}(T)$	A separate value of C_{ij} is determined for each binary system at each temperature.
3	$C_{ij}(T), D_{ij}(T)$	A separate value of C_{ij} and D_{ij} is determined for each binary system at each temperature. This case represents the correlative capability of the equation of state with two interaction parameters. The modified SPHCT equation was evaluated for this case both with and without the volume translation of Equations (85)-(88) in which δ_c was treated as a system-specific regressed parameter.
4	$C_{ij}(T), E_{ij}(T)$	A separate value of C_{ij} and E_{ij} is determined for each binary system at each temperature. This case represents the correlative capability of the equation of state with two interaction parameters. The modified SPHCT equation was evaluated for this case both with and without the volume translation of Equations (85)-(88) in which δ_c was treated as a system-specific regressed parameter.

were obtained for each isotherm by minimizing the squared percentage errors of both vapor and liquid phase densities. As discussed in Chapter II, the equilibrium calculations (bubble point pressures and vapor phase compositions) are unaffected by the volume translation. For Case 3, the PR equation is used with D_{ij} representing a second interaction parameter used in the co-volume mixing rules in the usual way (70). Since the volume translation used in this work was specifically developed for the constrained form of the SPHCT equation, no volume translations were included for either the PR or the original SPHCT equations.

The interaction parameters for each of these cases were obtained using the objective function of Equation (90) using bubble point pressure calculations. Since the interaction parameters were fit only to the bubble point pressure, the equation of state performance in predicting vapor phase compositions and phase densities provides a useful evaluation of the overall integrity of the equation.

A summary of the results is shown in Table XIII for the Peng-Robinson equation, the original SPHCT equation and the modified SPHCT equation, respectively. Only the average absolute percentage deviations (%AAD) are included in the summary table to simplify the comparisons. Complete statistics for every case studied appear in Tables G.XXXV through G.XLV of Appendix G.

The large errors shown for Case 1 in Table XIII are due to single phase convergence problems for all three equations when no interaction parameters are used. As shown in Table XIII, the modified equation is slightly better than the PR or original SPHCT equations for the prediction of phase densities, while the original SPHCT is the best for

TABLE XIII

SUMMARY OF RESULTS FOR REPRESENTATION OF BUBBLE POINT CALCULATIONS FOR THE DATA CONTAINING PHASE COMPOSITIONS AND DENSITIES

Case Number	Prop.*	Equation of State**		
		Peng-Robinson	SPHCT	Modified SPHCT
1	P	16.7	12.5	19.8
	y	18.1	2.5	11.1
	L	12.6	11.5	6.7
	V	69.5	79.8	55.0
2	P	2.9	2.9	3.9
	y	1.5	4.4	1.6
	L	13.2	14.4	8.7
	V	5.5	7.0	11.4
3	P	1.8	1.0	0.3
	y	1.6	2.8	1.4
	L	13.2	11.7	9.1
	V	4.7	6.5	8.6
	Lt			3.8
	Vt			5.4
4	P		2.0	0.3
	y		3.2	1.3
	L		13.4	8.9
	V		6.8	8.7
	Lt			3.6
	Vt			5.8

* P=pressure; y=solute vapor mole fraction; L=liquid density; V=vapor density; Lt=translated liquid density; Vt=translated vapor density

** Numbers in the table are average absolute percent deviations

prediction of vapor phase solute mole fraction in Case 1. However, no two-phase region existed for many of the data points for the SPHCT and modified SPHCT equations. This again emphasizes the danger of using these equations with no interaction parameters for the CO_2 + hydrocarbon mixtures. The results for Case 2 indicate that the modified SPHCT equation is comparable to the PR equation for prediction of vapor phase compositions (1.6% for the modified equation and 1.5% for PR) but is not quite as accurate for calculation of bubble point pressures as either of the other two equations (3.9% for the modified equation and 2.9% for the others). These results for bubble point pressure calculations for Case 2 ($C_{ij}(T)$) are the same as those obtained using the two solubility databases discussed previously. Case 3 demonstrates the effect of including the interaction parameter, D_{ij}, of Equation (84) for the prediction of the various phase properties. As shown in Table XIII, the modified equation (with no volume translation) is best in this case for the prediction of bubble point pressures (0.3 %AAD), vapor compositions (1.4 %AAD) and liquid densities (9.1 %AAD) while the PR equation is best for prediction of vapor densities (4.7 %AAD). Addition of the volume translation of Chapter III to the modified equation results in further improvement of phase density calculations. The addition of the interaction parameter, E_{ij}, of Equation (81) (Case 4) provides essentially the same results as Case 3 for both the original and modified equations.

The above evaluations which include two interaction parameters for each isotherm (Cases 3 and 4) stray from the ultimate objective of developing a strictly *a priori* predictive equation. In view of the inadequate representation of mixture properties for the more predictive

cases as discussed in the previous section, the comparisons of Cases 3 and 4 were done here as a remedial effort to demonstrate the purely correlative capability of the equation.

Overall, the modified SPHCT equation performs well for the representation of both vapor and liquid phase properties when used in a correlative fashion and compares favorably with both the PR and the original SPHCT equations. Use of the modified equation results in even distribution of vapor and liquid phase densities for both the untranslated and the translated equations for these cases.

CHAPTER V

CONCLUSIONS AND RECOMMENDATIONS

The goals of this work were to address some of the limitations of the simplified-perturbed-hard-chain theory (SPHCT) equation of state and to explore possible modifications to the equation to improve its performance for both equilibrium and volumetric calculations. Modifications to the equation were developed and evaluated using a database of 23 pure compounds and three separate mixture databases: one containing solubility data for ethane + n-paraffin binary mixtures, a second containing solubility data for CO_2 + n-paraffin binary mixtures and a third containing data for the complete two-phase envelope. The final database consists of vapor and liquid phase compositions and densities of binary mixtures at pressures up to the mixture critical point (including the experimental data of this work described in Section 1). Following are specific conclusions and recommendations which can be made based on this work.

Conclusions

1. A robust algorithm has been developed for solution of the SPHCT equation which consists of a new solution equation written in terms of the compressibility factor. The algorithm exhibits better behavior near both the liquid and vapor roots than previous solution equations. However, this routine is less efficient than

some of the previous methods resulting in increased computation time during parameter regressions.

2. A study of the SPHCT parameters (T*, v*, c, and Z_M) was undertaken to gain insight into the sensitivity of calculated properties to EOS parameter values and to investigate the behavior of the parameters required to produce accurate equilibrium and volumetric predictions over the full saturation range. The parameters T* and Z_M were found to have very strong influences on calculated vapor pressures and phase densities. This was interpreted as a deficiency of the attractive portion of the equation of state and further equation of state modifications were concentrated on improving the temperature functionality of this term.
3. The effect of applying the critical point constraints to the SPHCT equation was investigated. Application of the constraints results in more stable parameterization than the original SPHCT equation. This is because the parameters for the constrained equation are obtained by optimizing one of the pure fluid parameters using vapor pressure data only with the other parameters determined from the critical point constraints, thus avoiding parameter generation problems associated with the original SPHCT equation.
4. The simultaneous solution of the critical point constraint equations is quite cumbersome. Numerical implementation of these equations within equilibrium programs is difficult and computationally time-consuming. Therefore, simple correlations were developed for solving the critical point constraints. The correlations significantly reduce computation time and complexity,

and should allow other investigators to use the critical point constraints for this equation without the need to embed complicated numerical routines within their existing programs.

5. Several modifications for the attractive portion of the constrained SPHCT equation of state were investigated to improve the performance of equilibrium calculations. Significant improvement in the EOS predictive capability was realized by including a polynomial correction to the temperature dependence within the exponential part of the attractive term. The modifying function is intended to represent an empirical temperature dependence for the radial distribution function used in the original EOS development. The modified equation results in percent average absolute deviations (%AAD) for calculation of pure fluid vapor pressures of 1.1% for the 23 compounds considered.

6. A volume translation strategy similar to that developed by Chou and Prausnitz (38) has been proposed for improvement of phase density predictions of the constrained and modified SPHCT equation. The generalized volume translation improves the calculation of both vapor and liquid phase densities for pure fluids (1.8 %AAD for vapor densities and 2.6 %AAD for liquid densities).

7. The modified equation was evaluated for the prediction of bubble point pressures of ethane + n-paraffin and CO_2 + n-paraffin mixtures. The modified equation provides significant improvement for the prediction of bubble point pressures of the ethane systems when no interaction parameters are included. However, interaction parameters regressed for each isotherm of each mixture ($C_{ij}(T)$)

show stronger temperature dependence than those of the original SPHCT equation resulting in less flexibility. This is attributed to poor mixing characteristics for the EOS parameters.

8. The species coordination number and configurational energy for mixtures were developed without the simplifying assumption of the original SPHCT development. The earlier work assumed that the zero density limiting behavior of the radial distribution function was sufficient for description of real fluids at all conditions. The present work shows that the mixing rules used by Kim, et al. (7) can be inferred from the mixture configurational energy expression for the simplified radial distribution function. However, more realistic distribution functions will require the development of new mixing rules.

9. Two new interaction parameters were added to the equation of state to lend it additional flexibility and to account for the nonidealities in mixing for the hard core diameter, σ, and the degrees of freedom parameter, c. Inclusion of the new interaction parameters improves both the original and the modified SPHCT predictions when these equations are used in a correlative fashion.

10. The modified equation was further evaluated for the prediction of vapor phase compositions and phase densities using the database which contains information about the complete phase envelope. Evaluations were done through the use of bubble point calculations. Overall, the modified equation performs well for the prediction of bubble point pressures (0.3 %AAD), vapor phase compositions (1.4 %AAD), vapor densities (5.4 %AAD) and liquid

densities (3.8 %AAD) for the cases which contain C_{ij} and either D_{ij} or E_{ij} for each isotherm.

11. The proposed volume translation strategy was tested for the correlative cases using the third database. The volume translation results in even distribution of errors in calculated vapor and liquid phase densities when the volume translation parameter, δ_c, is treated as a system-specific parameter. The translation provides considerable improvement for liquid density predictions when compared to the original SPHCT equation (11.7 %AAD for the original equation and 3.8 %AAD for the modified and translated equation) and marginal improvements for the prediction of vapor density (6.5 %AAD for the original equation and 5.4 %AAD for the modified and translated equation).

Recommendations

1. The proposed solution algorithm for the modified and original SPHCT equations is computationally inefficient. The routine should be further improved to reduce the required computation time for equilibrium calculations. Such modifications can be made by improving the efficiency of the method used for location of the liquid root.
2. The modifications proposed in this work should be evaluated for the prediction of pure fluid densities in the compressed liquid, superheated vapor and dense gas regions. This will provide insight into the abilities of the modified SPHCT equation to describe the entire PVT surface.
3. Further improvements for the calculation of properties of hydrocarbon mixtures should be addressed through the development of better mixing rules. Efforts should be directed towards reducing the temperature and composition dependence of the required binary interaction parameters of the modified SPHCT equation.
4. Fundamental changes to the partition function of the original SPHCT equation should be addressed to improve the representation of mixtures containing compounds such as CO_2 which possess complex molecular interactions while maintaining the simple mathematical form of the SPHCT framework.
5. The mixture database should be expanded to include more types of chemical compounds for use in future EOS evaluations. The database should include other types of solute compounds (such as CH_4, H_2, H_2S and N_2) as well as a wider variety of solvent

compounds. The expanded database would then allow more comprehensive EOS evaluations for the predictions of mixtures commonly encountered in the chemical process industry.

LITERATURE CITED

1. Gasem, K. A. M. and R. L. Robinson, Jr., "Evaluation of the Simplified Perturbed Hard Chain Theory (SPHCT) for Prediction of Phase Behavior of n-Paraffins and Mixtures of n-Paraffins with Ethane," Fluid Phase Equilibria, 58, 13-33 (1990).

2. Ponce-Ramirez, L., C. Lira-Galeana, and C. Tapia-Medina, "Application of the SPHCT Model to the Prediction of Phase Equilibria in CO_2-Hydrocarbon Systems," Fluid Phase Equilibria, 70, 1-18 (1991).

3. van Pelt, A., C. J. Peters and J. de Swaan Arons, "Application of the Simplified-Perturbed-Hard-Chain Theory for Pure Components Near the Critical Point," Fluid Phase Equilibria, 74, 67-83 (1992).

4. van Pelt, A., U. K. Deiters, C. J. Peters and J. de Swaan Arons, "The Limiting Behavior at High Temperatures of the Simplified-Perturbed-Hard-Chain Theory," Fluid Phase Equilibria, In Press.

5. Beret, S. and J. M. Prausnitz, "Perturbed Hard-Chain Theory: An Equation of State for Fluids Containing Small or Large Molecules," AIChE Journal, 21, 1123-1132 (1975).

6. Donohue, M. D. and J. M. Prausnitz, "Perturbed Hard Chain Theory for Fluid Mixtures: Thermodynamic Properties for Mixtures in Natural Gas and Petroleum Technology," AIChE Journal, 24, 849-860 (1978).

7. Kim, C. H., P. Vimalchand, M. D. Donohue and S. I. Sandler, "Local Composition Model for Chainlike Molecules: A New Simplified Version of the Perturbed Hard Chain Theory," AIChE Journal, 32, 1726-1734 (1986).

8. Prausnitz, J. M. and M. D. Donohue, "Thermodynamic Properties of Fluid Mixtures from Perturbed-Hard-Chain Theory," Gas Processors Association, Proceedings of Fifty-Fifth Annual Convention, 10-17 (March, 1976).

9. Donohue, M. D., B. K. Kaul and J. M. Prausnitz, "Perturbed-Hard-Chain Theory for Correlation of Thermodynamic Properties," Gas Processors Association, Proceedings of Fifty-Sixth Annual Convention, 36-41 (March, 1977).

10. Donohue, M. D. and P. Vimalchand, "Recent Improvements in the Perturbed-Hard-Chain Equation," Gas Processors Association, Proceedings of Sixty-Sixth Annual Convention, 165-172 (March, 1987).

11. Chien, C. H., R. A. Greenkorn and K. C. Chao, "Chain-of-Rotators Equation of State," AIChE Journal, 29, 560-571 (1983).

12. Donohue, M. D. and P. Vimalchand, "The Perturbed-Hard-Chain Theory. Extensions and Applications," Fluid Phase Equilibria, 40, 185-211 (1988).

13. Walsh, J. M., G. Jin and M. D. Donohue, "Thermodynamics fo Short-Chain Polar Compounds," Fluid Phase Equilibria, 65, 209-237 (1991).

14. Vimalchand, P., "Thermodynamics of Multi-Polar Molecules: The Perturbed-Anisotropic-Chain Theory," Ph.D. Dissertation, The Johns Hopkins University (1986).

15. Martin, J. J., "Cubic Equations of State - Which?," Industrial and Engineering Chemistry Fundamentals, 18, 81-97 (1979).

16. Sandler, S. I., "From Molecular Theory to Thermodynamic Models," Chemical Engineering Education, 12 (1990).

17. Lee, L. L., "Molecular Thermodynamics of Nonideal Fluids," Butterworths, Boston (1988).

18. Carnahan, N. F. and K. E. Starling, "Intermolecular Repulsions and the Equation of State for Fluids," AIChE Journal, 18, 1184-1189 (1972).

19. Reed, T. M. and K. E. Gubbins, "Applied Statistical Mechanics," McGraw-Hill, New York (1973).

20. Prigogine, I., "The Molecular Theory of Solutions," North Holland Publishing Company, Amsterdam (1957).

21. Flory, P. J., "Thermodynamics of Polymer Solutions," Disc. Faraday Society, 49, 7 (1970).

22. Kaul, B., M. D. Donohue and J. M. Prausnitz, "Henry's Constants and Second Virial Coefficients from Perturbed-Hard-Chain Theory," Fluid Phase Equilibria, 4, 171-184 (1980).

23. Liu, D. D. and J. M. Prausnitz, "Thermodynamics of Gas Solubilities in Molten Polymers," Journal of Applied Polymer Science, 24, 725-733 (1979).

24. Alder, B. J., D. A. Young and M. A. Mark, "Studies in Molecular Dynamics. I. Corrections to the Augmented van der Waals Theory for Square-Well Fluids," Journal of Chemical Physics, 56, 3013 (1972).

25. Kim, C. H., "High Pressure Vapor-Liquid Equilibrium Measurements and a New Equation of State: The Simplified-Perturbed-Hard-Chain Theory," Ph.D. Dissertation, The Johns Hopkins University (1986).

26. Lee, K. H., M. Lombardo and S. I. Sandler, "The Generalized van der Waals Partition Function. II. Application to the Square-Well Fluids," Fluid Phase Equilibria, 21, 177-196 (1985).

27. Georgeton, G. K. and A. S. Teja, "A Group contribution Equation of State Based on the Simplified Perturbed Hard Chain Theory," Ind. Eng. Chem. Res., 27, 657-664 (1988).

28. Vimalchand, P. and M. D. Donohue, "Comparison of Equations of State for Chain Molecules," Journal of Physical Chemistry, 93, 4355-4360 (1989).

29. Garcia-Sanchez, F., J. L. Ruiz-Cortina, C. Lira-Galeana and L. Ponce-Ramirez, "Critical Point Calculations for Oil Reservoir Fluid Systems Using the SPHCT Equation of State," Submitted to Fluid Phase Equilibria.

30. Rumer, Y. B. and M. S. Ryvkin, "Thermodynamics, Statistical Physics, and Kinetics," Mir Publishers, Moscow (1980).

31. Dickman, R. and C. K. Hall, "Equation of State for Chain Molecules: Continuous-Space Analog of Flory Theory," Journal of Chemical Physics, 85, 4108-4115 (1986).

32. Honnell, K. G. and C. K. Hall, "A New Equation of State for Athermal Chains," Journal of Chemical Physics, 90, 1841-1855 (1989).

33. Honnel, K. G., C. K. Hall and R. Dickman, "On the Pressure Equation for Chain Molecules," Journal of Chemical Physics, 87, 664-674 (1987).

34. Bokis, C. P., M. D. Donohue and C. K. Hall, "A Local Composition Model for Square-Well Chains Using the Generalized Flory Dimer Theory," Journal of Physical Chemistry, 96, 11004-11009 (1992).

35. Jackson, L. W., "A Comparison of Selected Gradient Methods for Solving Nonlinear Least Squares Problems," M. S. Thesis, Oklahoma State University, Stillwater, Oklahoma (1978).

36. Sudibandriyo, M., "Improved Methods for Phase Density Prediction: CO_2 + Hydrocarbons," M. S. Thesis, Oklahoma State University (1988).

37. Peneloux, A. and E. Rauzy, "A Consistent Correction for Redlich-Kwong-Soave Volumes," Fluid Phase Equilibria, 8, 7-23 (1982).

38. Chou, G. F. and J. M. Prausnitz, "A Phenomenological Correction to an Equation of State for the Critical Region," AIChE Journal, 35, 1487-1496 (1989).

39. Angus, S., B. Armstrong and K. M. de Reuck, "International Thermodynamic Tables of the Fluid State - 5 Methane," International Union of Pure and Applied Chemistry, Pergamon Press, New York (1976).

40. Goodwin, R. D., H. M. Roder and G. C. Straty, "Thermophysical Properties of Ethane from 90 to 600 K at Pressures to 700 Bars," National Bureau of Standards (1976).

41. Goodwin, R. D. and W. M. Haynes, "Thermophysical Properties of Propane from 85 to 700 K at Pressures to 70 MPa," National Bureau of Standards Monogram 170 (1980).

42. Haynes, W. M. and R. D. Goodwin, "Thermophysical Properties of Normal Butane from 135 to 700 K at Pressures to 70 MPa," National Bureau of Standards Monogram 169 (1982).

43. Vargaftik, N. B., Tables on the Thermophysical Properties of Liquids and Gases, John Wiley and Sons, New York (1975).

44. "API Project 44. Selected Values of Properties of Hydrocarbons and Related Compounds," Thermodynamic Research Center, Texas A&M University.

45. Younglove, B. A., "Thermophysical Properties of Fluids. I. Argon, Ethylene, Parahydrogen, Nitrogen, Nitrogen Trifluoride, and Oxygen," Journal of Physical and Chemical Reference Data, Vol. 11, Supplement No. 1 (1982).

46. Angus, S., B. Armstrong and K. M. de Reuck, "International Thermodynamic Tables of the Fluid State - 7 Propylene (Propene)," International Union of Pure and Applied Chemistry, Pergamon Press, New York (1980).

47. Goodwin, R. D., "Benzene Thermophysical Properties from 279 to 900 K at Pressures to 1000 Bar," Journal of Physical and Chemical Reference Data, 17, 1541-1598 (1988).

48. Perry, R. H., D. W. Green and J. O. Maloney, eds., "Perry's Chemical Engineers Handbook," 6th Edition, McGraw-Hill, New York 1984).

49. Ely, J. F., J. W. Magee and W. M. Haynes, "Thermophysical Properties for Special High CO_2 Content Mixtures," Gas Processors Association, RR-110 (1987).

50. Haar, L., J. S. Gallager and G. S. Kell, NBS/NRC Steam Tables, McGraw-Hill, New York (1984).

51. Sherwood, A. E. and J. M. Prausnitz, "Intermolecular Potential Functions and the Second and Third Virial Coefficents," Journal of Chemical Physics, 41, 429-437 (1964).

52. Gosset, R., G. Heyen and B. Kalitventzeff, "An Efficient Algorithm to Solve Cubic Equations of State," Fluid Phase Equilibria, 25, 51-64 (1986).

53. Edmister, W. C. and B. I. Lee, "Applied Hydrocarbon Thermodynamics," Volume 1, Second Edition, Gulf Publishing Company, Houston, Texas (1984).

54. Mehra, V. S. and G. Thodos, "Vapor-Liquid Equilibrium in the Ethane-n-Butane System," Journal of Chemical and Engineering Data, 10, 307-309 (1965).

55. Reamer, H. H., B. H. Sage and W. N. Lacey, "Phase Equilibria in Hydrocarbon Systems. Volumetric and Phase Behavior of Ethane-n-Pentane System," Journal of Chemical and Engineering Data, 5, 44-50 (1960).

56. Raff, A. M., "Experimental Determination of the Solubilities of Ethane in Selected n-Paraffin Solvents," M. S. Thesis, Oklahoma State University, Stillwater, Oklahoma (1989).

57. Mehra, V. S. and G. Thodos, "Vapor-Liquid Equilibrium in the Ethane-n-Heptane System," Journal of Chemical and Engineering Data, 10, 211-214 (1965).

58. Rodrigues, R. B. J., D. S. McCaffrey, Jr. and J. P. Kohn, "Heterogeneous Phase and Volumetric Equilibrium in the Ethane-n-Octane System," Journal of Chemical and Engineering Data, 13, 164-168 (1968).

59. Bufkin, B. A., R. L. Robinson, Jr., S. S. Estera and K. D. Luks, "Solubility of Ethane in n-Decane at Pressures to 8.2 MPa and Temperatures from 278 to 411 K," Journal of Chemical and Engineering Data, 31, 421-423 (1986).

60. Robinson, R. L., Jr., J. M. Anderson, M. W. Barrick, B. A. Bufkin and C. H. Ross, "Phase Behavior of Coal Fluids: Data for Correlation Development," DE-FG22-86PC90523, Final Report, United States Department of Energy, January, 1987.

61. Olds, R. H., H. H. Reamer, B. H. Sage and W. N. Lacey, "Phase Equilibria in Hydrocarbon Systems. The n-Butane-Carbon Dioxide System," Industrial and Engineering Chemistry, 41, 475-482 (1949).

62. Besserer, G. J. and D. B. Robinson, Jr., "Equilibrium-Phase Properties of n-Pentane-Carbon Dioxide System," Journal of Chemical and Engineering Data, 18, 416-419 (1973).

63. Li, Y.-H., K. H. Dillard and R. L. Robinson, Jr., "Vapor-Liquid Phase Equilibrium for Carbon Dioxide-n-Hexane at 40, 80, and 120 °C," Journal of Chemical and Engineering Data, 26, 53-55 (1981).

64. Kalra, H., H. Kubota, D. B. Robinson and H. J. Ng, "Equilibrium Phase Properties of the Carbon Dioxide-n-Heptane System," Journal of Chemical and Engineering Data, 23, 317-321 (1978).

65. Reamer, H. H. and B. H. Sage, "Phase equilibria in Hydrocarbon Systems. Volumetric and Phase Behavior of the n-Decane-CO_2 System", Journal of Chemical and Engineering Data, 8, 508-513 (1963).

66. Sebastian, H. M., J. J. Simnick, H. -M. Lin and K. -C. Chao, "Vapor-Liquid Equilibrium in Binary Mixtures of Carbon Dioxide + n-Decane and Carbon Dioxide + n-Hexadecane," Journal of Chemical and Engineering Data, 25, 138-140 (1980).

67. Gasem, K. A. M. and R. L. Robinson, Jr., "Solubilities of Carbon Dioxide in Heavy Normal Paraffins (C_{20}-C_{44}) at Pressures to 9.6 MPa and Temperatures from 323 to 423 K," Journal of Chemical and Engineering Data, 30, 53-56 (1985).

68. Fall, D. J. and K. D. Luks, "Phase Equilibria Behavior of the Systems Carbon Dioxide + n-Dotriacontane and Carbon Dioxide + n-Docosane," Journal of Chemical and Engineering Data, 29, 413-417 (1984).

69. Reid, R. C., J. M. Prausnitz and T. K. Sherwood, "The Properties of Gases and Liquids," Second Edition, McGraw-Hill Book Company, New York (1977).

70. Gasem, K. A. M., "Binary Vapor-Liquid Phase Equilibrium for carbon Dioxide + Heavy Normal Paraffins," Ph.D. Dissertation, Oklahoma State University, Stillwater, Oklahoma (1986).

71. Gasem, K. A. M., C. H. Ross and R. L. Robinson, Jr., "Prediction of Ethane and CO_2 Solubilities in Heavy Normal Paraffins Using Generalized-Parameter Soave and Peng-Robinson Equations of State," Canadian Journal of Chemical Engineering, (Submitted for Publication October 7, 1992).

72. Hsu, J.-C., Nagarajan, N. and R. L. Robinson, Jr., "Equilibrium Phase Compositions, Phase Densities, and Interfacial Tensions for CO_2 + Hydrocarbon Systems. 1. CO_2 + n-Butane," Journal of Chemical and Engineering Data, 30, 485-491 (1985).

73. Nagarajan, N. and R. L. Robinson, Jr., "Equilibrium Phase Compositions, Phase Densities, and Interfacial Tensions for CO_2 + Hydrocarbon Systems. 2. CO_2 + n-Decane," Journal of Chemical and Engineering Data, 31, 168-171 (1986).

74. Gasem, K. A. M., K. B. Dickson, P. B. Dulcamara, N. Nagarajan and R. L. Robinson, Jr., "Equilibrium Phase Compositions, Phase Densities, and Interfacial Tensions for CO_2 + Hydrocarbon Systems. 5. CO_2 + n-Tetradecane," Journal of Chemical and Engineering Data, 34, 191-195 (1989).

75. Nagarajan, N., Y. K. Chen, and R. L. Robinson, Jr., "Interfacial Tensions in Carbon Dioxide-Hydrocarbon Systems: Development of Experimental Facilities and Acquisition of Experimental Data. Experimental Data for CO_2 + Benzene," Technical Progress Report (June 15, 1984).

76. Nagarajan, N., Y. K. Chen, and R. L. Robinson, Jr., "Interfacial Tensions in Carbon Dioxide-Hydrocarbon Systems: Development of Experimental Facilities and Acquisition of Experimental Data. Experimental Data for CO_2 + Cyclohexane," Technical Progress Report (May, 1984).

77. Anderson, J. M., "High Pressure Solubilities of Carbon Dioxide in Benzene, Cyclohexane, and Trans-Decalin," M.S. Thesis, Oklahoma State University, Stillwater, Oklahoma (1985).

78. Shaver, R. D., "A New Scaled-Variable-Reduced-Coordinate Framework for Correlation of Pure Fluid Saturation Properties," M.S. Thesis, Oklahoma State University, Stillwater, Oklahoma (1990).

79. Vimalchand, P., A. Thomas, I. G. Economou and M. D. Donohue, "Effect of Hard-Sphere Structure on Pure-Component Equation of State Calculations," Fluid Phase Equilibria, 73, 39-55 (1992).

80. Ciocca, G. and I. Nagata, "Density Dependence of the External Degrees of Freedom: Application to a Simplified Version of the Perturbed Hard Chain Theory," Fluid Phase Equilibria, 41, 59-80 (1988).

APPENDIX A

ADDITIONAL FIGURES FOR SPHCT PARAMETER STUDY

This appendix contains figures produced during the parameter study for the original SPHCT equation as described in Chapter III. Figures are included for carbon dioxide, benzene and water, respectively, which correspond to Figures 4-10 shown in Chapter III. The figures indicate similar trends for these compounds as for methane discussed previously. For all compounds, T* and Z_M show the strongest sensitivity to calculated vapor pressures and phase densities. All compounds also show the apparent linearity of v* with temperature. However, as discussed in Chapter III a linear temperature dependence for v* alone does not provide significant improvement in the accuracy of calculated properties. All compounds show strong similarities in the behavior of the regressed values for T* and Z_M. This is interpreted as a deficiency of the temperature dependence of the attractive portion of the SPHCT equation of state.

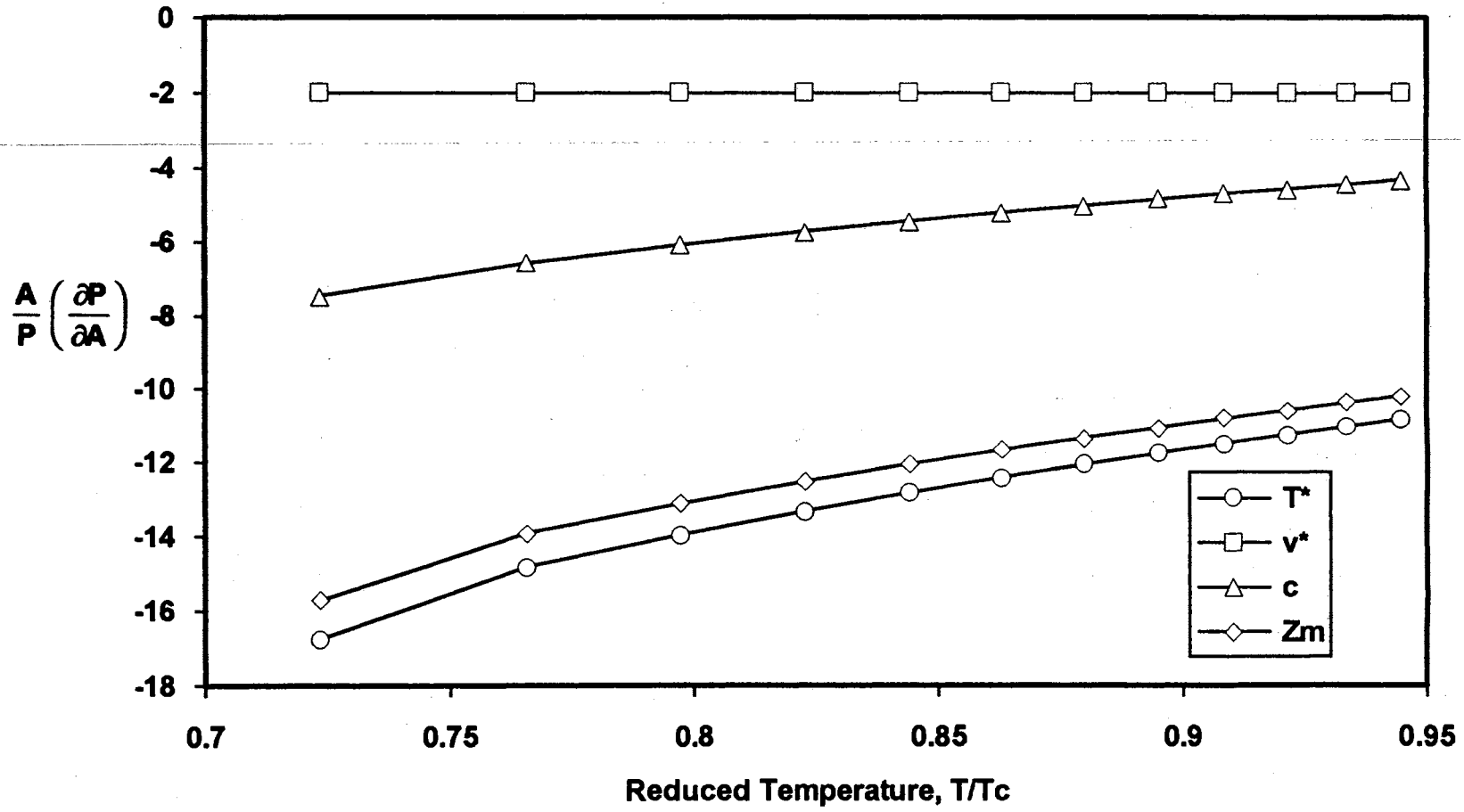

Figure A.1. Effect of Reduced Temperature on Vapor Pressure Sensitivity for Saturated Carbon Dioxide

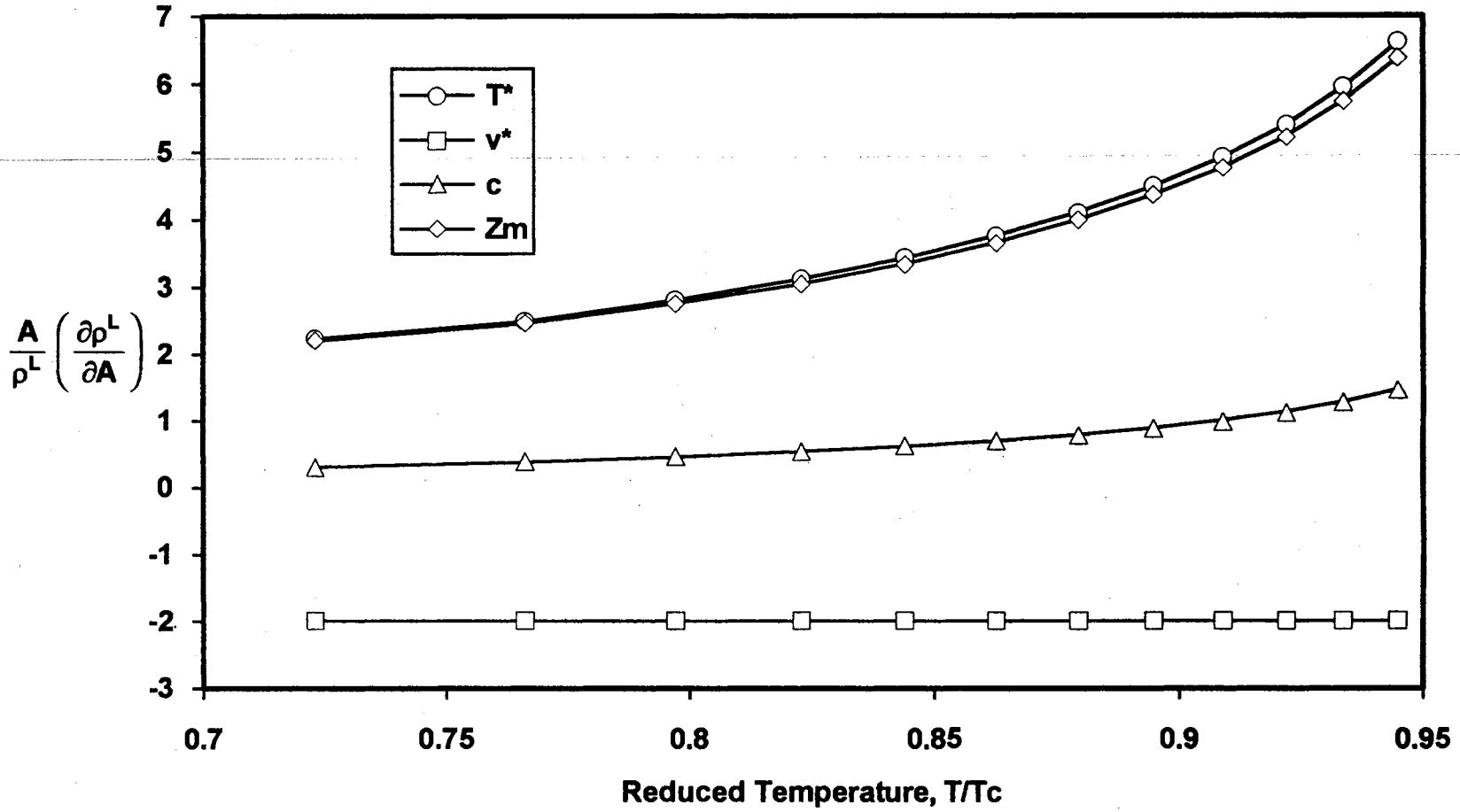

Figure A.2. Effect of Reduced Temperature on Liquid Density Sensitivity for Saturated Carbon Dioxide

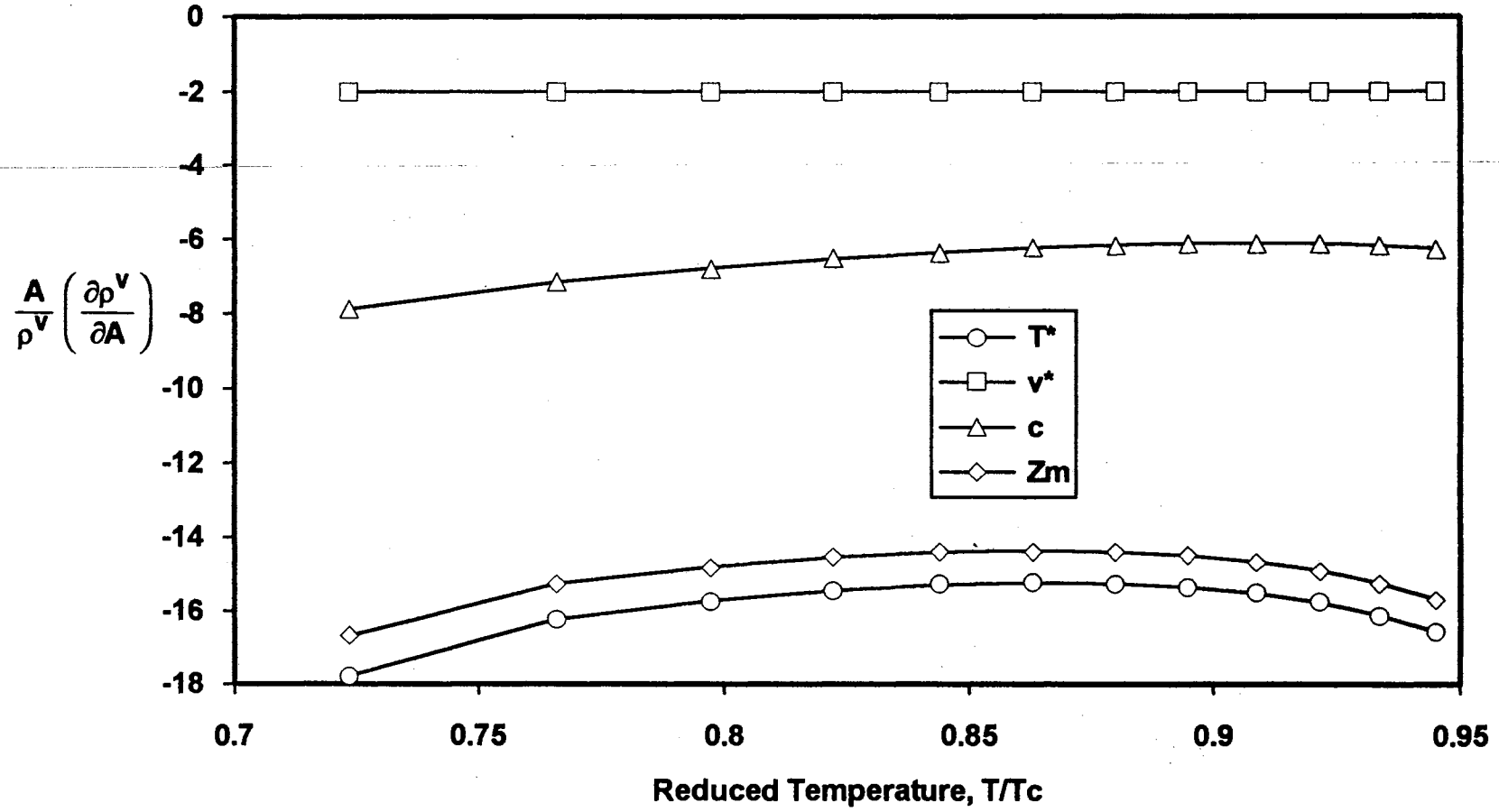

Figure A.3. Effect of Reduced Temperature on Vapor Density Sensitivity for Saturated Carbon Dioxide

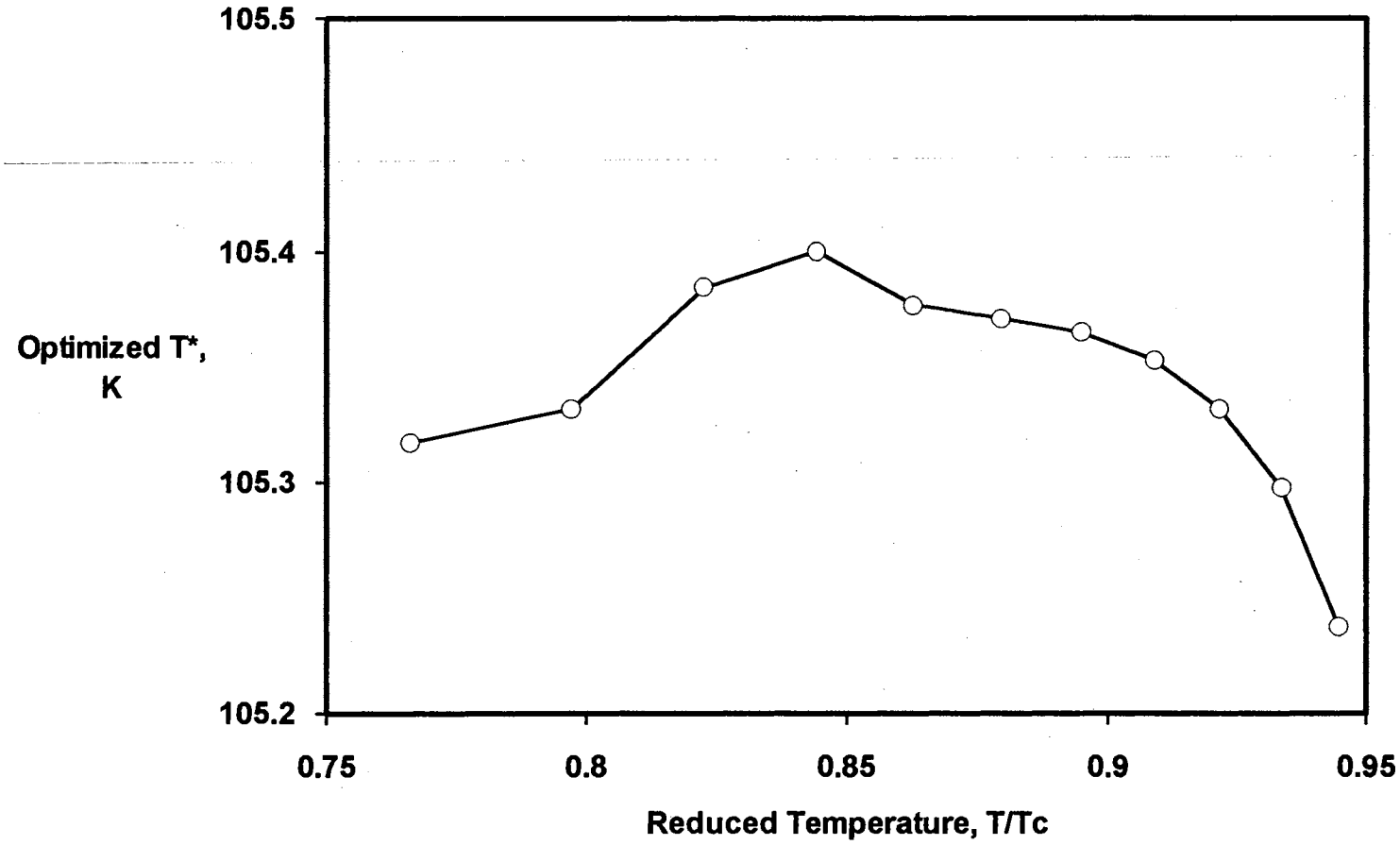

Figure A.4. Effect of Reduced Temperature on Optimized T* for Saturated Carbon Dioxide

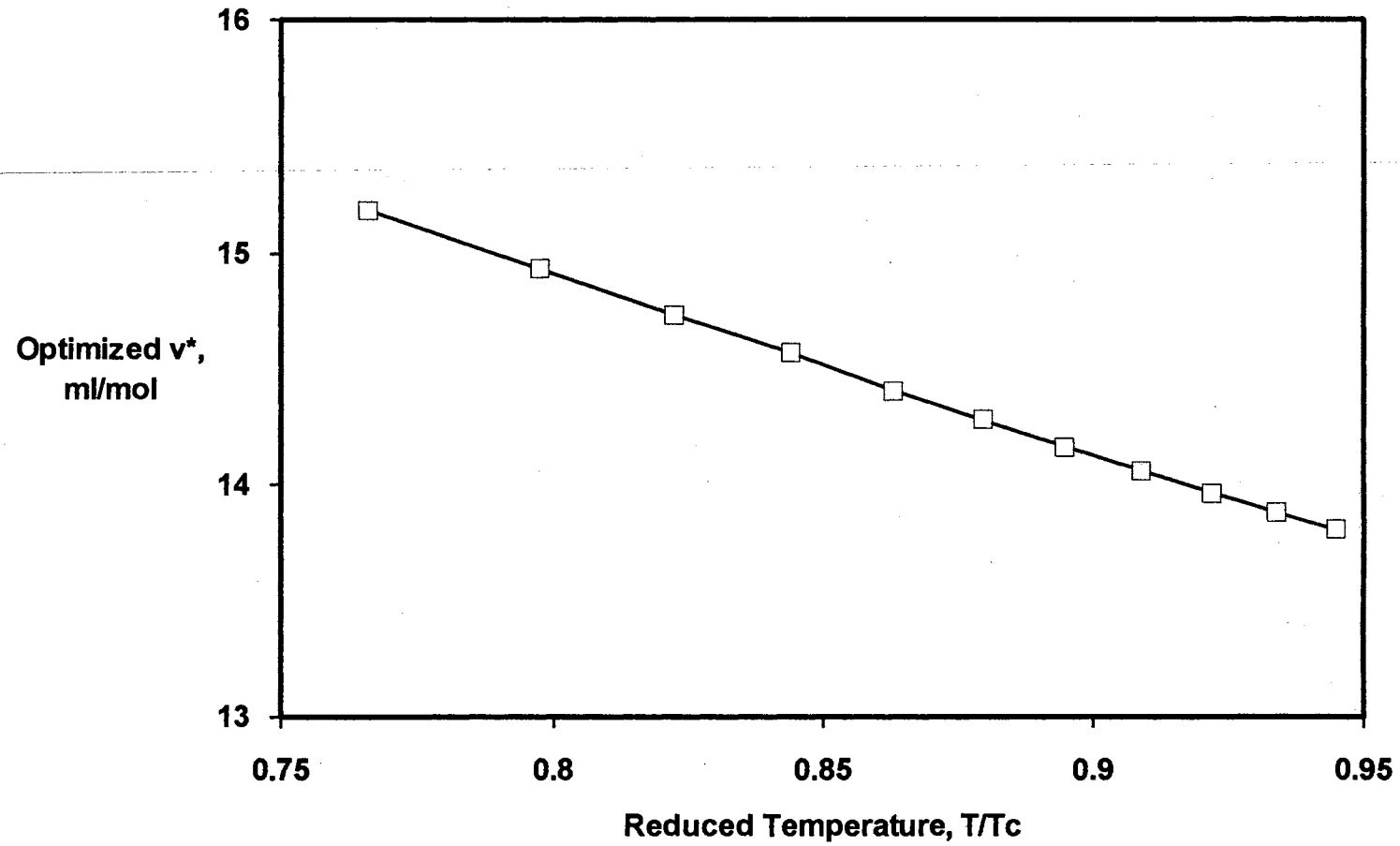

Figure A.5. Effect of Reduced Temperature on Optimized v* for Saturated Carbon Dioxide

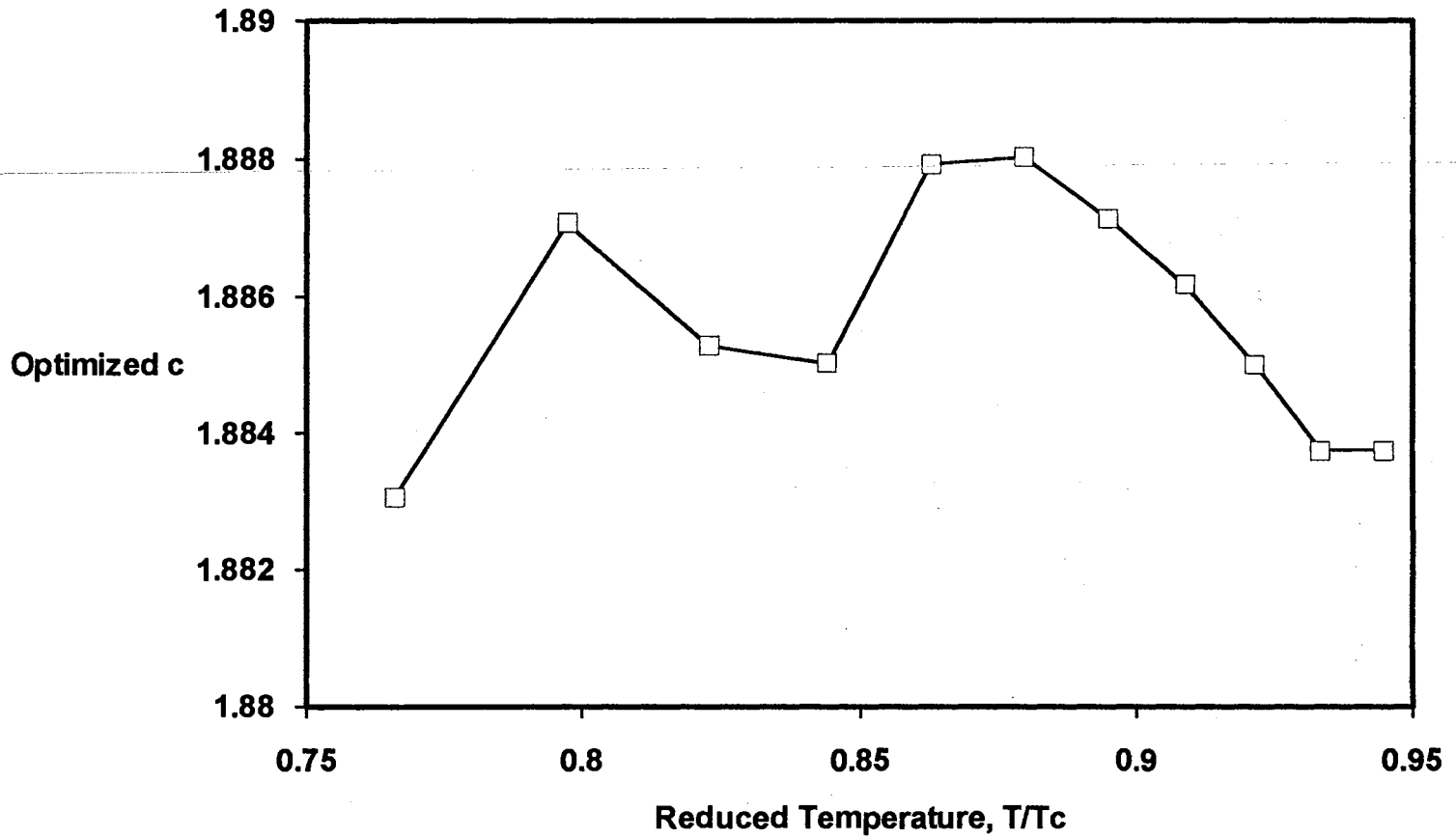

Figure A.6. Effect of Reduced Temperature on Optimized c for Saturated Carbon Dioxide

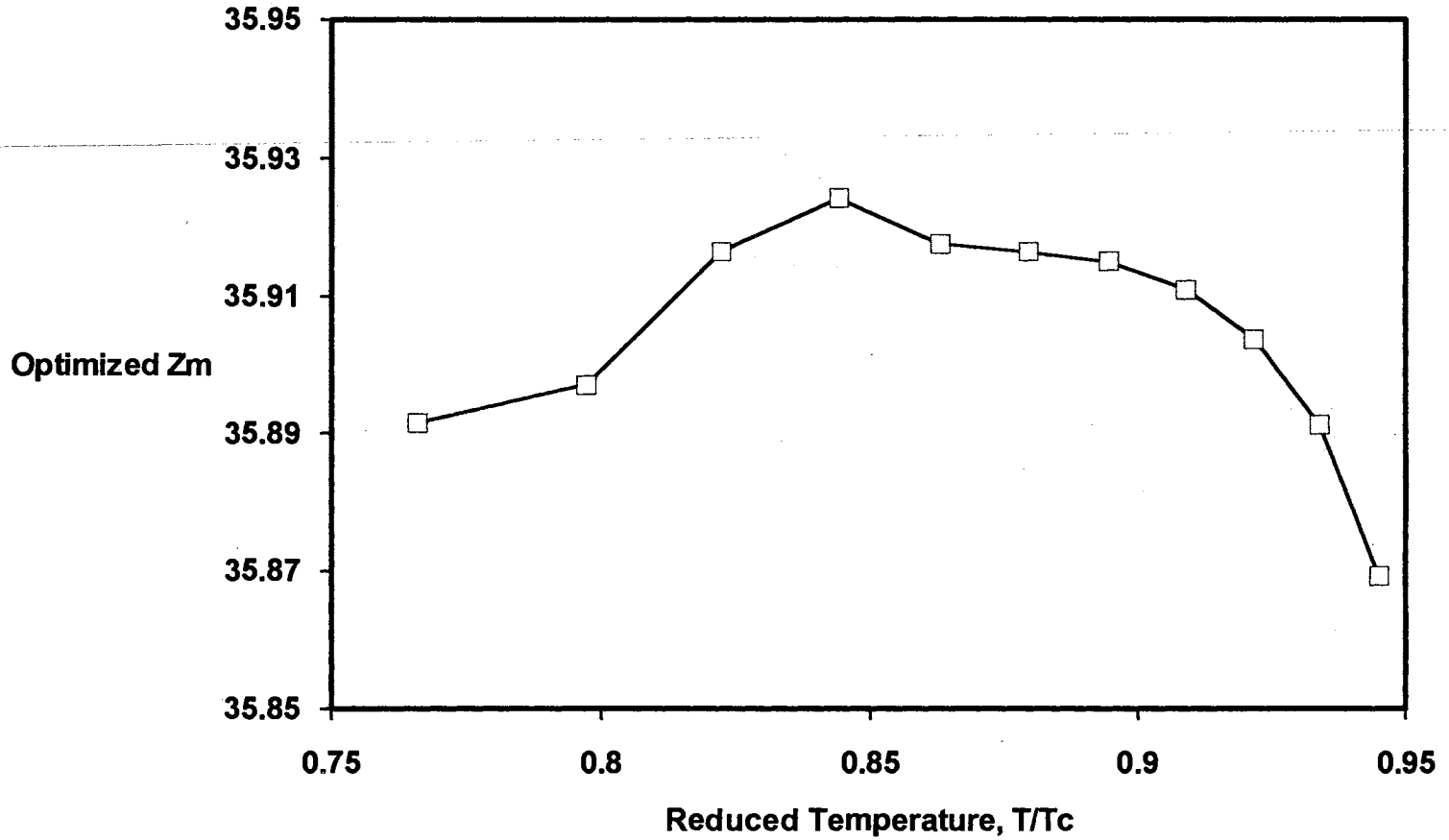

Figure A.7. Effect of Reduced Temperature on Optimized Z_M for Saturated Carbon Dioxide

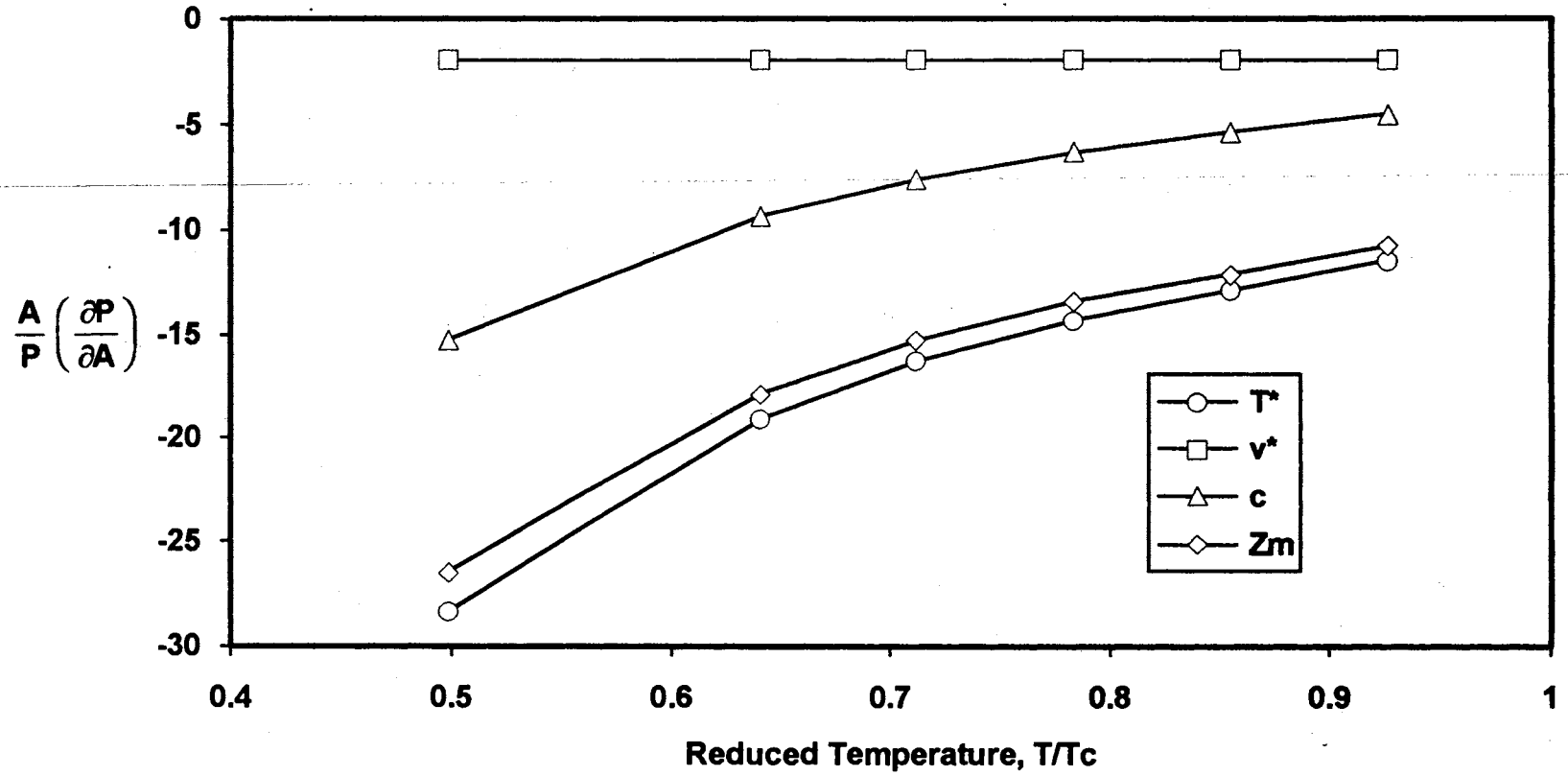

Figure A.8. Effect of Reduced Temperature on Vapor Pressure Sensitivity for Saturated Benzene

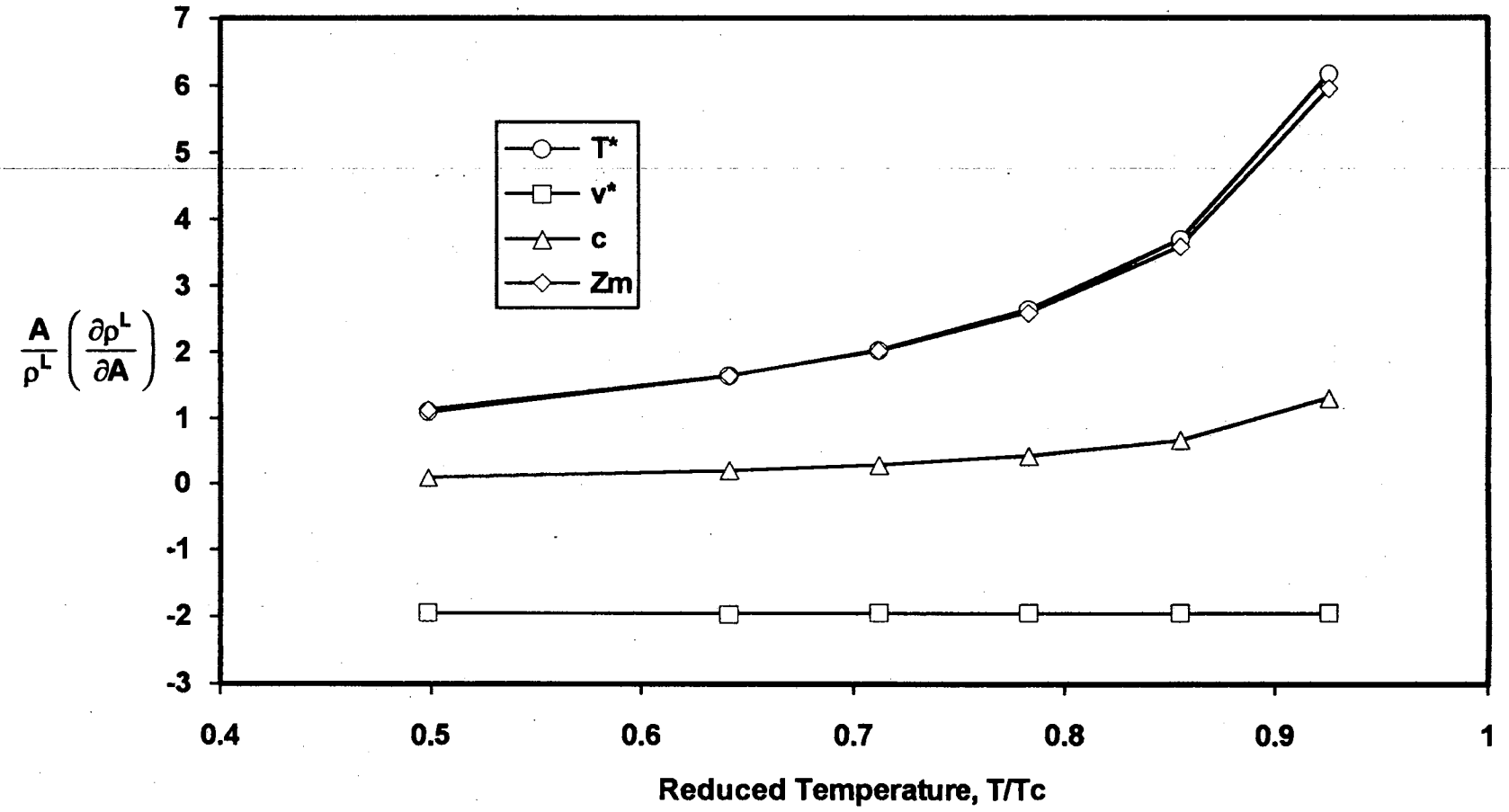

Figure A.9. Effect of Reduced Temperature on Liquid Density Sensitivity for Saturated Benzene

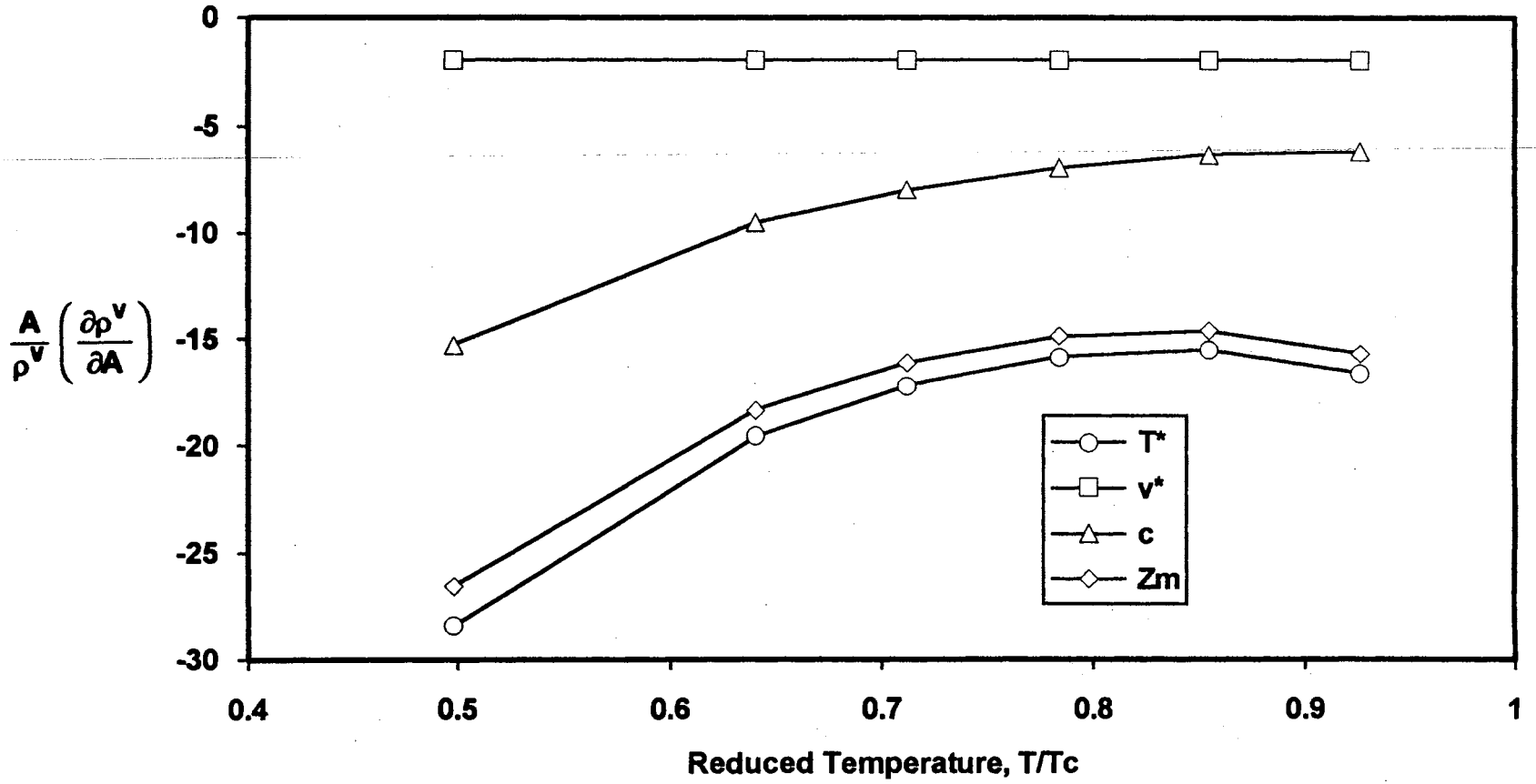

Figure A.10. Effect of Reduced Temperature on Vapor Density Sensitivity for Saturated Benzene

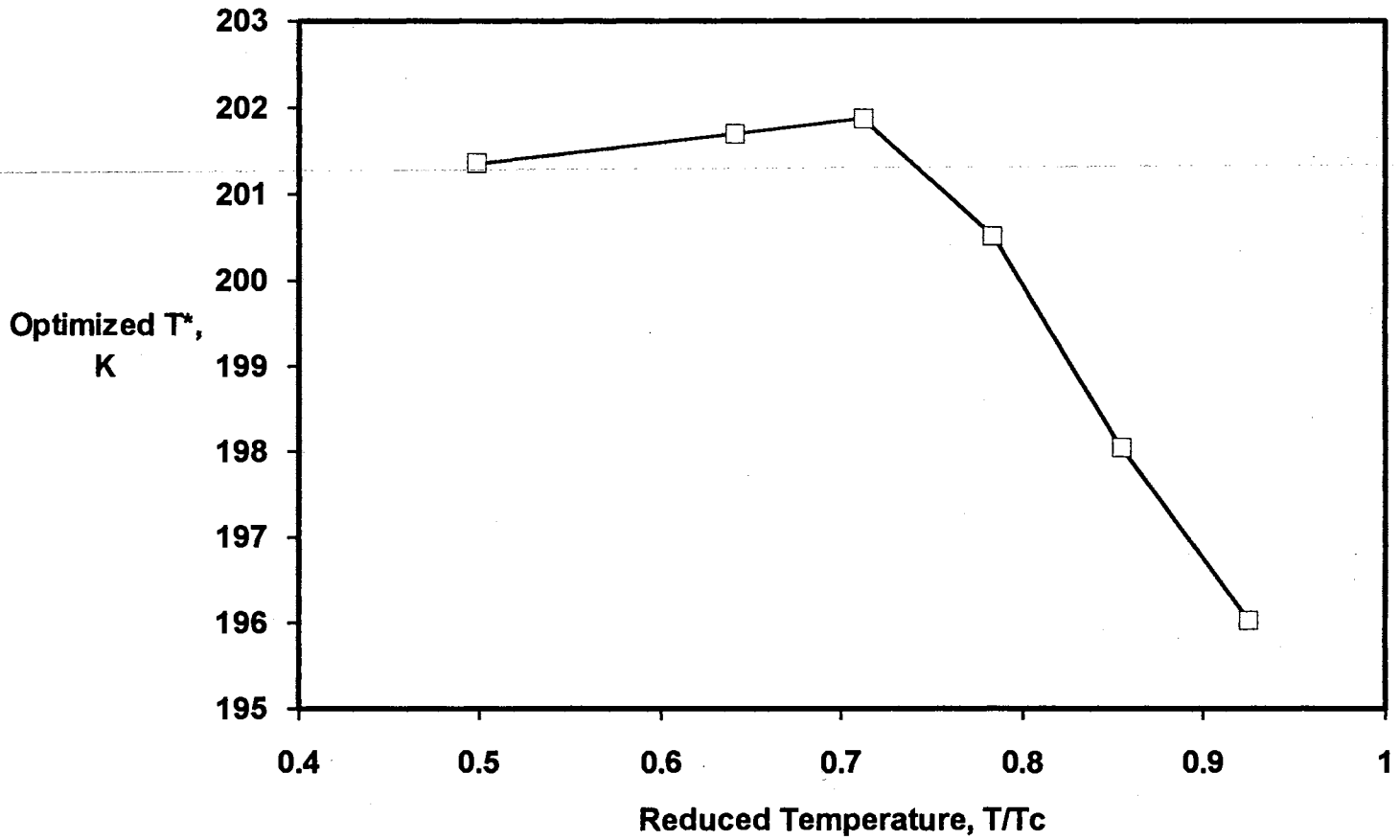

Figure A.11. Effect of Reduced Temperature on Optimized T* for Saturated Benzene

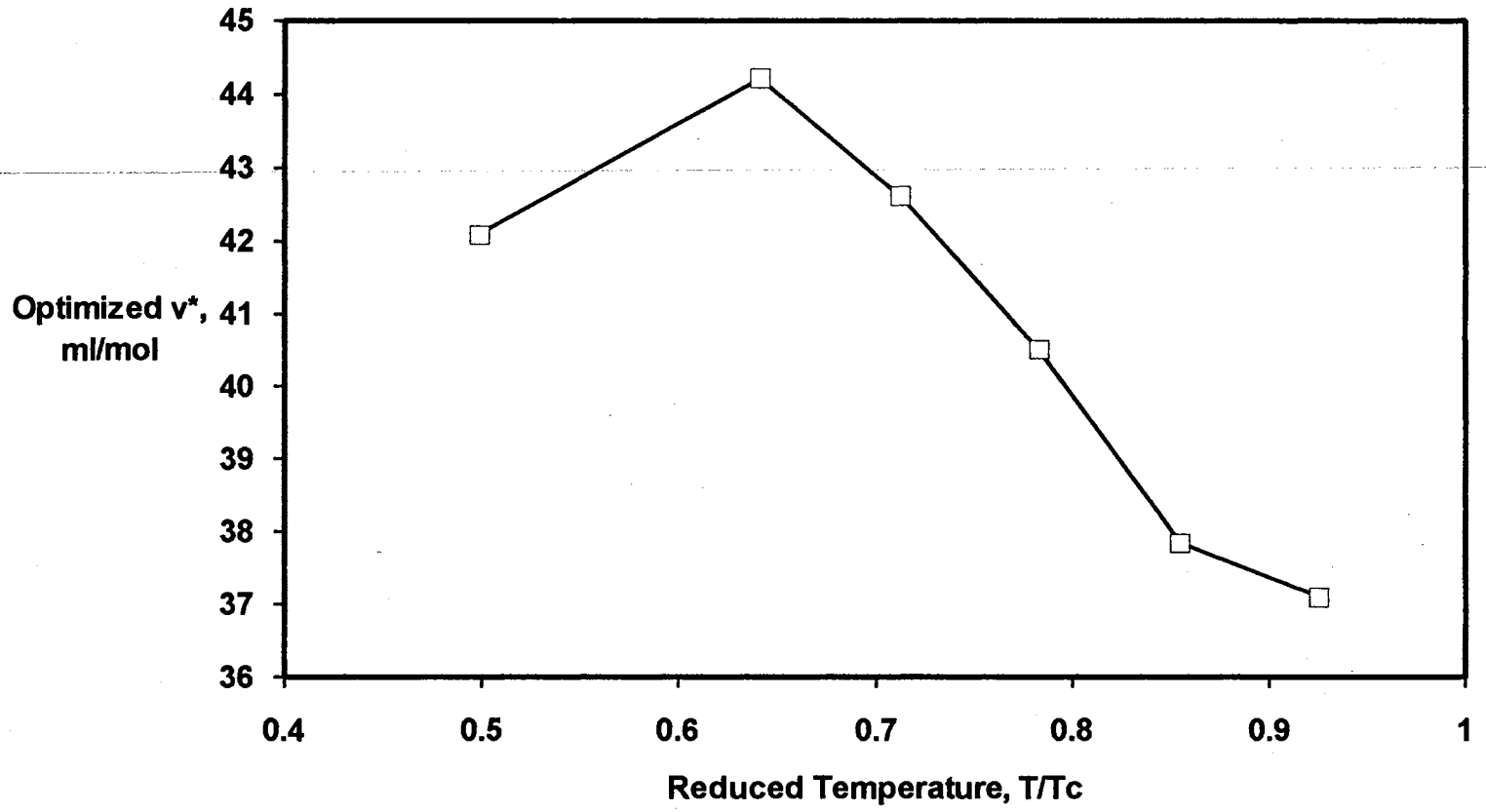

Figure A.12. Effect of Reduced Temperature on Optimized v* for Saturated Benzene

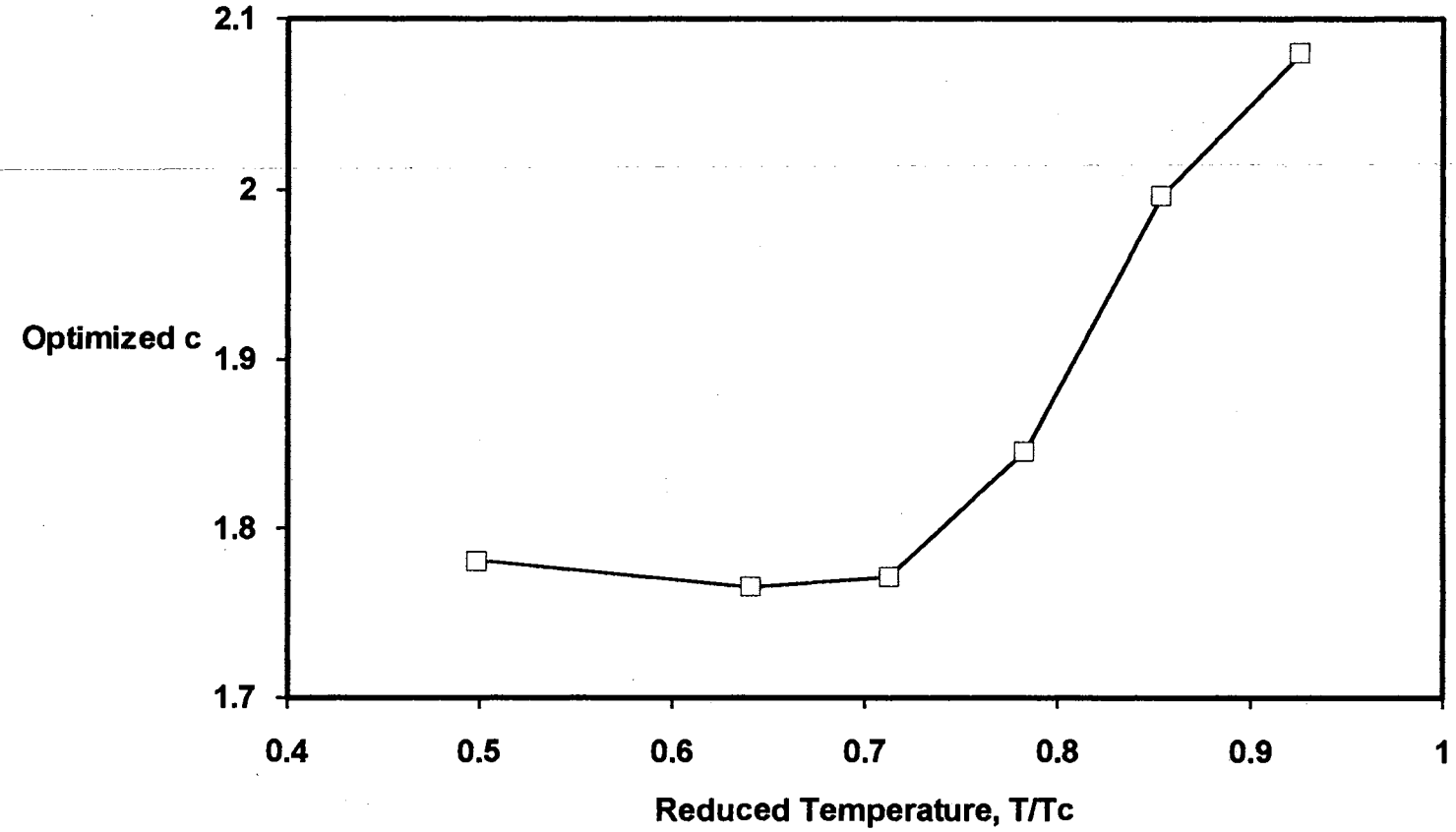

Figure A.13. Effect of Reduced Temperature on Optimized c for Saturated Benzene

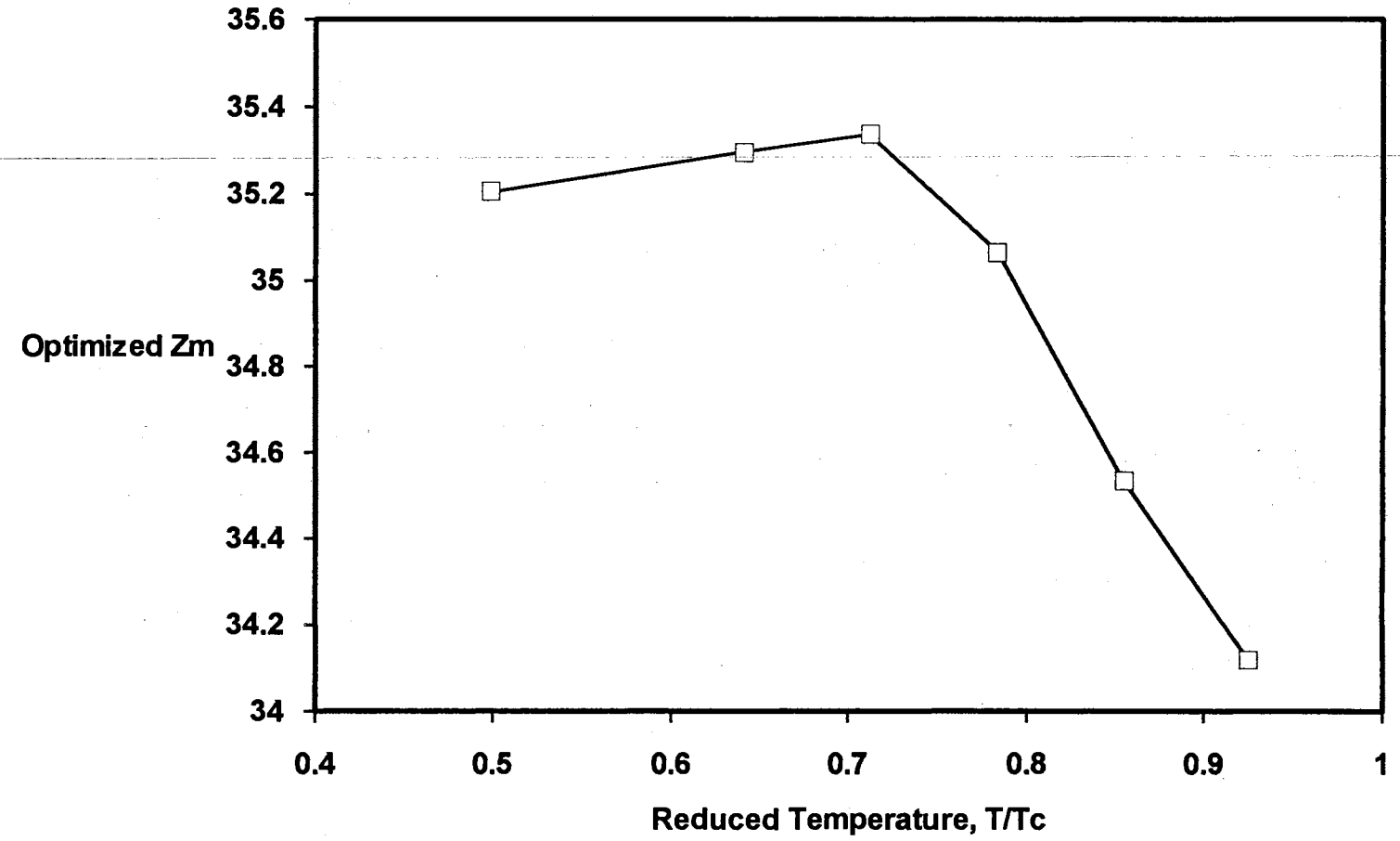

Figure A.14. Effect of Reduced Temperature on Optimized Z_M for Saturated Benzene

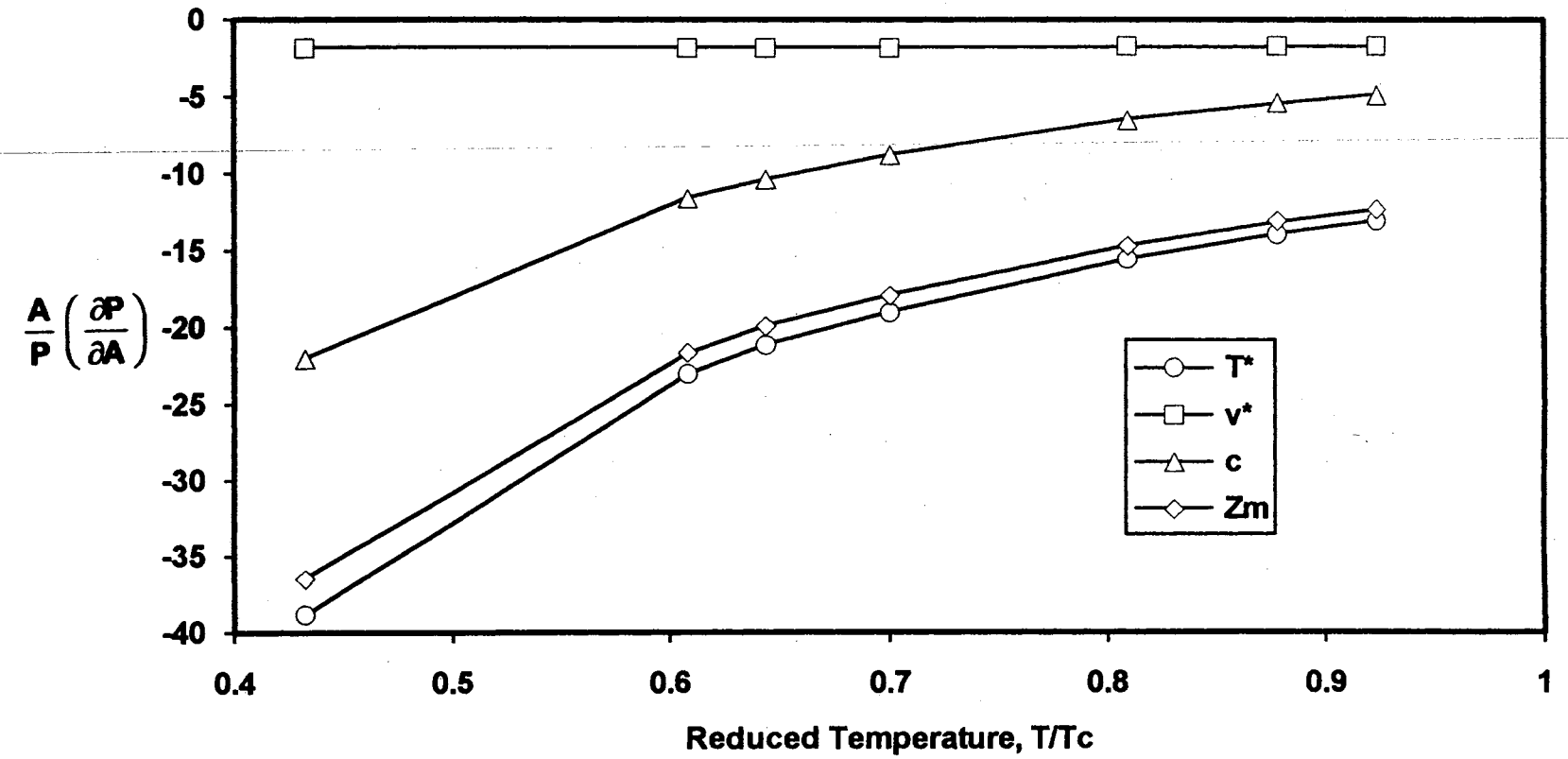

Figure A.15. Effect of Reduced Temperature on Vapor Pressure Sensitivity for Saturated Water

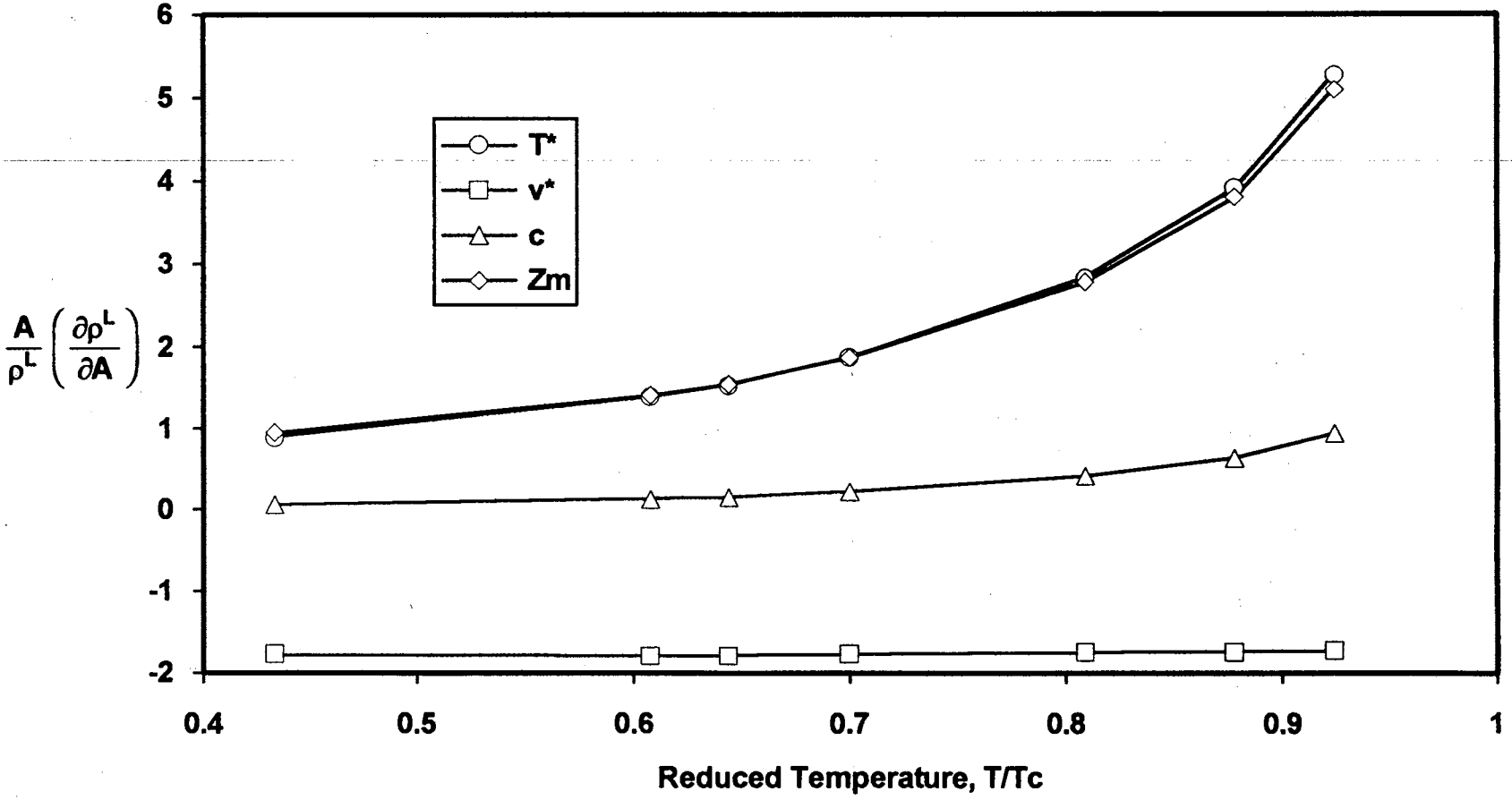

Figure A.16. Effect of Reduced Temperature on Liquid Density Sensitivity for Saturated Water

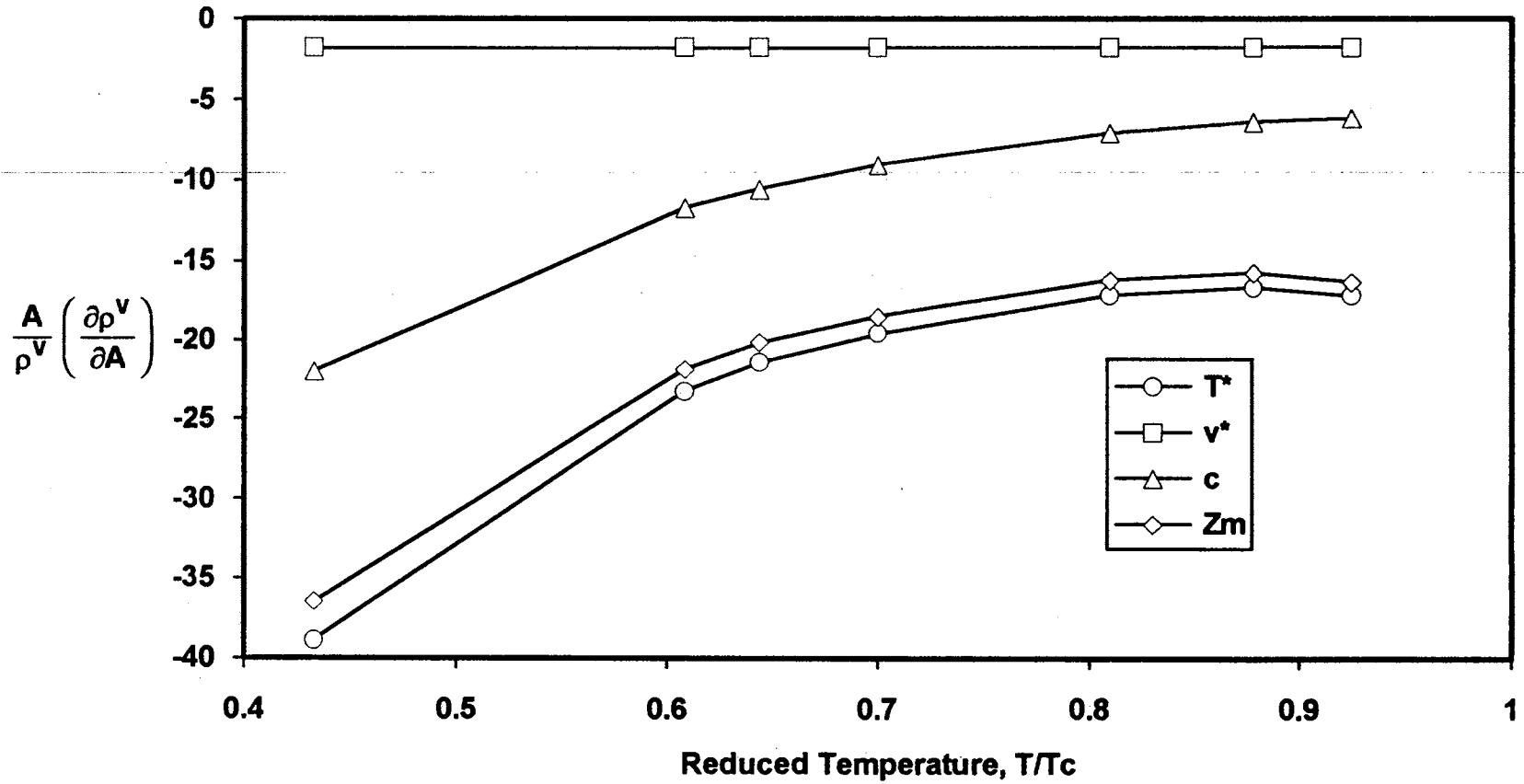

Figure A.17. Effect of Reduced Temperature on Vapor Density Sensitivity for Saturated Water

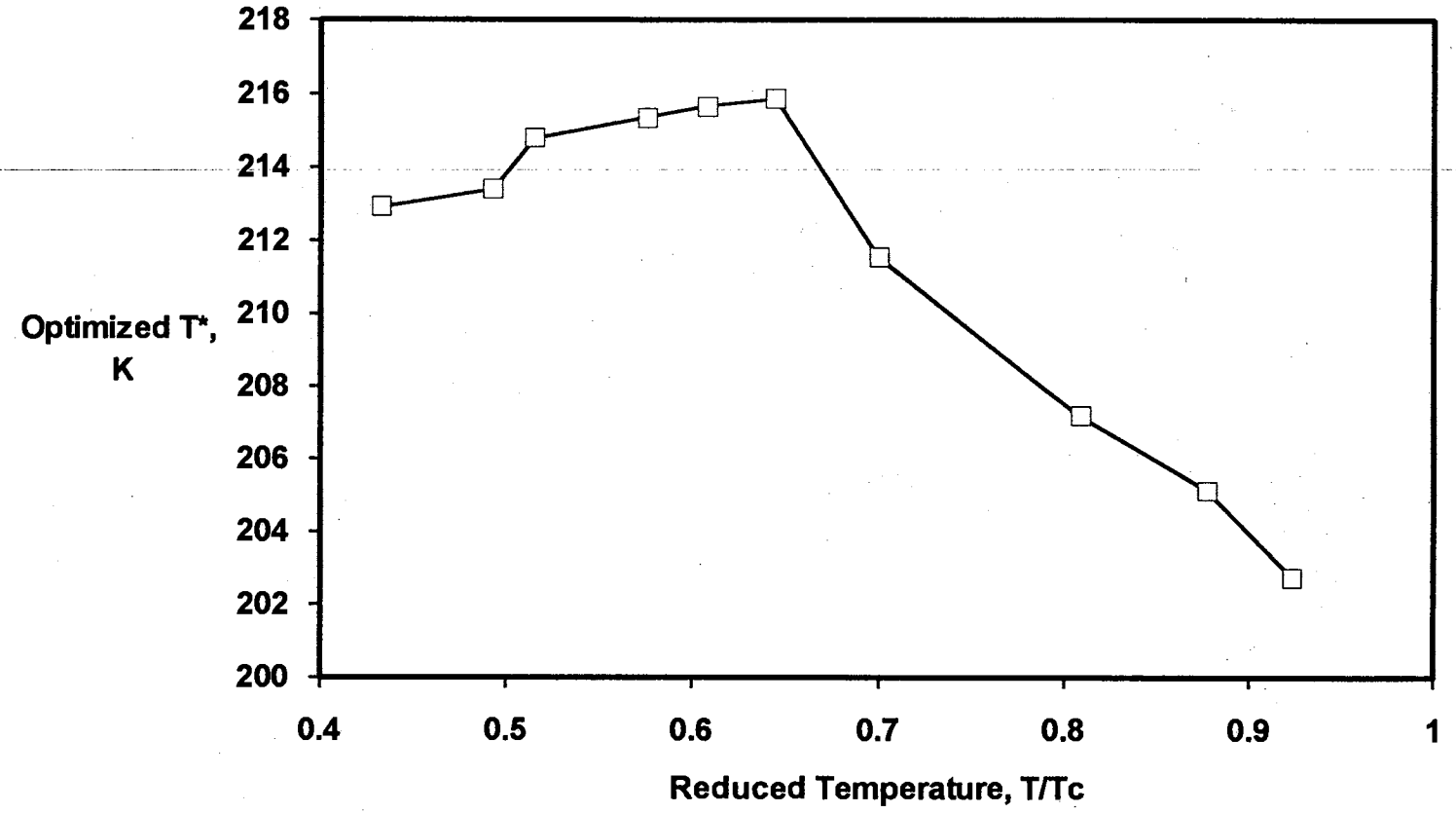

Figure A.18. Effect of Reduced Temperature on Optimized T* for Saturated Water

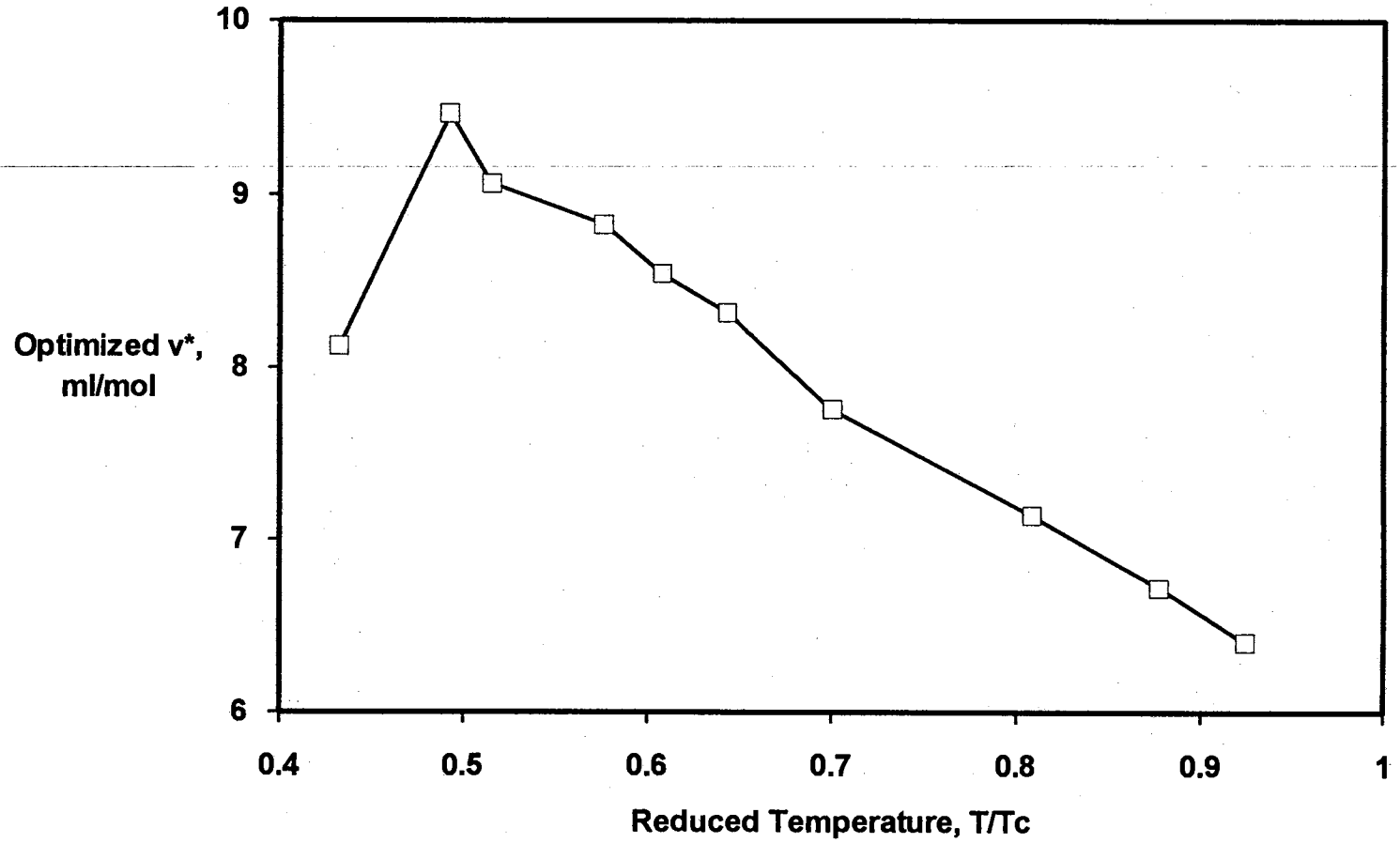

Figure A.19. Effect of Reduced Temperature on Optimized v* for Saturated Water

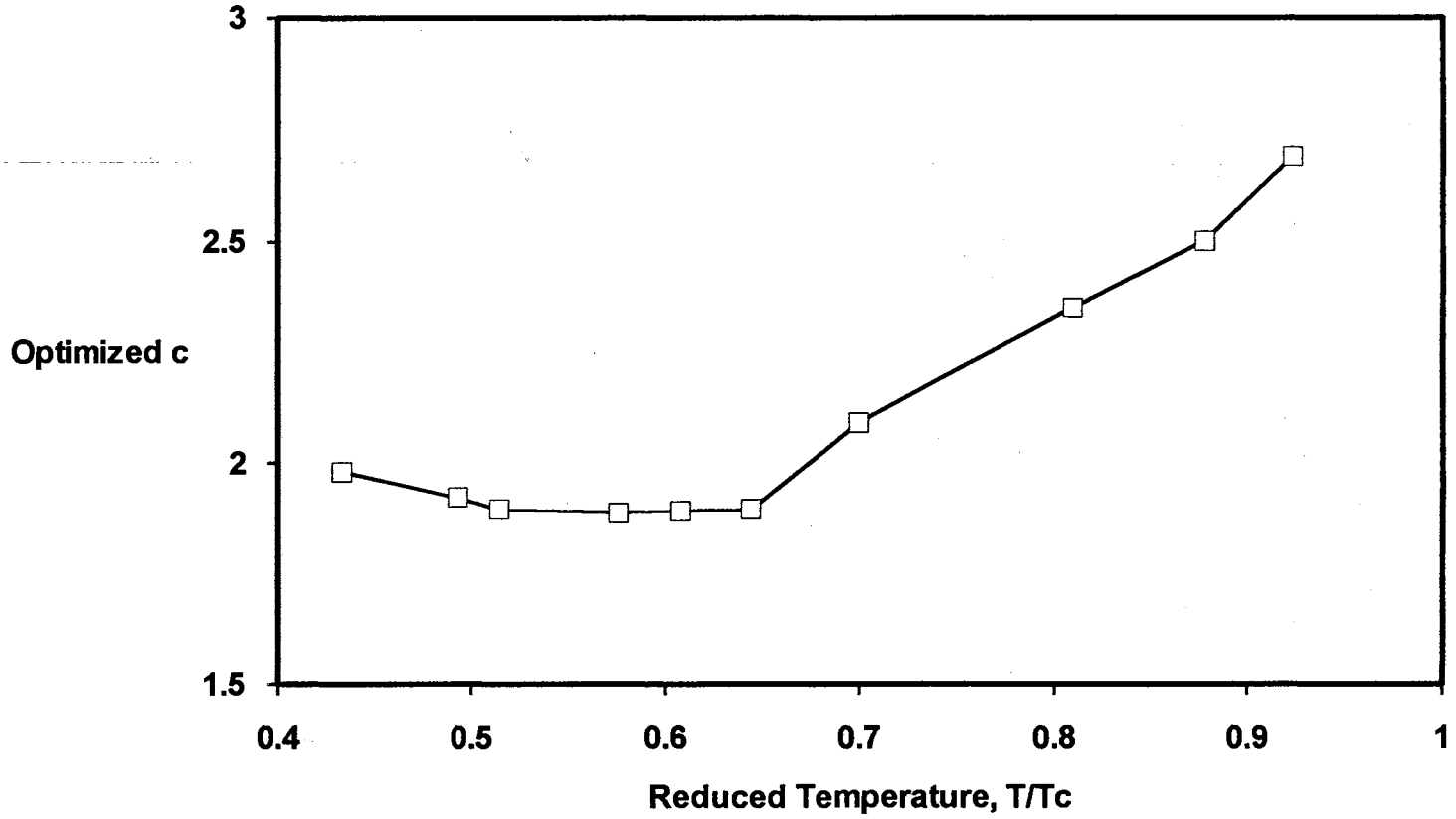

Figure A.20. Effect of Reduced Temperature on Optimized c for Saturated Water

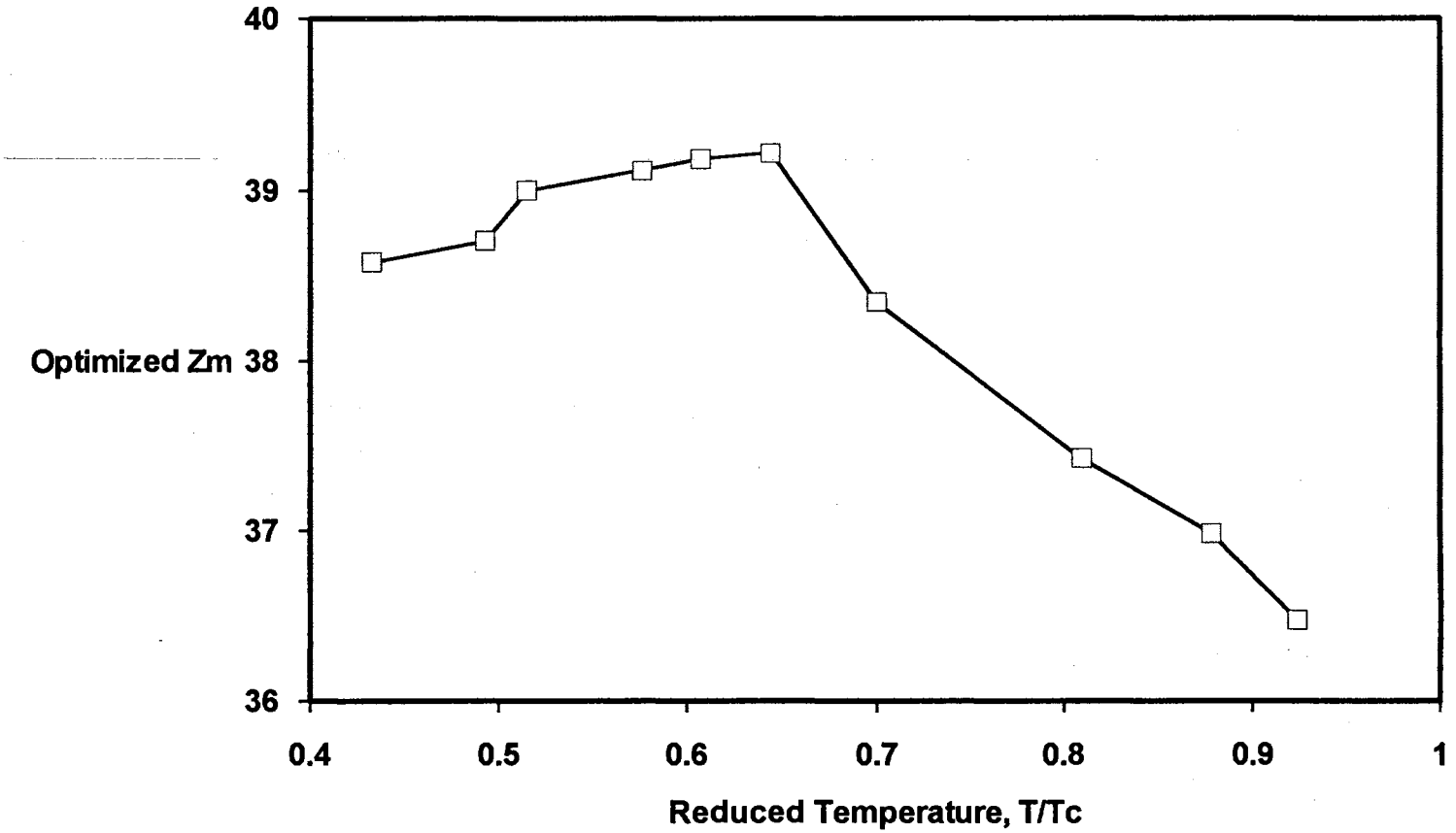

Figure A.21. Effect of Reduced Temperature on Optimized Z_M for Saturated Water

APPENDIX B

CRITICAL POINT CONSTRAINT EQUATIONS

The critical point constraints of Equations (63) and (64) can be rewritten in terms of derivatives of the compressibility factor as:

$$z + \eta\left(\frac{\partial z}{\partial \eta}\right)_{T=T_c} = 0$$

and

$$2\left(\frac{\partial z}{\partial \eta}\right)_{T=T_c} + \left(\frac{\partial^2 z}{\partial \eta^2}\right)_{T=T_c} = 0$$

where

$$\eta = \frac{v^*\tau}{v}$$

The first and second derivatives of z with respect to η are given by:

$$\left(\frac{\partial z}{\partial \eta}\right)_{T=T_c} = c\left[\frac{4(1-\eta)^2 + 3\left(4\eta - 2\eta^2\right)}{(1-\eta)^4}\right] - \frac{Z_M a c^2 \tau v^*}{\left(c\tau v^* + \eta a\right)^2}$$

$$\left(\frac{\partial^2 z}{\partial \eta^2}\right)_{T=T_c} = c\left[\frac{20(1-\eta)^2 + 12\left(4\eta - 2\eta^2\right)}{(1-\eta)^5}\right] + \frac{2Z_M a^2 c^2 \tau v^*}{\left(c\tau v^* + \eta a\right)^3}$$

These two equations along with the condition that $P(v_c, T_c)=P_c$ provide a set of three equations with five unknowns (c, v^*, T^*, v_c, and Z_M). The three equations were programmed in a subroutine which uses a Marquart non-linear regression scheme (35) to solve the three equations given two of the five parameters listed above. The subroutine then allows two of the five parameters to be optimized to experimental vapor pressures and saturation densities subject to the critical point constraints shown above. In Cases 1-5 for pure fluids of Chapter IV, Z_M was set at a

constant value of 18.0 and c was regressed to minimize percentage errors in calculated vapor pressures subject to the above constraints.

Since the above equations are cumbersome and time consuming to solve on the computer, simple correlations were developed to relate T* and v* to c for a value of Z_M of 18. The critical point constraints were solved at various values of c ranging from 1 to 15. Values of the reduced parameters, T^*/T_c and $v^*P_c/(RT_c)$ are shown in Figures B.1 and B.2, respectively. Simple correlations were then developed for these variables as functions of c. The resulting correlations are

$$\frac{T^*}{T_c} = A_1 + A_2 c^{A_3} + A_4 c^{A_5} \qquad \text{(B1)}$$

with

$A_1 = -0.1780022$
$A_2 = 0.3848355$
$A_3 = -0.7116849$
$A_4 = 0.5909591$
$A_5 = -0.03584398$

and

$$\frac{v^* P_c}{RT_c} = B_1 + B_2 c^{B_3} + B_4 c^{B_5} + B_6 c^{B_7} \qquad \text{(B2)}$$

with

$B_1 = 6.798509$
$B_2 = -6.749738$
$B_3 = 0.003224491$
$B_4 = 0.006775296$
$B_5 = 0.7167563$
$B_6 = -0.0009001604$
$B_7 = 1.114067$

The data used to generate the correlation coefficients along with the fitted values are shown in Tables B.I and B.II.

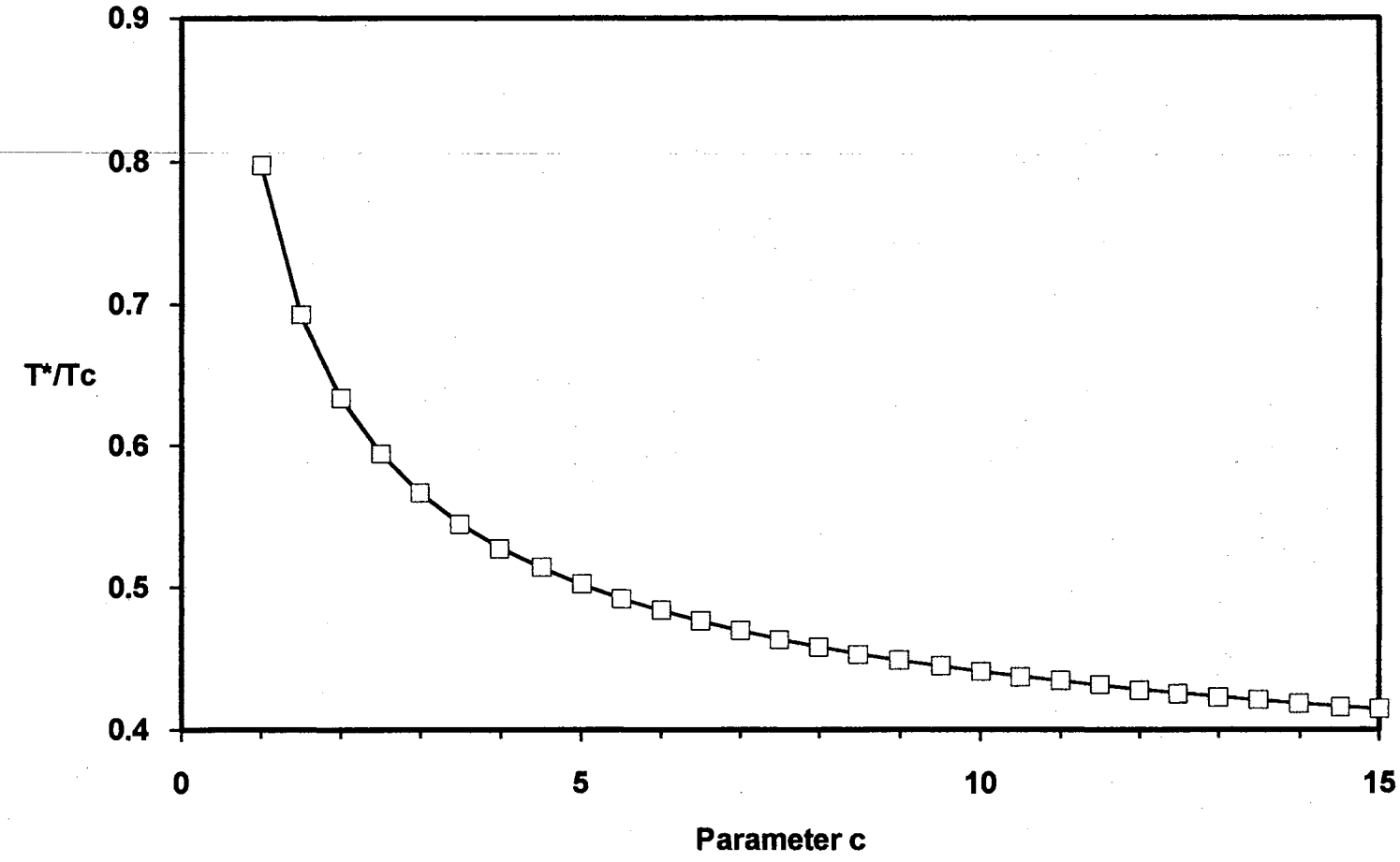

Figure B.1. Relation Between T^*/T_c and c from the Critical Point Constraints

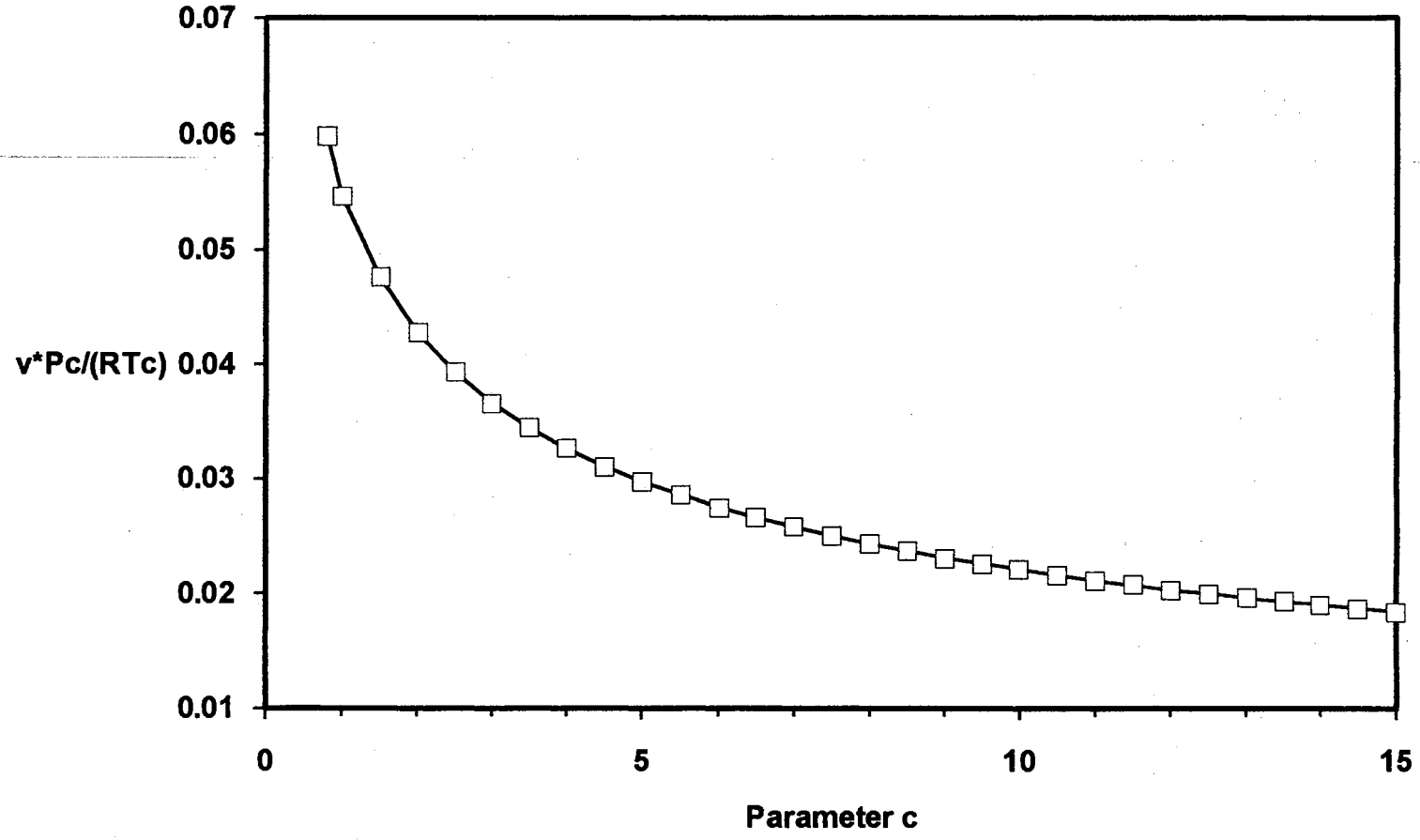

Figure B.2. Relation Between $v^*P_c/(RT_c)$ and c from the Critical Point Constraints

TABLE B.I

COMPARISON OF CALCULATED AND FITTED VALUES FOR T^*/T_c AS A FUNCTION OF THE PARAMETER C

C	T^*/T_c from critical pt constraints	T^*/T_c from Equation B1	% Dev.
1.0	0.7977	0.7978	-0.006
1.5	0.6927	0.6928	-0.012
2.0	0.6335	0.6334	0.012
2.5	0.5945	0.5943	0.024
3.0	0.5664	0.5662	0.026
3.5	0.5449	0.5448	0.022
4.0	0.5279	0.5278	0.015
4.5	0.5139	0.5139	0.007
5.0	0.5022	0.5022	-0.002
5.5	0.4923	0.4923	-0.009
6.0	0.4836	0.4837	-0.016
6.5	0.4761	0.4762	-0.021
7.0	0.4694	0.4695	-0.025
7.5	0.4634	0.4635	-0.028
8.0	0.4580	0.4581	-0.029
8.5	0.4531	0.4532	-0.029
9.0	0.4486	0.4488	-0.028
9.5	0.4446	0.4447	-0.026
10.0	0.4408	0.4409	-0.022
10.5	0.4373	0.4374	-0.018
11.0	0.4341	0.4341	-0.013
11.5	0.4311	0.4311	-0.006
12.0	0.4282	0.4282	0.000
12.5	0.4256	0.4256	0.008
13.0	0.4231	0.4231	0.016
13.5	0.4208	0.4207	0.026
14.0	0.4186	0.4184	0.035
14.5	0.4165	0.4163	0.045
15.0	0.4145	0.4143	0.056

RMSE = 0.0001 AAPD = 0.020

TABLE B.II

COMPARISON OF CALCULATED AND FITTED VALUES FOR $v^*P_c/(RT_c)$ AS A FUNCTION OF THE PARAMETER C

C	$v^*P_c/(RT_c)$ from critical pt constraints	$v^*P_c/(RT_c)$ from Equation B2	% Dev.
1.0	0.0547	0.0546	0.101
1.5	0.0476	0.0476	0.052
2.0	0.0428	0.0429	-0.027
2.5	0.0393	0.0394	-0.063
3.0	0.0366	0.0366	-0.065
3.5	0.0344	0.0344	-0.049
4.0	0.0326	0.0326	-0.024
4.5	0.0311	0.0311	0.001
5.0	0.0297	0.0297	0.022
5.5	0.0286	0.0285	0.039
6.0	0.0275	0.0275	0.049
6.5	0.0266	0.0266	0.053
7.0	0.0258	0.0258	0.051
7.5	0.0250	0.0250	0.044
8.0	0.0243	0.0243	0.034
8.5	0.0237	0.0237	0.020
9.0	0.0231	0.0231	0.004
9.5	0.0226	0.0226	-0.012
10.0	0.0221	0.0221	-0.028
10.5	0.0216	0.0216	-0.041
11.0	0.0211	0.0212	-0.052
11.5	0.0207	0.0207	-0.058
12.0	0.0203	0.0203	-0.059
12.5	0.0200	0.0200	-0.054
13.0	0.0196	0.0196	-0.041
13.5	0.0193	0.0193	-0.020
14.0	0.0190	0.0190	0.010
14.5	0.0187	0.0187	0.050
15.0	0.0184	0.0184	0.102

RMSE = 0.00002 AAPD = 0.043

APPENDIX C

DERIVATION OF THE COORDINATION NUMBER AND CONFIGURATIONAL ENERGY EXPRESSIONS FOR MIXTURES

Strictly speaking, the derivation of the SPHCT equation given in Chapter II is valid only for pure fluids. The mixing rules for multicomponent systems using the same equation are then obtained by deriving key expressions such as the coordination number expression and inferring the type of mixing required to produce a pseudo-pure compound. Because of difficulties encountered during this work when dealing with prediction of mixture properties, the coordination number for a pure fluid (given by Equation (30) of Chapter II) was rederived for a mixture without the simplifying assumptions regarding the function Ψ of Equation (26). This was done for two reasons: first, to determine if the mixing rule used in the attractive portion of the equation of state (Equation (39)) is the best choice that can be inferred from sound theoretical arguments, and, second, to remove the restrictions of the assumptions outlined in Chapter II and in the process illustrate how the equation may be improved based on more accurate molecular descriptions.

The maximum coordination number of Equation (24) can be extended to mixtures in the following way

$$Z_M = \sum_{i=0}^{n} N_{ij} \qquad (C1)$$

in which Z_M represents the maximum coordination number for a single segment of species j, N_{ij} represents the number of segments of species i interacting with a central segment of species j, the subscript 0 is used to represent unoccupied lattice sites (holes) and the subscripts 1 through n represent the different chemical components of the mixture. The distribution of the various components about a central segment of

type j can be given by a local composition model of the type used in Chapter II such that

$$\frac{N_{ij}}{N_{jj}} = \frac{N_i}{N_j} \Psi_{ij} \tag{C2}$$

where

$$\Psi_{ij} = \frac{\sigma_{ij}^3}{\sigma_{jj}^3} \frac{\int_1^{R_{ij}} g_{ij} 4\pi\tilde{r}^2 d\tilde{r}}{\int_1^{R_{jj}} g_{jj} 4\pi\tilde{r}^2 d\tilde{r}} = \frac{v_{ij}^*}{v_{jj}^*} \frac{G_{ij}}{G_{jj}} \tag{C3}$$

and $$G_{ij} = \int_1^{R_{ij}} g_{ij} 4\pi\tilde{r}^2 d\tilde{r} \tag{C4}$$

By combining Equations (C1) through (C4) an expression for the coordination number of species i around a central segment of species j is given by

$$N_{ij} = \frac{Z_M x_i v_{ij}^* \frac{G_{ij}}{G_{0j}}}{x_0 v_{0j}^* + \sum_{k=1}^{n} x_k v_{kj}^* \frac{G_{kj}}{G_{0j}}} \tag{C5}$$

Recognizing that the specific volume can be written in terms of the v*'s as

$$v = \frac{V}{\sum_{i=0}^{n} N_i} = x_0 v_{0j}^* + \sum_{i=1}^{n} x_i v_{ij}^* \tag{C6}$$

the individual coordination numbers, N_{ij}, can be written as

$$N_{ij} = \frac{z_M x_k v_{ij}^* \frac{G_{ij}}{G_{0j}}}{v + \sum_{k=1}^{n}\left[x_k v_{kj}^*\left(\frac{G_{kj}}{G_{0j}} - 1\right)\right]} \tag{C7}$$

where the x's now represent conventional mole fractions of the chemical components. The total coordination number for species of all types around a central segment of species j can then be expressed as

$$N_{cj} = \sum_{i=1}^{n} N_{ij} = \frac{z_M \sum_{i=1}^{n} x_i v_{ij}^* \frac{G_{ij}}{G_{0j}}}{v + \sum_{i=1}^{n}\left[x_i v_{ij}^*\left(\frac{G_{ij}}{G_{0j}} - 1\right)\right]} \tag{C8}$$

For a pure square-well fluid the configurational energy of Equation (22) can be related to the coordination number by

$$E^{CONF} = -\varepsilon \frac{NN_c}{2} \tag{C9}$$

For a mixture, the configurational energy due to i-j interactions is

$$E_{ij}^{CONF} = -\varepsilon_{ij} \frac{N_j N_{ij}}{2} \tag{C10}$$

The total configurational energy for a mixture is then given by

$$E^{CONF} = \sum_{i=1}^{n}\sum_{j=1}^{n}\left(-\varepsilon_{ij} \frac{N_j N_{ij}}{2}\right) \tag{C11}$$

Substituting the expression for the species coordination number, N_{ij}, of Equation (C5), the configurational energy is

$$\frac{E^{CONF}}{N} = -\frac{1}{2}\sum_{i=1}^{n}\sum_{j=1}^{n}\frac{\varepsilon_{ij}Z_M x_i x_j v^*_{ij}\frac{G_{ij}}{G_{0j}}}{v + \sum_{k=1}^{n}\left[x_k v^*_{kj}\left(\frac{G_{kj}}{G_{0j}} - 1\right)\right]} \qquad \text{(C12)}$$

Comparison of Equation (C12) with Equation (C9) and Equation (30) of Chapter II suggest that a pseudo-pure component can be defined when mixing is done in the following manner

$$Y_{pseudo\text{-}pure} = \sum_{i=1}^{n}\sum_{j=1}^{n} x_i x_j v^*_{ij}\frac{G_{ij}}{G_{0j}} \qquad \text{(C13)}$$

which is precisely the type of mixing used in Equation (39) of Chapter II.

The above equations imply that the mixing rules used for multicomponent systems are valid as they are currently used. However, the simple expression for G_{ij} developed in Chapter II may be inadequate for complex mixtures. A more accurate expression for the exponential term of the original SPHCT equation may be a ratio of two similar functions (as suggested by Equation (C13)) based on more realistic radial distributions functions which are functions of both temperature and density.

APPENDIX D

MODIFIED SPHCT FUGACITY COEFFICIENT EXPRESSIONS

During the course of this work, several modifications were studied which affect the expression for the component fugacities. Accordingly, the necessary equations are listed here for completeness. For the SPHCT equation in its original form, with the mixing rules listed in Equations (37) through (41) of Chapter II, the fugacity coefficient expression is identical to the one reported by Kim, et al. (7).

$$\ln \phi_i = c_i \frac{4\tau\tilde{\rho} - 3(\tau\tilde{\rho})^2}{(1-\tau\tilde{\rho})^2} + \frac{\langle c\rangle v_i^*}{\langle v^*\rangle} \frac{4\tau\tilde{\rho} - 2(\tau\tilde{\rho})^2}{(1-\tau\tilde{\rho})^3}$$

$$-\langle c\rangle Z_M \left[2 - \frac{c_i}{\langle c\rangle} + \frac{c_i}{\langle c\rangle} \ln\left(1 + \frac{\langle cv^*Y\rangle}{\langle c\rangle v} \right) \right.$$

$$\left. + \frac{v(c_i - 2\langle c\rangle) + \frac{1}{n}\frac{\partial}{\partial n_i}\left(n^2\langle cv^*Y\rangle\right) - 2\langle cv^*Y\rangle}{\langle c\rangle v + \langle cv^*Y\rangle} \right] - \ln z \qquad \text{(D1)}$$

where

$$\frac{1}{n}\frac{\partial}{\partial n_i}\left(n^2\langle cv^*Y\rangle\right) = \sum_j x_j \left[c_i v_{ji}^* \left(\exp \frac{\varepsilon_{ij} q_i}{2c_i kT} \right) + c_j v_{ij}^* \left(\exp \frac{\varepsilon_{ji} q_j}{2c_j kT} \right) \right] \qquad \text{(D2)}$$

For the case in which <v*> is calculated by the following mixing rule

$$\langle v^*\rangle = \sum_i \sum_j x_i x_j v_{ij}^* \qquad \text{(D3)}$$

with

$$v_{ij}^* = \frac{s_j \sigma_{ij}^3}{\sqrt{2}} \qquad \text{(D4)}$$

and

$$\sigma_{ij} = \frac{\left(\sigma_{ii} + \sigma_{jj}\right)}{2}\left(1 + D_{ij}\right) \tag{D5}$$

where D_{ij} is a binary interaction parameter, the second term in the fugacity coefficient expression given above (Equation (D1)) should be changed to

$$\frac{\langle c\rangle\left[\sum_j x_j\left(v^*_{ij} + v^*_{ji}\right) - \left\langle v^*\right\rangle\right]}{\left\langle v^*\right\rangle}\frac{4\tau\tilde{\rho} - 2(\tau\tilde{\rho})^2}{(1 - \tau\tilde{\rho})^3} \tag{D6}$$

For the case when <c> is calculated from the following mixing rule

$$\langle c\rangle = \sum_i \sum_j x_i x_j c_{ij} \tag{D7}$$

with

$$c_{ij} = \frac{\left(c_i + c_j\right)}{2}\left(1 + E_{ij}\right) \tag{D8}$$

where E_{ij} is a binary interaction parameter, and c_i of Equation (D1) should be replaced with

$$\sum_j x_j\left(c_{ij} + c_{ji}\right) - \langle c\rangle \tag{D9}$$

For the case in which Z_M is a function of temperature and/or other parameters and the mixture Z_M is given by

$$\left\langle Z_M\right\rangle = \sum_i \sum_j x_i x_j Z_{Mij} \tag{D10}$$

and Z_{Mij} is given by a mixing expression for Z_M such as

$$Z_{Mij} = \sqrt{Z_{Mi} Z_{Mj}} \tag{D11}$$

the following term should be added to the fugacity coefficient expression

$$-\langle c\rangle\left[\sum_j x_j\left(Z_{Mij} + Z_{Mji}\right) - 2\langle Z_M\rangle\right]\ln\left(1 + \frac{\langle cv^*Y\rangle}{\langle c\rangle v}\right) \qquad \text{(D12)}$$

The above equations for component fugacities were used in the investigation of the EOS modifications discussed in Chapter III.

APPENDIX E

DATABASE USED

This appendix contains the sources and ranges of all data used in the equation of state development and evaluations of this work. Table E.I contains the sources and ranges of pure fluids used in Chapter IV. Table E.II contains the sources and ranges of solubility data for ethane + n-paraffin binary mixtures and Table E.III contains a similar summary for the CO_2 + n-paraffin solubility data. Table IV describes the database used for evaluation of the modified and original SPHCT equations for the prediction of bubble point pressures, vapor phase compositions and vapor and liquid phase densities. This database consists mostly of CO_2 + hydrocarbon systems with the exception of the ethane + 1-methylnaphthalene data taken during this work.

TABLE E.I

SOURCES AND RANGES OF SATURATED DATA USED FOR PURE FLUIDS

Compound	Temperature Range, K	Pressure Range, bar	Liquid Density Range, g/cm^3	Vapor Density Range, g/cm^3	Source
Methane	90.68-188.0	0.1172-42.412	0.2299-0.4512	2.514×10^{-4}-0.0986	39
Ethane	90.348-295.0	1.131×10^{-5}-39.16	0.3309-0.6519	4.557×10^{-8}-0.0925	40
Propane	85.47-360.0	3.0×10^{-9}-35.55	0.3453-0.6574	2.72×10^{-5}-0.1054	41
n-Butane	134.86-420.0	6.736×10^{-6}-34.83	0.3281-0.7353	3.492×10^{-8}-0.1335	42
n-Octane	243.15-553.15	3.16×10^{-4}-19.97	0.3818-0.7102	0.0003-0.0983	43
n-Decane	330.85-613.15	0.01333-20.366	0.324-0.6996	*	44
n-Tetradecane	394.26-573.15	0.0129-2.605	0.6685**	*	44
n-Eicosane	473.15-623.15	0.01533-1.11	0.704**	*	44
Ethene	103.986-276.0	0.0012-43.73	0.3242-0.6549	4.01×10^{-6}-0.1115	45
Propene	87.89-360.0	9.54×10^{-9}-42.202	0.3292-0.7688	5.49×10^{-11}-0.1338	46
1-Butene	119.95-413.15	5.0×10^{-7}-36.18	0.345-0.618	*	44
1-Hexene	156.15-493.15	5.0×10^{-7}-26.86	*	*	44
Cyclopropane	171.85-393.15	0.01333-51.252	*	*	44
Cyclobutane	204.95-453.15	0.01333-45.191	*	*	44
Cyclohexane	279.82-543.15	0.05328-35.889	0.3130-0.7102	*	44

TABLE E.I (Continued)

Compound	Temperature Range, K	Pressure Range, bar	Liquid Density Range, g/cm^3	Vapor Density Range, g/cm^3	Source
Cyclooctane	308.45-633.15	0.01333-31.309	*	*	44
trans-Decalin	334.06-492.03	0.01333-1.9998	0.7726-0.8355	*	44,77
Benzene	278.68-555.0	0.0478-44.8502	0.4355-0.8965	1.62×10^{-4}-0.1750	47
Toluene	270.0-580.0	0.0076-35.56	0.2914-0.8873	2.87×10^{-5}-0.1318	48
1-Methyl naphthalene	380.83-551.47	0.01333-1.9998	0.9230-0.9619	*	44
Argon	84.0-146.0	0.7052-49.05	0.8296-1.413	0.004194-0.2680	45
Carbon Dioxide	216.55-298.15	5.179-64.356	0.7138-1.1778	0.0138-0.2424	49
Water	273.16-633.15	0.006117-186.55	0.5281-0.9998	4.855×10^{-6}-0.1437	50

* Saturated density data for these compounds was not available.
** Only one saturated liquid density value was available for n-tetradecane and n-eicosane.

TABLE E.II

ETHANE BINARY SYSTEM SOLUBILITY DATA USED IN EQUATION OF STATE EVALUATIONS

Solvent	Temperature Range, K	Pressure Range, bar	Ethane Mole Fraction Range	Reference Number
$n\text{-}C_4$	338.7-394.3	32.4-50.3	0.118-0.753	54
$n\text{-}C_5$	310.9-444.3	3.4-62.1	0.013-0.927	55
$n\text{-}C_6$	310.9-394.3	3.9-54.0	0.072-0.652	56
$n\text{-}C_7$	338.7-449.8	31.4-49.4	0.333-0.517	57
$n\text{-}C_8$	323.2-373.2	4.1-52.7	0.047-0.863	58
$n\text{-}C_{10}$	310.9-410.9	4.2-82.4	0.105-0.638	59
$n\text{-}C_{12}$	373.2	11.1-53.2	0.155-0.554	60
$n\text{-}C_{20}$	323.2-423.2	5.0-76.9	0.118-0.653	56
$n\text{-}C_{28}$	348.2-423.2	5.6-51.8	0.102-0.520	60
$n\text{-}C_{36}$	373.2-423.2	3.7-47.6	0.087-0.531	56
$n\text{-}C_{44}$	373.2-423.2	3.9-31.7	0.099-0.516	56

TABLE E.III

CARBON DIOXIDE BINARY SYSTEM SOLUBILITY DATA
USED IN EQUATION OF STATE EVALUATIONS

Solvent	Temperature Range, K	Pressure Range, bar	CO_2 Mole Fraction Range	Reference Number
$n\text{-}C_4$	310.9-410.9	5.5-75.4	0.002-0.908	61
$n\text{-}C_5$	311.0-377.6	4.1-96.3	0.007-0.942	62
$n\text{-}C_6$	313.2-393.2	8.6-116.0	0.052-0.915	63
$n\text{-}C_7$	310.7-477.2	1.8-133.1	0.022-0.949	64
$n\text{-}C_{10}$	310.9-510.9	3.5-172.4	0.045-0.864	65
$n\text{-}C_{16}$	463.1	9.3-68.8	0.109-0.258	66
$n\text{-}C_{20}$	323.2-373.2	6.2-67.6	0.073-0.501	67
$n\text{-}C_{22}$	323.2-373.2	9.6-71.8	0.083-0.593	68
$n\text{-}C_{28}$	323.2-423.2	8.1-96.0	0.070-0.617	67
$n\text{-}C_{32}$	348.2-398.2	9.5-72.3	0.096-0.562	68
$n\text{-}C_{36}$	373.2-423.2	5.2-86.5	0.062-0.502	67
$n\text{-}C_{44}$	373.2-423.2	5.8-70.8	0.082-0.502	67

TABLE E.IV

MIXTURE PHASE DENSITY DATABASE USED IN EQUATION OF STATE EVALUATIONS

Mixture	Temperature, K	Pressure Range, bar	Liquid Density Range, g/cm^3	Vapor Density Range, g/cm^3	Source
CO_2 + n-Butane	319.26	21.79-76.26	0.5634-0.4060	0.0501-0.4060	72
	344.26	32.06-81.22	0.5201-0.3735	0.0691-0.3735	72
	377.59	28.82-75.70	0.4565-0.3196	0.0714-0.3195	72
CO_2 + n-Decane	344.26	34.47-127.14	0.6987-0.5875	0.0629-0.5875	This work
	377.59	103.42-164.85	0.6760-0.5535	0.2051-0.5535	73
CO_2 + n-Tetradecane	344.26	110.32-163.82	0.7509-0.7085	0.2961-0.7085	74
CO_2 + Benzene	344.26	68.95-109.56	0.8150-0.5330	0.1560-0.5330	75
CO_2 + Cyclohexane	344.26	103.42-158.37	0.8343-0.7658	0.2709-0.7658	76
CO_2 + *trans*-Decalin	344.26	68.95-227.06	0.8353-0.7635	0.1422-0.7635	This work
Ethane + 1-Methylnaphthalene	344.26	82.74-158.23	0.8115-0.5687	0.1930-0.5687	This work

TABLE E.V

MIXTURE PHASE COMPOSITION DATABASE USED IN EQUATION OF STATE EVALUATIONS

Mixture	Temperature, K	Pressure Range, bar	Liquid Mole Fraction Solute	Vapor Mole Fraction Solute	Source
CO_2 + n-Butane	319.26	21.79-76.26	0.1880-0.8750	0.7446-0.8750	72
	344.26	32.06-81.22	0.2079-0.7200	0.6821-0.7200	72
	377.59	28.82-75.70	0.0880-0.5100	0.3403-0.5100	72
CO_2 + n-Decane	344.26	34.47-127.14	0.2624-0.9349	0.9941-0.9349	This work
	377.59	103.42-164.85	0.5651-0.8950	0.9872-0.8950	73
CO_2 + n-Tetradecane	344.26	110.32-163.82	0.6830-0.9240	0.9910-0.9240	74
CO_2 + Benzene	344.26	68.95-109.56	0.4258-0.8800	0.9515-0.8800	75
CO_2 + Cyclohexane	344.26	103.42-158.37	0.5245-0.8620	0.9815-0.8620	76
CO_2 + *trans*-Decalin	344.26	68.95-227.06	0.3399-0.8732	0.9960-0.8732	This work
Ethane + 1-Methylnaphthalene	344.26	82.74-158.23	0.5095-0.8238	0.9949-0.8238	This work

APPENDIX F

PURE FLUID EQUATION OF STATE PARAMETERS USED

This appendix contains the equation of state parameters generated during the regression procedures described for pure fluids in Chapter IV. Table F.I contains the parameters for the original SPHCT equation of state. Table F.II contains the parameters for the constrained SPHCT equation (Case 1 of Table III). Table F.III contains the parameters for the modified SPHCT equation including the modified attractive term of Equations (73) and (74) (Case 2 of Table III). Table F.IV contains the volume translation parameters for Equation (86) for Cases 3 and 4 of Table III.

TABLE F.I

PURE FLUID PARAMETERS FOR THE ORIGINAL SPHCT EQUATION

Compound	c	T* (K)	v* (ml/mol)
Methane	1.0298	80.05	18.889
Ethane	1.2485	120.73	26.988
Propane	1.5015	136.94	35.876
n-Butane	1.6867	151.73	43.922
n-Octane	2.6453	177.91	74.084
n-Decane	3.0697	186.03	93.130
n-Tetradecane	3.9218	196.70	127.416
n-Eicosane	5.1600	205.98	181.657
Ethene	1.2379	111.58	24.684
Propene	1.5267	133.85	31.881
1-Butene	1.5212	157.89	40.457
1-Hexene	1.0854	255.90	26.597
Cyclopropane	0.6646	252.76	13.699
Cyclobutane	0.6413	312.12	13.976
Cyclohexane	1.7077	199.49	49.825
Cyclooctane	2.1068	212.41	69.815
trans-Decalin	0.9682	381.13	29.826
Benzene	1.8866	192.59	41.457
Toluene	1.8921	205.78	52.971
1-Methylnaphthalene	1.1351	398.18	28.382
Argon	1.0270	63.25	14.275
Carbon Dioxide	1.9258	104.32	14.486
Water	2.0233	225.08	9.071

TABLE F.II

PURE FLUID PARAMETERS FOR THE CONSTRAINED SPHCT EQUATION (CASE 1)

Compound	c	T* (K)	v* (ml/mol)
Methane	1.0409	149.78	18.614
Ethane	1.3096	221.34	26.310
Propane	1.5779	252.01	33.886
n-Butane	1.7827	278.85	41.640
n-Octane	2.7671	329.34	71.710
n-Decane	3.3758	339.48	85.527
n-Tetradecane	4.4354	356.57	115.020
n-Eicosane	5.7281	378.41	162.967
Ethene	1.2942	205.46	23.358
Propene	1.5638	249.85	30.562
1-Butene	1.7477	277.12	38.900
1-Hexene	2.1929	310.86	55.166
Cyclopropane	1.4774	277.25	28.431
Cyclobutane	1.6942	306.51	34.954
Cyclohexane	1.9255	354.63	49.087
Cyclooctane	2.1144	403.37	63.286
trans-Decalin	2.2677	419.73	74.317
Benzene	1.9049	361.08	41.794
Toluene	2.0912	370.03	50.508
1-Methylnaphthalene	2.5359	457.15	69.756
Argon	1.0422	118.52	13.799
Carbon Dioxide	2.2271	186.79	14.104
Water	2.3534	391.20	9.824

TABLE F.III

PURE FLUID PARAMETERS FOR THE MODIFIED SPHCT EQUATION (CASE 2)

Compound	c	T* (K)	v* (ml/mol)
Methane	1.0003	95.23	18.858
Ethane	1.2423	142.28	26.795
Propane	1.4273	165.27	35.123
n-Butane	1.5594	185.28	43.721
n-Octane	2.1875	227.31	78.542
n-Decane	2.4906	239.20	96.459
n-Tetradecane	3.0646	256.16	133.675
n-Eicosane	3.7096	276.49	195.231
Ethene	1.2299	131.95	23.773
Propene	1.3884	164.70	31.885
1-Butene	1.5329	183.89	40.798
1-Hexene	1.8164	210.80	59.210
Cyclopropane	1.3473	181.03	29.372
Cyclobutane	1.4884	203.12	36.629
Cyclohexane	1.6060	239.26	52.475
Cyclooctane	1.7514	273.29	67.898
trans-Decalin	1.8482	286.08	80.275
Benzene	1.6142	242.48	44.417
Toluene	1.7578	249.65	53.890
1-Methylnaphthalene	2.0217	314.20	76.076
Argon	0.9760	76.03	14.098
Carbon Dioxide	1.6258	131.05	15.858
Water	1.9416	266.06	10.568

TABLE F.IV

PARAMETERS USED IN MODIFIED SPHCT VOLUME TRANSLATIONS

Compound	Case 3		Case 4
	c_1	c_2	c_2
Methane	0.041298	1.280774	1.290430
Ethane	0.042916	1.238858	1.258637
Propane	0.042398	1.541326	1.565299
n-Butane	0.037364	1.661840	1.632381
n-Octane	0.018802	2.187511	1.949292
n-Decane	0.034410	2.304688	2.257884
n-Tetradecane	0.035403	1.437548	1.383026
n-Eicosane	0.028532	1.289396	1.160417
Ethene	0.039102	1.460464	1.451348
Propene	0.040846	1.722680	1.731145
1-Butene	0.028353	1.574936	1.505023
Cyclohexane	0.017662	1.507541	1.384786
Benzene	0.043828	1.271750	1.297716
Toluene	0.016215	1.834757	1.523969
Argon	0.051681	1.353512	1.438851
Carbon Dioxide	0.026912	1.561819	1.499169
Water	-0.022018	1.485624	1.004126

Case 3: 2 constant volume translation.
Case 4: 1 constant volume translation. c_1=0.04 for all compounds.

APPENDIX G

MIXTURE EQUATION OF STATE EVALUATIONS

This appendix contains detailed tables for all cases studied during the evaluations of the modified SPHCT, the original SPHCT and the PR equations as described in Chapter IV. Tables G.I through G.XVII contain the detailed results for the cases of Table IX for the PR, original SPHCT and modified SPHCT equations, respectively, for the calculation of bubble point pressures of ethane + n-paraffin systems. Table G.XVIII through G.XXXIV contain similar tables for the calculation of bubble point pressures of CO_2 + n-paraffin systems. The statistics in Tables G.I through G.XXXIV are RMSE (root mean square error in bars), RMSPE (root mean square fractional error), BIAS (bias in bars), AAD (average absolute deviation) and %AAD (percent average absolute deviation). Tables G.XXXV through G.XLV contain the results for the cases of Table XII for the evaluation of the data set containing phase densities and compositions for the PR, the original SPHCT and the modified SPHCT equations, respectively. Table XLVI lists the physical properties used as input variables for the mixture equation of state evaluations.

TABLE G.I

BUBBLE-POINT CALCULATIONS USING PENG-ROBINSON EQUATION OF STATE FOR ETHANE + N-PARAFFIN SYSTEMS (CASE 1)

ISO	CN	T(K)	C(I,J)	D(I,J)	RMSE	RMSPE	BIAS	AAD	%AAD	NPT
1	4	338.7	0.0000	0.0000	1.71	0.0390	-1.50	1.50	3.4	6
2	4	366.5	0.0000	0.0000	2.08	0.0481	-1.80	1.80	4.2	8
3	4	394.3	0.0000	0.0000	0.77	0.0206	-0.60	0.60	1.6	5
4	5	310.9	0.0000	0.0000	0.32	0.0172	-0.25	0.25	1.4	12
5	5	377.6	0.0000	0.0000	0.98	0.0214	-0.71	0.71	1.9	13
6	5	444.3	0.0000	0.0000	0.58	0.0175	-0.41	0.41	1.2	6
7	6	310.9	0.0000	0.0000	0.18	0.0121	-0.17	0.17	1.2	15
8	6	338.7	0.0000	0.0000	0.08	0.0085	0.00	0.07	0.6	11
9	6	366.5	0.0000	0.0000	0.09	0.0063	0.07	0.07	0.5	11
10	6	394.3	0.0000	0.0000	0.50	0.0113	-0.35	0.35	0.9	11
11	7	338.7	0.0000	0.0000	1.04	0.0331	1.04	1.04	3.3	1
12	7	394.3	0.0000	0.0000	1.73	0.0434	1.73	1.73	4.3	1
13	7	449.8	0.0000	0.0000	3.47	0.0702	-3.47	3.47	7.0	1
14	8	323.1	0.0000	0.0000	1.44	0.0457	-1.35	1.35	4.4	11
15	8	348.1	0.0000	0.0000	1.92	0.0772	-1.78	1.78	7.2	13
16	8	373.1	0.0000	0.0000	1.37	0.0701	-1.28	1.28	6.7	9
17	10	310.9	0.0000	0.0000	0.58	0.0325	-0.47	0.47	3.1	10
18	10	344.3	0.0000	0.0000	0.66	0.0171	-0.44	0.50	1.5	7
19	10	377.6	0.0000	0.0000	0.56	0.0195	-0.10	0.47	1.7	6
20	10	410.9	0.0000	0.0000	1.22	0.0300	-0.32	1.02	2.6	7
21	12	373.1	0.0000	0.0000	0.64	0.0292	0.14	0.56	2.4	9
22	20	323.1	0.0000	0.0000	1.40	0.1392	0.78	1.30	11.4	6
23	20	373.1	0.0000	0.0000	1.94	0.0923	0.61	1.79	7.1	6
24	20	423.1	0.0000	0.0000	2.80	0.1217	2.27	2.60	9.7	7
25	28	348.1	0.0000	0.0000	2.54	0.1891	2.51	2.51	17.2	10
26	28	373.1	0.0000	0.0000	2.46	0.1758	2.39	2.39	15.8	7
27	28	423.1	0.0000	0.0000	3.38	0.1751	3.28	3.28	15.9	7
28	36	373.1	0.0000	0.0000	2.67	0.2236	2.58	2.58	20.3	7
29	36	423.1	0.0000	0.0000	2.35	0.1439	2.07	2.07	11.6	6
30	44	373.1	0.0000	0.0000	3.30	0.2965	3.23	3.23	26.2	9
31	44	423.1	0.0000	0.0000	2.33	0.1692	2.25	2.25	15.7	7

MODEL OVERALL STATISTICS

RMSE	= 1.6844 BAR	NO PT	= 245
AAD	= 1.2428 BAR	%AAD	= 6.492
MIN DEV=	-3.4701 BAR	MIN %DEV	= -13.093
MAX DEV=	4.2122 BAR	MAX %DEV	= 48.666
BIAS	= 0.2365 BAR	C-VAR	= 0.092
RESTRICTIONS	: NONE	R-SQR	=0.958991

TABLE G.II

BUBBLE-POINT CALCULATIONS USING PENG-ROBINSON EQUATION OF STATE FOR ETHANE + N-PARAFFIN SYSTEMS (CASE 2)

ISO	CN	T(K)	C(I,J)	D(I,J)	RMSE	RMSPE	BIAS	AAD	%AAD	NPT
1	4	338.7	-0.0117	0.0000	2.21	0.0518	-1.85	1.85	4.4	6
2	4	366.5	-0.0117	0.0000	2.27	0.0551	-1.88	1.88	4.6	8
3	4	394.3	-0.0117	0.0000	0.84	0.0238	-0.56	0.56	1.6	5
4	5	310.9	-0.0117	0.0000	0.77	0.0477	-0.74	0.74	4.3	12
5	5	377.6	-0.0117	0.0000	1.57	0.0408	-1.30	1.30	3.9	13
6	5	444.3	-0.0117	0.0000	0.71	0.0216	-0.49	0.49	1.5	6
7	6	310.9	-0.0117	0.0000	0.80	0.0551	-0.76	0.76	5.3	15
8	6	338.7	-0.0117	0.0000	0.79	0.0354	-0.72	0.72	3.5	11
9	6	366.5	-0.0117	0.0000	0.66	0.0301	-0.60	0.60	3.0	11
10	6	394.3	-0.0117	0.0000	1.27	0.0346	-1.11	1.11	3.4	11
11	7	338.7	-0.0117	0.0000	0.07	0.0023	-0.07	0.07	0.2	1
12	7	394.3	-0.0117	0.0000	0.54	0.0135	0.54	0.54	1.4	1
13	7	449.8	-0.0117	0.0000	4.36	0.0882	-4.36	4.36	8.8	1
14	8	323.1	-0.0117	0.0000	2.33	0.0800	-2.23	2.23	7.7	11
15	8	348.1	-0.0117	0.0000	2.96	0.1138	-2.75	2.75	11.0	13
16	8	373.1	-0.0117	0.0000	2.18	0.1062	-2.02	2.02	10.4	9
17	10	310.9	-0.0117	0.0000	1.33	0.0848	-1.19	1.19	8.4	10
18	10	344.3	-0.0117	0.0000	1.81	0.0548	-1.55	1.55	5.4	7
19	10	377.6	-0.0117	0.0000	1.69	0.0356	-1.32	1.32	3.3	6
20	10	410.9	-0.0117	0.0000	2.41	0.0343	-1.71	1.78	2.9	7
21	12	373.1	-0.0117	0.0000	1.56	0.0358	-1.13	1.17	3.1	9
22	20	323.1	-0.0117	0.0000	1.63	0.1001	-0.23	1.33	8.7	6
23	20	373.1	-0.0117	0.0000	2.86	0.0736	-1.20	2.31	6.5	6
24	20	423.1	-0.0117	0.0000	2.33	0.0943	0.65	2.10	7.4	7
25	28	348.1	-0.0117	0.0000	1.68	0.1424	1.58	1.58	12.0	10
26	28	373.1	-0.0117	0.0000	1.56	0.1355	1.43	1.43	11.2	7
27	28	423.1	-0.0117	0.0000	2.43	0.1421	2.27	2.27	12.2	7
28	36	373.1	-0.0117	0.0000	1.98	0.1861	1.85	1.85	16.1	7
29	36	423.1	-0.0117	0.0000	1.86	0.1195	1.17	1.67	9.4	6
30	44	373.1	-0.0117	0.0000	2.67	0.2617	2.57	2.57	22.3	9
31	44	423.1	-0.0117	0.0000	1.79	0.1435	1.73	1.73	12.9	7

MODEL OVERALL STATISTICS

RMSE	= 1.8481 BAR	NO PT	= 245
AAD	= 1.5076 BAR	%AAD	= 7.262
MIN DEV=	-5.5034 BAR	MIN %DEV	= -17.331
MAX DEV=	3.4746 BAR	MAX %DEV	= 44.475
BIAS	= -0.5634 BAR	C-VAR	= 0.101
RESTRICTIONS	: NONE	R-SQR	=0.912685

TABLE G.III

BUBBLE-POINT CALCULATIONS USING PENG-ROBINSON EQUATION OF STATE FOR ETHANE + N-PARAFFIN SYSTEMS (CASE 3)

ISO	CN	T(K)	C(I,J)	D(I,J)	RMSE	RMSPE	BIAS	AAD	%AAD	NPT
1	4	338.7	0.0002	0.0000	1.70	0.0387	-1.49	1.49	3.4	6
2	4	366.5	0.0002	0.0000	2.07	0.0479	-1.79	1.79	4.2	8
3	4	394.3	0.0002	0.0000	0.82	0.0214	-0.63	0.63	1.6	5
4	5	310.9	0.0072	0.0000	0.28	0.0090	0.04	0.20	0.8	12
5	5	377.6	0.0072	0.0000	0.68	0.0119	-0.34	0.34	0.7	13
6	5	444.3	0.0072	0.0000	0.50	0.0150	-0.36	0.37	1.1	6
7	6	310.9	0.0012	0.0000	0.11	0.0077	-0.10	0.10	0.7	15
8	6	338.7	0.0012	0.0000	0.09	0.0110	0.07	0.07	0.7	11
9	6	366.5	0.0012	0.0000	0.15	0.0093	0.14	0.14	0.8	11
10	6	394.3	0.0012	0.0000	0.43	0.0096	-0.27	0.30	0.8	11
11	7	338.7	-0.0056	0.0000	0.50	0.0160	0.50	0.50	1.6	1
12	7	394.3	-0.0056	0.0000	1.15	0.0289	1.15	1.15	2.9	1
13	7	449.8	-0.0056	0.0000	3.90	0.0789	-3.90	3.90	7.9	1
14	8	323.1	0.0185	0.0000	0.38	0.0210	0.14	0.32	1.5	11
15	8	348.1	0.0185	0.0000	0.33	0.0253	-0.14	0.30	1.8	13
16	8	373.1	0.0185	0.0000	0.30	0.0201	-0.04	0.27	1.8	9
17	10	310.9	0.0027	0.0000	0.40	0.0208	-0.30	0.30	1.9	10
18	10	344.3	0.0027	0.0000	0.42	0.0155	-0.18	0.34	1.3	7
19	10	377.6	0.0027	0.0000	0.49	0.0252	0.19	0.46	2.1	6
20	10	410.9	0.0027	0.0000	1.06	0.0339	0.01	0.95	2.8	7
21	12	373.1	-0.0045	0.0000	0.87	0.0239	-0.36	0.65	2.0	9
22	20	323.1	-0.0220	0.0000	2.27	0.0867	-1.07	1.54	7.5	6
23	20	373.1	-0.0220	0.0000	4.21	0.0780	-2.69	3.23	7.1	6
24	20	423.1	-0.0220	0.0000	2.89	0.0787	-0.71	2.27	6.4	7
25	28	348.1	-0.0454	0.0000	1.64	0.0715	-0.81	1.22	6.3	10
26	28	373.1	-0.0454	0.0000	2.11	0.0724	-1.07	1.60	6.8	7
27	28	423.1	-0.0454	0.0000	1.97	0.0737	-0.39	1.53	6.4	7
28	36	373.1	-0.0572	0.0000	1.91	0.0891	-0.66	1.27	7.5	7
29	36	423.1	-0.0572	0.0000	3.47	0.0873	-2.01	2.54	7.6	6
30	44	373.1	-0.0854	0.0000	2.34	0.1235	-1.00	1.71	10.4	9
31	44	423.1	-0.0854	0.0000	1.88	0.0691	-1.16	1.34	6.0	7

MODEL OVERALL STATISTICS

RMSE	= 1.5109 BAR	NO PT	= 245
AAD	= 0.8409 BAR	%AAD	= 3.232
MIN DEV=	-7.8599 BAR	MIN %DEV	= -14.727
MAX DEV=	1.8140 BAR	MAX %DEV	= 20.781
BIAS	= -0.5033 BAR	C-VAR	= 0.083
RESTRICTIONS	: NONE	R-SQR	=0.891059

TABLE G.IV

BUBBLE-POINT CALCULATIONS USING PENG-ROBINSON EQUATION OF STATE FOR ETHANE + N-PARAFFIN SYSTEMS (CASE 4)

ISO	CN	T(K)	C(I,J)	D(I,J)	RMSE	RMSPE	BIAS	AAD	%AAD	NPT
1	4	338.7	0.0250	0.0000	1.05	0.0209	-0.75	0.88	1.8	6
2	4	366.5	0.0378	0.0000	0.90	0.0192	-0.29	0.71	1.5	8
3	4	394.3	-0.0018	0.0000	0.70	0.0194	-0.52	0.52	1.4	5
4	5	310.9	0.0055	0.0000	0.26	0.0077	-0.03	0.16	0.6	12
5	5	377.6	0.0102	0.0000	0.60	0.0105	-0.18	0.31	0.7	13
6	5	444.3	0.0223	0.0000	0.39	0.0110	-0.29	0.32	0.9	6
7	6	310.9	0.0031	0.0000	0.04	0.0025	0.00	0.03	0.2	15
8	6	338.7	-0.0012	0.0000	0.13	0.0076	-0.08	0.11	0.6	11
9	6	366.5	-0.0015	0.0000	0.08	0.0043	-0.02	0.07	0.3	11
10	6	394.3	0.0035	0.0000	0.32	0.0081	-0.11	0.22	0.7	11
11	7	338.7	-0.0109	0.0000	0.00	0.0001	0.00	0.00	0.0	1
12	7	394.3	-0.0171	0.0000	0.00	0.0001	0.00	0.00	0.0	1
13	7	449.8	0.0426	0.0000	0.00	0.0001	0.00	0.00	0.0	1
14	8	323.1	0.0137	0.0000	0.44	0.0134	-0.26	0.40	1.3	11
15	8	348.1	0.0211	0.0000	0.34	0.0234	0.10	0.29	1.7	13
16	8	373.1	0.0199	0.0000	0.33	0.0194	0.06	0.28	1.7	9
17	10	310.9	0.0064	0.0000	0.20	0.0106	-0.06	0.15	1.0	10
18	10	344.3	0.0020	0.0000	0.48	0.0152	-0.24	0.35	1.3	7
19	10	377.6	-0.0025	0.0000	0.75	0.0175	-0.37	0.51	1.5	6
20	10	410.9	-0.0043	0.0000	1.60	0.0275	-0.84	1.19	2.5	7
21	12	373.1	-0.0045	0.0000	0.87	0.0239	-0.36	0.65	2.0	9
22	20	323.1	-0.0224	0.0000	2.30	0.0866	-1.10	1.56	7.4	6
23	20	373.1	-0.0144	0.0000	3.20	0.0729	-1.60	2.48	6.4	6
24	20	423.1	-0.0305	0.0000	3.72	0.0744	-1.79	2.70	6.3	7
25	28	348.1	-0.0424	0.0000	1.48	0.0707	-0.62	1.11	6.1	10
26	28	373.1	-0.0439	0.0000	2.02	0.0722	-0.96	1.56	6.9	7
27	28	423.1	-0.0552	0.0000	2.53	0.0688	-1.10	1.75	5.9	7
28	36	373.1	-0.0634	0.0000	2.18	0.0872	-0.97	1.42	7.5	7
29	36	423.1	-0.0458	0.0000	2.80	0.0831	-1.26	2.22	7.7	6
30	44	373.1	-0.0923	0.0000	2.60	0.1222	-1.29	1.86	10.5	9
31	44	423.1	-0.0706	0.0000	1.36	0.0624	-0.63	0.99	5.4	7

MODEL OVERALL STATISTICS

RMSE	= 1.4246 BAR	NO PT	= 245
AAD	= 0.7447 BAR	%AAD	= 2.846
MIN DEV=	-8.0781 BAR	MIN %DEV	= -16.314
MAX DEV=	1.3728 BAR	MAX %DEV	= 18.781
BIAS	= -0.4505 BAR	C-VAR	= 0.078
RESTRICTIONS	: NONE	R-SQR	=0.880946

TABLE G.V

BUBBLE-POINT CALCULATIONS USING PENG-ROBINSON EQUATION OF STATE FOR ETHANE + N-PARAFFIN SYSTEMS (CASE 5)

ISO	CN	T(K)	C(I,J)	D(I,J)	RMSE	RMSPE	BIAS	AAD	%AAD	NPT
1	4	338.7	0.0069	0.0440	0.84	0.0183	-0.44	0.66	1.5	6
2	4	366.5	-0.0051	0.0631	0.88	0.0198	-0.42	0.70	1.6	8
3	4	394.3	-0.0749	0.1262	0.30	0.0085	-0.09	0.25	0.7	5
4	5	310.9	0.0009	0.0055	0.26	0.0065	-0.08	0.13	0.4	12
5	5	377.6	0.0227	-0.0165	0.36	0.0075	-0.05	0.23	0.6	13
6	5	444.3	-0.0595	0.1074	0.22	0.0068	-0.06	0.19	0.6	6
7	6	310.9	0.0035	-0.0004	0.04	0.0024	0.00	0.03	0.2	15
8	6	338.7	0.0052	-0.0070	0.07	0.0040	0.01	0.05	0.3	11
9	6	366.5	0.0030	-0.0047	0.05	0.0034	0.00	0.03	0.2	11
10	6	394.3	0.0160	-0.0148	0.08	0.0025	-0.01	0.06	0.2	11
11	7	338.7	-0.0054	-0.0100	0.01	0.0002	0.01	0.01	0.0	1
12	7	394.3	-0.0085	-0.0130	0.00	0.0001	0.00	0.00	0.0	1
13	7	449.8	0.0216	0.0315	0.00	0.0000	0.00	0.00	0.0	1
14	8	323.1	0.0224	-0.0114	0.10	0.0034	0.01	0.09	0.3	11
15	8	348.1	0.0158	0.0054	0.36	0.0219	-0.05	0.32	1.7	13
16	8	373.1	0.0143	0.0047	0.24	0.0189	0.01	0.22	1.5	9
17	10	310.9	0.0099	-0.0027	0.12	0.0091	-0.02	0.10	0.8	10
18	10	344.3	0.0098	-0.0068	0.12	0.0070	-0.01	0.11	0.6	7
19	10	377.6	0.0098	-0.0107	0.12	0.0032	-0.01	0.09	0.3	6
20	10	410.9	0.0153	-0.0192	0.15	0.0043	-0.02	0.13	0.4	7
21	12	373.1	0.0153	-0.0152	0.12	0.0054	0.00	0.09	0.4	9
22	20	323.1	0.0228	-0.0217	0.16	0.0074	-0.01	0.13	0.7	6
23	20	373.1	0.0211	-0.0222	0.37	0.0090	-0.04	0.32	0.9	6
24	20	423.1	0.0279	-0.0310	0.31	0.0056	-0.01	0.23	0.5	7
25	28	348.1	0.0176	-0.0198	0.18	0.0107	-0.01	0.14	0.9	10
26	28	373.1	0.0122	-0.0171	0.24	0.0136	-0.02	0.20	1.2	7
27	28	423.1	0.0225	-0.0238	0.23	0.0079	-0.01	0.18	0.7	7
28	36	373.1	0.0225	-0.0186	0.11	0.0078	-0.01	0.09	0.6	7
29	36	423.1	0.0534	-0.0245	0.32	0.0123	-0.02	0.29	1.1	6
30	44	373.1	0.0429	-0.0242	0.19	0.0123	-0.01	0.15	1.0	9
31	44	423.1	0.0309	-0.0164	0.17	0.0090	0.00	0.15	0.9	7

MODEL OVERALL STATISTICS

RMSE	= 0.2916 BAR	NO PT	= 245
AAD	= 0.1748 BAR	%AAD	= 0.694
MIN DEV=	-1.8173 BAR	MIN %DEV	= -3.815
MAX DEV=	1.0377 BAR	MAX %DEV	= 5.638
BIAS	= -0.0412 BAR	C-VAR	= 0.016
RESTRICTIONS	: NONE	R-SQR	=0.988438

TABLE G.VI

BUBBLE-POINT CALCULATIONS USING SPHCT EQUATION OF STATE
FOR ETHANE + N-PARAFFIN SYSTEMS (CASE 1)

ISO	CN	T(K)	C(I,J)	D(I,J)	RMSE	RMSPE	BIAS	AAD	%AAD	NPT
1	4	366.5	0.0000	0.0000	4.43	0.1081	-3.69	3.69	9.0	8
2	4	338.7	0.0000	0.0000	3.54	0.0875	-2.91	2.91	7.1	6
3	4	394.3	0.0000	0.0000	2.61	0.0755	-1.84	1.84	5.2	5
4	5	310.9	0.0000	0.0000	1.58	0.0602	-1.27	1.27	5.7	12
5	5	377.6	0.0000	0.0000	4.69	0.1092	-3.63	3.63	10.3	13
6	5	444.3	0.0000	0.0000	2.89	0.0947	-2.41	2.41	8.0	6
7	6	310.9	0.0000	0.0000	0.99	0.0592	-0.91	0.91	5.9	15
8	6	338.7	0.0000	0.0000	1.73	0.0720	-1.52	1.52	7.2	11
9	6	366.5	0.0000	0.0000	1.99	0.0900	-1.81	1.81	9.0	11
10	6	394.3	0.0000	0.0000	3.95	0.1130	-3.54	3.54	11.2	11
11	7	338.7	0.0000	0.0000	1.30	0.0415	-1.30	1.30	4.1	1
12	7	394.3	0.0000	0.0000	3.06	0.0769	-3.06	3.06	7.7	1
13	7	449.8	0.0000	0.0000	9.23	0.1868	-9.23	9.23	18.7	1
14	8	323.1	0.0000	0.0000	3.39	0.1056	-3.25	3.25	10.5	11
15	8	348.1	0.0000	0.0000	4.43	0.1655	-4.10	4.10	16.1	13
16	8	373.1	0.0000	0.0000	3.91	0.1861	-3.59	3.59	18.5	9
17	10	310.9	0.0000	0.0000	1.54	0.1213	-1.47	1.47	11.8	10
18	10	344.3	0.0000	0.0000	2.97	0.1151	-2.75	2.75	11.3	7
19	10	377.6	0.0000	0.0000	4.35	0.1279	-3.94	3.94	12.7	6
20	10	410.9	0.0000	0.0000	6.85	0.1359	-6.14	6.14	13.6	7
21	12	373.1	0.0000	0.0000	4.39	0.1406	-4.11	4.11	14.0	9
22	20	323.1	0.0000	0.0000	2.85	0.1471	-2.54	2.54	14.6	6
23	20	373.1	0.0000	0.0000	6.21	0.1558	-5.75	5.75	15.4	6
24	20	423.1	0.0000	0.0000	7.93	0.1677	-7.13	7.13	16.8	7
25	28	348.1	0.0000	0.0000	3.98	0.2092	-3.70	3.70	20.9	10
26	28	373.1	0.0000	0.0000	4.87	0.2181	-4.31	4.31	21.7	7
27	28	423.1	0.0000	0.0000	6.07	0.2042	-5.42	5.42	20.4	7
28	36	373.1	0.0000	0.0000	4.98	0.2596	-4.39	4.39	25.9	7
29	36	423.1	0.0000	0.0000	7.80	0.2508	-7.02	7.02	25.1	6
30	44	373.1	0.0000	0.0000	5.10	0.2563	-4.46	4.46	25.6	9
31	44	423.1	0.0000	0.0000	5.42	0.2764	-4.86	4.86	27.6	7

MODEL OVERALL STATISTICS

RMSE	= 4.2817 BAR	NO PT	= 245
AAD	= 3.4550 BAR	%AAD	= 13.682
MIN DEV=	-12.3584 BAR	MIN %DEV	= -30.459
MAX DEV=	0.0000 BAR	MAX %DEV	= 0.000
BIAS	= -3.4550 BAR	C-VAR	= 0.158
RESTRICTIONS	: NONE	R-SQR	=0.859661

TABLE G.VII

BUBBLE-POINT CALCULATIONS USING SPHCT EQUATION OF STATE
FOR ETHANE + N-PARAFFIN SYSTEMS (CASE 2)

ISO	CN	T(K)	C(I,J)	D(I,J)	RMSE	RMSPE	BIAS	AAD	%AAD	NPT
1	4	366.5	0.0254	0.0000	3.29	0.0757	-3.02	3.02	7.0	8
2	4	338.7	0.0254	0.0000	2.79	0.0630	-2.26	2.26	5.2	6
3	4	394.3	0.0254	0.0000	2.75	0.0714	-2.29	2.29	5.9	5
4	5	310.9	0.0254	0.0000	1.21	0.0647	0.10	0.94	5.5	12
5	5	377.6	0.0254	0.0000	2.23	0.0432	-1.47	1.47	3.5	13
6	5	444.3	0.0254	0.0000	2.47	0.0812	-2.23	2.23	7.2	6
7	6	310.9	0.0254	0.0000	1.13	0.0961	1.09	1.09	8.7	15
8	6	338.7	0.0254	0.0000	0.87	0.0666	0.81	0.81	5.7	11
9	6	366.5	0.0254	0.0000	0.44	0.0300	0.41	0.41	2.6	11
10	6	394.3	0.0254	0.0000	1.47	0.0337	-1.09	1.09	2.8	11
11	7	338.7	0.0254	0.0000	2.28	0.0727	2.28	2.28	7.3	1
12	7	394.3	0.0254	0.0000	0.77	0.0194	0.77	0.77	1.9	1
13	7	449.8	0.0254	0.0000	6.26	0.1266	-6.26	6.26	12.7	1
14	8	323.1	0.0254	0.0000	1.59	0.0439	-0.43	1.22	3.8	11
15	8	348.1	0.0254	0.0000	1.12	0.0406	-0.86	0.88	3.4	13
16	8	373.1	0.0254	0.0000	1.11	0.0582	-1.03	1.03	5.5	9
17	10	310.9	0.0254	0.0000	1.36	0.0859	1.22	1.22	8.5	10
18	10	344.3	0.0254	0.0000	1.30	0.0490	1.20	1.20	4.8	7
19	10	377.6	0.0254	0.0000	0.36	0.0142	0.28	0.30	1.2	6
20	10	410.9	0.0254	0.0000	1.95	0.0285	-1.49	1.49	2.6	7
21	12	373.1	0.0254	0.0000	0.55	0.0180	0.50	0.50	1.7	9
22	20	323.1	0.0254	0.0000	1.69	0.0779	1.42	1.42	7.7	6
23	20	373.1	0.0254	0.0000	1.87	0.0318	1.38	1.40	2.7	6
24	20	423.1	0.0254	0.0000	1.21	0.0262	-1.10	1.10	2.6	7
25	28	348.1	0.0254	0.0000	0.26	0.0177	-0.12	0.21	1.4	10
26	28	373.1	0.0254	0.0000	0.56	0.0487	-0.55	0.55	4.1	7
27	28	423.1	0.0254	0.0000	1.56	0.0614	-1.46	1.46	6.0	7
28	36	373.1	0.0254	0.0000	1.54	0.0924	-1.41	1.41	9.1	7
29	36	423.1	0.0254	0.0000	3.42	0.1138	-3.11	3.11	11.3	6
30	44	373.1	0.0254	0.0000	1.82	0.0877	-1.57	1.57	8.6	9
31	44	423.1	0.0254	0.0000	2.62	0.1444	-2.40	2.40	14.3	7

MODEL OVERALL STATISTICS

RMSE	= 1.7348 BAR	NO PT	= 245
AAD	= 1.2885 BAR	%AAD	= 5.366
MIN DEV=	-6.2594 BAR	MIN %DEV	= -17.673
MAX DEV=	3.5472 BAR	MAX %DEV	= 14.033
BIAS	= -0.5740 BAR	C-VAR	= 0.064
RESTRICTIONS	: NONE	R-SQR	=0.926618

TABLE G.VIII

BUBBLE-POINT CALCULATIONS USING SPHCT EQUATION OF STATE
FOR ETHANE + N-PARAFFIN SYSTEMS (CASE 3)

ISO	CN	T(K)	C(I,J)	D(I,J)	RMSE	RMSPE	BIAS	AAD	%AAD	NPT
1	4	366.5	0.0601	0.0000	1.65	0.0326	-0.93	1.25	2.6	8
2	4	338.7	0.0601	0.0000	1.72	0.0365	-0.74	1.46	3.2	6
3	4	394.3	0.0601	0.0000	2.07	0.0458	-1.94	1.94	4.5	5
4	5	310.9	0.0205	0.0000	1.14	0.0468	-0.18	0.77	4.0	12
5	5	377.6	0.0205	0.0000	2.56	0.0536	-1.84	1.84	4.8	13
6	5	444.3	0.0205	0.0000	2.53	0.0834	-2.21	2.21	7.2	6
7	6	310.9	0.0153	0.0000	0.35	0.0332	0.26	0.32	2.8	15
8	6	338.7	0.0153	0.0000	0.45	0.0227	-0.16	0.34	1.9	11
9	6	366.5	0.0153	0.0000	0.65	0.0244	-0.51	0.51	2.2	11
10	6	394.3	0.0153	0.0000	2.46	0.0647	-2.10	2.10	6.3	11
11	7	338.7	0.0229	0.0000	1.90	0.0607	1.90	1.90	6.1	1
12	7	394.3	0.0229	0.0000	0.37	0.0094	0.37	0.37	0.9	1
13	7	449.8	0.0229	0.0000	6.56	0.1328	-6.56	6.56	13.3	1
14	8	323.1	0.0290	0.0000	1.65	0.0567	0.00	1.39	4.9	11
15	8	348.1	0.0290	0.0000	0.74	0.0277	-0.36	0.54	2.3	13
16	8	373.1	0.0290	0.0000	0.69	0.0395	-0.64	0.64	3.5	9
17	10	310.9	0.0190	0.0000	0.58	0.0331	0.49	0.49	3.1	10
18	10	344.3	0.0190	0.0000	0.20	0.0094	0.12	0.15	0.8	7
19	10	377.6	0.0190	0.0000	1.03	0.0258	-0.86	0.86	2.6	6
20	10	410.9	0.0190	0.0000	3.24	0.0556	-2.73	2.73	5.5	7
21	12	373.1	0.0229	0.0000	0.11	0.0054	0.00	0.09	0.4	9
22	20	323.1	0.0216	0.0000	0.92	0.0406	0.75	0.75	4.0	6
23	20	373.1	0.0216	0.0000	0.70	0.0201	0.17	0.57	1.7	6
24	20	423.1	0.0216	0.0000	2.31	0.0491	-2.09	2.09	4.9	7
25	28	348.1	0.0292	0.0000	0.67	0.0274	0.50	0.50	2.4	10
26	28	373.1	0.0292	0.0000	0.45	0.0296	0.10	0.37	2.4	7
27	28	423.1	0.0292	0.0000	0.83	0.0385	-0.79	0.79	3.6	7
28	36	373.1	0.0391	0.0000	0.95	0.0275	0.51	0.52	1.9	7
29	36	423.1	0.0391	0.0000	0.67	0.0301	-0.65	0.65	2.8	6
30	44	373.1	0.0401	0.0000	0.55	0.0348	0.45	0.45	3.1	9
31	44	423.1	0.0401	0.0000	0.78	0.0592	-0.76	0.76	5.4	7

MODEL OVERALL STATISTICS

RMSE	= 1.4549 BAR	NO PT	= 245
AAD	= 0.9499 BAR	%AAD	= 3.384
MIN DEV=	-6.5645 BAR	MIN %DEV	= -13.279
MAX DEV=	2.4000 BAR	MAX %DEV	= 9.231
BIAS	= -0.5358 BAR	C-VAR	= 0.080
RESTRICTIONS	: NONE	R-SQR	=0.941131

TABLE G.IX

BUBBLE-POINT CALCULATIONS USING SPHCT EQUATION OF STATE
FOR ETHANE + N-PARAFFIN SYSTEMS (CASE 4)

ISO	CN	T(K)	C(I,J)	D(I,J)	RMSE	RMSPE	BIAS	AAD	%AAD	NPT
1	4	338.7	0.0546	0.0000	1.47	0.0314	-0.82	1.20	2.6	6
2	4	366.5	0.0653	0.0000	1.45	0.0304	-0.43	1.19	2.6	8
3	4	394.3	0.0874	0.0000	0.41	0.0096	-0.06	0.34	0.8	5
4	5	310.9	0.0126	0.0000	1.19	0.0320	-0.61	0.67	2.2	12
5	5	377.6	0.0352	0.0000	1.69	0.0305	-0.71	0.93	2.1	13
6	5	444.3	0.1287	0.0000	0.73	0.0290	-0.21	0.52	1.9	6
7	6	310.9	0.0102	0.0000	0.29	0.0121	-0.15	0.20	1.0	15
8	6	338.7	0.0138	0.0000	0.54	0.0212	-0.30	0.40	1.9	11
9	6	366.5	0.0198	0.0000	0.30	0.0124	-0.11	0.23	1.1	11
10	6	394.3	0.0327	0.0000	0.86	0.0210	-0.33	0.59	1.8	11
11	7	338.7	0.0097	0.0000	0.01	0.0002	0.01	0.01	0.0	1
12	7	394.3	0.0205	0.0000	0.00	0.0001	0.00	0.00	0.0	1
13	7	449.8	0.0719	0.0000	0.00	0.0001	0.00	0.00	0.0	1
14	8	323.1	0.0209	0.0000	1.70	0.0370	-0.97	1.21	3.1	11
15	8	348.1	0.0308	0.0000	0.63	0.0255	-0.10	0.50	2.1	13
16	8	373.1	0.0350	0.0000	0.29	0.0185	0.05	0.25	1.6	9
17	10	310.9	0.0157	0.0000	0.22	0.0176	0.12	0.18	1.4	10
18	10	344.3	0.0184	0.0000	0.15	0.0086	0.02	0.12	0.7	7
19	10	377.6	0.0233	0.0000	0.31	0.0062	-0.10	0.22	0.5	6
20	10	410.9	0.0302	0.0000	1.06	0.0166	-0.51	0.75	1.4	7
21	12	373.1	0.0229	0.0000	0.11	0.0054	0.00	0.09	0.4	9
22	20	323.1	0.0174	0.0000	0.18	0.0081	0.04	0.12	0.7	6
23	20	373.1	0.0222	0.0000	0.84	0.0195	0.35	0.65	1.7	6
24	20	423.1	0.0295	0.0000	0.15	0.0052	0.00	0.14	0.4	7
25	28	348.1	0.0266	0.0000	0.29	0.0141	0.07	0.22	1.2	10
26	28	373.1	0.0304	0.0000	0.64	0.0279	0.31	0.49	2.4	7
27	28	423.1	0.0347	0.0000	0.51	0.0140	0.20	0.34	1.2	7
28	36	373.1	0.0369	0.0000	0.64	0.0206	0.19	0.34	1.6	7
29	36	423.1	0.0432	0.0000	0.30	0.0125	0.14	0.25	1.0	6
30	44	373.1	0.0364	0.0000	0.26	0.0158	-0.09	0.23	1.5	9
31	44	423.1	0.0482	0.0000	0.52	0.0263	0.23	0.42	2.4	7

MODEL OVERALL STATISTICS

RMSE	= 0.8195 BAR	NO PT	= 245
AAD	= 0.4597 BAR	%AAD	= 1.581
MIN DEV=	-4.7500 BAR	MIN %DEV	= -8.384
MAX DEV=	1.7721 BAR	MAX %DEV	= 5.046
BIAS	= -0.1688 BAR	C-VAR	= 0.045
RESTRICTIONS	: NONE	R-SQR	=0.965414

TABLE G.X

BUBBLE-POINT CALCULATIONS USING SPHCT EQUATION OF STATE
FOR ETHANE + N-PARAFFIN SYSTEMS (CASE 5)

ISO	CN	T(K)	C(I,J)	D(I,J)	RMSE	RMSPE	BIAS	AAD	%AAD	NPT
1	4	338.7	0.0616	0.0042	1.40	0.0308	-0.63	1.15	2.6	6
2	4	366.5	0.0235	-0.0464	0.23	0.0057	0.00	0.19	0.5	8
3	4	394.3	0.0806	-0.0161	0.12	0.0033	0.00	0.12	0.3	5
4	5	310.9	0.0112	-0.0062	1.00	0.0264	-0.35	0.52	1.7	12
5	5	377.6	0.0317	-0.0146	0.68	0.0144	-0.11	0.43	1.2	13
6	5	444.3	0.1260	0.0165	0.75	0.0280	-0.21	0.61	2.1	6
7	6	310.9	0.0101	-0.0023	0.14	0.0064	-0.03	0.09	0.5	15
8	6	338.7	0.0136	-0.0052	0.10	0.0043	-0.01	0.07	0.4	11
9	6	366.5	0.0204	-0.0048	0.07	0.0038	-0.01	0.06	0.3	11
10	6	394.3	0.0318	-0.0086	0.21	0.0054	-0.02	0.14	0.4	11
11	7	338.7	0.0043	-0.0043	0.00	0.0000	0.00	0.00	0.0	1
12	7	394.3	0.0188	-0.0021	0.01	0.0002	-0.01	0.01	0.0	1
13	7	449.8	0.0715	-0.0011	0.01	0.0002	0.01	0.01	0.0	1
14	8	323.1	0.0179	-0.0060	1.10	0.0240	-0.38	0.69	1.9	11
15	8	348.1	0.0308	0.0002	0.66	0.0255	-0.12	0.51	2.1	13
16	8	373.1	0.0345	0.0007	0.23	0.0182	0.02	0.20	1.4	9
17	10	310.9	0.0143	0.0017	0.12	0.0087	-0.01	0.10	0.8	10
18	10	344.3	0.0183	0.0003	0.17	0.0080	-0.02	0.14	0.7	7
19	10	377.6	0.0235	-0.0005	0.19	0.0048	-0.03	0.15	0.4	6
20	10	410.9	0.0306	-0.0021	0.31	0.0064	-0.06	0.23	0.6	7
21	12	373.1	0.0229	0.0000	0.11	0.0054	0.00	0.09	0.4	9
22	20	323.1	0.0172	0.0001	0.14	0.0078	0.02	0.10	0.6	6
23	20	373.1	0.0213	0.0011	0.20	0.0039	0.02	0.14	0.3	6
24	20	423.1	0.0296	-0.0001	0.19	0.0051	0.01	0.16	0.4	7
25	28	348.1	0.0249	0.0005	0.18	0.0112	0.02	0.14	0.9	10
26	28	373.1	0.0255	0.0012	0.13	0.0062	0.01	0.11	0.5	7
27	28	423.1	0.0312	0.0008	0.11	0.0030	0.01	0.08	0.3	7
28	36	373.1	0.0330	0.0006	0.30	0.0108	0.00	0.21	0.9	7
29	36	423.1	0.0403	0.0005	0.13	0.0058	-0.04	0.11	0.5	6
30	44	373.1	0.0387	-0.0003	0.27	0.0122	0.02	0.18	1.0	9
31	44	423.1	0.0394	0.0010	0.08	0.0070	0.00	0.06	0.5	7

MODEL OVERALL STATISTICS

RMSE	= 0.4857 BAR	NO PT	= 245
AAD	= 0.2436 BAR	%AAD	= 0.889
MIN DEV=	-3.1509 BAR	MIN %DEV	= -7.617
MAX DEV=	1.1910 BAR	MAX %DEV	= 5.271
BIAS	= -0.0711 BAR	C-VAR	= 0.027
RESTRICTIONS	: NONE	R-SQR	=0.983889

TABLE G.XI

BUBBLE-POINT CALCULATIONS USING SPHCT EQUATION OF STATE
FOR ETHANE + N-PARAFFIN SYSTEMS (CASE 6)

ISO	CN	T(K)	C(I,J)	E(I,J)	RMSE	RMSPE	BIAS	AAD	%AAD	NPT
1	4	338.7	0.0484	0.0235	1.41	0.0309	-0.64	1.16	2.6	6
2	4	366.5	0.1742	-0.2405	0.24	0.0057	0.00	0.19	0.4	8
3	4	394.3	0.0875	-0.0006	0.41	0.0096	-0.08	0.34	0.8	5
4	5	310.9	0.0291	-0.0348	1.00	0.0265	-0.36	0.52	1.8	12
5	5	377.6	0.0767	-0.0733	0.71	0.0149	-0.12	0.44	1.2	13
6	5	444.3	0.0645	0.0902	0.75	0.0280	-0.20	0.61	2.1	6
7	6	310.9	0.0167	-0.0133	0.14	0.0064	-0.03	0.09	0.5	15
8	6	338.7	0.0286	-0.0279	0.10	0.0044	-0.01	0.07	0.4	11
9	6	366.5	0.0346	-0.0245	0.07	0.0038	0.00	0.06	0.3	11
10	6	394.3	0.0576	-0.0419	0.22	0.0055	-0.02	0.15	0.5	11
11	7	338.7	0.0159	-0.0211	0.00	0.0000	0.00	0.00	0.0	1
12	7	394.3	0.0251	-0.0106	0.00	0.0001	0.00	0.00	0.0	1
13	7	449.8	0.0749	-0.0053	0.00	0.0000	0.00	0.00	0.0	1
14	8	323.1	0.0350	-0.0353	1.11	0.0242	-0.37	0.70	1.9	11
15	8	348.1	0.0303	0.0009	0.65	0.0255	-0.12	0.51	2.1	13
16	8	373.1	0.0325	0.0036	0.23	0.0182	0.01	0.20	1.4	9
17	10	310.9	0.0095	0.0106	0.12	0.0088	-0.02	0.10	0.7	10
18	10	344.3	0.0173	0.0019	0.18	0.0080	-0.03	0.15	0.7	7
19	10	377.6	0.0249	-0.0026	0.20	0.0048	-0.02	0.15	0.4	6
20	10	410.9	0.0367	-0.0107	0.30	0.0065	-0.05	0.23	0.6	7
21	12	373.1	0.0229	0.0000	0.11	0.0054	0.00	0.09	0.4	9
22	20	323.1	0.0169	0.0008	0.14	0.0078	0.03	0.10	0.6	6
23	20	373.1	0.0183	0.0065	0.20	0.0039	0.02	0.14	0.3	6
24	20	423.1	0.0299	-0.0004	0.19	0.0051	0.04	0.16	0.4	7
25	28	348.1	0.0237	0.0029	0.18	0.0111	0.00	0.14	0.9	10
26	28	373.1	0.0224	0.0070	0.12	0.0060	-0.01	0.11	0.6	7
27	28	423.1	0.0291	0.0043	0.11	0.0030	0.00	0.08	0.3	7
28	36	373.1	0.0314	0.0038	0.30	0.0107	0.01	0.20	0.9	7
29	36	423.1	0.0389	0.0030	0.12	0.0055	-0.01	0.10	0.4	6
30	44	373.1	0.0396	-0.0020	0.27	0.0121	0.01	0.18	0.9	9
31	44	423.1	0.0368	0.0056	0.08	0.0070	-0.01	0.06	0.5	7

MODEL OVERALL STATISTICS

RMSE	= 0.4932 BAR	NO PT	= 245
AAD	= 0.2494 BAR	%AAD	= 0.903
MIN DEV=	-3.1671 BAR	MIN %DEV	= -7.656
MAX DEV=	1.1852 BAR	MAX %DEV	= 5.199
BIAS	= -0.0736 BAR	C-VAR	= 0.027
RESTRICTIONS	: NONE	R-SQR	=0.983058

TABLE G.XII

BUBBLE-POINT CALCULATIONS USING MODIFIED SPHCT EQUATION OF STATE FOR ETHANE + N-PARAFFIN SYSTEMS (CASE 1)

ISO	CN	T(K)	C(I,J)	D(I,J)	RMSE	RMSPE	BIAS	AAD	%AAD	NPT
1	4	366.5	0.0000	0.0000	2.98	0.0629	-2.82	2.82	6.1	8
2	4	338.7	0.0000	0.0000	2.55	0.0526	-2.43	2.43	5.2	6
3	4	394.3	0.0000	0.0000	1.42	0.0337	-1.22	1.22	2.9	5
4	5	310.9	0.0000	0.0000	0.81	0.0236	-0.29	0.44	1.8	12
5	5	377.6	0.0000	0.0000	0.91	0.0202	-0.60	0.64	1.8	13
6	5	444.3	0.0000	0.0000	1.47	0.0370	-0.96	1.04	2.8	6
7	6	310.9	0.0000	0.0000	0.29	0.0302	-0.11	0.26	2.4	15
8	6	338.7	0.0000	0.0000	0.25	0.0088	0.12	0.18	0.8	11
9	6	366.5	0.0000	0.0000	0.17	0.0065	0.11	0.14	0.6	11
10	6	394.3	0.0000	0.0000	0.20	0.0050	-0.15	0.15	0.4	11
11	7	338.7	0.0000	0.0000	1.53	0.0486	1.53	1.53	4.9	1
12	7	394.3	0.0000	0.0000	2.37	0.0595	2.37	2.37	6.0	1
13	7	449.8	0.0000	0.0000	3.12	0.0631	-3.12	3.12	6.3	1
14	8	323.1	0.0000	0.0000	1.20	0.0574	-0.88	1.10	4.7	11
15	8	348.1	0.0000	0.0000	1.69	0.1019	-1.60	1.60	8.5	13
16	8	373.1	0.0000	0.0000	1.64	0.0965	-1.56	1.56	9.1	9
17	10	310.9	0.0000	0.0000	1.66	0.1511	-1.62	1.62	14.1	10
18	10	344.3	0.0000	0.0000	1.04	0.0736	-0.81	0.94	5.8	7
19	10	377.6	0.0000	0.0000	0.95	0.0368	0.04	0.75	3.0	6
20	10	410.9	0.0000	0.0000	2.02	0.0283	1.40	1.44	2.4	7
21	12	373.1	0.0000	0.0000	1.20	0.0561	-1.11	1.11	4.9	9
22	20	323.1	0.0000	0.0000	3.84	0.2278	-3.58	3.58	22.3	6
23	20	373.1	0.0000	0.0000	2.44	0.0988	-2.27	2.27	8.3	6
24	20	423.1	0.0000	0.0000	1.40	0.0246	0.54	0.99	2.2	7
25	28	348.1	0.0000	0.0000	4.04	0.2251	-3.83	3.83	22.3	10
26	28	373.1	0.0000	0.0000	3.02	0.1656	-2.82	2.82	16.0	7
27	28	423.1	0.0000	0.0000	0.95	0.0333	0.17	0.70	2.9	7
28	36	373.1	0.0000	0.0000	2.58	0.1614	-2.40	2.40	15.8	7
29	36	423.1	0.0000	0.0000	1.27	0.0322	0.82	0.97	2.9	6
30	44	373.1	0.0000	0.0000	1.28	0.0748	-1.16	1.16	7.3	9
31	44	423.1	0.0000	0.0000	2.38	0.0883	1.82	1.82	7.8	7

MODEL OVERALL STATISTICS

RMSE	= 1.8222 BAR	NO PT	= 245
AAD	= 1.3232 BAR	%AAD	= 6.270
MIN DEV=	-5.6507 BAR	MIN %DEV	= -26.777
MAX DEV=	4.1967 BAR	MAX %DEV	= 13.239
BIAS	= -0.9151 BAR	C-VAR	= 0.067
RESTRICTIONS	: NONE	R-SQR	=0.969956

TABLE G.XIII

BUBBLE-POINT CALCULATIONS USING MODIFIED SPHCT EQUATION OF STATE FOR ETHANE + N-PARAFFIN SYSTEMS (CASE 2)

ISO	CN	T(K)	C(I,J)	D(I,J)	RMSE	RMSPE	BIAS	AAD	%AAD	NPT
1	4	366.5	0.0090	0.0000	2.17	0.0443	-1.94	1.94	4.1	8
2	4	338.7	0.0090	0.0000	1.96	0.0386	-1.72	1.72	3.5	6
3	4	394.3	0.0090	0.0000	2.00	0.0420	-1.65	1.66	3.6	5
4	5	310.9	0.0090	0.0000	0.98	0.0338	0.25	0.77	3.2	12
5	5	377.6	0.0090	0.0000	0.60	0.0197	0.18	0.49	1.8	13
6	5	444.3	0.0090	0.0000	1.32	0.0323	-0.86	0.96	2.5	6
7	6	310.9	0.0090	0.0000	0.77	0.0358	0.64	0.64	3.4	15
8	6	338.7	0.0090	0.0000	1.18	0.0521	1.05	1.05	5.2	11
9	6	366.5	0.0090	0.0000	1.10	0.0510	1.01	1.01	5.1	11
10	6	394.3	0.0090	0.0000	0.95	0.0323	0.90	0.90	3.2	11
11	7	338.7	0.0090	0.0000	2.99	0.0952	2.99	2.99	9.5	1
12	7	394.3	0.0090	0.0000	4.05	0.1018	4.05	4.05	10.2	1
13	7	449.8	0.0090	0.0000	1.80	0.0363	-1.80	1.80	3.6	1
14	8	323.1	0.0090	0.0000	0.69	0.0217	0.24	0.56	1.8	11
15	8	348.1	0.0090	0.0000	0.81	0.0616	-0.30	0.65	4.2	13
16	8	373.1	0.0090	0.0000	0.70	0.0506	-0.53	0.58	4.1	9
17	10	310.9	0.0090	0.0000	0.81	0.0922	-0.75	0.77	7.9	10
18	10	344.3	0.0090	0.0000	1.37	0.0432	0.70	1.04	3.9	7
19	10	377.6	0.0090	0.0000	2.47	0.0486	1.79	1.81	4.1	6
20	10	410.9	0.0090	0.0000	4.26	0.0700	3.54	3.54	6.8	7
21	12	373.1	0.0090	0.0000	1.29	0.0291	0.70	0.88	2.4	9
22	20	323.1	0.0090	0.0000	2.54	0.1667	-2.42	2.42	16.0	6
23	20	373.1	0.0090	0.0000	2.03	0.0597	0.43	1.67	5.1	6
24	20	423.1	0.0090	0.0000	4.18	0.0673	3.22	3.22	6.2	7
25	28	348.1	0.0090	0.0000	2.79	0.1630	-2.68	2.68	16.0	10
26	28	373.1	0.0090	0.0000	1.47	0.1072	-1.43	1.43	9.6	7
27	28	423.1	0.0090	0.0000	2.80	0.0640	2.00	2.00	5.4	7
28	36	373.1	0.0090	0.0000	1.30	0.0975	-1.17	1.17	9.0	7
29	36	423.1	0.0090	0.0000	3.56	0.0921	2.89	2.89	8.6	6
30	44	373.1	0.0090	0.0000	0.56	0.0195	0.24	0.33	1.4	9
31	44	423.1	0.0090	0.0000	4.11	0.1650	3.34	3.34	15.8	7

MODEL OVERALL STATISTICS

RMSE	= 1.9608 BAR	NO PT	= 245
AAD	= 1.3660 BAR	%AAD	= 5.533
MIN DEV=	-3.5876 BAR	MIN %DEV	= -20.584
MAX DEV=	8.1449 BAR	MAX %DEV	= 21.900
BIAS	= 0.2824 BAR	C-VAR	= 0.072
RESTRICTIONS	: NONE	R-SQR	=0.911284

TABLE G.XIV

BUBBLE-POINT CALCULATIONS USING MODIFIED SPHCT EQUATION OF STATE FOR ETHANE + N-PARAFFIN SYSTEMS (CASE 3)

ISO	CN	T(K)	C(I,J)	D(I,J)	RMSE	RMSPE	BIAS	AAD	%AAD	NPT
1	4	366.5	0.0087	0.0000	2.20	0.0449	-1.97	1.97	4.2	8
2	4	338.7	0.0087	0.0000	1.98	0.0390	-1.74	1.74	3.6	6
3	4	394.3	0.0087	0.0000	1.88	0.0399	-1.57	1.58	3.4	5
4	5	310.9	0.0038	0.0000	0.84	0.0207	-0.06	0.50	1.6	12
5	5	377.6	0.0038	0.0000	0.67	0.0147	-0.27	0.35	1.0	13
6	5	444.3	0.0038	0.0000	1.38	0.0345	-0.90	0.99	2.6	6
7	6	310.9	0.0015	0.0000	0.29	0.0238	0.01	0.26	2.0	15
8	6	338.7	0.0015	0.0000	0.38	0.0127	0.28	0.28	1.0	11
9	6	366.5	0.0015	0.0000	0.31	0.0126	0.26	0.26	1.2	11
10	6	394.3	0.0015	0.0000	0.10	0.0040	0.03	0.09	0.3	11
11	7	338.7	-0.0061	0.0000	0.58	0.0186	0.58	0.58	1.9	1
12	7	394.3	-0.0061	0.0000	1.28	0.0321	1.28	1.28	3.2	1
13	7	449.8	-0.0061	0.0000	3.99	0.0807	-3.99	3.99	8.1	1
14	8	323.1	0.0143	0.0000	1.10	0.0273	0.93	0.93	2.5	11
15	8	348.1	0.0143	0.0000	1.14	0.0476	0.52	0.96	3.9	13
16	8	373.1	0.0143	0.0000	0.67	0.0321	0.11	0.54	2.7	9
17	10	310.9	0.0104	0.0000	0.70	0.0832	-0.60	0.67	7.0	10
18	10	344.3	0.0104	0.0000	1.59	0.0441	0.94	1.18	3.9	7
19	10	377.6	0.0104	0.0000	2.77	0.0559	2.08	2.08	4.8	6
20	10	410.9	0.0104	0.0000	4.63	0.0776	3.89	3.89	7.6	7
21	12	373.1	0.0074	0.0000	1.02	0.0268	0.37	0.73	2.3	9
22	20	323.1	0.0132	0.0000	1.92	0.1369	-1.84	1.84	12.8	6
23	20	373.1	0.0132	0.0000	3.24	0.0615	1.79	2.35	5.4	6
24	20	423.1	0.0132	0.0000	5.67	0.0963	4.55	4.55	9.2	7
25	28	348.1	0.0189	0.0000	1.32	0.0901	-1.28	1.28	8.4	10
26	28	373.1	0.0189	0.0000	1.00	0.0565	0.25	0.85	5.0	7
27	28	423.1	0.0189	0.0000	5.29	0.1365	4.17	4.17	13.1	7
28	36	373.1	0.0095	0.0000	1.24	0.0939	-1.10	1.10	8.6	7
29	36	423.1	0.0095	0.0000	3.69	0.0961	3.01	3.01	9.1	6
30	44	373.1	0.0007	0.0000	1.17	0.0690	-1.06	1.06	6.7	9
31	44	423.1	0.0007	0.0000	2.51	0.0938	1.94	1.94	8.4	7

MODEL OVERALL STATISTICS

RMSE	= 2.0895 BAR	NO PT	= 245
AAD	= 1.2641 BAR	%AAD	= 4.541
MIN DEV=	-3.9885 BAR	MIN %DEV	= -17.511
MAX DEV=	10.6594 BAR	MAX %DEV	= 19.631
BIAS	= 0.3511 BAR	C-VAR	= 0.115
RESTRICTIONS	: NONE	R-SQR	=0.873662

TABLE G.XV

BUBBLE-POINT CALCULATIONS USING MODIFIED SPHCT EQUATION OF STATE FOR ETHANE + N-PARAFFIN SYSTEMS (CASE 4)

ISO	CN	T(K)	C(I,J)	D(I,J)	RMSE	RMSPE	BIAS	AAD	%AAD	NPT
1	4	366.5	0.0225	0.0000	1.17	0.0236	-0.60	0.88	1.8	8
2	4	338.7	0.0253	0.0000	1.32	0.0281	-0.42	1.17	2.5	6
3	4	394.3	0.0069	0.0000	1.70	0.0370	-1.43	1.43	3.2	5
4	5	310.9	0.0028	0.0000	0.82	0.0203	-0.12	0.47	1.6	12
5	5	377.6	0.0047	0.0000	0.63	0.0145	-0.20	0.33	1.0	13
6	5	444.3	0.0096	0.0000	1.33	0.0323	-0.87	0.97	2.5	6
7	6	310.9	0.0040	0.0000	0.39	0.0185	0.22	0.29	1.7	15
8	6	338.7	-0.0002	0.0000	0.24	0.0088	0.10	0.18	0.8	11
9	6	366.5	-0.0008	0.0000	0.11	0.0053	0.03	0.09	0.4	11
10	6	394.3	0.0009	0.0000	0.12	0.0034	-0.04	0.09	0.3	11
11	7	338.7	-0.0100	0.0000	0.00	0.0000	0.00	0.00	0.0	1
12	7	394.3	-0.0135	0.0000	0.01	0.0001	0.01	0.01	0.0	1
13	7	449.8	0.0206	0.0000	0.01	0.0001	-0.01	0.01	0.0	1
14	8	323.1	0.0107	0.0000	0.77	0.0197	0.46	0.60	1.7	11
15	8	348.1	0.0157	0.0000	1.32	0.0468	0.74	1.09	4.0	13
16	8	373.1	0.0156	0.0000	0.78	0.0311	0.27	0.60	2.7	9
17	10	310.9	0.0194	0.0000	0.79	0.0445	0.35	0.54	3.6	10
18	10	344.3	0.0091	0.0000	1.38	0.0432	0.71	1.05	3.9	7
19	10	377.6	0.0031	0.0000	1.34	0.0314	0.63	0.94	2.7	6
20	10	410.9	-0.0032	0.0000	1.36	0.0227	0.67	0.94	1.9	7
21	12	373.1	0.0074	0.0000	1.02	0.0268	0.37	0.73	2.3	9
22	20	323.1	0.0284	0.0000	1.45	0.0516	0.52	0.95	4.5	6
23	20	373.1	0.0107	0.0000	2.47	0.0581	0.97	1.94	5.2	6
24	20	423.1	-0.0001	0.0000	1.37	0.0246	0.51	0.98	2.2	7
25	28	348.1	0.0286	0.0000	0.80	0.0360	0.24	0.58	3.1	10
26	28	373.1	0.0208	0.0000	1.32	0.0544	0.59	1.01	4.9	7
27	28	423.1	0.0013	0.0000	1.15	0.0319	0.43	0.77	2.7	7
28	36	373.1	0.0195	0.0000	1.28	0.0439	0.40	0.71	3.5	7
29	36	423.1	-0.0021	0.0000	0.82	0.0278	0.36	0.63	2.3	6
30	44	373.1	0.0081	0.0000	0.46	0.0178	0.09	0.29	1.4	9
31	44	423.1	-0.0096	0.0000	0.78	0.0382	0.34	0.61	3.5	7

MODEL OVERALL STATISTICS

RMSE	= 1.0349 BAR	NO PT	= 245
AAD	= 0.6565 BAR	%AAD	= 2.349
MIN DEV=	-2.7695 BAR	MIN %DEV	= -10.078
MAX DEV=	5.0862 BAR	MAX %DEV	= 9.034
BIAS	= 0.1962 BAR	C-VAR	= 0.057
RESTRICTIONS	: NONE	R-SQR	=0.921248

TABLE G.XVI

BUBBLE-POINT CALCULATIONS USING MODIFIED SPHCT EQUATION OF STATE FOR ETHANE + N-PARAFFIN SYSTEMS (CASE 5)

ISO	CN	T(K)	C(I,J)	D(I,J)	RMSE	RMSPE	BIAS	AAD	%AAD	NPT
1	4	366.5	-0.0042	-0.0347	0.24	0.0059	0.00	0.20	0.5	8
2	4	338.7	-0.0354	-0.0454	0.09	0.0022	-0.01	0.08	0.2	6
3	4	394.3	0.0093	-0.0451	0.20	0.0057	0.00	0.17	0.5	5
4	5	310.9	0.0037	0.0037	0.82	0.0176	-0.28	0.36	0.9	12
5	5	377.6	0.0025	-0.0057	0.33	0.0107	-0.02	0.24	0.8	13
6	5	444.3	0.0279	0.0316	0.98	0.0252	-0.28	0.73	2.0	6
7	6	310.9	0.0044	0.0044	0.08	0.0039	0.01	0.05	0.3	15
8	6	338.7	0.0001	0.0020	0.10	0.0049	0.02	0.07	0.4	11
9	6	366.5	-0.0008	0.0018	0.05	0.0035	0.00	0.04	0.2	11
10	6	394.3	0.0007	-0.0012	0.07	0.0022	0.00	0.05	0.2	11
11	7	338.7	-0.0016	0.0078	0.00	0.0001	0.00	0.00	0.0	1
12	7	394.3	0.0001	0.0190	0.00	0.0000	0.00	0.00	0.0	1
13	7	449.8	0.0189	-0.0040	0.00	0.0001	0.00	0.00	0.0	1
14	8	323.1	0.0130	0.0043	0.27	0.0061	0.08	0.19	0.5	11
15	8	348.1	0.0153	0.0068	0.26	0.0209	-0.03	0.23	1.4	13
16	8	373.1	0.0124	0.0056	0.27	0.0200	0.01	0.25	1.6	9
17	10	310.9	0.0158	0.0056	0.08	0.0062	0.00	0.07	0.5	10
18	10	344.3	0.0078	0.0052	0.23	0.0077	0.03	0.18	0.7	7
19	10	377.6	0.0017	0.0045	0.23	0.0047	0.03	0.15	0.4	6
20	10	410.9	-0.0034	0.0036	0.28	0.0045	0.03	0.21	0.4	7
21	12	373.1	0.0051	0.0039	0.18	0.0070	0.00	0.14	0.5	9
22	20	323.1	0.0239	0.0028	0.39	0.0179	0.04	0.29	1.6	6
23	20	373.1	0.0081	0.0039	0.55	0.0114	0.05	0.39	1.0	6
24	20	423.1	-0.0030	0.0020	0.41	0.0096	0.04	0.34	0.9	7
25	28	348.1	0.0223	0.0020	0.25	0.0138	0.01	0.19	1.1	10
26	28	373.1	0.0114	0.0027	0.14	0.0051	0.03	0.11	0.5	7
27	28	423.1	-0.0062	0.0021	0.20	0.0057	0.04	0.13	0.5	7
28	36	373.1	0.0113	0.0016	0.45	0.0159	0.02	0.30	1.4	7
29	36	423.1	-0.0084	0.0015	0.11	0.0042	0.01	0.10	0.4	6
30	44	373.1	0.0063	0.0003	0.34	0.0150	-0.01	0.24	1.2	9
31	44	423.1	-0.0202	0.0016	0.09	0.0076	0.01	0.07	0.5	7

MODEL OVERALL STATISTICS

RMSE	= 0.3366 BAR	NO PT	= 245
AAD	= 0.1862 BAR	%AAD	= 0.735
MIN DEV=	-2.6738 BAR	MIN %DEV	= -5.540
MAX DEV=	1.1621 BAR	MAX %DEV	= 5.902
BIAS	= -0.0095 BAR	C-VAR	= 0.018
RESTRICTIONS	: NONE	R-SQR	=0.995996

TABLE G.XVII

BUBBLE-POINT CALCULATIONS USING MODIFIED SPHCT EQUATION OF STATE FOR ETHANE + N-PARAFFIN SYSTEMS (CASE 6)

ISO	CN	T(K)	C(I,J)	E(I,J)	RMSE	RMSPE	BIAS	AAD	%AAD	NPT
1	4	366.5	0.0940	-0.2020	0.24	0.0058	0.00	0.20	0.5	8
2	4	338.7	0.0935	-0.2827	0.12	0.0027	-0.01	0.10	0.2	6
3	4	394.3	-0.0398	-0.4455	0.15	0.0040	-0.14	0.14	0.4	5
4	5	310.9	-0.0061	0.0254	0.82	0.0175	-0.27	0.36	0.9	12
5	5	377.6	0.0176	-0.0313	0.34	0.0108	-0.02	0.24	0.9	13
6	5	444.3	-0.1994	0.3785	0.47	0.0146	-0.12	0.42	1.3	6
7	6	310.9	-0.0072	0.0311	0.07	0.0038	0.01	0.05	0.3	15
8	6	338.7	-0.0051	0.0125	0.10	0.0049	0.01	0.07	0.4	11
9	6	366.5	-0.0054	0.0103	0.05	0.0035	0.00	0.03	0.2	11
10	6	394.3	0.0037	-0.0063	0.07	0.0023	-0.01	0.05	0.2	11
11	7	338.7	-0.0002	-0.0423	0.01	0.0002	0.01	0.01	0.0	1
12	7	394.3	0.0043	-0.0536	0.01	0.0002	0.01	0.01	0.0	1
13	7	449.8	0.0258	-0.0121	0.01	0.0001	0.01	0.01	0.0	1
14	8	323.1	0.0021	0.0302	0.27	0.0061	0.08	0.19	0.5	11
15	8	348.1	-0.0016	0.0437	0.26	0.0209	-0.02	0.23	1.4	13
16	8	373.1	-0.0015	0.0333	0.27	0.0199	0.01	0.24	1.6	9
17	10	310.9	0.0010	0.0458	0.07	0.0064	0.00	0.07	0.6	10
18	10	344.3	-0.0053	0.0361	0.21	0.0075	0.02	0.17	0.6	7
19	10	377.6	-0.0093	0.0275	0.22	0.0046	0.02	0.15	0.4	6
20	10	410.9	-0.0120	0.0198	0.28	0.0046	0.03	0.22	0.4	7
21	12	373.1	-0.0044	0.0253	0.18	0.0069	0.01	0.14	0.5	9
22	20	323.1	0.0163	0.0262	0.36	0.0167	0.04	0.27	1.5	6
23	20	373.1	-0.0016	0.0289	0.51	0.0108	0.03	0.36	0.9	6
24	20	423.1	-0.0075	0.0122	0.42	0.0095	0.05	0.34	0.9	7
25	28	348.1	0.0165	0.0186	0.24	0.0135	0.00	0.19	1.1	10
26	28	373.1	0.0042	0.0218	0.14	0.0047	-0.01	0.10	0.4	7
27	28	423.1	-0.0113	0.0140	0.20	0.0054	0.00	0.14	0.5	7
28	36	373.1	0.0065	0.0145	0.43	0.0156	0.02	0.29	1.4	7
29	36	423.1	-0.0122	0.0108	0.10	0.0041	0.01	0.10	0.4	6
30	44	373.1	0.0052	0.0032	0.34	0.0148	0.01	0.24	1.3	9
31	44	423.1	-0.0248	0.0124	0.09	0.0075	0.00	0.07	0.5	7

MODEL OVERALL STATISTICS

RMSE	= 0.3045 BAR	NO PT	= 245
AAD	= 0.1763 BAR	%AAD	= 0.708
MIN DEV=	-2.6684 BAR	MIN %DEV	= -5.529
MAX DEV=	1.0511 BAR	MAX %DEV	= 5.879
BIAS	= -0.0107 BAR	C-VAR	= 0.017
RESTRICTIONS	: NONE	R-SQR	=0.995549

TABLE G.XVIII

BUBBLE-POINT CALCULATIONS USING PENG-ROBINSON EQUATION OF STATE FOR CARBON DIOXIDE + N-PARAFFIN SYSTEMS (CASE 1)

ISO	CN	T(K)	C(I,J)	D(I,J)	RMSE	RMSPE	BIAS	AAD	%AAD	NPT
1	4	310.9	0.0000	0.0000	6.93	0.2650	-5.84	5.84	24.2	18
2	4	344.3	0.0000	0.0000	4.72	0.1643	-3.22	3.22	12.4	17
3	4	377.6	0.0000	0.0000	2.44	0.0803	-1.54	1.54	5.2	12
4	4	410.9	0.0000	0.0000	0.64	0.0186	-0.35	0.35	1.0	5
5	5	311.0	0.0000	0.0000	7.39	0.2683	-6.59	6.59	22.6	14
6	5	344.1	0.0000	0.0000	6.92	0.2208	-4.76	4.76	18.2	15
7	5	377.6	0.0000	0.0000	5.45	0.1709	-4.14	4.14	13.7	9
8	6	313.1	0.0000	0.0000	10.81	0.2700	-10.19	10.19	23.6	8
9	6	353.1	0.0000	0.0000	10.82	0.2566	-8.40	8.40	20.9	14
10	6	393.1	0.0000	0.0000	8.59	0.1851	-6.69	6.69	14.8	15
11	7	310.6	0.0000	0.0000	8.35	0.2709	-7.10	7.10	23.1	23
12	7	352.6	0.0000	0.0000	10.78	0.2282	-8.55	8.55	19.5	17
13	7	394.3	0.0000	0.0000	13.44	0.1749	-12.16	12.16	16.9	16
14	7	477.2	0.0000	0.0000	7.41	0.0977	-6.51	6.51	9.4	7
15	10	310.9	0.0000	0.0000	14.61	0.3874	-13.21	13.21	37.0	11
16	10	344.3	0.0000	0.0000	16.06	0.3074	-13.05	13.05	26.9	8
17	10	377.6	0.0000	0.0000	16.06	0.2494	-12.95	12.95	21.7	10
18	10	410.9	0.0000	0.0000	14.96	0.2089	-12.26	12.26	18.6	10
19	10	444.3	0.0000	0.0000	17.91	0.1980	-15.90	15.90	19.3	11
20	10	477.6	0.0000	0.0000	29.98	0.2459	-23.13	23.13	23.1	11
21	10	510.9	0.0000	0.0000	15.86	0.1839	-13.75	13.75	18.3	9
22	16	463.0	0.0000	0.0000	4.54	0.1213	-4.31	4.31	12.1	4
23	20	323.1	0.0000	0.0000	11.36	0.3472	-9.91	9.91	34.7	13
24	20	373.1	0.0000	0.0000	11.52	0.2380	-10.17	10.17	23.7	9
25	22	323.1	0.0000	0.0000	17.96	0.3530	-15.99	15.99	35.2	14
26	22	348.1	0.0000	0.0000	12.95	0.2647	-11.15	11.15	26.2	19
27	22	373.1	0.0000	0.0000	9.28	0.2100	-7.76	7.76	20.8	11
28	28	348.1	0.0000	0.0000	18.25	0.2746	-13.90	13.90	26.4	8
29	28	373.1	0.0000	0.0000	13.09	0.2102	-9.49	9.49	20.0	9
30	28	423.1	0.0000	0.0000	10.46	0.1456	-7.31	7.31	13.2	6
31	32	348.1	0.0000	0.0000	13.02	0.2409	-10.83	10.83	23.5	11
32	32	373.1	0.0000	0.0000	12.03	0.2112	-10.79	10.79	20.7	11
33	32	398.1	0.0000	0.0000	7.96	0.1367	-6.37	6.37	12.5	14
34	36	373.1	0.0000	0.0000	6.73	0.1603	-5.09	5.09	15.1	10
35	36	423.1	0.0000	0.0000	9.85	0.1508	-7.11	7.11	13.6	8
36	44	373.1	0.0000	0.0000	7.43	0.1580	-5.09	5.09	13.9	7
37	44	423.1	0.0000	0.0000	7.99	0.1455	-5.60	5.60	12.9	7

MODEL OVERALL STATISTICS

RMSE	= 12.0754 BAR	NO PT	= 421
AAD	= 9.0106 BAR	%AAD	= 20.170
MIN DEV=	-62.8435 BAR	MIN %DEV	= -46.201
MAX DEV=	0.0000 BAR	MAX %DEV	= 0.000
BIAS	= -9.0106 BAR	C-VAR	= 0.241
RESTRICTIONS	: NONE	R-SQR	=0.900957

TABLE G.XIX

BUBBLE-POINT CALCULATIONS USING PENG-ROBINSON EQUATION OF STATE FOR CARBON DIOXIDE + N-PARAFFIN SYSTEMS (CASE 2)

ISO	CN	T(K)	C(I,J)	D(I,J)	RMSE	RMSPE	BIAS	AAD	%AAD	NPT
1	4	310.9	0.1009	0.0000	1.87	0.0805	-1.64	1.64	7.3	18
2	4	344.3	0.1009	0.0000	2.69	0.0637	-2.33	2.33	6.1	17
3	4	377.6	0.1009	0.0000	2.90	0.0557	-2.45	2.45	5.1	12
4	4	410.9	0.1009	0.0000	1.33	0.0270	-0.79	0.79	1.7	5
5	5	311.0	0.1009	0.0000	1.60	0.0853	-1.50	1.50	6.2	14
6	5	344.1	0.1009	0.0000	2.84	0.0757	-2.46	2.46	7.2	15
7	5	377.6	0.1009	0.0000	3.49	0.0803	-3.18	3.18	7.7	9
8	6	313.1	0.1009	0.0000	2.58	0.0674	-2.51	2.51	5.8	8
9	6	353.1	0.1009	0.0000	3.31	0.0811	-3.19	3.19	7.2	14
10	6	393.1	0.1009	0.0000	4.21	0.0679	-3.94	3.94	6.6	15
11	7	310.6	0.1009	0.0000	1.04	0.0370	-0.77	0.80	2.6	23
12	7	352.6	0.1009	0.0000	1.15	0.0147	-0.64	0.72	1.2	17
13	7	394.3	0.1009	0.0000	1.51	0.0487	0.90	1.41	3.1	16
14	7	477.2	0.1009	0.0000	1.12	0.0152	-0.64	0.84	1.3	7
15	10	310.9	0.1009	0.0000	2.70	0.0993	-2.49	2.49	8.6	11
16	10	344.3	0.1009	0.0000	2.73	0.0590	-1.64	2.49	5.2	8
17	10	377.6	0.1009	0.0000	2.22	0.0337	-1.63	1.87	2.9	10
18	10	410.9	0.1009	0.0000	2.07	0.0243	-1.65	1.65	2.0	10
19	10	444.3	0.1009	0.0000	2.88	0.0279	-2.45	2.45	2.6	11
20	10	477.6	0.1009	0.0000	4.27	0.0417	-3.70	3.70	4.1	11
21	10	510.9	0.1009	0.0000	6.14	0.0711	-5.28	5.28	7.1	9
22	16	463.0	0.1009	0.0000	3.05	0.0793	2.86	2.86	7.9	4
23	20	323.1	0.1009	0.0000	0.95	0.0208	-0.60	0.62	1.7	13
24	20	373.1	0.1009	0.0000	1.94	0.0577	1.89	1.89	5.5	9
25	22	323.1	0.1009	0.0000	1.13	0.0214	-0.65	0.83	1.7	14
26	22	348.1	0.1009	0.0000	2.03	0.0707	1.96	1.96	6.3	19
27	22	373.1	0.1009	0.0000	2.72	0.0858	2.52	2.52	8.2	11
28	28	348.1	0.1009	0.0000	2.31	0.0742	-0.13	1.89	6.1	8
29	28	373.1	0.1009	0.0000	1.92	0.0901	1.21	1.80	7.7	9
30	28	423.1	0.1009	0.0000	2.10	0.1032	1.88	1.88	8.7	6
31	32	348.1	0.1009	0.0000	1.85	0.0709	1.70	1.70	5.9	11
32	32	373.1	0.1009	0.0000	2.31	0.0685	2.22	2.22	5.8	11
33	32	398.1	0.1009	0.0000	4.18	0.1292	4.05	4.05	11.9	14
34	36	373.1	0.1009	0.0000	1.81	0.1008	1.64	1.69	8.9	10
35	36	423.1	0.1009	0.0000	2.43	0.0838	0.79	2.04	7.1	8
36	44	373.1	0.1009	0.0000	1.68	0.1010	0.60	1.49	8.6	7
37	44	423.1	0.1009	0.0000	2.33	0.0735	-0.15	1.78	6.5	7

MODEL OVERALL STATISTICS

RMSE	= 2.5940 BAR	NO PT	= 421
AAD	= 2.0928 BAR	%AAD	= 5.533
MIN DEV=	-10.0497 BAR	MIN %DEV	= -19.133
MAX DEV=	5.3257 BAR	MAX %DEV	= 21.258
BIAS	= -0.7041 BAR	C-VAR	= 0.052
RESTRICTIONS	: NONE	R-SQR	=0.946255

TABLE G.XX

BUBBLE-POINT CALCULATIONS USING PENG-ROBINSON EQUATION OF STATE FOR CARBON DIOXIDE + N-PARAFFIN SYSTEMS (CASE 3)

ISO	CN	T(K)	C(I,J)	D(I,J)	RMSE	RMSPE	BIAS	AAD	%AAD	NPT
1	4	310.9	0.1363	0.0000	0.57	0.0140	0.15	0.39	1.1	18
2	4	344.3	0.1363	0.0000	0.41	0.0079	-0.21	0.24	0.6	17
3	4	377.6	0.1363	0.0000	1.05	0.0190	-0.84	0.84	1.7	12
4	4	410.9	0.1363	0.0000	1.08	0.0244	-0.92	0.93	2.1	5
5	5	311.0	0.1327	0.0000	1.24	0.0451	0.46	1.06	3.6	14
6	5	344.1	0.1327	0.0000	1.07	0.0339	0.16	0.84	2.7	15
7	5	377.6	0.1327	0.0000	0.72	0.0409	-0.63	0.63	2.6	9
8	6	313.1	0.1302	0.0000	1.48	0.0268	0.39	1.29	2.4	8
9	6	353.1	0.1302	0.0000	1.42	0.0276	0.63	1.16	2.3	14
10	6	393.1	0.1302	0.0000	0.57	0.0192	-0.30	0.43	1.2	15
11	7	310.6	0.1038	0.0000	0.92	0.0306	-0.55	0.73	2.2	23
12	7	352.6	0.1038	0.0000	0.98	0.0112	-0.18	0.58	0.8	17
13	7	394.3	0.1038	0.0000	1.79	0.0535	1.36	1.74	3.7	16
14	7	477.2	0.1038	0.0000	0.95	0.0145	-0.44	0.74	1.2	7
15	10	310.9	0.1149	0.0000	1.65	0.0564	-0.16	1.43	4.8	11
16	10	344.3	0.1149	0.0000	5.13	0.0485	2.41	3.23	3.8	8
17	10	377.6	0.1149	0.0000	4.20	0.0307	2.44	2.54	2.2	10
18	10	410.9	0.1149	0.0000	2.91	0.0239	1.84	1.94	2.0	10
19	10	444.3	0.1149	0.0000	1.21	0.0109	0.37	0.79	0.9	11
20	10	477.6	0.1149	0.0000	1.94	0.0189	-1.48	1.56	1.7	11
21	10	510.9	0.1149	0.0000	4.57	0.0535	-3.92	3.92	5.3	9
22	16	463.0	0.0639	0.0000	0.21	0.0065	0.03	0.19	0.6	4
23	20	323.1	0.0984	0.0000	1.27	0.0294	-0.90	0.91	2.5	13
24	20	373.1	0.0984	0.0000	1.56	0.0496	1.52	1.52	4.6	9
25	22	323.1	0.0908	0.0000	3.38	0.0576	-2.73	2.73	5.2	14
26	22	348.1	0.0908	0.0000	1.01	0.0412	0.30	0.90	3.2	19
27	22	373.1	0.0908	0.0000	1.40	0.0544	1.28	1.28	4.8	11
28	28	348.1	0.0833	0.0000	5.61	0.0751	-3.20	3.64	6.3	8
29	28	373.1	0.0833	0.0000	3.22	0.0622	-1.03	1.97	5.3	9
30	28	423.1	0.0833	0.0000	2.03	0.0731	0.05	1.67	6.3	6
31	32	348.1	0.0755	0.0000	3.29	0.0541	-2.10	2.38	4.5	11
32	32	373.1	0.0755	0.0000	2.45	0.0438	-1.59	1.93	3.8	11
33	32	398.1	0.0755	0.0000	1.80	0.0730	1.07	1.61	5.8	14
34	36	373.1	0.0702	0.0000	1.92	0.0523	-0.65	1.27	4.6	10
35	36	423.1	0.0702	0.0000	4.22	0.0651	-1.86	2.58	5.4	8
36	44	373.1	0.0750	0.0000	2.85	0.0748	-1.04	1.83	6.6	7
37	44	423.1	0.0750	0.0000	3.68	0.0668	-1.68	2.23	5.5	7

MODEL OVERALL STATISTICS

RMSE	= 2.2532 BAR	NO PT	= 421
AAD	= 1.3854 BAR	%AAD	= 3.151
MIN DEV	=-12.7345 BAR	MIN %DEV	= -13.259
MAX DEV	= 11.8494 BAR	MAX %DEV	= 17.447
BIAS	= -0.2521 BAR	C-VAR	= 0.069
RESTRICTIONS	: NONE	R-SQR	=0.984991

TABLE G.XXI

BUBBLE-POINT CALCULATIONS USING PENG-ROBINSON EQUATION OF STATE FOR CARBON DIOXIDE + N-PARAFFIN SYSTEMS (CASE 4)

ISO	CN	T(K)	C(I,J)	D(I,J)	RMSE	RMSPE	BIAS	AAD	%AAD	NPT
1	4	310.9	0.1346	0.0000	0.51	0.0133	0.05	0.36	1.1	18
2	4	344.3	0.1388	0.0000	0.36	0.0065	-0.06	0.23	0.6	17
3	4	377.6	0.1530	0.0000	0.21	0.0044	-0.04	0.17	0.4	12
4	4	410.9	0.1297	0.0000	0.80	0.0170	-0.61	0.61	1.4	5
5	5	311.0	0.1301	0.0000	1.08	0.0446	0.30	0.92	3.3	14
6	5	344.1	0.1323	0.0000	1.05	0.0339	0.13	0.82	2.6	15
7	5	377.6	0.1431	0.0000	0.71	0.0365	0.27	0.64	2.4	9
8	6	313.1	0.1247	0.0000	1.18	0.0215	-0.18	0.94	1.8	8
9	6	353.1	0.1309	0.0000	1.45	0.0272	0.61	1.12	2.3	14
10	6	393.1	0.1346	0.0000	0.70	0.0167	0.29	0.60	1.2	15
11	7	310.6	0.1103	0.0000	0.93	0.0229	-0.05	0.74	2.0	23
12	7	352.6	0.1042	0.0000	0.98	0.0111	-0.11	0.59	0.8	17
13	7	394.3	0.0872	0.0000	2.06	0.0369	-1.23	1.49	2.2	16
14	7	477.2	0.1047	0.0000	0.91	0.0139	-0.45	0.69	1.1	7
15	10	310.9	0.1205	0.0000	2.30	0.0500	0.89	1.74	4.5	11
16	10	344.3	0.1099	0.0000	3.71	0.0441	0.91	2.73	4.1	8
17	10	377.6	0.1087	0.0000	2.43	0.0210	0.57	1.73	1.8	10
18	10	410.9	0.1081	0.0000	1.44	0.0143	0.11	1.14	1.3	10
19	10	444.3	0.1128	0.0000	1.06	0.0097	-0.07	0.80	0.9	11
20	10	477.6	0.1240	0.0000	1.23	0.0095	0.03	0.80	0.8	11
21	10	510.9	0.1532	0.0000	0.97	0.0111	0.08	0.64	0.9	9
22	16	463.0	0.0639	0.0000	0.21	0.0065	0.03	0.19	0.6	4
23	20	323.1	0.1045	0.0000	0.53	0.0140	-0.17	0.31	1.0	13
24	20	373.1	0.0852	0.0000	0.97	0.0214	-0.36	0.71	1.8	9
25	22	323.1	0.1028	0.0000	0.75	0.0195	-0.24	0.58	1.5	14
26	22	348.1	0.0852	0.0000	1.49	0.0353	-0.57	1.11	2.9	19
27	22	373.1	0.0763	0.0000	1.12	0.0277	-0.40	0.81	2.3	11
28	28	348.1	0.0926	0.0000	3.81	0.0676	-1.63	2.64	6.0	8
29	28	373.1	0.0793	0.0000	3.72	0.0611	-1.51	2.21	5.2	9
30	28	423.1	0.0652	0.0000	3.75	0.0602	-1.73	2.45	5.5	6
31	32	348.1	0.0851	0.0000	1.92	0.0440	-0.72	1.51	3.8	11
32	32	373.1	0.0825	0.0000	1.60	0.0388	-0.58	1.26	3.0	11
33	32	398.1	0.0562	0.0000	2.53	0.0547	-1.01	1.94	4.8	14
34	36	373.1	0.0678	0.0000	2.06	0.0512	-0.86	1.30	4.3	10
35	36	423.1	0.0750	0.0000	3.85	0.0645	-1.46	2.38	5.4	8
36	44	373.1	0.0706	0.0000	3.12	0.0742	-1.30	1.95	6.5	7
37	44	423.1	0.0822	0.0000	3.27	0.0657	-1.27	2.01	5.5	7

MODEL OVERALL STATISTICS

RMSE	= 1.7946 BAR	NO PT	= 421
AAD	= 1.0680 BAR	%AAD	= 2.437
MIN DEV=	-10.0015 BAR	MIN %DEV	= -12.555
MAX DEV=	8.5003 BAR	MAX %DEV	= 12.913
BIAS	= -0.2693 BAR	C-VAR	= 0.055
RESTRICTIONS	: NONE	R-SQR	=0.981475

TABLE G.XXII

BUBBLE-POINT CALCULATIONS USING PENG-ROBINSON EQUATION OF STATE FOR CARBON DIOXIDE + N-PARAFFIN SYSTEMS (CASE 5)

ISO	CN	T(K)	C(I,J)	D(I,J)	RMSE	RMSPE	BIAS	AAD	%AAD	NPT
1	4	310.9	0.1171	0.0209	0.30	0.0061	-0.07	0.16	0.4	18
2	4	344.3	0.1385	0.0005	0.37	0.0065	-0.06	0.23	0.5	17
3	4	377.6	0.1607	-0.0113	0.16	0.0028	0.02	0.11	0.2	12
4	4	410.9	0.2334	-0.1387	0.52	0.0133	-0.42	0.42	1.0	5
5	5	311.0	0.0939	0.0411	1.12	0.0281	-0.56	0.85	2.4	14
6	5	344.1	0.1207	0.0145	1.38	0.0312	-0.33	0.90	2.5	15
7	5	377.6	0.1276	0.0215	0.89	0.0336	-0.19	0.83	2.6	9
8	6	313.1	0.1078	0.0101	3.37	0.0516	-2.15	2.15	3.9	8
9	6	353.1	0.1160	0.0194	1.08	0.0137	-0.21	0.79	1.2	14
10	6	393.1	0.1275	0.0107	0.66	0.0133	-0.08	0.58	1.1	15
11	7	310.6	0.1067	0.0032	0.84	0.0222	-0.19	0.67	1.9	23
12	7	352.6	0.1043	-0.0001	0.98	0.0111	-0.10	0.59	0.8	17
13	7	394.3	0.1075	-0.0262	0.89	0.0225	0.10	0.75	1.5	16
14	7	477.2	0.1124	-0.0150	0.46	0.0079	0.01	0.33	0.6	7
15	10	310.9	0.1028	0.0162	0.63	0.0116	-0.06	0.45	1.0	11
16	10	344.3	0.0991	0.0138	1.03	0.0167	0.01	0.86	1.4	8
17	10	377.6	0.1036	0.0059	1.29	0.0157	0.05	1.05	1.4	10
18	10	410.9	0.1076	0.0006	1.36	0.0142	0.06	1.08	1.3	10
19	10	444.3	0.1138	-0.0012	1.16	0.0095	-0.02	0.83	0.8	11
20	10	477.6	0.1238	0.0004	1.21	0.0095	0.03	0.80	0.8	11
21	10	510.9	0.1490	0.0040	0.86	0.0106	-0.04	0.66	0.9	9
22	16	463.0	0.0524	0.0042	0.23	0.0058	-0.01	0.21	0.6	4
23	20	323.1	0.1151	-0.0037	0.14	0.0042	0.00	0.10	0.3	13
24	20	373.1	0.1084	-0.0083	0.13	0.0027	-0.01	0.10	0.2	9
25	22	323.1	0.1107	-0.0037	0.29	0.0089	0.01	0.24	0.7	14
26	22	348.1	0.1098	-0.0088	0.39	0.0137	0.01	0.32	1.0	19
27	22	373.1	0.1004	-0.0072	0.49	0.0168	-0.01	0.40	1.4	11
28	28	348.1	0.1270	-0.0106	0.38	0.0060	-0.02	0.26	0.5	8
29	28	373.1	0.1299	-0.0124	0.08	0.0036	0.01	0.07	0.3	9
30	28	423.1	0.1373	-0.0161	0.05	0.0016	0.01	0.04	0.1	6
31	32	348.1	0.1111	-0.0069	0.44	0.0196	-0.01	0.37	1.4	11
32	32	373.1	0.1214	-0.0104	0.41	0.0088	-0.03	0.33	0.7	11
33	32	398.1	0.1238	-0.0150	0.60	0.0140	-0.01	0.45	1.1	14
34	36	373.1	0.1363	-0.0111	0.31	0.0073	0.00	0.20	0.6	10
35	36	423.1	0.1729	-0.0173	0.46	0.0078	-0.03	0.29	0.6	8
36	44	373.1	0.1673	-0.0124	0.16	0.0052	-0.01	0.11	0.4	7
37	44	423.1	0.2032	-0.0157	0.19	0.0046	-0.02	0.12	0.4	7

MODEL OVERALL STATISTICS

RMSE	= 0.8792 BAR	NO PT	= 421
AAD	= 0.5148 BAR	%AAD	= 1.093
MIN DEV=	-8.9168 BAR	MIN %DEV	= -11.920
MAX DEV=	3.4133 BAR	MAX %DEV	= 7.435
BIAS	= -0.1073 BAR	C-VAR	= 0.027
RESTRICTIONS	: NONE	R-SQR	=0.999498

TABLE G.XXIII

BUBBLE-POINT CALCULATIONS USING SPHCT EQUATION OF STATE
FOR CARBON DIOXIDE + N-PARAFFIN SYSTEMS (CASE 1)

ISO	CN	T(K)	C(I,J)	D(I,J)	RMSE	RMSPE	BIAS	AAD	%AAD	NPT
1	4	310.9	0.0000	0.0000	8.07	0.2808	-7.17	7.17	26.7	18
2	4	344.3	0.0000	0.0000	6.27	0.1946	-4.60	4.60	15.7	17
3	4	377.6	0.0000	0.0000	4.24	0.1285	-3.16	3.16	9.9	12
4	4	410.9	0.0000	0.0000	1.53	0.0488	-0.89	0.89	2.7	5
5	5	311.0	0.0000	0.0000	8.51	0.2791	-7.81	7.81	24.6	14
6	5	344.1	0.0000	0.0000	9.00	0.2370	-6.50	6.50	20.5	15
7	5	377.6	0.0000	0.0000	7.99	0.2034	-6.25	6.25	17.4	9
8	6	313.1	0.0000	0.0000	12.04	0.2878	-11.55	11.55	25.9	8
9	6	353.1	0.0000	0.0000	12.41	0.2691	-10.48	10.48	23.3	14
10	6	393.1	0.0000	0.0000	11.02	0.2099	-8.98	8.98	17.8	15
11	7	310.6	0.0000	0.0000	9.37	0.2804	-8.15	8.15	24.7	23
12	7	352.6	0.0000	0.0000	12.56	0.2404	-10.79	10.79	21.8	17
13	7	394.3	0.0000	0.0000	11.67	0.1770	-10.36	10.36	16.0	16
14	7	477.2	0.0000	0.0000	8.50	0.1236	-7.71	7.71	12.1	7
15	10	310.9	0.0000	0.0000	16.08	0.4107	-14.94	14.94	40.2	11
16	10	344.3	0.0000	0.0000	19.91	0.3317	-17.09	17.09	31.1	8
17	10	377.6	0.0000	0.0000	19.91	0.2694	-16.61	16.61	24.7	10
18	10	410.9	0.0000	0.0000	16.17	0.2176	-13.86	13.86	19.9	10
19	10	444.3	0.0000	0.0000	17.63	0.2058	-15.89	15.89	19.9	11
20	10	477.6	0.0000	0.0000	20.34	0.2067	-17.89	17.89	20.5	11
21	10	510.9	0.0000	0.0000	22.72	0.2390	-18.54	18.54	23.6	9
22	16	463.0	0.0000	0.0000	6.18	0.1703	-5.95	5.95	17.0	4
23	20	323.1	0.0000	0.0000	14.42	0.4695	-12.95	12.95	46.9	13
24	20	373.1	0.0000	0.0000	14.04	0.3119	-12.76	12.76	31.2	9
25	22	323.1	0.0000	0.0000	22.08	0.4660	-20.22	20.22	46.6	14
26	22	348.1	0.0000	0.0000	16.45	0.3707	-14.77	14.77	37.1	19
27	22	373.1	0.0000	0.0000	12.12	0.3096	-10.67	10.67	30.9	11
28	28	348.1	0.0000	0.0000	22.62	0.4166	-18.74	18.74	41.6	8
29	28	373.1	0.0000	0.0000	16.47	0.3407	-13.36	13.36	34.1	9
30	28	423.1	0.0000	0.0000	12.10	0.2316	-9.66	9.66	23.2	6
31	32	348.1	0.0000	0.0000	19.04	0.4156	-16.97	16.97	41.5	11
32	32	373.1	0.0000	0.0000	17.39	0.3386	-16.35	16.35	33.9	11
33	32	398.1	0.0000	0.0000	11.71	0.2489	-10.54	10.54	24.9	14
34	36	373.1	0.0000	0.0000	11.60	0.3585	-9.94	9.94	35.8	10
35	36	423.1	0.0000	0.0000	11.95	0.2440	-10.11	10.11	24.4	8
36	44	373.1	0.0000	0.0000	12.32	0.3757	-10.10	10.10	37.6	7
37	44	423.1	0.0000	0.0000	9.89	0.2501	-8.30	8.30	25.0	7

MODEL OVERALL STATISTICS

RMSE = 13.9298 BAR	NO PT = 421
AAD = 11.3087 BAR	%AAD = 26.518
MIN DEV=-44.2786 BAR	MIN %DEV = -49.084
MAX DEV= 0.0000 BAR	MAX %DEV = 0.000
BIAS =-11.3087 BAR	C-VAR = 0.425
RESTRICTIONS : NONE	R-SQR =0.991702

TABLE G.XXIV

BUBBLE-POINT CALCULATIONS USING SPHCT EQUATION OF STATE
FOR CARBON DIOXIDE + N-PARAFFIN SYSTEMS (CASE 2)

ISO	CN	T(K)	C(I,J)	D(I,J)	RMSE	RMSPE	BIAS	AAD	%AAD	NPT
1	4	310.9	0.0654	0.0000	2.97	0.0901	-2.51	2.51	8.6	18
2	4	344.3	0.0654	0.0000	4.45	0.0892	-3.56	3.56	8.4	17
3	4	377.6	0.0654	0.0000	4.69	0.0927	-4.09	4.09	9.1	12
4	4	410.9	0.0654	0.0000	2.23	0.0571	-1.73	1.73	4.3	5
5	5	311.0	0.0654	0.0000	2.98	0.0806	-2.75	2.75	7.5	14
6	5	344.1	0.0654	0.0000	6.30	0.0916	-4.44	4.44	8.5	15
7	5	377.6	0.0654	0.0000	6.04	0.0968	-4.91	4.91	9.5	9
8	6	313.1	0.0654	0.0000	4.14	0.0800	-4.02	4.02	7.9	8
9	6	353.1	0.0654	0.0000	7.51	0.0933	-6.17	6.17	9.1	14
10	6	393.1	0.0654	0.0000	7.75	0.0862	-6.40	6.40	8.3	15
11	7	310.6	0.0654	0.0000	2.62	0.0485	-2.07	2.12	4.4	23
12	7	352.6	0.0654	0.0000	7.17	0.0770	-3.77	4.63	6.3	17
13	7	394.3	0.0654	0.0000	5.41	0.0866	-1.26	4.24	6.8	16
14	7	477.2	0.0654	0.0000	0.80	0.0088	-0.07	0.55	0.7	7
15	10	310.9	0.0654	0.0000	3.09	0.0677	-2.59	2.59	6.6	11
16	10	344.3	0.0654	0.0000	4.21	0.0374	-2.07	2.27	2.5	8
17	10	377.6	0.0654	0.0000	3.70	0.0470	-0.51	2.61	3.9	10
18	10	410.9	0.0654	0.0000	2.84	0.0506	0.42	2.29	4.1	10
19	10	444.3	0.0654	0.0000	1.73	0.0316	0.27	1.49	2.5	11
20	10	477.6	0.0654	0.0000	2.07	0.0160	-1.40	1.58	1.4	11
21	10	510.9	0.0654	0.0000	4.00	0.0507	-3.48	3.48	4.9	9
22	16	463.0	0.0654	0.0000	5.89	0.1484	5.44	5.44	14.7	4
23	20	323.1	0.0654	0.0000	1.07	0.0508	-1.04	1.04	4.7	13
24	20	373.1	0.0654	0.0000	6.24	0.1263	5.46	5.46	12.5	9
25	22	323.1	0.0654	0.0000	0.90	0.0389	-0.51	0.77	2.8	14
26	22	348.1	0.0654	0.0000	4.76	0.0931	3.97	3.97	8.9	19
27	22	373.1	0.0654	0.0000	6.27	0.1339	5.06	5.06	12.9	11
28	28	348.1	0.0654	0.0000	3.46	0.0398	2.03	2.03	2.8	8
29	28	373.1	0.0654	0.0000	5.99	0.0959	4.28	4.28	9.2	9
30	28	423.1	0.0654	0.0000	9.99	0.1655	7.50	7.50	16.3	6
31	32	348.1	0.0654	0.0000	3.33	0.0583	2.15	2.46	5.1	11
32	32	373.1	0.0654	0.0000	6.73	0.1141	5.85	5.85	10.9	11
33	32	398.1	0.0654	0.0000	9.94	0.1955	8.65	8.65	19.3	14
34	36	373.1	0.0654	0.0000	2.30	0.0550	1.75	1.75	5.1	10
35	36	423.1	0.0654	0.0000	7.66	0.1484	6.36	6.36	14.8	8
36	44	373.1	0.0654	0.0000	1.36	0.0275	0.87	0.87	2.2	7
37	44	423.1	0.0654	0.0000	5.63	0.1321	4.57	4.57	13.1	7

MODEL OVERALL STATISTICS

RMSE	= 5.1145 BAR	NO PT	= 421
AAD	= 3.6391 BAR	%AAD	= 7.483
MIN DEV	=-21.1684 BAR	MIN %DEV	= -18.466
MAX DEV	= 19.6735 BAR	MAX %DEV	= 24.818
BIAS	= -0.3624 BAR	C-VAR	= 0.156
RESTRICTIONS	: NONE	R-SQR	=0.959339

TABLE G.XXV

BUBBLE-POINT CALCULATIONS USING SPHCT EQUATION OF STATE
FOR CARBON DIOXIDE + N-PARAFFIN SYSTEMS (CASE 3)

ISO	CN	T(K)	C(I,J)	D(I,J)	RMSE	RMSPE	BIAS	AAD	%AAD	NPT
1	4	310.9	0.0937	0.0000	1.18	0.0329	-0.25	0.88	3.1	18
2	4	344.3	0.0937	0.0000	2.12	0.0308	-1.12	1.26	2.2	17
3	4	377.6	0.0937	0.0000	2.19	0.0436	-1.88	1.88	4.3	12
4	4	410.9	0.0937	0.0000	3.28	0.0859	-3.20	3.20	8.3	5
5	5	311.0	0.0854	0.0000	1.74	0.0382	-0.84	1.45	3.5	14
6	5	344.1	0.0854	0.0000	3.71	0.0513	-1.89	2.41	4.3	15
7	5	377.6	0.0854	0.0000	3.52	0.0527	-2.37	2.44	4.4	9
8	6	313.1	0.0841	0.0000	2.43	0.0395	-1.28	2.01	3.6	8
9	6	353.1	0.0841	0.0000	4.27	0.0479	-2.28	2.95	4.0	14
10	6	393.1	0.0841	0.0000	4.41	0.0435	-2.66	3.08	3.5	15
11	7	310.6	0.0638	0.0000	2.75	0.0494	-2.25	2.29	4.7	23
12	7	352.6	0.0638	0.0000	7.47	0.0771	-4.17	4.76	6.2	17
13	7	394.3	0.0638	0.0000	5.54	0.0834	-1.68	4.24	6.5	16
14	7	477.2	0.0638	0.0000	0.87	0.0100	-0.31	0.64	0.8	7
15	10	310.9	0.0667	0.0000	2.80	0.0593	-2.26	2.26	5.7	11
16	10	344.3	0.0667	0.0000	3.91	0.0365	-1.55	2.10	2.6	8
17	10	377.6	0.0667	0.0000	3.46	0.0514	0.15	2.65	4.3	10
18	10	410.9	0.0667	0.0000	2.77	0.0556	1.05	2.44	4.5	10
19	10	444.3	0.0667	0.0000	1.68	0.0356	0.83	1.50	2.8	11
20	10	477.6	0.0667	0.0000	1.60	0.0138	-0.95	1.26	1.3	11
21	10	510.9	0.0667	0.0000	3.67	0.0470	-3.19	3.19	4.6	9
22	16	463.0	0.0380	0.0000	0.43	0.0140	0.13	0.37	1.1	4
23	20	323.1	0.0626	0.0000	1.82	0.0738	-1.75	1.75	7.2	13
24	20	373.1	0.0626	0.0000	5.05	0.1014	4.40	4.40	10.0	9
25	22	323.1	0.0586	0.0000	3.64	0.0924	-3.49	3.49	8.9	14
26	22	348.1	0.0586	0.0000	1.70	0.0321	1.27	1.34	2.9	19
27	22	373.1	0.0586	0.0000	3.74	0.0764	2.90	2.90	7.0	11
28	28	348.1	0.0553	0.0000	2.94	0.0671	-2.63	2.63	6.6	8
29	28	373.1	0.0553	0.0000	1.21	0.0153	0.59	0.66	1.2	9
30	28	423.1	0.0553	0.0000	5.54	0.0897	4.12	4.12	8.8	6
31	32	348.1	0.0518	0.0000	3.32	0.1004	-3.18	3.18	9.3	11
32	32	373.1	0.0518	0.0000	0.87	0.0236	-0.15	0.70	1.8	11
33	32	398.1	0.0518	0.0000	4.23	0.0816	3.61	3.61	7.9	14
34	36	373.1	0.0531	0.0000	1.09	0.0469	-1.02	1.02	4.5	10
35	36	423.1	0.0531	0.0000	3.01	0.0586	2.52	2.52	5.8	8
36	44	373.1	0.0551	0.0000	1.50	0.0569	-1.33	1.33	5.6	7
37	44	423.1	0.0551	0.0000	2.58	0.0591	2.07	2.07	5.9	7

MODEL OVERALL STATISTICS

RMSE = 3.3881 BAR	NO PT = 421
AAD = 2.3382 BAR	%AAD = 4.801
MIN DEV=-21.9212 BAR	MIN %DEV = -18.880
MAX DEV= 11.0374 BAR	MAX %DEV = 23.893
BIAS = -0.8309 BAR	C-VAR = 0.103
RESTRICTIONS : NONE	R-SQR =0.918052

TABLE G.XXVI

BUBBLE-POINT CALCULATIONS USING SPHCT EQUATION OF STATE
FOR CARBON DIOXIDE + N-PARAFFIN SYSTEMS (CASE 4)

ISO	CN	T(K)	C(I,J)	D(I,J)	RMSE	RMSPE	BIAS	AAD	%AAD	NPT
1	4	310.9	0.0885	0.0000	1.35	0.0249	-0.72	0.86	2.1	18
2	4	344.3	0.0970	0.0000	1.90	0.0293	-0.79	1.19	2.4	17
3	4	377.6	0.1138	0.0000	0.56	0.0179	-0.18	0.49	1.4	12
4	4	410.9	0.1634	0.0000	2.18	0.0591	-0.81	1.94	5.1	5
5	5	311.0	0.0830	0.0000	1.79	0.0366	-1.08	1.45	3.4	14
6	5	344.1	0.0848	0.0000	3.76	0.0512	-1.96	2.44	4.3	15
7	5	377.6	0.0953	0.0000	2.50	0.0432	-1.00	1.86	3.9	9
8	6	313.1	0.0817	0.0000	2.51	0.0378	-1.65	2.00	3.3	8
9	6	353.1	0.0823	0.0000	4.45	0.0477	-2.64	3.02	3.8	14
10	6	393.1	0.0875	0.0000	3.88	0.0415	-1.92	2.80	3.5	15
11	7	310.6	0.0656	0.0000	2.60	0.0485	-2.05	2.10	4.3	23
12	7	352.6	0.0638	0.0000	7.47	0.0771	-4.17	4.76	6.2	17
13	7	394.3	0.0554	0.0000	6.65	0.0754	-3.81	4.61	5.8	16
14	7	477.2	0.0657	0.0000	0.72	0.0080	-0.07	0.50	0.6	7
15	10	310.9	0.0736	0.0000	1.87	0.0275	-0.40	1.05	2.0	11
16	10	344.3	0.0666	0.0000	3.93	0.0365	-1.59	2.10	2.6	8
17	10	377.6	0.0619	0.0000	4.79	0.0416	-2.22	3.01	3.4	10
18	10	410.9	0.0596	0.0000	4.62	0.0393	-2.29	3.19	3.4	10
19	10	444.3	0.0614	0.0000	2.83	0.0257	-1.38	2.12	2.3	11
20	10	477.6	0.0678	0.0000	1.28	0.0133	-0.60	1.06	1.2	11
21	10	510.9	0.0809	0.0000	0.89	0.0148	0.15	0.57	1.0	9
22	16	463.0	0.0380	0.0000	0.43	0.0140	0.13	0.37	1.1	4
23	20	323.1	0.0703	0.0000	0.81	0.0230	0.27	0.57	2.0	13
24	20	373.1	0.0504	0.0000	0.37	0.0100	0.17	0.32	0.9	9
25	22	323.1	0.0673	0.0000	1.27	0.0332	0.40	1.01	2.7	14
26	22	348.1	0.0557	0.0000	0.64	0.0185	0.20	0.51	1.5	19
27	22	373.1	0.0496	0.0000	0.90	0.0249	0.28	0.57	1.7	11
28	28	348.1	0.0621	0.0000	1.49	0.0221	0.40	0.91	1.9	8
29	28	373.1	0.0554	0.0000	1.25	0.0157	0.63	0.69	1.2	9
30	28	423.1	0.0422	0.0000	0.57	0.0079	0.21	0.33	0.7	6
31	32	348.1	0.0619	0.0000	1.77	0.0475	0.68	1.35	3.7	11
32	32	373.1	0.0528	0.0000	1.02	0.0220	0.26	0.77	1.7	11
33	32	398.1	0.0411	0.0000	0.67	0.0155	0.12	0.49	1.2	14
34	36	373.1	0.0589	0.0000	0.56	0.0172	0.24	0.42	1.5	10
35	36	423.1	0.0444	0.0000	0.26	0.0061	0.04	0.17	0.5	8
36	44	373.1	0.0624	0.0000	0.58	0.0142	0.20	0.37	1.2	7
37	44	423.1	0.0462	0.0000	0.19	0.0048	0.08	0.15	0.4	7

MODEL OVERALL STATISTICS

RMSE	= 2.9497 BAR	NO PT	= 421
AAD	= 1.5646 BAR	%AAD	= 2.664
MIN DEV=	-21.9212 BAR	MIN %DEV	= -18.880
MAX DEV=	3.8670 BAR	MAX %DEV	= 19.166
BIAS	= -0.9090 BAR	C-VAR	= 0.090
RESTRICTIONS	: NONE	R-SQR	=0.908576

TABLE G.XXVII

BUBBLE-POINT CALCULATIONS USING SPHCT EQUATION OF STATE
FOR CARBON DIOXIDE + N-PARAFFIN SYSTEMS (CASE 5)

ISO	CN	T(K)	C(I,J)	D(I,J)	RMSE	RMSPE	BIAS	AAD	%AAD	NPT
1	4	310.9	0.0866	-0.0163	0.83	0.0134	-0.28	0.46	1.0	18
2	4	344.3	0.0904	-0.0235	0.38	0.0103	-0.07	0.29	0.9	17
3	4	377.6	0.1113	-0.0069	0.38	0.0171	-0.09	0.30	1.1	12
4	4	410.9	0.1918	0.1397	1.33	0.0402	-0.49	1.14	3.2	5
5	5	311.0	0.0831	-0.0024	1.65	0.0362	-0.93	1.34	3.3	14
6	5	344.1	0.0846	-0.0161	1.75	0.0336	-0.48	1.16	2.9	15
7	5	377.6	0.0932	-0.0117	0.99	0.0368	-0.21	0.92	2.9	9
8	6	313.1	0.0793	-0.0111	1.77	0.0266	-0.87	1.31	2.2	8
9	6	353.1	0.0836	-0.0111	2.10	0.0254	-0.58	1.47	2.1	14
10	6	393.1	0.0856	-0.0126	0.92	0.0165	-0.11	0.76	1.3	15
11	7	310.6	0.0708	-0.0072	1.83	0.0285	-0.95	1.31	2.5	23
12	7	352.6	0.0663	-0.0129	2.38	0.0257	-0.57	1.51	2.0	17
13	7	394.3	0.0541	-0.0197	0.64	0.0179	-0.01	0.58	1.2	16
14	7	477.2	0.0652	-0.0001	0.78	0.0087	-0.10	0.54	0.7	7
15	10	310.9	0.0733	0.0003	1.91	0.0273	-0.49	1.03	1.9	11
16	10	344.3	0.0681	-0.0031	2.34	0.0217	-0.30	1.35	1.6	8
17	10	377.6	0.0634	-0.0045	1.27	0.0094	-0.05	0.75	0.7	10
18	10	410.9	0.0614	-0.0048	0.74	0.0054	-0.03	0.51	0.4	10
19	10	444.3	0.0629	-0.0040	0.27	0.0029	0.02	0.22	0.3	11
20	10	477.6	0.0683	-0.0021	0.62	0.0061	-0.03	0.47	0.6	11
21	10	510.9	0.0800	0.0016	0.77	0.0134	-0.05	0.63	1.1	9
22	16	463.0	0.0245	0.0037	0.23	0.0057	-0.01	0.21	0.6	4
23	20	323.1	0.0650	0.0014	0.15	0.0045	0.01	0.11	0.4	13
24	20	373.1	0.0475	0.0008	0.12	0.0026	0.01	0.10	0.2	9
25	22	323.1	0.0640	0.0015	0.29	0.0091	-0.02	0.22	0.7	14
26	22	348.1	0.0532	0.0007	0.39	0.0137	-0.04	0.33	1.1	19
27	22	373.1	0.0441	0.0012	0.49	0.0167	-0.04	0.40	1.4	11
28	28	348.1	0.0597	0.0007	0.45	0.0084	0.05	0.30	0.7	8
29	28	373.1	0.0517	0.0005	0.17	0.0042	-0.01	0.12	0.4	9
30	28	423.1	0.0400	0.0003	0.18	0.0042	-0.06	0.15	0.4	6
31	32	348.1	0.0551	0.0015	0.37	0.0177	-0.05	0.31	1.3	11
32	32	373.1	0.0482	0.0010	0.47	0.0098	-0.06	0.35	0.7	11
33	32	398.1	0.0386	0.0004	0.59	0.0132	-0.08	0.48	1.1	14
34	36	373.1	0.0535	0.0006	0.20	0.0057	-0.07	0.12	0.4	10
35	36	423.1	0.0434	0.0001	0.32	0.0057	-0.07	0.21	0.5	8
36	44	373.1	0.0589	0.0004	0.17	0.0080	0.09	0.12	0.5	7
37	44	423.1	0.0447	0.0001	0.12	0.0043	-0.08	0.11	0.4	7

MODEL OVERALL STATISTICS

RMSE	= 1.1294 BAR	NO PT	= 421
AAD	= 0.6323 BAR	%AAD	= 1.286
MIN DEV=	-7.3615 BAR	MIN %DEV	= -8.400
MAX DEV=	2.6562 BAR	MAX %DEV	= 5.493
BIAS	= -0.2262 BAR	C-VAR	= 0.034
RESTRICTIONS	: NONE	R-SQR	=0.979183

TABLE G.XXVIII

BUBBLE-POINT CALCULATIONS USING SPHCT EQUATION OF STATE
FOR CARBON DIOXIDE + N-PARAFFIN SYSTEMS (CASE 6)

ISO	CN	T(K)	C(I,J)	E(I,J)	RMSE	RMSPE	BIAS	AAD	%AAD	NPT
1	4	310.9	0.1048	-0.0278	0.87	0.0142	-0.32	0.48	1.0	18
2	4	344.3	0.1225	-0.0430	0.65	0.0133	-0.15	0.43	1.1	17
3	4	377.6	0.1222	-0.0131	0.40	0.0172	-0.10	0.32	1.1	12
4	4	410.9	0.0445	0.0006	1.78	0.0510	-1.29	1.29	3.4	5
5	5	311.0	0.0847	-0.0030	1.72	0.0365	-1.00	1.40	3.4	14
6	5	344.1	0.1047	-0.0324	2.20	0.0373	-0.71	1.40	3.2	15
7	5	377.6	0.1097	-0.0236	1.21	0.0380	-0.30	1.08	3.1	9
8	6	313.1	0.0931	-0.0295	1.92	0.0285	-0.98	1.44	2.4	8
9	6	353.1	0.0983	-0.0267	2.57	0.0296	-0.80	1.78	2.5	14
10	6	393.1	0.1037	-0.0288	1.26	0.0190	-0.22	1.00	1.6	15
11	7	310.6	0.0796	-0.0208	1.92	0.0296	-1.04	1.38	2.6	23
12	7	352.6	0.0831	-0.0340	3.01	0.0313	-0.95	1.87	2.4	17
13	7	394.3	0.0838	-0.0522	1.08	0.0174	-0.09	0.88	1.4	16
14	7	477.2	0.0838	-0.0522	3.25	0.0579	-0.39	2.87	5.3	7
15	10	310.9	0.0727	0.0016	1.92	0.0272	-0.51	1.03	1.8	11
16	10	344.3	0.0719	-0.0102	2.60	0.0235	-0.45	1.39	1.6	8
17	10	377.6	0.0695	-0.0144	1.55	0.0113	-0.10	0.88	0.8	10
18	10	410.9	0.0681	-0.0145	0.88	0.0059	-0.02	0.55	0.5	10
19	10	444.3	0.0683	-0.0111	0.19	0.0028	0.00	0.16	0.2	11
20	10	477.6	0.0713	-0.0056	0.59	0.0060	0.00	0.43	0.5	11
21	10	510.9	0.0781	0.0039	0.73	0.0133	-0.01	0.62	1.1	9
22	16	463.0	0.0206	0.0118	0.23	0.0057	0.00	0.21	0.6	4
23	20	323.1	0.0634	0.0067	0.15	0.0045	0.00	0.11	0.3	13
24	20	373.1	0.0467	0.0033	0.11	0.0025	0.01	0.10	0.2	9
25	22	323.1	0.0621	0.0077	0.29	0.0090	-0.02	0.22	0.7	14
26	22	348.1	0.0524	0.0033	0.39	0.0137	-0.03	0.33	1.1	19
27	22	373.1	0.0428	0.0053	0.48	0.0167	-0.02	0.40	1.4	11
28	28	348.1	0.0590	0.0033	0.48	0.0083	0.02	0.32	0.7	8
29	28	373.1	0.0512	0.0024	0.18	0.0042	0.02	0.12	0.3	9
30	28	423.1	0.0397	0.0015	0.18	0.0035	0.02	0.13	0.3	6
31	32	348.1	0.0533	0.0080	0.37	0.0176	-0.04	0.31	1.3	11
32	32	373.1	0.0470	0.0051	0.46	0.0097	-0.03	0.34	0.7	11
33	32	398.1	0.0382	0.0020	0.59	0.0130	-0.02	0.47	1.1	14
34	36	373.1	0.0529	0.0032	0.18	0.0047	-0.01	0.11	0.3	10
35	36	423.1	0.0433	0.0006	0.31	0.0054	-0.01	0.20	0.5	8
36	44	373.1	0.0585	0.0018	0.13	0.0068	-0.01	0.12	0.6	7
37	44	423.1	0.0445	0.0007	0.09	0.0029	-0.01	0.07	0.2	7

MODEL OVERALL STATISTICS

RMSE	= 1.3768 BAR	NO PT	= 421
AAD	= 0.7451 BAR	%AAD	= 1.445
MIN DEV	= -8.9772 BAR	MIN %DEV	= -10.459
MAX DEV	= 6.2737 BAR	MAX %DEV	= 6.323
BIAS	= -0.2910 BAR	C-VAR	= 0.042
RESTRICTIONS	: NONE	R-SQR	=0.974317

TABLE G.XXIX

BUBBLE-POINT CALCULATIONS USING MODIFIED SPHCT EQUATION OF STATE FOR CARBON DIOXIDE + N-PARAFFIN SYSTEMS (CASE 1)

ISO	CN	T(K)	C(I,J)	D(I,J)	RMSE	RMSPE	BIAS	AAD	%AAD	NPT
1	4	310.9	0.0000	0.0000	7.19	0.2681	-6.32	6.32	24.9	18
2	4	344.3	0.0000	0.0000	6.28	0.1749	-4.87	4.88	14.7	17
3	4	377.6	0.0000	0.0000	3.85	0.0983	-2.87	2.92	7.8	12
4	4	410.9	0.0000	0.0000	0.56	0.0155	-0.39	0.42	1.1	5
5	5	311.0	0.0000	0.0000	7.40	0.2774	-6.55	6.55	23.0	14
6	5	344.1	0.0000	0.0000	10.89	0.2338	-9.07	9.07	22.7	15
7	5	377.6	0.0000	0.0000	9.76	0.1867	-8.63	8.63	18.3	9
8	6	313.1	0.0000	0.0000	10.82	0.2788	-9.92	9.92	23.6	8
9	6	353.1	0.0000	0.0000	12.36	0.2546	-11.60	11.60	23.7	14
10	6	393.1	0.0000	0.0000	11.78	0.1800	-10.97	10.97	17.6	15
11	7	310.6	0.0000	0.0000	8.47	0.3068	-6.83	6.83	24.8	23
12	7	352.6	0.0000	0.0000	11.56	0.2240	-10.86	10.86	21.2	17
13	7	394.3	0.0000	0.0000	8.06	0.1094	-7.55	7.55	10.5	16
14	7	477.2	0.0000	0.0000	2.03	0.0290	-1.69	1.72	2.6	7
15	10	310.9	0.0000	0.0000	16.70	0.4714	-15.65	15.65	45.0	11
16	10	344.3	0.0000	0.0000	18.73	0.3455	-17.76	17.76	33.0	8
17	10	377.6	0.0000	0.0000	16.36	0.2372	-15.42	15.42	22.7	10
18	10	410.9	0.0000	0.0000	10.44	0.1479	-9.76	9.76	14.0	10
19	10	444.3	0.0000	0.0000	5.87	0.0858	-5.31	5.31	7.8	11
20	10	477.6	0.0000	0.0000	3.77	0.0545	-2.10	3.32	4.9	11
21	10	510.9	0.0000	0.0000	3.34	0.0571	-2.87	3.03	5.3	9
22	16	463.0	0.0000	0.0000	1.13	0.0447	-1.07	1.07	3.8	4
23	20	323.1	0.0000	0.0000	18.64	0.6252	-16.96	16.96	62.5	13
24	20	373.1	0.0000	0.0000	16.37	0.3835	-15.17	15.17	38.3	9
25	22	323.1	0.0000	0.0000	27.54	0.6056	-25.60	25.60	60.4	14
26	22	348.1	0.0000	0.0000	20.80	0.4955	-19.07	19.07	49.4	19
27	22	373.1	0.0000	0.0000	14.45	0.3951	-13.05	13.05	39.3	11
28	28	348.1	0.0000	0.0000	25.94	0.5263	-22.28	22.28	52.5	8
29	28	373.1	0.0000	0.0000	17.60	0.4105	-14.96	14.96	40.9	9
30	28	423.1	0.0000	0.0000	5.75	0.1574	-5.12	5.12	15.3	6
31	32	348.1	0.0000	0.0000	22.55	0.5190	-20.47	20.47	51.7	11
32	32	373.1	0.0000	0.0000	18.48	0.3769	-17.64	17.64	37.5	11
33	32	398.1	0.0000	0.0000	9.13	0.2200	-8.55	8.55	21.7	14
34	36	373.1	0.0000	0.0000	12.33	0.4071	-10.83	10.83	40.6	10
35	36	423.1	0.0000	0.0000	3.11	0.0970	-2.99	2.99	9.2	8
36	44	373.1	0.0000	0.0000	10.95	0.3716	-9.35	9.35	37.0	7
37	44	423.1	0.0000	0.0000	1.62	0.0359	0.47	1.06	3.2	7

MODEL OVERALL STATISTICS

RMSE = 13.3489 BAR
AAD = 10.5021 BAR
MIN DEV=-44.5329 BAR
MAX DEV= 6.5140 BAR
BIAS =-10.4385 BAR
RESTRICTIONS : NONE

NO PT = 421
%AAD = 26.500
MIN %DEV = -67.487
MAX %DEV = 5.638
C-VAR = 0.407
R-SQR =0.985688

TABLE G.XXX

BUBBLE-POINT CALCULATIONS USING MODIFIED SPHCT EQUATION
OF STATE FOR CARBON DIOXIDE + N-PARAFFIN SYSTEMS (CASE 2)

ISO	CN	T(K)	C(I,J)	D(I,J)	RMSE	RMSPE	BIAS	AAD	%AAD	NPT
1	4	310.9	0.0529	0.0000	2.84	0.1090	-2.57	2.57	10.1	18
2	4	344.3	0.0529	0.0000	3.19	0.0659	-2.59	2.61	6.1	17
3	4	377.6	0.0529	0.0000	2.76	0.0486	-2.11	2.18	4.3	12
4	4	410.9	0.0529	0.0000	1.54	0.0338	-1.23	1.32	3.0	5
5	5	311.0	0.0529	0.0000	2.42	0.1184	-2.25	2.25	9.1	14
6	5	344.1	0.0529	0.0000	2.89	0.0682	-2.43	2.43	6.6	15
7	5	377.6	0.0529	0.0000	2.22	0.0498	-1.94	1.94	4.6	9
8	6	313.1	0.0529	0.0000	3.61	0.1014	-3.36	3.36	8.3	8
9	6	353.1	0.0529	0.0000	2.02	0.0630	-1.90	1.90	5.0	14
10	6	393.1	0.0529	0.0000	0.68	0.0158	0.29	0.56	1.2	15
11	7	310.6	0.0529	0.0000	2.22	0.1131	-1.74	1.74	8.1	23
12	7	352.6	0.0529	0.0000	2.15	0.0271	1.50	1.64	2.2	17
13	7	394.3	0.0529	0.0000	8.79	0.1389	8.41	8.41	13.2	16
14	7	477.2	0.0529	0.0000	8.02	0.1094	7.14	7.14	10.9	7
15	10	310.9	0.0529	0.0000	6.71	0.2491	-6.13	6.13	21.5	11
16	10	344.3	0.0529	0.0000	6.93	0.1147	0.73	5.65	10.3	8
17	10	377.6	0.0529	0.0000	16.70	0.1238	11.09	11.15	9.3	10
18	10	410.9	0.0529	0.0000	26.62	0.1958	19.80	19.80	18.1	10
19	10	444.3	0.0529	0.0000	29.40	0.2315	23.08	23.08	22.2	11
20	10	477.6	0.0529	0.0000	29.97	0.2336	23.36	23.36	22.3	11
21	10	510.9	0.0529	0.0000	17.44	0.1649	13.49	13.49	15.4	9
22	16	463.0	0.0529	0.0000	11.51	0.2857	10.53	10.53	28.3	4
23	20	323.1	0.0529	0.0000	11.68	0.4180	-10.89	10.89	41.5	13
24	20	373.1	0.0529	0.0000	2.65	0.0991	-2.48	2.48	8.4	9
25	22	323.1	0.0529	0.0000	15.69	0.3826	-15.01	15.01	37.6	14
26	22	348.1	0.0529	0.0000	8.06	0.2334	-7.77	7.77	22.5	19
27	22	373.1	0.0529	0.0000	2.61	0.1203	-2.20	2.46	10.3	11
28	28	348.1	0.0529	0.0000	9.94	0.2714	-9.25	9.25	26.0	8
29	28	373.1	0.0529	0.0000	3.50	0.1336	-2.16	3.28	12.1	9
30	28	423.1	0.0529	0.0000	17.40	0.2387	11.92	11.92	21.8	6
31	32	348.1	0.0529	0.0000	8.59	0.2589	-8.27	8.27	24.4	11
32	32	373.1	0.0529	0.0000	2.68	0.0809	-0.88	2.31	6.3	11
33	32	398.1	0.0529	0.0000	10.66	0.1802	8.39	8.39	16.3	14
34	36	373.1	0.0529	0.0000	2.05	0.1164	-1.90	1.90	10.2	10
35	36	423.1	0.0529	0.0000	19.88	0.3374	15.37	15.37	32.6	8
36	44	373.1	0.0529	0.0000	2.53	0.0731	0.52	1.65	6.5	7
37	44	423.1	0.0529	0.0000	22.22	0.4760	17.21	17.21	46.7	7

MODEL OVERALL STATISTICS

RMSE	= 11.3903 BAR	NO PT	= 421
AAD	= 6.7718 BAR	%AAD	= 14.373
MIN DEV=-20.1819 BAR		MIN %DEV	= -49.529
MAX DEV= 62.6196 BAR		MAX %DEV	= 64.898
BIAS	= 1.2177 BAR	C-VAR	= 0.348
RESTRICTIONS	: NONE	R-SQR	=0.703323

TABLE G.XXXI

BUBBLE-POINT CALCULATIONS USING MODIFIED SPHCT EQUATION OF STATE FOR CARBON DIOXIDE + N-PARAFFIN SYSTEMS (CASE 3)

ISO	CN	T(K)	C(I,J)	D(I,J)	RMSE	RMSPE	BIAS	AAD	%AAD	NPT
1	4	310.9	0.0786	0.0000	0.59	0.0146	-0.35	0.39	1.3	18
2	4	344.3	0.0786	0.0000	0.83	0.0203	0.08	0.64	1.9	17
3	4	377.6	0.0786	0.0000	0.64	0.0177	0.09	0.59	1.6	12
4	4	410.9	0.0786	0.0000	0.76	0.0172	-0.55	0.67	1.6	5
5	5	311.0	0.0727	0.0000	0.70	0.0558	-0.29	0.56	3.0	14
6	5	344.1	0.0727	0.0000	1.44	0.0324	0.36	1.15	2.9	15
7	5	377.6	0.0727	0.0000	1.54	0.0383	1.02	1.34	3.5	9
8	6	313.1	0.0626	0.0000	2.08	0.0623	-1.89	1.89	4.8	8
9	6	353.1	0.0626	0.0000	1.26	0.0322	0.36	1.08	2.6	14
10	6	393.1	0.0626	0.0000	3.34	0.0437	2.92	2.93	4.1	15
11	7	310.6	0.0500	0.0000	2.59	0.1254	-2.07	2.07	9.2	23
12	7	352.6	0.0500	0.0000	1.38	0.0215	0.65	1.15	2.0	17
13	7	394.3	0.0500	0.0000	7.59	0.1230	7.26	7.26	11.6	16
14	7	477.2	0.0500	0.0000	7.53	0.1019	6.67	6.67	10.1	7
15	10	310.9	0.0375	0.0000	10.00	0.3227	-9.42	9.42	29.5	11
16	10	344.3	0.0375	0.0000	7.30	0.1767	-6.31	6.53	15.1	8
17	10	377.6	0.0375	0.0000	5.77	0.0725	0.85	4.54	6.5	10
18	10	410.9	0.0375	0.0000	12.80	0.0850	8.56	8.56	6.5	10
19	10	444.3	0.0375	0.0000	16.74	0.1253	12.70	12.70	11.6	11
20	10	477.6	0.0375	0.0000	18.73	0.1407	14.23	14.23	13.1	11
21	10	510.9	0.0375	0.0000	10.69	0.0964	7.93	7.93	8.6	9
22	16	463.0	0.0070	0.0000	0.84	0.0256	0.24	0.76	2.3	4
23	20	323.1	0.0856	0.0000	5.34	0.2343	-5.16	5.16	22.3	13
24	20	373.1	0.0856	0.0000	12.19	0.2136	9.60	9.60	19.2	9
25	22	323.1	0.0811	0.0000	6.37	0.2169	-5.83	5.83	18.4	14
26	22	348.1	0.0811	0.0000	4.76	0.1024	1.62	3.53	9.0	19
27	22	373.1	0.0811	0.0000	9.51	0.1660	6.42	6.48	13.2	11
28	28	348.1	0.0572	0.0000	8.28	0.2461	-7.74	7.74	23.1	8
29	28	373.1	0.0572	0.0000	3.89	0.1141	-0.74	2.99	10.2	9
30	28	423.1	0.0572	0.0000	19.95	0.2777	13.78	13.78	25.6	6
31	32	348.1	0.0518	0.0000	8.95	0.2654	-8.61	8.61	25.1	11
32	32	373.1	0.0518	0.0000	2.70	0.0849	-1.34	2.42	6.7	11
33	32	398.1	0.0518	0.0000	10.14	0.1705	7.94	7.94	15.3	14
34	36	373.1	0.0368	0.0000	5.51	0.2142	-5.09	5.09	21.0	10
35	36	423.1	0.0368	0.0000	11.59	0.1883	8.74	8.74	17.8	8
36	44	373.1	0.0224	0.0000	6.51	0.2481	-5.79	5.79	24.5	7
37	44	423.1	0.0224	0.0000	8.80	0.1753	6.55	6.55	16.7	7

MODEL OVERALL STATISTICS

RMSE	= 7.6565 BAR	NO PT	= 421
AAD	= 4.7778 BAR	%AAD	= 10.553
MIN DEV=	-13.1983 BAR	MIN %DEV	= -46.801
MAX DEV=	41.7127 BAR	MAX %DEV	= 45.081
BIAS	= 1.3100 BAR	C-VAR	= 0.234
RESTRICTIONS	: NONE	R-SQR	=0.787493

TABLE G.XXXII

BUBBLE-POINT CALCULATIONS USING MODIFIED SPHCT EQUATION OF STATE FOR CARBON DIOXIDE + N-PARAFFIN SYSTEMS (CASE 4)

ISO	CN	T(K)	C(I,J)	D(I,J)	RMSE	RMSPE	BIAS	AAD	%AAD	NPT
1	4	310.9	0.0809	0.0000	0.55	0.0108	-0.14	0.34	0.9	18
2	4	344.3	0.0747	0.0000	0.95	0.0162	-0.35	0.55	1.3	17
3	4	377.6	0.0760	0.0000	0.75	0.0169	-0.15	0.63	1.6	12
4	4	410.9	0.1011	0.0000	0.24	0.0065	0.08	0.22	0.6	5
5	5	311.0	0.0792	0.0000	1.09	0.0477	0.40	0.94	3.4	14
6	5	344.1	0.0690	0.0000	1.25	0.0285	-0.20	0.88	2.4	15
7	5	377.6	0.0654	0.0000	0.59	0.0286	0.00	0.55	2.1	9
8	6	313.1	0.0748	0.0000	1.15	0.0253	0.11	0.99	2.0	8
9	6	353.1	0.0645	0.0000	1.61	0.0308	0.83	1.30	2.6	14
10	6	393.1	0.0528	0.0000	0.66	0.0158	0.26	0.54	1.1	15
11	7	310.6	0.0732	0.0000	1.93	0.0457	0.81	1.47	3.9	23
12	7	352.6	0.0499	0.0000	1.36	0.0215	0.62	1.13	2.0	17
13	7	394.3	0.0258	0.0000	1.05	0.0282	-0.70	0.85	1.5	16
14	7	477.2	0.0140	0.0000	0.43	0.0113	-0.01	0.36	0.8	7
15	10	310.9	0.0757	0.0000	9.03	0.1801	2.13	5.82	15.1	11
16	10	344.3	0.0561	0.0000	8.50	0.1121	2.54	6.29	10.1	8
17	10	377.6	0.0405	0.0000	7.18	0.0696	2.59	5.14	6.3	10
18	10	410.9	0.0267	0.0000	6.05	0.0492	2.30	4.36	4.6	10
19	10	444.3	0.0164	0.0000	4.65	0.0363	1.65	2.99	3.1	11
20	10	477.6	0.0098	0.0000	4.82	0.0364	1.58	2.98	3.1	11
21	10	510.9	0.0142	0.0000	2.98	0.0301	0.86	1.66	2.3	9
22	16	463.0	0.0070	0.0000	0.84	0.0256	0.24	0.76	2.3	4
23	20	323.1	0.1095	0.0000	4.44	0.1183	0.72	2.74	9.8	13
24	20	373.1	0.0631	0.0000	2.59	0.0622	0.82	2.00	5.3	9
25	22	323.1	0.0942	0.0000	6.50	0.1669	0.27	5.27	14.3	14
26	22	348.1	0.0796	0.0000	4.22	0.1015	1.02	3.28	8.9	19
27	22	373.1	0.0646	0.0000	3.44	0.0821	1.05	2.37	7.0	11
28	28	348.1	0.0774	0.0000	8.52	0.1577	1.18	5.76	14.2	8
29	28	373.1	0.0638	0.0000	6.14	0.1000	1.62	3.46	8.5	9
30	28	423.1	0.0235	0.0000	3.59	0.0566	1.36	2.20	5.0	6
31	32	348.1	0.0790	0.0000	5.52	0.1401	1.30	4.37	12.2	11
32	32	373.1	0.0568	0.0000	3.33	0.0740	0.77	2.71	6.2	11
33	32	398.1	0.0324	0.0000	2.44	0.0541	0.77	1.70	4.4	14
34	36	373.1	0.0651	0.0000	2.50	0.0688	0.88	1.70	6.1	10
35	36	423.1	0.0133	0.0000	2.19	0.0398	0.80	1.46	3.5	8
36	44	373.1	0.0549	0.0000	3.04	0.0711	1.01	1.84	6.3	7
37	44	423.1	0.0006	0.0000	1.76	0.0356	0.62	1.12	3.1	7

MODEL OVERALL STATISTICS

RMSE	= 3.8664 BAR	NO PT	= 421
AAD	= 2.1591 BAR	%AAD	= 4.981
MIN DEV=	-5.5676 BAR	MIN %DEV	= -28.701
MAX DEV=	26.6151 BAR	MAX %DEV	= 35.093
BIAS	= 0.7312 BAR	C-VAR	= 0.118
RESTRICTIONS	: NONE	R-SQR	=0.862670

TABLE G.XXXIII

BUBBLE-POINT CALCULATIONS USING MODIFIED SPHCT EQUATION OF STATE FOR CARBON DIOXIDE + N-PARAFFIN SYSTEMS (CASE 5)

ISO	CN	T(K)	C(I,J)	D(I,J)	RMSE	RMSPE	BIAS	AAD	%AAD	NPT
1	4	310.9	0.0811	0.0016	0.57	0.0105	-0.18	0.33	0.8	18
2	4	344.3	0.0721	-0.0103	0.28	0.0089	0.00	0.21	0.7	17
3	4	377.6	0.0703	-0.0167	0.32	0.0094	0.07	0.26	0.7	12
4	4	410.9	0.1022	0.0050	0.21	0.0062	0.07	0.18	0.5	5
5	5	311.0	0.0789	0.0149	1.12	0.0291	-0.62	0.94	2.6	14
6	5	344.1	0.0692	0.0017	1.41	0.0280	-0.35	0.93	2.4	15
7	5	377.6	0.0658	0.0020	0.77	0.0283	-0.14	0.72	2.3	9
8	6	313.1	0.0769	0.0079	0.99	0.0150	-0.46	0.72	1.2	8
9	6	353.1	0.0652	0.0067	1.25	0.0158	-0.30	0.91	1.4	14
10	6	393.1	0.0536	0.0029	0.68	0.0130	-0.09	0.59	1.0	15
11	7	310.6	0.0700	0.0072	0.78	0.0199	-0.24	0.60	1.6	23
12	7	352.6	0.0500	0.0034	1.03	0.0114	-0.16	0.63	0.9	17
13	7	394.3	0.0250	-0.0047	0.91	0.0219	0.16	0.76	1.5	16
14	7	477.2	0.0118	0.0007	0.71	0.0124	-0.03	0.55	1.0	7
15	10	310.9	0.0783	0.0133	0.62	0.0116	-0.07	0.44	1.0	11
16	10	344.3	0.0585	0.0106	0.82	0.0138	0.08	0.69	1.2	8
17	10	377.6	0.0412	0.0077	1.13	0.0138	0.14	0.93	1.2	10
18	10	410.9	0.0263	0.0062	1.31	0.0136	0.10	1.04	1.2	10
19	10	444.3	0.0156	0.0058	1.24	0.0098	0.05	0.86	0.8	11
20	10	477.6	0.0098	0.0064	1.60	0.0111	0.34	0.91	0.9	11
21	10	510.9	0.0112	0.0080	0.90	0.0102	-0.06	0.68	0.9	9
22	16	463.0	-0.0173	0.0080	0.21	0.0054	0.02	0.20	0.5	4
23	20	323.1	0.0860	0.0077	0.49	0.0138	0.01	0.29	1.1	13
24	20	373.1	0.0458	0.0056	0.15	0.0044	-0.02	0.14	0.4	9
25	22	323.1	0.0810	0.0090	1.07	0.0241	0.02	0.86	2.1	14
26	22	348.1	0.0617	0.0064	0.61	0.0178	0.05	0.52	1.5	19
27	22	373.1	0.0422	0.0058	0.58	0.0177	0.02	0.43	1.4	11
28	28	348.1	0.0644	0.0055	1.97	0.0331	-0.01	1.34	2.9	8
29	28	373.1	0.0465	0.0042	1.10	0.0179	0.05	0.68	1.5	9
30	28	423.1	0.0087	0.0030	0.56	0.0095	0.06	0.39	0.9	6
31	32	348.1	0.0603	0.0055	0.86	0.0225	0.01	0.69	1.9	11
32	32	373.1	0.0407	0.0043	0.80	0.0163	-0.01	0.62	1.3	11
33	32	398.1	0.0180	0.0030	0.70	0.0141	-0.01	0.54	1.3	14
34	36	373.1	0.0451	0.0029	0.23	0.0075	0.03	0.17	0.6	10
35	36	423.1	0.0012	0.0020	0.21	0.0050	0.03	0.18	0.5	8
36	44	373.1	0.0381	0.0021	0.52	0.0151	0.02	0.36	1.3	7
37	44	423.1	-0.0108	0.0014	0.24	0.0063	-0.05	0.19	0.5	7

MODEL OVERALL STATISTICS

RMSE	= 0.8960 BAR	NO PT	= 421
AAD	= 0.5957 BAR	%AAD	= 1.278
MIN DEV	= -3.4893 BAR	MIN %DEV	= -6.393
MAX DEV	= 4.9012 BAR	MAX %DEV	= 7.233
BIAS	= -0.0571 BAR	C-VAR	= 0.027
RESTRICTIONS	: NONE	R-SQR	=0.993384

TABLE G.XXXIV

BUBBLE-POINT CALCULATIONS USING MODIFIED SPHCT EQUATION OF STATE FOR CARBON DIOXIDE + N-PARAFFIN SYSTEMS (CASE 6)

ISO	CN	T(K)	C(I,J)	E(I,J)	RMSE	RMSPE	BIAS	AAD	%AAD	NPT
1	4	310.9	0.0786	0.0053	0.57	0.0104	-0.20	0.33	0.8	18
2	4	344.3	0.0868	-0.0282	0.38	0.0095	-0.03	0.26	0.8	17
3	4	377.6	0.0986	-0.0484	0.28	0.0089	0.07	0.22	0.6	12
4	4	410.9	0.1084	-0.0117	0.27	0.0070	0.10	0.24	0.6	5
5	5	311.0	0.0586	0.0518	1.05	0.0282	-0.58	0.88	2.5	14
6	5	344.1	0.0659	0.0074	1.44	0.0277	-0.41	0.93	2.3	15
7	5	377.6	0.0623	0.0071	0.79	0.0281	-0.17	0.75	2.3	9
8	6	313.1	0.0657	0.0320	0.92	0.0139	-0.46	0.65	1.1	8
9	6	353.1	0.0554	0.0239	1.11	0.0142	-0.30	0.81	1.2	14
10	6	393.1	0.0494	0.0091	0.65	0.0127	-0.09	0.56	1.0	15
11	7	310.6	0.0598	0.0316	0.72	0.0191	-0.21	0.55	1.6	23
12	7	352.6	0.0450	0.0132	0.97	0.0107	-0.17	0.58	0.8	17
13	7	394.3	0.0319	-0.0161	0.86	0.0213	0.15	0.74	1.4	16
14	7	477.2	0.0131	-0.0029	0.95	0.0132	0.16	0.68	1.1	7
15	10	310.9	0.0593	0.0711	0.50	0.0082	-0.07	0.31	0.7	11
16	10	344.3	0.0438	0.0493	0.94	0.0145	0.12	0.75	1.2	8
17	10	377.6	0.0307	0.0319	1.30	0.0151	0.11	1.04	1.4	10
18	10	410.9	0.0182	0.0229	1.50	0.0148	0.14	1.17	1.3	10
19	10	444.3	0.0083	0.0195	1.41	0.0108	0.11	0.95	0.9	11
20	10	477.6	0.0004	0.0216	1.49	0.0116	0.03	0.97	1.0	11
21	10	510.9	0.0013	0.0231	0.96	0.0105	-0.04	0.72	0.9	9
22	16	463.0	-0.0262	0.0311	0.21	0.0053	0.00	0.19	0.5	4
23	20	323.1	0.0715	0.0589	0.33	0.0096	0.00	0.20	0.8	13
24	20	373.1	0.0376	0.0331	0.11	0.0036	0.00	0.10	0.3	9
25	22	323.1	0.0652	0.0708	0.76	0.0176	-0.02	0.62	1.5	14
26	22	348.1	0.0511	0.0446	0.53	0.0164	-0.01	0.47	1.4	19
27	22	373.1	0.0333	0.0363	0.56	0.0174	-0.02	0.43	1.4	11
28	28	348.1	0.0551	0.0416	1.73	0.0290	-0.04	1.18	2.6	8
29	28	373.1	0.0399	0.0285	1.01	0.0163	0.04	0.63	1.4	9
30	28	423.1	0.0048	0.0167	0.54	0.0091	0.02	0.39	0.8	6
31	32	348.1	0.0497	0.0447	0.73	0.0206	-0.02	0.60	1.7	11
32	32	373.1	0.0332	0.0311	0.74	0.0154	-0.02	0.58	1.3	11
33	32	398.1	0.0132	0.0196	0.68	0.0140	-0.02	0.53	1.3	14
34	36	373.1	0.0394	0.0222	0.20	0.0069	0.01	0.15	0.6	10
35	36	423.1	-0.0018	0.0124	0.20	0.0049	0.02	0.17	0.5	8
36	44	373.1	0.0335	0.0175	0.49	0.0144	0.04	0.33	1.2	7
37	44	423.1	-0.0133	0.0097	0.23	0.0056	0.02	0.16	0.5	7

MODEL OVERALL STATISTICS

RMSE	= 0.8670 BAR	NO PT	= 421
AAD	= 0.5729 BAR	%AAD	= 1.210
MIN DEV=	-3.5844 BAR	MIN %DEV	= -6.303
MAX DEV=	4.2267 BAR	MAX %DEV	= 6.902
BIAS	= -0.0679 BAR	C-VAR	= 0.026
RESTRICTIONS	: NONE	R-SQR	=0.993983

TABLE G.XXXV

BUBBLE POINT CALCULATIONS FOR THE PENG-ROBINSON EQUATION FOR THE DATA SET CONTAINING DENSITIES AND COMPOSITIONS (CASE 1)

Solvent	T(K)	C(I,J)	D(I,J)	PROP	RMSE	BIAS	AAD	%AAD	PT
n-Butane	319.3	0.0000	0.0000	P	9.16	-9.07	9.07	21.38	11
				y	0.024	-0.004	0.019	2.36	11
				L	32.00	-31.00	31.00	5.38	11
				V	36.00	-34.00	34.00	27.76	11
n-Butane	344.3	0.0000	0.0000	P	7.63	-5.13	6.49	13.38	7
				y	0.216	-0.175	0.175	22.56	7
				L	24.00	21.00	21.00	4.17	7
				V	273.00	195.00	214.00	131.41	7
n-Butane	377.6	0.0000	0.0000	P	5.52	-1.68	5.08	10.96	8
				y	0.228	-0.208	0.208	39.60	8
				L	14.00	2.00	13.00	2.97	8
				V	255.00	217.00	222.00	160.28	8
n-Decane	344.3	0.0000	0.0000	P	21.26	-20.66	20.66	12.85	6
				y	0.003	0.003	0.003	0.29	6
				L	26.00	-26.00	26.00	3.72	6
				V	66.00	-60.00	60.00	38.93	6
n-Decane	377.6	0.0000	0.0000	P	17.78	-8.93	15.30	12.85	9
				y	0.213	-0.170	0.173	17.74	9
				L	22.00	-20.00	20.00	2.98	9
				V	272.00	194.00	242.00	79.56	9
n-Tetra decane	344.3	0.0000	0.0000	P	19.45	-9.91	16.06	13.20	6
				y	0.206	-0.184	0.187	18.89	6
				L	83.00	-82.00	82.00	10.93	6
				V	237.00	179.00	227.00	58.71	6
Cyclo-hexane	344.3	0.0000	0.0000	P	6.10	6.06	6.06	5.02	6
				y	0.371	-0.365	0.365	37.51	6
				L	35.00	-35.00	35.00	4.22	6
				V	416.00	406.00	406.00	115.62	6
Benzene	344.3	0.0000	0.0000	P	19.73	-19.63	19.63	24.32	5
				y	0.027	0.026	0.026	2.79	5
				L	109.00	109.00	109.00	15.02	5
				V	72.00	-71.00	71.00	34.67	5

TABLE G.XXXV (Continued)

Solvent	T(K)	C(I,J)	D(I,J)	PROP	RMSE	BIAS	AAD	%AAD	PT
trans-Decalin	344.3	0.0000	0.0000	P		-33.56	33.56	11	11
				y	0.131		0.060	6.08	11
				L	18.69	-15.28		1. 3	11
				V	190.	-58.49	173.06	57. 8	11
1-Methyl naphthalene**	344.3	0.0000	0.0000	P	16.19	-7.84	14.91	29.90	9
				y	0.217	-0.118	0.130	13.36	9
				L	363.00	-22.00	357.00	24.47	9
				V	53.00	16.00	44.00	10.26	9

* P=pressure, bar; y=solute vapor mole fraction; L=liquid density, kg/m^3; V=vapor density, kg/m^3

** The solute for the first nine mixtures is CO_2. The last mixture is ethane + 1-methylnaphthalene.

TABLE G.XXXVI

BUBBLE POINT CALCULATIONS FOR THE PENG-ROBINSON EQUATION FOR THE DATA SET CONTAINING DENSITIES AND COMPOSITIONS (CASE 2)

Solvent	T(K)	C(I,J)	D(I,J)	PROP	RMSE	BIAS	AAD	%AAD	PT
n-Butane	319.3	0.1213	0.0000	P	0.30	0.01	0.26	0.60	11
				y	0.009	-0.002	0.009	1.01	11
				L	19.00	-5.00	16.00	2.88	11
				V	6.00	4.00	5.00	4.55	11
n-Butane	344.3	0.1237	0.0000	P	0.29	-0.09	0.21	0.34	7
				y	0.014	-0.014	0.014	1.80	7
				L	19.00	-13.00	15.00	2.97	7
				V	6.00	5.00	5.00	3.60	7
n-Butane	377.6	0.1371	0.0000	P	0.36	-0.08	0.31	0.64	8
				y	0.011	-0.010	0.010	2.00	8
				L	26.00	-25.00	25.00	5.67	8
				V	1.00	0.00	1.00	0.82	8
n-Decane	344.3	0.1035	0.0000	P	2.16	5.54	1.74	2.56	6
				y	0.002	0.001	0.002	0.18	6
				L	28.00	-28.00	28.00	3.89	6
				V	23.00	6.00	9.00	5.34	6
n-Decane	377.6	0.0943	0.0000	P	0.98	0.09	0.91	0.73	9
				y	0.002	-0.001	0.001	0.15	9
				L	31.00	-31.00	31.00	4.66	9
				V	5.00	3.00	4.00	1.31	9
n-Tetra decane	344.3	0.0948	0.0000	P	2.14	-0.28	1.82	1.46	6
				y	0.005	0.003	0.004	0.41	6
				L	90.00	-90.00	90.00	11.98	6
				V	7.00	-7.00	7.00	1.85	6
Cyclo-hexane	344.3	0.1795	0.0000	P	0.60	0.05	0.50	0.43	6
				y	0.070	-0.064	0.064	6.58	6
				L	82.00	-82.00	82.00	9.83	6
				V	83.00	81.00	81.00	20.83	6
Benzene	344.3	0.0928	0.0000	P	1.87	0.40	1.54	1.84	5
				y	0.019	0.019	0.019	2.00	5
				L	97.00	97.00	97.00	13.29	5
				V	9.00	4.00	7.00	2.90	5

TABLE G.XXXVI (Continued)

Solvent	T(K)	C(I,J)	D(I,J)	PROP	RMSE	BIAS	AAD	%AAD	PT
trans-Decalin	344.3	0.1260	0.0000	P	9.52	-2.05	8.29	8.38	11
				y	0.005	-0.001	0.003	0.35	11
				L	441.00	-437.00	437.00	52.52	11
				V	24.00	-17.00	22.00	9.80	11
1-Methyl naphthalene**	344.3	0.0518	0.0000	P	5.38	0.16	4.57	11.62	9
				y	0.014	0.009	0.009	0.88	9
				L	364.00	-23.00	357.00	24.57	9
				V	57.00	20.00	45.00	3.80	9

* P=pressure, bar; y=solute vapor mole fraction; L=liquid density, kg/m^3; V=vapor density, kg/m^3

** The solute for the first nine mixtures is CO_2. The last mixture is ethane + 1-methylnaphthalene.

TABLE G.XXXVII

BUBBLE POINT CALCULATIONS FOR THE PENG-ROBINSON EQUATION FOR THE DATA SET CONTAINING DENSITIES AND COMPOSITIONS (CASE 3)

Solvent	T(K)	C(I,J)	D(I,J)	PROP	RMSE	BIAS	AAD	%AAD	PT
n-Butane	319.3	0.1212	0.0004	P	0.30	0.02	0.27	0.60	11
				y	0.009	-0.002	0.009	1.02	11
				L	19.00	-6.00	16.00	2.90	11
				V	6.00	4.00	5.00	4.56	11
n-Butane	344.3	0.1250	-0.0025	P	0.25	-0.08	0.17	0.26	7
				y	0.013	-0.013	0.013	1.72	7
				L	18.00	-12.00	14.00	2.81	7
				V	5.00	5.00	5.00	3.46	7
n-Butane	377.6	0.1564	-0.0294	P	0.04	0.00	0.03	0.08	8
				y	0.004	-0.004	0.004	0.82	8
				L	18.00	-18.00	18.00	4.06	8
				V	2.00	-2.00	2.00	1.42	8
n-Decane	344.3	0.0908	0.0162	P	0.21	0.01	0.16	0.24	6
				y	0.002	0.001	0.002	0.16	6
				L	34.00	-34.00	34.00	4.78	6
				V	4.00	2.00	3.00	1.73	6
n-Decane	377.6	0.0910	0.0128	P	0.48	-0.01	0.37	0.27	9
				y	0.003	-0.003	0.003	0.29	9
				L	38.00	-38.00	38.00	5.64	9
				V	5.00	5.00	5.00	1.57	9
n-Tetra decane	344.3	0.0884	0.0252	P	0.07	-0.00	0.07	0.05	6
				y	0.004	0.001	0.004	0.40	6
				L	103.00	-103.00	103.00	13.72	6
				V	5.00	2.00	4.00	1.10	6
Cyclo-hexane	344.3	0.1794	0.0003	P	0.60	0.05	0.49	0.43	6
				y	0.070	-0.064	0.064	6.58	6
				L	82.00	-82.00	82.00	9.83	6
				V	83.00	81.00	81.00	20.86	6
Benzene	344.3	0.0771	0.0381	P	0.13	0.00	0.11	0.13	5
				y	0.016	0.016	0.016	1.66	5
				L	76.00	75.00	75.00	10.28	5
				V	4.00	3.00	3.00	1.54	5

TABLE G.XXXVII (Continued)

Solvent	T(K)	C(I,J)	D(I,J)	PROP	RMSE	BIAS	AAD	%AAD	PT
trans-Decalin	344.3	0.1168	0.0209	P	12.05	1.79	7.12	6.42	11
				y	0.085	-0.027	0.028	2.87	11
				L	445.00	-442.00	442.00	53.05	11
				V	20.00	-14.00	16.00	5.88	11
1-Methyl naphthalene**	344.3	0.0324	0.0347	P	4.21	0.06	3.75	9.82	9
				y	0.014	0.008	0.008	0.83	9
				L	366.00	-28.00	359.00	25.01	9
				V	7.00	24.00	56.00	4.96	9

* P=pressure, bar; y=solute vapor mole fraction; L=liquid density, kg/m^3; V=vapor density, kg/m^3

** The solute for the first nine mixtures is CO_2. The last mixture is ethane + 1-methylnaphthalene.

TABLE G.XXXVIII

BUBBLE POINT CALCULATIONS FOR THE SPHCT EQUATION
FOR THE DATA SET CONTAINING DENSITIES
AND COMPOSITIONS (CASE 1)

Solvent	T(K)	C(I,J)	D(I,J)	PROP	RMSE	BIAS	AAD	%AAD	PT
n-Butane	319.3	0.0000	0.0000	P*	7.82	-6.62	6.62	17.30	11
				y	0.121	-0.097	0.097	11.22	11
				L	60.62	-59.66	59.66	10.37	11
				V	195.83	99.30	134.66	79.81	11
n-Butane	344.3	0.0000	0.0000	P	6.42	-4.59	4.59	10.80	7
				y	0.220	-0.192	0.192	24.82	7
				L	67.13	-66.23	66.23	12.84	7
				V	207.73	145.63	165.95	102.40	7
n-Butane	377.6	0.0000	0.0000	P	2.98	-2.02	2.02	5.20	8
				y	0.206	-0.187	0.187	35.82	8
				L	75.22	-74.12	74.12	16.72	8
				V	165.83	125.83	133.98	89.74	8
n-Decane	344.3	0.0000	0.0000	P	21.52	-20.81	20.81	31.10	6
				y	0.003	0.003	0.003	0.28	6
				L	29.38	-19.88	22.95	3.22	6
				V	70.15	-63.19	63.19	40.39	6
n-Decane	377.6	0.0000	0.0000	P	19.45	-16.69	16.69	14.00	9
				y	0.212	-0.170	0.170	17.66	9
				L	59.64	-59.57	59.57	8.91	9
				V	237.80	161.08	215.57	71.85	9
n-Tetra decane	344.3	0.0000	0.0000	P	21.60	-16.23	16.23	13.80	6
				y	0.172	-0.140	0.140	14.32	6
				L	31.25	-30.50	30.50	4.05	6
				V	241.95	128.78	230.04	57.52	6
Cyclo-hexane	344.3	0.0000	0.0000	P	1.10	-1.08	1.08	0.90	6
				y	0.070	-0.360	0.360	37.42	6
				L	154.96	-154.89	154.89	18.66	6
				V	302.53	286.07	286.07	83.57	6
Benzene	344.3	0.0000	0.0000	P	14.13	-14.12	14.12	17.30	5
				y	0.022	0.022	0.022	2.73	5
				L	20.69	11.63	17.09	2.34	5
				V	59.32	-57.81	57.81	27.61	5

TABLE G.XXXVIII (Continued)

Solvent	T(K)	C(I,J)	D(I,J)	PROP	RMSE	BIAS	AAD	%AAD	PT
trans-decalin	344.3	0.0000	0.0000	P	9.97	-5.02	5.02	6.60	11
				y	0.450	-0.420	0.420	42.21	11
				L	182.53	-181.99	181.99	21.89	11
				V	344.97	297.65	310.96	132.40	11
1-Methyl naphthalene	344.3	0.0000	0.0000	P	8.45	-7.80	7.80	7.70	9
				y	0.380	-0.380	0.380	38.06	9
				L	124.49	-124.25	124.25	16.36	9
				V	329.18	314.00	314.00	112.49	9

* P=pressure, bar; y=solute vapor fraction; L=liquid density, kg/m^3; V=vapor density, kg/m^3

** The solute for the first nine mixtures is CO_2. The last mixture is ethane + 1-methylnaphthalene.

TABLE G.XXXVIX

BUBBLE POINT CALCULATIONS FOR THE SPHCT EQUATION
FOR THE DATA SET CONTAINING DENSITIES
AND COMPOSITIONS (CASE 2)

Solvent	T(K)	C(I,J)	D(I,J)	PROP	RMSE	BIAS	AAD	%AAD	PT
n-Butane	319.3	0.0827	0.0000	P*	2.04	-1.21	1.68	3.30	11
				y	0.027	-0.030	0.030	3.16	11
				L	107.85	-104.82	104.82	12.28	11
				V	9.49	-5.64	6.94	4.38	11
n-Butane	344.3	0.0937	0.0000	P	2.72	-1.24	2.21	3.90	7
				y	0.530	-0.530	0.530	6.90	7
				L	113.64	-112.10	112.10	21.86	7
				V	5.22	1.60	4.52	4.00	7
n-Butane	377.6	0.1015	0.0000	P	2.13	-0.64	1.83	3.80	8
				y	0.053	-0.051	0.051	9.88	8
				L	107.46	-107.00	107.00	24.32	8
				V	3.41	-0.15	3.06	2.57	8
n-Decane	344.3	0.0592	0.0000	P	0.93	-0.19	0.62	0.70	6
				y	0.002	0.001	0.001	0.15	6
				L	34.62	-24.49	27.11	3.80	6
				V	4.49	-3.57	3.57	2.45	6
n-Decane	377.6	0.0644	0.0000	P	2.34	-0.33	1.97	1.50	9
				y	0.010	-0.009	0.009	0.94	9
				L	74.34	-73.55	73.55	11.01	9
				V	5.79	4.80	5.53	2.06	9
n-Tetra decane	344.3	0.0504	0.0000	P	0.35	-0.01	0.30	0.20	6
				y	0.005	0.001	0.005	0.46	6
				L	43.56	-41.29	41.29	5.49	6
				V	15.42	-13.59	13.59	3.17	6
Cyclo-hexane	344.3	0.1020	0.0000	P	7.63	-3.73	4.98	3.80	6
				y	0.149	-0.147	0.147	15.11	6
				L	202.83	-202.27	202.27	24.37	6
				V	125.56	111.68	111.68	33.07	6
Benzene	344.3	0.0396	0.0000	P	1.45	-0.43	1.20	1.40	5
				y	0.014	0.014	0.014	1.48	5
				L	20.30	1.02	17.70	2.44	5
				V	8.36	-5.06	6.23	2.65	5

TABLE G.XXXVIX (Continued)

Solvent	T(K)	C(I,J)	D(I,J)	PROP	RMSE	BIAS	AAD	%AAD	PT
trans-decalin***	344.3	0.0823	0.0000	P	5.27	-2.31	4.24	4.90	5
				y	0.025	-0.024	0.024	2.40	5
				L	178.83	-178.41	178.41	21.37	5
				V	16.31	15.28	15.28	8.89	5
1-Methyl naphthalene**	344.3	0.0469	0.0000	P	6.87	-1.10	5.97	5.60	9
				y	0.031	-0.029	0.029	3.03	9
				L	131.48	-131.23	131.23	17.28	9
				V	19.00	-18.41	18.41	6.26	9

* P=pressure, bar; y=solute vapor fraction; L=liquid density, kg/m^3; V=vapor density, kg/m^3

** The solute for the first nine mixtures is CO_2. The last mixture is ethane + 1-methylnaphthalene.

*** The equation indicates no two-phase region for the higher pressure data of *trans*-decalin. Therefore, only the lower pressure points were included here.

TABLE G.XL

BUBBLE POINT CALCULATIONS FOR THE SPHCT EQUATION
FOR THE DATA SET CONTAINING DENSITIES
AND COMPOSITIONS (CASE 3)

Solvent	T(K)	C(I,J)	D(I,J)	PROP	RMSE	BIAS	AAD	%AAD	PT
n-Butane	319.3	0.0662	-0.0326	P*	0.47	-0.10	0.37	0.70	11
				y	0.014	-0.013	0.013	1.60	11
				L	71.41	-69.73	69.73	12.17	11
				V	6.86	-4.50	4.92	3.72	11
n-Butane	344.3	0.0642	-0.0455	P	0.18	-0.02	0.14	0.20	7
				y	0.021	-0.018	0.018	2.43	7
				L	65.57	-65.40	65.40	12.73	7
				V	6.28	-4.52	4.52	2.57	7
n-Butane	377.6	0.0636	-0.0703	P	0.29	0.01	0.25	0.57	8
				y	0.020	-0.005	0.017	3.84	8
				L	65.62	-65.18	65.18	14.73	8
				V	15.08	-12.88	12.88	8.74	8
n-Decane	344.3	0.0591	-0.0008	P	0.65	-0.00	0.51	0.71	6
				y	0.002	0.001	0.002	0.16	6
				L	33.60	-23.39	26.20	3.67	6
				V	3.11	-2.70	2.70	2.27	6
n-Decane	377.6	0.0541	-0.0069	P	0.65	0.01	0.50	0.37	9
				y	0.006	-0.005	0.005	0.53	9
				L	61.96	-61.24	61.24	9.17	9
				V	3.23	0.21	2.92	1.02	9
n-Tetra decane	344.3	0.0504	0.0000	P	0.35	-0.01	0.30	0.20	6
				y	0.005	0.001	0.005	0.46	6
				L	43.56	-41.29	41.29	5.49	6
				V	15.42	-13.59	13.59	3.17	6
Cyclo-hexane	344.3	0.0935	-0.0131	P	2.16	-0.76	1.98	1.60	6
				y	0.124	-0.119	0.119	12.27	6
				L	180.71	-180.35	180.35	21.73	6
				V	106.74	100.74	100.74	28.58	6
Benzene	344.3	0.0312	-0.0085	P	0.24	-0.01	0.23	0.28	5
				y	0.016	0.016	0.016	1.72	5
				L	24.67	15.73	20.94	2.87	5
				V	4.58	-4.12	4.12	1.95	5

TABLE G.XL (Continued)

Solvent	T(K)	C(I,J)	D(I,J)	PROP	RMSE	BIAS	AAD	%AAD	PT
trans-decalin**	344.3	0.0835	-0.0368	P	0.19	-0.00	0.17	0.22	5
				y	0.016	-0.150	0.150	1.52	5
				L	142.93	-142.72	142.72	17.10	5
				V	17.41	14.08	14.08	6.80	5
1-Methyl naphthalene***	344.3	0.0469	0.0000	P	6.87	-1.10	5.97	5.60	9
				y	0.031	-0.029	0.029	3.03	9
				L	131.48	-131.23	131.23	17.28	9
				V	19.00	-18.41	18.41	6.26	9

* P=pressure, bar; y=solute vapor fraction; L=liquid density, kg/m^3; V=vapor density, kg/m^3

** The equation indicates no two-phase region for the higher pressure data of *trans*-decalin. Therefore, only the lower pressure points were included here.

*** The solute for the first nine mixtures is CO_2. The last mixture is ethane + 1-methylnaphthalene.

TABLE G.XLI

BUBBLE POINT CALCULATIONS FOR THE SPHCT EQUATION
FOR THE DATA SET CONTAINING DENSITIES
AND COMPOSITIONS (CASE 4)

Solvent	T(K)	C(I,J)	E(I,J)	PROP	RMSE	BIAS	AAD	%AAD	PT
n-Butane	319.3	0.1125	-0.0671	P*	0.70	-0.20	0.56	1.13	11
				y	0.020	-0.020	0.020	2.32	11
				L	97.76	-93.96	93.96	11.39	11
				V	4.93	-2.39	3.52	3.11	11
n-Butane	344.3	0.1376	-0.0993	P	0.45	-0.05	0.36	0.64	7
				y	0.030	-0.029	0.029	3.91	7
				L	91.90	-91.00	91.00	17.74	7
				V	2.75	-1.01	1.54	0.82	7
n-Butane	377.6	0.1910	-0.1446	P	0.18	0.01	0.15	0.35	8
				y	0.026	-0.023	0.023	5.23	8
				L	87.62	-87.59	87.59	19.87	8
				V	10.61	-8.85	8.85	5.92	8
n-Decane	344.3	0.0602	-0.0028	P	0.68	-0.04	0.53	0.72	6
				y	0.002	0.001	0.002	0.16	6
				L	34.09	-23.93	26.64	3.74	6
				V	3.19	-2.74	2.74	2.27	6
n-Decane	377.6	0.0648	-0.0261	P	0.69	-0.01	0.53	0.39	9
				y	0.007	-0.006	0.006	0.59	9
				L	66.17	-65.47	65.47	9.80	9
				V	3.58	0.93	3.29	1.14	9
n-Tetra decane	344.3	0.0504	0.0011	P	0.36	-0.03	0.30	0.23	6
				y	0.005	0.001	0.005	0.46	6
				L	43.89	-41.62	41.62	5.53	6
				V	14.89	-13.07	13.07	3.04	6
Cyclo-hexane	344.3	0.0979	0.0259	P	9.63	-2.16	7.45	5.93	6
				y	0.165	-0.160	0.160	16.42	6
				L	208.60	-207.94	207.94	25.05	6
				V	133.41	116.20	116.20	34.36	6
Benzene	344.3	0.0465	-0.0299	P	0.29	-0.02	0.28	0.34	5
				y	0.016	0.016	0.016	1.69	5
				L	21.59	9.34	18.69	2.56	5
				V	4.18	-3.73	3.73	1.78	5

TABLE G.XLI (Continued)

Solvent	T(K)	C(I,J)	E(I,J)	PROP	RMSE	BIAS	AAD	%AAD	PT
trans-decalin**	344.3	0.0823	0.0001	P	5.27	-2.31	4.29	4.87	5
				y	0.025	-0.024	0.024	2.42	5
				L	178.93	-178.40	178.40	21.37	5
				V	16.31	15.27	15.27	8.89	5
1-Methyl naphthalene***	344.3	0.0469	0.0001	P	6.85	-1.05	5.96	5.57	9
				y	0.031	-0.029	0.029	3.03	9
				L	131.49	-131.20	131.20	17.28	9
				V	18.96	-18.36	18.36	6.24	9

* P=pressure, bar; y=solute vapor fraction; L=liquid density, kg/m^3; V=vapor density, kg/m^3

** The equation indicates no two-phase region for the higher pressure data of *trans*-decalin. Therefore, only the lower pressure points were included here.

*** The solute for the first nine mixtures is CO_2. The last mixture is ethane + 1-methylnaphthalene.

TABLE G.XLII

BUBBLE POINT CALCULATIONS FOR THE MODIFIED SPHCT EQUATION FOR THE DATA SET CONTAINING DENSITIES AND COMPOSITIONS (CASE 1)

Solvent	T(K)	C(I,J)	D(I,J)	PROP	RMSE	BIAS	AAD	%AAD	PT
n-Butane	319.3	0.0000	0.0000	P	9.65	-9.56	9.56	22.40	11
				y	0.021	0.001	0.021	2.57	11
				L	38.21	-37.93	37.93	6.60	11
				V	43.67	-40.52	40.52	32.38	11
n-Butane	344.3	0.0000	0.0000	P	8.41	-7.79	7.79	16.10	7
				y	0.122	-0.122	0.122	15.70	7
				L	48.38	-47.62	47.62	9.23	7
				V	179.80	100.08	132.51	77.48	7
n-Butane	377.6	0.0304	0.0000	P	4.56	-3.98	3.98	9.10	8
				y	0.140	-0.140	0.140	26.32	8
				L	61.65	-60.72	60.72	13.70	8
				V	148.87	95.68	113.25	71.98	8
n-Decane	344.3	0.0550	0.0000	P	21.04	-20.76	20.76	32.40	6
				y	0.004	0.004	0.004	0.37	6
				L	24.47	-17.93	19.43	2.72	6
				V	68.77	-63.78	63.78	42.40	6
n-Decane	377.6	0.0304	0.0000	P	19.70	-19.68	19.68	15.60	9
				y	0.011	-0.010	0.010	8.36	9
				L	56.36	-55.89	55.89	8.36	9
				V	84.16	-82.93	82.93	28.60	9
n-Tetra decane	344.3	0.0426	0.0000	P	30.73	-27.87	27.87	22.80	6
				y	0.106	-0.055	0.067	6.80	6
				L	39.90	-39.18	39.18	5.21	6
				V	192.50	-50.48	190.14	47.55	6
Cyclo-hexane	344.3	0.0826	0.0000	P	2.16	-1.85	1.85	1.60	6
				y	0.365	-0.365	0.365	37.51	6
				L	119.52	-119.41	119.41	14.38	6
				V	336.39	321.57	321.57	93.21	6
Benzene	344.3	0.0306	0.0000	P	12.15	-11.89	11.89	14.90	5
				y	0.028	0.028	0.028	2.96	5
				L	34.92	31.98	31.98	4.38	5
				V	56.07	-55.62	55.62	27.18	5

TABLE G.XLII (Continued)

Solvent	T(K)	C(I,J)	D(I,J)	PROP	RMSE	BIAS	AAD	%AAD	PT
trans-Decalin	344.3	0.0461	0.0000	P	35.63	-33.56	33.56	35.11	11
				y	0.131	-0.051	0.060	6.08	11
				L	18.69	-15.28	10.73	1.83	11
				V	190.90	-58.49	173.06	57.58	11
1-Methyl naphthalene**	344.3	0.0358	0.0000	P	33.46	-28.77	28.77	28.40	9
				y	0.168	0.083	0.108	11.42	9
				L	5.93	4.68	4.68	0.63	9
				V	246.66	-14.85	234.54	72.02	9

* P=pressure, bar; y=solute vapor mole fraction; L=liquid density, kg/m^3; V=vapor density, kg/m^3

** The solute for the first nine mixtures is CO_2. The last mixture is ethane + 1-methylnaphthalene.

TABLE G.XLIII

BUBBLE POINT CALCULATIONS FOR THE MODIFIED SPHCT EQUATION FOR THE DATA SET CONTAINING DENSITIES AND COMPOSITIONS (CASE 2)

Solvent	T(K)	C(I,J)	D(I,J)	PROP	RMSE	BIAS	AAD	%AAD	PT
n-Butane	319.3	0.0740	0.0000	P	0.67	-0.30	0.48	0.90	11
				y	0.010	0.004	0.008	0.99	11
				L	75.21	-72.40	72.40	12.63	11
				V	9.18	-6.64	6.68	4.91	11
n-Butane	344.3	0.0710	0.0000	P	0.83	-0.32	0.64	1.10	7
				y	0.007	-0.007	0.007	0.88	7
				L	77.69	-76.71	76.71	14.95	7
				V	8.09	-5.68	5.68	3.18	7
n-Butane	377.6	0.0304	0.0000	P	0.65	-0.16	0.57	1.20	8
				y	0.005	-0.004	0.004	0.79	8
				L	80.00	-79.84	79.84	18.13	8
				V	11.29	-9.52	9.52	6.50	8
n-Decane	344.3	0.0550	0.0000	P	5.30	1.12	4.39	6.70	6
				y	0.003	0.002	0.002	0.23	6
				L	27.00	-20.36	21.54	3.02	6
				V	13.92	-1.03	11.94	9.21	6
n-Decane	377.6	0.0304	0.0000	P	2.41	0.31	2.27	1.80	9
				y	0.005	0.005	0.005	0.48	9
				L	55.38	-54.96	54.96	8.22	9
				V	28.56	-28.14	28.14	9.77	9
n-Tetra decane	344.3	0.0426	0.0000	P	4.70	-0.47	4.10	3.30	6
				y	0.007	0.007	0.007	0.71	6
				L	42.92	-41.72	41.72	5.54	6
				V	59.24	-58.93	58.93	14.81	6
Cyclo-hexane	344.3	0.0826	0.0000	P	0.55	0.31	0.39	0.30	6
				y	0.068	-0.062	0.062	6.41	6
				L	156.16	-155.81	155.81	18.77	6
				V	37.03	34.69	34.69	9.38	6
Benzene	344.3	0.0306	0.0000	P	2.44	0.53	2.05	2.50	5
				y	0.023	0.023	0.023	2.45	5
				L	29.55	24.82	24.82	3.34	5
				V	12.35	-11.87	11.87	6.23	5

TABLE G.XLIII (Continued)

Solvent	T(K)	C(I,J)	D(I,J)	PROP	RMSE	BIAS	AAD	%AAD	PT
trans-Decalin	344.3	0.0461	0.0000	P	15.57	-5.17	13.91	14.40	11
				y	0.004	0.001	0.004	0.38	11
				L	18.38	9.90	15.31	1.84	11
				V	51.18	-45.81	47.61	20.60	11
1-Methyl naphthalene**	344.3	0.0358	0.0000	P	9.54	-0.61	7.95	7.30	9
				y	0.027	0.023	0.023	2.39	9
				L	3.97	3.79	3.79	0.50	9
				V	94.71	-93.84	93.84	30.01	9

* P=pressure, bar; y=solute vapor mole fraction; L=liquid density, kg/m^3; V=vapor density, kg/m^3

** The solute for the first nine mixtures is CO_2. The last mixture is ethane + 1-methylnaphthalene.

TABLE G.XLIV

BUBBLE POINT CALCULATIONS FOR THE MODIFIED SPHCT EQUATION FOR THE DATA SET CONTAINING DENSITIES AND COMPOSITIONS (CASE 3)

Solvent	T(K)	C(I,J)	D(I,J)	PROP	RMSE	BIAS	AAD	%AAD	PT
n-Butane	319.3	0.0720	-0.0048	P*	0.47	-0.11	0.39	0.80	11
				y	0.010	0.006	0.008	0.94	11
				L	69.86	-67.24	67.24	11.73	11
				V	8.48	-6.24	6.35	4.71	11
		δ_c = 0.02956		Lt	15.21	-8.25	13.77	2.40	11
				Vt	2.61	-0.14	1.89	2.41	11
n-Butane	344.3	0.0650	-0.0110	P	0.20	-0.02	0.18	0.30	7
				y	0.002	0.001	0.001	0.18	7
				L	65.88	-65.26	65.26	12.72	7
				V	8.77	-6.95	6.95	4.29	7
		δ_c = 0.03487		Lt	8.90	-3.83	7.85	1.52	7
				Vt	1.46	0.56	1.34	0.97	7
n-Butane	377.6	0.0646	-0.0185	P	0.05	0.00	0.04	0.10	8
				y	0.010	0.008	0.009	1.70	8
				L	68.73	-68.72	68.72	15.58	8
				V	14.42	-12.71	12.71	8.97	8
		δ_c = 0.04654		Lt	8.71	2.73	7.60	1.75	8
				Vt	4.46	-4.26	4.26	3.32	8
n-Decane	344.3	0.0582	0.0115	P	0.06	0.00	0.05	0.10	6
				y	0.002	0.002	0.002	0.19	6
				L	41.97	-35.44	35.44	4.97	6
				V	10.06	-8.50	8.50	5.20	6
		δ_c = 0.11510		Lt	15.97	-11.05	15.57	2.20	6
				Vt	4.18	-3.46	3.99	3.35	6
n-Decane	377.6	0.0411	0.0087	P	0.49	0.00	0.35	0.30	9
				y	0.002	0.002	0.002	0.23	9
				L	69.97	-69.47	69.47	10.40	9
				V	27.56	-25.93	25.93	8.64	9
		δ_c = 0.08470		Lt	14.90	-3.09	13.38	1.99	9
				Vt	5.08	-2.84	4.10	1.66	9
n-Tetra decane	344.3	0.0615	0.0139	P	0.38	0.01	0.31	0.20	6
				y	0.005	0.005	0.005	0.52	6
				L	69.23	-68.19	68.19	9.07	6
				V	53.02	-49.14	49.14	11.60	6
		δ_c = 0.16698		Lt	22.99	-0.53	19.16	2.55	6
				Vt	13.46	-10.55	12.80	3.47	6

TABLE G.XLIV (Continued)

Solvent	T(K)	C(I,J)	D(I,J)	PROP	RMSE	BIAS	AAD	%AAD	PT
Cyclo-hexane	344.3	0.0786	-0.0047	P	0.82	0.49	0.60	0.50	6
				y	0.060	-0.054	0.054	5.62	6
				L	148.57	-148.23	148.23	17.86	6
				V	29.80	26.63	26.63	7.17	6
		δ_c = 0.03859		Lt	101.26	-101.24	101.24	12.19	6
				Vt	50.22	45.86	45.86	11.56	6
Benzene	344.3	0.0439	0.0151	P	0.07	0.00	0.05	0.10	5
				y	0.020	0.020	0.020	2.09	5
				L	18.28	-0.57	15.60	2.15	5
				V	14.23	-12.93	12.93	5.88	5
		δ_c = 0.01709		Lt	21.16	18.32	18.32	2.51	5
				Vt	11.57	-10.72	10.72	4.94	5
trans-Decalin	344.3	0.0647	0.0262	P	0.22	0.00	0.20	0.20	11
				y	0.005	-0.002	0.004	0.37	11
				L	39.01	-30.36	31.46	3.79	11
				V	27.78	-22.71	22.71	6.72	11
		δ_c = 0.14030		Lt	28.86	-26.71	27.11	3.25	11
				Vt	17.07	-16.04	16.04	5.72	11
1-Methyl naphthalene**	344.3	0.0583	0.0175	P	1.18	0.01	0.88	0.80	9
				y	0.022	0.018	0.018	1.90	9
				L	23.44	-23.39	23.39	3.10	9
				V	80.92	-76.54	76.54	23.11	9
		δ_c = -0.3343		Lt	67.97	62.18	62.18	8.05	9
				Vt	61.60	-56.50	56.50	16.63	9

* P=pressure, bar; y=solute vapor mole fraction; L=liquid density, kg/m^3; V=vapor density, kg/m^3; Lt=translated liquid density, kg/m^3; Vt=translated vapor density, kg/m^3

** The solute for the first nine mixtures is CO_2. The last mixture is ethane + 1-methylnaphthalene.

TABLE G.XLV

BUBBLE POINT CALCULATIONS FOR THE MODIFIED SPHCT EQUATION FOR THE DATA SET CONTAINING DENSITIES AND COMPOSITIONS (CASE 4)

Solvent	T(K)	C(I,J) E(I,J)	PROP	RMSE	BIAS	AAD	%AAD	PT
n-Butane	319.3	0.0782 -0.0129	P*	0.50	-0.14	0.41	0.80	11
			y	0.010	0.005	0.008	0.95	11
			L	73.37	-70.57	70.57	12.31	11
			V	8.48	-6.14	6.30	4.66	11
		δ_c = 0.03101	Lt	16.01	-9.17	14.35	2.50	11
			Vt	2.83	0.30	2.34	2.61	11
n-Butane	344.3	0.0814 -0.0323	P	0.26	-0.02	0.22	0.40	7
			y	0.002	-0.001	0.001	0.18	7
			L	71.86	-71.06	71.06	13.85	7
			V	8.02	-6.28	6.28	3.86	7
		δ_c = 0.03789	Lt	9.28	-5.78	8.17	1.58	7
			Vt	3.19	2.10	2.49	1.49	7
n-Butane	377.6	0.0951 -0.0526	P	0.04	0.00	0.04	0.10	8
			y	0.006	0.004	0.005	0.97	8
			L	74.11	-74.05	74.05	16.80	8
			V	13.32	-11.75	11.75	8.30	8
		δ_c = 0.05033	Lt	5.97	1.48	5.19	1.19	8
			Vt	2.58	-2.51	2.51	2.12	8
n-Decane	344.3	0.0426 0.0528	P	0.12	0.01	0.09	0.10	6
			y	0.002	0.002	0.002	0.20	6
			L	35.36	-28.69	28.68	4.02	6
			V	10.17	-8.64	8.64	5.28	6
		δ_c = 0.09897	Lt	14.07	-5.43	10.48	1.48	6
			Vt	4.42	-4.06	4.06	3.40	6
n-Decane	377.6	0.0293 0.0394	P	0.46	0.00	0.35	0.30	9
			y	0.003	0.003	0.003	0.27	9
			L	64.77	-64.26	64.26	9.62	9
			V	28.08	-26.40	26.40	8.78	9
		δ_c = 0.07864	Lt	13.65	0.31	12.16	1.82	9
			Vt	5.50	-4.44	4.44	1.79	9
n-Tetra decane	344.3	0.0432 0.0788	P	0.30	0.00	0.25	0.20	6
			y	0.006	0.006	0.006	0.58	6
			L	59.17	-58.00	58.00	7.71	6
			V	55.52	-51.20	51.20	12.04	6
		δ_c = 0.14826	Lt	23.22	10.07	17.12	2.24	6
			Vt	15.03	-14.39	14.39	3.83	6

TABLE G.XLV (Continued)

Solvent	T(K)	C(I,J)	E(I,J)	PROP	RMSE	BIAS	AAD	%AAD	PT
Cyclo-hexane	344.3	0.0838	-0.0112	P	0.32	-0.06	0.28	0.20	6
				y	0.061	-0.056	0.056	5.76	6
				L	153.85	-153.49	153.49	18.49	6
				V	30.11	26.27	26.27	7.22	6
		δ_c = 0.03532		Lt	111.35	-111.34	111.34	13.41	6
				Vt	52.68	49.77	49.77	12.73	6
Benzene	344.3	0.0181	0.0681	P	0.10	0.00	0.08	0.10	5
				y	0.020	0.020	0.020	2.16	5
				L	20.28	10.25	17.14	2.35	5
				V	14.86	-13.48	13.48	6.12	5
		δ_c = 0.00914		Lt	24.88	21.03	21.03	2.87	5
				Vt	13.40	-12.26	12.26	5.60	5
trans-Decalin	344.3	0.0302	0.1232	P	0.15	-0.01	0.13	0.10	11
				y	0.003	0.000	0.002	0.22	11
				L	23.99	-10.48	19.71	2.38	11
				V	35.04	-27.17	27.17	7.75	11
		δ_c = 0.13996		Lt	16.93	1.44	12.86	1.55	11
				Vt	20.13	-18.62	18.62	6.21	11
1-Methyl naphthalene**	344.3	0.0122	0.1436	P	0.98	0.00	0.77	0.70	9
				y	0.022	0.018	0.018	1.90	9
				L	14.50	-14.41	14.41	1.91	9
				V	80.34	-76.18	76.18	23.06	9
		δ_c = -0.3562		Lt	67.11	59.83	59.83	7.72	9
				Vt	65.15	-59.99	59.99	17.72	9

* P=pressure, bar; y=solute vapor mole fraction; L=liquid density, kg/m^3; V=vapor density, kg/m^3; Lt=translated liquid density, kg/m^3; Vt=translated vapor density, kg/m^3

** The solute for the first nine mixtures is CO_2. The last mixture is ethane + 1-methylnaphthalene.

TABLE G.XLVI

PHYSICAL PROPERTIES USED IN MIXTURE EOS EVALUATIONS

Compound	T_c, K	P_c, bar	ω	Ref.
C_2	305.4	48.2	0.1004	49,69
C_4	425.16	37.96	0.2004	42,69
C_5	469.8	33.76	0.2511	1
C_6	507.9	29.88	0.2978	1
C_7	540.1	27.35	0.3499	1
C_8	568.8	24.98	0.3995	1
C_{10}	617.6	20.97	0.4885	1
C_{12}	658.3	18.06	0.5708	1
C_{14}	691.6	15.62	0.6442	70
C_{16}	720.6	13.76	0.7311	70
C_{20}*	770.5	11.17		70
	766.6	10.69	0.8791	71
C_{22}	791.7	10.22		70
	785.0	9.44	0.9521	71
C_{28}	845.43	8.26		70
	827.4	6.61	1.1617	71
C_{32}	875.10	7.42		70
	847.9	5.29	1.2947	71
C_{36}	901.07	6.82		70
	864.0	4.28	1.4228	71
C_{44}	944.29	6.04		70
	886.6	2.90	1.6664	71
CO_2	304.2	48.2	0.2390	49,69
Benzene	561.75	48.76	0.2120	47,69
Cyclohexane	553.5	40.70	0.2120	69
trans-Decalin	687.1	31.4	0.2700	69
1-Methyl naphthalene	772.0	36.0	0.3100	69

* For the n-paraffins of C_{20} and heavier the properties used with the SPHCT equation were taken from Gasem (70) and those used with the PR equation were the ones determined as optimum for the PR equation by Gasem, et al. (71).

VITA

Ronald D. Shaver

Candidate for the Degree of

Doctor of Philosophy

Thesis: VAPOR-LIQUID EQUILIBRIUM MEASUREMENTS FOR SELECTED ETHANE AND CARBON DIOXIDE MIXTURES AND MODIFICATION OF THE SPHCT EQUATION OF STATE

Major Filed: Chemical Engineering

Biographical:

Personal Data: Born in Oklahoma City, Oklahoma, August 23, 1966, the son of Jim R. and Carole Shaver.

Education: Graduated from Yukon High School, Yukon, Oklahoma, in May 1984; received Bachelor of Science Degree in Chemical Engineering from Oklahoma State University in December 1988; received Master of Science Degree in Chemical Engineering from Oklahoma State University in May 1990; completed requirements for the Doctor of Philosophy Degree at Oklahoma State University in July 1993.

Professional Experience: Employed by ARCO Oil and Gas Company, Summer, 1988 and 1989; employed by CONOCO, Summer, 1990 and 1991; Research Assistant, School of Chemical Engineering, Oklahoma State University, January, 1989 to June, 1993.